

University of Naples “Federico II”

Department of Chemical, Materials and Production Engineering



Thesis Submitted

By

Firas Khaleel Ismael AL-Zuhairi

In Partial Fulfillment of the Requirements

for the Degree of

Doctor of Philosophy in Chemical Engineering

XXVIII Cycle

Combined use of anaerobic digestion and Fischer-Tropsch reaction to convert organic wastes into biodiesel

Supervisor

Prof. Domenico Pirozzi

CO-Supervisor

Prof. Maria Turco

Dr. Luca Micoli

Course Coordinator

Prof. Andrea D'Anna

Naples- Italy

2017

Abstract

Transportation sector consumes a high amount of energy (e.g., gasoline and diesel) and is the main responsible for a large part of the CO₂ and other pollutants emissions. Replacing the energy derived from fossil fuel required in this sector with that derived from a renewable resource, such as biomass, is a solution that can relieve global warming and other environmental problems.

This work focuses the attention on the overall process that includes the anaerobic digestion of organic wastes, and the conversion of the biogas produced to Biofuels by Fischer-Tropsch (FT) synthesis.

The first aim of the present work is the optimization of the anaerobic digestion processes for biogas production from Municipal Solid Wastes (MSW) under mesophilic conditions, the anaerobic co-digestion of Municipal Solid Wastes (MSW) with lignocellulosic biomasses from Giant reed (GR), the effect of mineral solution "M9 10x" and 400x salts addition, and the effect of trace metals addition in individual and mixed form.

The results show that the highest amount of biogas as well as the highest methane fraction were obtained adopting a suitable combination of the operating parameters (15 wt. % of TS, 10 V/V% of inoculum, co-digestion of 75% GR and 25% MSW, with the addition a mineral and salt solution and addition of 5mg/L from individual elements of Ni, Co and Zn, however higher production was with the addition a mixture of three above elements at concentration 5mg/L for each one).

The second aim is the optimization of the FT synthesis reaction for the exploitation of the synthesis gas (H₂ and CO) obtained by a reforming step of the methane produced by anaerobic digestion. Under the operating conditions adopted, the main product of the FT reaction were liquid hydrocarbons.

The FT reaction was studied under diluted conditions with H₂/CO ratio equal to 2 and extruded cylindrical pellets (d = 2 mm) of Cobalt-Alumina based catalyst. Working with diluted condition (4% H₂, 2% CO, 94% He) drastically reduces the influence of the temperature, since the FT reactions are highly exothermic, allowing to hypothesize a kinetic mechanism at isotherm conditions.

The catalyst was prepared by impregnation technique under vacuum condition with 15% wt. of Cobalt, and it has been characterized using a temperature-programmed reduction (TPR) technique and a N₂ adsorption isotherm.

The experimental investigation on FT reaction was conducted varying the GHSV, from 370 to 820 h⁻¹, and the temperature from 220 to 250 °C, using a fixed bed reactor with 5 g of catalyst. Liquid and gaseous phases products were analyzed by gas-chromatography techniques, in the range C₁, C₂-C₄, C₅-C₁₁, C₁₂-C₂₀ and C₂₁₊ according to the number of C atoms in the chains.

The results indicated that changes in the temperatures and GHSV do not have a significant effect on the conversion of diluted syngas. On the other hand, the results show that the value of CO conversion obtained at steady state with lowest temperatures and GHSV is about 27%, which is higher than the values reported in the literature with the same H₂/CO ratio for a not diluted condition.

The optimum conditions were obtained adopting the lowest values of temperatures and GHSVs. Under these conditions, the liquid hydrocarbon yield at steady state was about 26% and the selectivities towards gasoline and diesel hydrocarbons were about 40.30% and 47.18% respectively.

Acknowledgment

I would like to express my deep and sincere gratitude to my Ph.D. supervisors, Prof. Domenico Pirozzi, Prof. Maria Turco and Dr. Luca Micoli, for their invaluable guidance, constant encouragement, inspiration and assistance throughout this Ph.D. project.

My gratitude and appreciation are also extended to the Ph.D. course coordinator Prof. Andrea D'Anna and Head of the Department of Chemical, Materials and Production Engineering Prof. Pier Luca Maffettone for their cooperation in all the administrative and academic activities related to this research.

I would like to also extend my gratitude and appreciation to members of the biochemical engineering laboratory and catalysts laboratory at Department of Chemical, Materials and Production Engineering / University of Naples "Federico II". I would like to thank Prof. Giuseppe Toscano, Angelo Ausiello, Gaetano Zuccaro, Maria Abagnale, Ciro Florio, Felicia Rugari and Andrea Guidone.

I wish to thank the office of secretary and teaching management Mrs. Paola Desidery, for her assistance.

I would also like to express my acknowledgment to the staff of Department of Chemical, Materials and Production Engineering / University of Naples "Federico II".

Special thanks to my wife Suhair Shabaa for her love, support, and encouragement.

Finally, I would like to thank, the University of Technology/ Ministry of Higher Education & Scientific Research in the Republic of Iraq for allowing me the opportunity to study this Ph.D. program.

Firas

List of Contents

Contents	Page no.
Abstract	I
Acknowledgment	III
List of Contents	IV
List of Tables	X
List of Figures	XI
List of Abbreviations and Nomenclature	XXI
Chapter One: Introduction	1
1.1 General Introduction.....	1
1.2 Objective of Thesis.....	3
1.3 Thesis Outline.....	4
Chapter Two: Literature Review	5
2 Introduction	5
2.1 Anaerobic Digestion.....	5
2.1.1 Hydrolysis.....	7
2.1.2 Acidogenesis.....	8
2.1.3 Acetogenesis.....	9
2.1.4 Methanogenesis.....	10
2.2 Parameters Effect on Anaerobic Digestion Process.....	11
2.2.1 pH value.....	11
2.2.2 Temperature.....	12
2.2.3 Substrate Characteristics.....	12
2.2.4 Mixing (Agitation).....	13
2.2.5 Carbon/Nitrogen ratio.....	14

2.2.6 Volatile Fatty Acids (VFAs).	14
2.2.7 Retention time (RT).....	16
2.3 Types or Operation Modes of Anaerobic Digestion Processes.	17
2.3.1 Liquid and Solid-State Anaerobic Digestion Processes.	17
2.3.2 Batch and Continuous Anaerobic Digestion Processes.	18
2.3.3 Single and Two Stages Anaerobic Digestion Process.	19
2.4 Inhibition /toxicity of anaerobic digestion process.	20
2.4.1 Ammonia.....	20
2.4.2 Sulfide.....	20
2.4.3 Light metals ions.....	21
2.4.4 Heavy metals.....	22
2.4.5 Organics.	22
2.5 Improvement of AD process.	23
2.5.1 Co-digestion.	23
2.5.2 Pretreatment of substrates.	24
2.5.2.1 Mechanical pretreatment.	25
2.5.2.2 Thermal pretreatment.	25
2.5.2.3 Chemical Pretreatment.	25
2.5.2.4 Biological pretreatment.	26
2.5.2.5 Physicochemical pretreatment.....	27
2.5.3 Trace Metals Addition.	28
2.6 Composition of Biogas.	30
2.7 Upgrading of Biogas.....	31
2.7.1 Adsorption technology.....	31
2.7.2 Absorption technology.....	31
2.7.3 Cryogenic separation technology.	32
2.7.4 Membrane separation technology.	32
2.8 production of Synthesis gas.	33
2.9 Fischer-Tropsch Synthesis (FTS).	35
2.9.1 Fischer-Tropsch Synthesis reactions.	37

2.9.2 Catalysts for Fischer-Tropsch synthesis.	38
2.9.3 Mechanisms of Fischer –Tropsch Synthesis.	48
2.9.3.1 Alkyl mechanism.	49
2.9.3.2 Alkenyl mechanism.	50
2.9.3.3 Enol mechanism.	51
2.9.3.4 CO-insertion mechanism.	52
2.9.4 Product distribution or (product selectivity).....	53
2.9.4.1 Parameter Effect on the catalyst activity and product selectivity of F-T Reaction..	55
2.9.4.1.1 Temperature.	55
2.9.4.1.2 Pressure.	55
2.9.4.1.3 H ₂ /CO Feed Ratio.	56
2.9.4.1.4 Space velocity.	56
2.9.5 Fischer-Tropsch Reactors.	58
2.9.6 Catalyst Preparation Methods.	59
2.9.6.1 Impregnation.....	59
2.9.6.2 Precipitation and co-precipitation.	60
2.9.6.3 Gel formation and related processes.	60
2.9.6.4 Selective removal.	61
2.9.7 Catalyst Characterization.....	61
2.9.8 Operating Modes.	61
Chapter Three: Materials and Methods.....	62
3.1 Raw materials, experimental and analysis equipment, analytical methods and procedures for biogas production anaerobic digestion Process.	62
3.1.1 Municipal Solid Wastes (MSW).	62
3.1.2 Giant reed (GR).	63
3.1.3 Inoculum.	64
3.1.4 Trace elements.....	65
3.1.5 Chemical analysis of the liquid phase producing from anaerobic digestion processes.....	66
3.1.5.1 Measurement of biomass growth (microbial biomass).	66

3.1.5.2 Measurement of reducing sugars (colorimetric method) or glucose (enzymatic).	66
3.1.5.3 Analysis of Volatile Fatty Acids (VFAs) and Alcohols.	68
3.1.5.4 Power of Hydrogen (pH).	68
3.1.6 Chemical analysis of the gas phase (Biogas) production anaerobic digestion processes and gas phase products from FT reaction.	69
3.1.7 Analysis of Total solid (TS), Total volatile solids (TVS), Moisture content and Ash percentage.	69
3.1.7.1 Total solid percent (%TS).	70
3.1.7.2 Total volatile solids (%TVS).	70
3.1.7.3 Moisture content.	71
3.1.7.4 Ash.	71
3.1.8 Batch anaerobic digestion experiments.	72
3.1.9 Collection of Producing Biogas.	73
3.2 Catalyst preparation, experimental and analysis equipment, analytical methods and procedures for Fisher-Tropsch Process.	75
3.2.1 Fischer –Tropsch catalyst preparation method.	75
3.2.2 Catalyst characterization techniques.	77
3.2.2.1 Temperature Programmed Reduction (TPR).	77
3.2.2.2 Nitrogen adsorption measurement.	77
3.2.3 Fischer-Tropsch Experimental setup.	78
3.2.4 Calculation of Fischer-Tropsch Synthesis reactor.	81
3.2.4.1 Reactant conversion.	81
3.2.4.2 Product yield.	82
3.2.4.3 Product selectivity.	83
Chapter Four: Results and Discussion	84
4.1 Optimization of Anaerobic Digestion Process.	85
4.1.1 Optimization of a total solid percentage for biogas production by anaerobic digestion process form Municipal Solid Waste (MSW).	85
4.1.1.1 VFAs production and pH variation.	86
4.1.1.2 Biogas yield.	89
4.1.1.3 Biomass growth and glucose concentration.	92

4.1.2 Optimization of the inoculum for biogas production by solid-state anaerobic digestion of Municipal Solid Waste (MSW).....	94
4.1.2.1 VFAs production and pH variation.....	95
4.1.2.2 Biogas yield.....	98
4.1.2.3 Biomass growth and glucose concentration.	101
4.1.3 Optimization of anaerobic co-digestion of Municipal Solid Wastes (MSW) with lignocellulosic biomasses from Giant reed (GR) under mesophilic conditions.....	103
4.1.3.1 VFAs production and pH variation.....	104
4.1.3.2 Biogas yield.....	108
4.1.3.3 Biomass growth and glucose concentration.....	113
4.1.4 Effect mineral solution "M9 10x" and 400x salts addition on a performance of anaerobic digestion for Municipal Solid Waste (MSW).....	116
4.1.4.1 VFAs production and pH variation.....	116
4.1.4.2 Biogas yield.....	118
4.1.4.3 Biomass growth and glucose concentration.....	120
4.1.5 Optimization of trace metals addition for biogas production from solid-state anaerobic digestion process of Municipal Solid Waste (MSW).....	121
4.1.5.1 VFA and pH variation during (AD).....	122
4.1.5.1.1 VFA and pH variation during (AD) for individual trace element.....	122
4.1.5.1.2 VFA and pH variation during (AD) for mixed trace element.....	130
4.1.5.2 Biogas yield.....	134
4.1.5.2.1 Effect of individual trace element addition on biogas yield.....	134
4.1.5.2.2 Effect mixed trace element addition on Biogas yield.....	142
4.1.5.3 Biomass growth and glucose concentration.....	146
4.1.5.3.1 Effect of individual trace element addition on biomass growth.....	146
4.1.5.3.2 Effect of mixed trace element addition biomass growth and glucose concentration.....	150
4.2 Catalyst Characterization.....	152
4.2.1 Temperature-programmed reduction (TPR).....	152
4.2.2 Nitrogen adsorption measurement.....	154
4.3 Fischer –Tropsch Synthesis Parameter Study.....	155
4.3.1 Description of transitory condition (Time on Stream) for single test as an example.....	157

4.3.2 Description the results at steady-state conditions.	161
4.3.2.1 Effect of reaction temperature and GHSV on the conversion of synthesis gas.	162
4.3.2.1.1 Effect of reaction temperature on synthesis gas conversion (CO and H ₂).	162
4.3.2.1.2 Effect of gas hourly space velocity (GHSV) on synthesis gas conversion (CO and H ₂).	164
4.3.2.2 Effect of reaction temperature and GHSV on gases product selectivity.	166
4.3.2.2.1 Effect of reaction temperature on light hydrocarbon selectivity.	166
4.3.2.2.2 Effect of reaction temperature on Carbon dioxide selectivity.	168
4.3.2.2.3 Effect of gas hourly space velocity (GHSV) on light hydrocarbon selectivity.	169
4.3.2.2.4 Effect of gas hourly space velocity (GHSV) on Carbon dioxide (CO ₂) selectivity.	170
4.3.2.3 Effect of reaction temperature and GHSV on liquid products selectivity.....	171
4.3.2.3.1 Effect of reaction temperature on liquid hydrocarbon selectivity.	171
4.3.2.3.2 Effect of gas hourly space velocity (GHSV) on liquid product selectivity.	173
Chapter Five: Conclusions	174
5.1 Conclusions - optimization of an anaerobic digestion process.....	174
5.2 Conclusions - catalyst characterization.	176
5.3 Conclusions - FT reaction.	176
References	178
Appendices	i
Appendix A.....	i
Appendix B	iii
Appendix C	vi

List of Tables

Table	Page no.
Table (2.1): Formulae and structure of major AD intermediate products.....	15
Table (2.2): Functions of elements.	29
Table (2.3): Typical Composition of biogas in volume fraction.	30
Table (2.4): Summary Parameter studies by using Iron-based catalysts.....	39
Table (2.5): Summary Parameter studies by using cobalt-based catalysts.	42
Table (3.1): Materials used for simulating the MSW and its composition.	63
Table (3.2): Characterization of raw materials (MSW and GR).	69
Table (4.1): Batch tests conditions for the effect of a total solid percentage.	85
Table (4.2): Batch tests conditions for effect of different percentage of Inoculum.	94
Table (4.3): Batch tests conditions for anaerobic co-digestion of Municipal Solid Wastes (MSW) with lignocellulosic biomasses from Giant reed (GR).....	103
Table (4.4): Batch tests conditions for the effect of trace metals addition.....	121
Table (4.5): Final concentrations of VFAs and ethanol obtained in each experimental test for the effect of trace metals addition.	122
Table (4.6): BET surface area and pore volume for the support and catalyst...154	
Table (4.7): F-T Synthesis experiments conditions and results at steady-state conditions.....	156

List of Figures

Figures	Page no.
Figure 1.1 Short flow chart of experimental activity.....	3
Figure 2.1 Anaerobic Digestion Flow Scheme.....	6
Figure 2.2 Scheme diagram of overall Fischer-Tropsch Synthesis process. ...	35
Figure 2.3 Alkyl mechanism.....	49
Figure 2.4 Alkenyl mechanism.....	50
Figure 2.5 Enol mechanism.....	51
Figure 2.6 CO-insertion mechanism.....	52
Figure 3.1 Experimental apparatus of the batch anaerobic digester.....	72
Figure 3.2 View of experimental equipment used to measure of biogas production by anaerobic fermentation.....	73
Figure 3.3 Schematic diagram of experimental equipment used to measure of biogas production by anaerobic fermentation.....	74
Figure 3.4 Experimental apparatus and procedure for catalyst preparation by vacuum impregnation.....	76
Figure 3.5 Schematic diagram of Fischer – Tropsch reaction System on fixed bed reactor.....	80
Figure 4.1a VFA variation during digestion at T= 37°C, 150 rpm and MSW: 5gm. Products: Ethanol (◇), Acetic Acid (□), Propionic Acid (Δ) and Butyric Acid (x).....	87
Figure 4.1b VFA variation during digestion at T= 37°C, 150 rpm and MSW: 10gm. Products: Ethanol (◇), Acetic Acid (□), Propionic Acid (Δ) and Butyric Acid (x).....	87
Figure 4.1c VFA variation during digestion at T= 37°C, 150 rpm and MSW: 15gm. Products: Ethanol (◇), Acetic Acid (□), Propionic Acid (Δ) and Butyric Acid (x).....	88
Figure 4.2 pH variation during AD tests at T= 37°C, 150 rpm and Feed load: 15 gm. (◇), 10 gm. (□) and 5 gm. (Δ).....	88
Figure 4.3 Cumulative biogas yield during AD tests at T= 37°C, 150 rpm. Feed load: 5gm. (◇), 10 gm. (□), and 15gm. (Δ).....	90

Figure 4.4a	Biogas composition during digestion at T= 37°C, 150 rpm and MSW: 5 gm.	90
Figure 4.4b	Biogas composition during digestion at T= 37°C, 150 rpm and MSW: 10 gm.	91
Figure 4.4c	Biogas composition during digestion at T= 37°C, 150 rpm and MSW: 15 gm.	91
Figure 4.5	Biomass growth during digestion period at T = 37 °C, 150 rpm and feeds load: 5gm. (◇), 10gm. (□) and 15gm. (Δ).....	92
Figure 4.6	Concentration of glucose during digestion period at T= 37°C, 150 rpm and feeds load: 5gm. (◇), 10gm. (□) and 15gm. (Δ).	93
Figure 4.7a	VFA variation during digestion at T= 37°C, 150 rpm and Inoculum: 10 mL. Products: Ethanol (◇), Acetic Acid (□), Propionic Acid (Δ) and Butyric Acid (x).....	96
Figure 4.7b	VFA variation during digestion at T= 37°C, 150 rpm and inoculum: 15 mL. Products: Ethanol (◇), Acetic Acid (□), Propionic Acid (Δ) and Butyric Acid (x).....	96
Figure 4.7c	VFA variation during digestion at T = 37 °C, 150 rpm and Inoculum: 20 mL. Products: Ethanol (◇), Acetic Acid (□), Propionic Acid (Δ) and Butyric Acid (x).....	97
Figure 4.8	pH variation during AD tests at T= 37°C, 150 rpm and volumes of inoculum: 10 mL (◇), 15 mL (□) and 20 mL (Δ).	97
Figure 4.9a	Cumulative biogas yield during AD tests at T= 37°C, 150 rpm and volumes of inoculum: 10 mL (◇), 15 mL (□) and 20 mL (Δ).	99
Figure 4.9b	Cumulative biogas/gm VS yield during AD tests at T= 37°C, 150 rpm and volumes of inoculum: 10 mL (◇), 15 mL (□) and 20 mL (Δ).	99
Figure 4.10a	Biogas composition during digestion at T= 37°C, 150 rpm and inoculum: 10 mL.....	100
Figure 4.10b	Biogas composition during digestion at T= 37°C, 150 rpm and inoculum: 15 mL.....	100
Figure 4.10c	Biogas composition during digestion at T= 37°C, 150 rpm and inoculum: 20 mL.....	101
Figure 4.11	Biomass growth during digestion period at T= 37°C, 150 rpm and volumes of inoculum: 10 mL (◇), 15 mL (□) and 20 mL (Δ).	102

Figure 4.12	Concentration of glucose during digestion period at T = 37°C, 150 rpm and volumes of inoculum: 10 mL (◇), 15 mL (□) and 20 mL (Δ).	102
Figure 4.13a	VFA variation during digestion period at T = 37 °C, 150 rpm, 15% TS (25% GR+75% MSW) and 10 mL inoculum, where (◇) Ethanol, (□) Acetic Acid, (Δ) Propionic Acid and (×) Butyric Acid.....	105
Figure 4.13b	VFA variation during digestion period at T= 37 °C, 150 rpm, 15% TS (50%GR+50% MSW) and 10 mL inoculum, where (◇) Ethanol, (□) Acetic Acid., (Δ) Propionic Acid and (×) Butyric Acid.....	105
Figure 4.13c	VFA variation during digestion period at T= 37 °C, 150 rpm, 15% TS (75% GR+25% MSW) and 10mL inoculum, where (◇) Ethanol, (□) Acetic Acid, (Δ) Propionic Acid and (×) Butyric Acid.....	106
Figure 4.13d	VFA variation during digestion period at T = 37 °C, 150 rpm, 15% TS (100% GR) and 10 mL inoculum, where (◇) Acetic Acid, (□) Propionic Acid and (Δ) Butyric Acid.	106
Figure 4.13e	VFA variation during digestion period at T= 37 °C, 150 rpm, 15% TS (15gm MSW) and 10 mL inoculum, where (◇) Ethanol, (□) Acetic Acid, (Δ) Propionic Acid and (×) Butyric Acid.	107
Figure 4.14	pH variation n during digestion period at T= 37°C, 150 rpm, 10mL Inoc.and15%TS,where(o)100%MSW,(◇)25%GR+75%MSW,(□)50%GR+50%MSW, (Δ) 75%GR+25%MSW and (x) 100%GR. ...	107
Figure 4.15	Specific cumulative biogas yield during digestion period at T=37°C, 150rpm,10mLInoc.and15%TS,where(o)100%MSW(◇)25%GR+75%MSW,(□)50%GR+50%MSW,(Δ)75%GR+25%MSWand(x)100%GR.....	108
Figure 4.16a	Composition of biogas for the sample 25%GR + 75% MSW at T = 37°C, 150 rpm, 10mL Inoc. and 15% TS.	110
Figure 4.16b	Composition of biogas for the sample 50%GR + 50% MSW at T = 37 °C, 150 rpm, 10mL Inoc. and 15% TS.	110
Figure 4.16c	Composition of biogas for the sample 75%GR + 25% MSW at T = 37 °C, 150 rpm, 10mL Inoc. and 15% TS..	111
Figure 4.16d	Composition of biogas for the sample 100% GR at T = 37 °C, 150 rpm, 10mL Inoc. and 15% TS.	111
Figure 4.16e	Composition of biogas for the sample 100% MSW at T = 37 °C, 150 rpm, 10mL Inoc. and 15% TS.....	112

Figure 4.17 Cumulative biogas , H₂ and CO₂ yield during digestion period at T =37°C,150 rpm,10mL of inoculum from synthetic medium prepared by adapted Clostridium bacteria and 15%TS,where Cumulative biogas (◇),Cumulative H₂ (□) and Cumulative CO₂ (Δ). 112

Figure 4.18 Biomass growth during digestion period at T= 37°C, 150 rpm, 10mL Inoc.and15% TS(100%MSW,25%GR+75%MSW,50%GR+50%MSW,75%GR+25%MSWand100%GRrespectively),where(o)100%MSW,(◇)25%GR+75%MSW,(□)50%GR+50%MSW,(Δ)75%GR+25%MSW and (x) 100%GR. 114

Figure 4.19 Concentration of glucose during digestion period at T= 37°C, 150 rpm,10mLInoc.and15% TS(100%MSW,25%GR+75%MSW,50%GR+50%MSW,75%GR+25%MSWand100%GRrespectively),where(o)100%MSW,(◇)25%GR+75%MSW,(□)50%GR+50%MSW,(Δ)75%GR+25%MSW and (x) 100%GR..... 115

Figure 4.20 VFA variation during digestion period at T= 37°C, 150 rpm, 15%TS and 10 mL Inoculum for effect of mineral and salts solution addition ,where (◇) Ethanol,(□)Acetic Acid, (Δ) Propionic Acid and (x) Butyric Acid..... 117

Figure 4.21 pH variation during digestion period at T= 37°C, 150 rpm, 15%TS and 10 mL Inoculum for effect of mineral and salts solution addition. 117

Figure 4.22 Cumulative biogas yield during digestion period with mineral and salts solution addition at T= 37 °C, 150rpm, 10v/v Inoc. and 15%TS. 118

Figure 4.23 Composition of biogas for the test with mineral and salts solution addition at T= 37 °C, 150rpm, 10v/v Inoc. and 15%TS..... 119

Figure 4.24 Biomass growth and glucose concentration during digestion period at T= 37°C, 150 rpm, 15%TS and mineral and salts solution addition. 120

Figure 4.25a VFA variation during digestion period at T= 37 °C, 150 rpm, 15%TS MSW ,10 mL Inoculum and Zero trace elements Conc., where (◇) Ethanol, (□) Acetic Acid (Δ) Propionic Acid and (×) Butyric Acid. 123

Figure 4.25b VFA variation during digestion period at T= 37 °C, 150 rpm, 15%TS MSW ,10 mL Inoculum and 5mg/L Ni Conc., where (◇) Ethanol, (□) Acetic Acid,(Δ) Propionic Acid and (×) Butyric Acid. 124

- Figure 4.25c VFA variation during digestion period at T = 37 °C, 150 rpm, 15% TS MSW, 10 mL Inoculum and 50mg/L Ni Conc., where (◇) Ethanol, (□) Acetic Acid., (Δ) Propionic Acid and (×) Butyric Acid..... 124
- Figure 4.25d VFA variation during digestion period at T= 37 °C, 150 rpm, 15% TS MSW, 10 mL Inoculum and 100 mg/L Ni Conc., where (◇) Ethanol, (□) Acetic Acid, (Δ) Propionic Acid and (×) Butyric Acid..... 125
- Figure 4.25e VFA variation during digestion period at T= 37 °C, 150 rpm, 15% TS MSW, 10 mL Inoculum and 5 mg/L Zn Conc., where (◇) Ethanol, (□) Acetic Acid.,(Δ) Propionic Acid and (×) Butyric Acid..... 125
- Figure 4.25f VFA variation during digestion period at T= 37 °C, 150 rpm, 15% TS MSW ,10 mL Inoculum and 50mg/L Zn Conc., where (◇) Ethanol, (□) Acetic Acid., (Δ) Propionic Acid and (×) Butyric Acid 126
- Figure 4.25g VFA variation during digestion period at T= 37 °C, 150 rpm, 15% TS MSW, 10 mL Inoculum and 100 mg/L Ni Conc., where (◇) Ethanol, (□) Acetic Acid,(Δ) Propionic Acid and (×) Butyric Acid 126
- Figure 4.25h VFA variation during digestion period at T= 37 °C, 150 rpm, 15% TS MSW ,10 mL Inoculum and 5 mg/L Co Conc., where (◇) Ethanol, (□) Acetic Acid.,(Δ) Propionic Acid and (×) Butyric Acid 127
- Figure 4.25i VFA variation during digestion period at T= 37 °C, 150 rpm, 15% TS MSW, 10 mL Inoculum and 50mg/L Co Conc., where (◇) Ethanol, (□) Acetic Acid,(Δ) Propionic Acid and (×) Butyric Acid..... 127
- Figure 4.25j VFA variation during digestion period at T= 37 °C, 150 rpm, 15% TS MSW, 10 mL Inoculum and 100 mg/L Co Conc., where (◇) Ethanol, (□) Acetic Acid, (Δ) Propionic Acid and (×) Butyric Acid..... 128
- Figure 4.26a pH variation during digestion period at T= 37 °C, 150 rpm, 10mL Inoculum, 15% TS MSW and different Ni Concentration, where (◇) Zero, (□) 5mg/L, (Δ) 50mg/L and (x) 100mg/L..... 128
- Figure 4.26b pH variation during digestion period at T = 37 °C, 150 rpm, 10mL Inoculum,15% TS MSW and different Zn Concentration, where (◇) Zero, (□) 5mg/L , (Δ) 50mg/L and (x) 100mg/L..... 129
- Figure 4.26c pH variation during digestion period at T= 37 °C, 150 rpm, 10mL Inoculum, 15% TS MSW and different Co Concentration, where (◇) Zero, (□) 5mg/L, (Δ) 50mg/L and (x) 100mg/L..... 129

Figure 4.27a VFA and ethanol variation during digestion period at T= 37 °C, 150 rpm, 15% TS MSW ,10 mL Inoculum and mix of three trace elements (Ni, Zn and Co) with concentration 5mg/L For each one , where (◇) Ethanol, (□) Acetic Acid, (Δ) Propionic Acid and (×) Butyric Acid .
..... 131

Figure 4.27b VFA and ethanol variation during digestion period at T= 37 °C, 150 rpm, 15% TS MSW, 10 mL Inoculum and mix of two trace elements (Ni and Co) with concentration 5mg/L For each one, where (◇) Ethanol, (□) Acetic Acid., (Δ) Propionic Acid and (×) Butyric Acid.
..... 131

Figure 4.27c VFA and ethanol variation during digestion period at T= 37 °C, 150 rpm, 15% TS MSW,10 mL Inoculum and mix of two trace elements (Ni and Zn) with concentration 5mg/L For each one, where (◇) Ethanol, (□) Acetic Acid., (Δ) Propionic Acid and (×) Butyric Acid.
..... 132

Figure 4.27d VFA and ethanol variation during digestion period at T= 37 °C, 150 rpm, 15% TS MSW, 10 mL Inoculum and mix of trace elements (Zn and Co) with concentration 5mg/L For each one, where (◇) Ethanol, (□) Acetic Acid, (Δ) Propionic Acid and (×) Butyric Acid..... 132

Figure 4.28 pH variation during digestion period at T= 37 °C, 150 rpm, 10mL Inoculum , 15% TS MSW and different mix of trace elements ,where (◇)Ni/Co/Zn, (□) Ni/Co , (Δ) Ni/Zn and (x) Zn/Co..... 133

Figure 4.29a Cumulative biogas yield during digestion period at T= 37°C, 150 rpm, 10mL Inoculum, 15% TS MSW and different Ni concentration, where (◇) Zero, (□) 5mg/L, (Δ) 50mg/L and (x) 100mg/L. 135

Figure 4.29b Cumulative biogas yield during digestion period at T= 37°C, 150 rpm, 10mL Inoculum, 15% TS MSW and different Zn concentration, where (◇) Zero, (□) 5mg/L, (Δ) 50mg/L and (x) 100mg/L. 135

Figure 4.29c Cumulative biogas yield during digestion period at T= 37°C, 150 rpm, 10mL Inoculum,15% TS MSW and different Co concentration, where (◇) Zero, (□) 5mg/L , (Δ) 50mg/L and (x) 100mg/L. 136

Figure 4.30a Composition of biogas for the sample without trace element addition at T= 37°C,15% TS, 150 rpm and 10mL Inoculum. ... 136

Figure 4.30b Composition of biogas for the sample with Ni concentration 5mg/L at T= 37°C,15 % TS, 150 rpm and 10mL Inoculum..... 137

Figure 4.30c	Composition of biogas for the sample with Ni concentration 50mg/L at T= 37°C, 15 %TS, 150 rpm and 10mL Inoculum. .	137
Figure 4.30d	Composition of biogas for the sample with Ni concentration 100 mg/L at T= 37°C,15%TS, 150 rpm and 10mL Inoculum.....	138
Figure 4.30e	Composition of biogas for the sample with Zn concentration 5mg/L at T= 37°C,15%TS, 150 rpm and 10mL Inoculum.....	138
Figure 4.30f	Composition of biogas for the sample with Zn concentration 50 mg/L at T= 37°C, 15%TS, 150 rpm and 10mL Inoculum.....	139
Figure 4.30g	Composition of biogas for the sample with Zn concentration 100 mg/L at T= 37°C,15%TS, 150 rpm and 10mL Inoculum.....	139
Figure 4.30h	Composition of biogas for the sample with Co concentration 5mg/L at T= 37°C,15%TS, 150 rpm and 10mL Inoculum.....	140
Figure 4.30i	Composition of biogas for the sample with Co concentration 50 mg/L at T= 37°C,15%TS, 150 rpm and 10mL Inoculum.....	140
Figure 4.30j	Composition of biogas for the sample with Co concentration 100 mg/L at T= 37°C,15%TS, 150 rpm and 10mL Inoculum.....	141
Figure 4.31	Cumulative biogas yield during digestion period at T= 37°C, 150 rpm, 10mL Inoculum,15%TS MSW and different mix of trace elements ,where (◇)Ni/Co/Zn, (□) Ni/Co , (Δ) Ni/Zn and (x) Zn/Co.....	143
Figure 4.32a	Composition of biogas for the sample with mix from three trace elements Ni/Co/Zn at T=37°C, 15%TS, 150 rpm and 10mL Inoculum.	144
Figure 4.32b	Composition of biogas for the sample with mix from two trace elements Ni/Co at T= 37°C,15% TS, 150 rpm and 10mL Inoculum.	144
Figure 4.32c	Composition of biogas for the sample with mix from two trace elements Ni/Zn at T=37°C,15%TS, 150 rpm and 10mL Inoculum.	145
Figure 4.32d	Composition of biogas for the sample with mix from two trace elements Zn/Co at T=37°C,15%TS, 150 rpm and 10mL Inoculum.	145
Figure 4.33a	Biomass growth during digestion period at T= 37°C, 150 rpm, 10mLInoculum, 15%TS MSW and different Ni concentration where (◇) Zero, (□) 5mg/L, (Δ) 50mg/L and (x) 100mg/L.....	147

Figure 4.33b Biomass growth during digestion period at T= 37 °C, 150 rpm, 10mL Inoculum, 15%TS MSW and different Zn concentration ,where (◇) Zero, (□) 5mg/L , (Δ) 50mg/L and (x) 100mg/L. 147

Figure 4.33c Biomass growth during digestion period at T = 37°C, 150 rpm, 10mL Inoculum, 15%TS MSW and different Co concentration, where (◇) Zero, (□) 5mg/L, (Δ) 50mg/L and (x) 100mg/L..... 148

Figure 4.34a Concentration of glucose during digestion period at T= 37 °C, 150 rpm, 10mL Inoculum, 15%TS MSW and different Ni concentration, where (◇) Zero, (□) 5mg/L , (Δ) 50mg/L and (x) 100mg/L..... 148

Figure 4.34b Concentration of glucose during digestion period at T = 37°C, 150 rpm, 10mL Inoculum, 15%TS MSW and different Zn concentration, where (◇) Zero, (□) 5mg/L, (Δ) 50mg/L and (x) 100mg/L..... 149

Figure 4.34c Concentration of glucose during digestion period at T= 37°C, 150 rpm, 10mL Inoculum, 15%TS MSW and different Co concentration, where (◇) Zero, (□) 5mg/L, (Δ) 50mg/L and (x) 100mg/L..... 149

Figure 4.35 Biomass growth during digestion period at T= 37°C, 150 rpm, 10mL Inoculum,15%TS MSW and different mix of trace elements addition ,where (◇)Ni/Co/Zn, (□) Ni/Co , (Δ) Ni/Zn and (x) Zn/Co..... 151

Figure 4.36 Concentration of glucose during digestion period at T= 37°C, 150 rpm, 10mL Inoculum, 15%TS MSW and different mix of trace elements addition, where (◇) Ni/Co/Zn, (□) Ni/Co , (Δ) Ni/Zn and (x) Zn/Co. 151

Figure 4.37 TPR profiles of the catalysts..... 153

Figure 4.38 Conversion of CO and H₂ on time stream at P= 1 atm., H₂/CO = 2, T=220 °C , GHSV = 370 h⁻¹ and 5gm of catalyst, where (□) CO and (◇)H₂..... 158

Figure 4.39 Mole percentage of products on time stream at P= 1 atm., H₂/CO = 2, T=220 °C , GHSV = 370 h⁻¹ and 5gm of catalyst, where (x) Liquid products , (Δ)C₂-C₄, (◇) CH₄ and (□) CO₂..... 160

Figure 4.40 Yield percentage of products on time stream at P = 1 atm., H₂/CO = 2, T=220 °C , GHSV = 370 h⁻¹ and 5gm of catalyst, where (Δ) Liquid products, (◇)CO₂ and (□) CH₄+(C₂-C₄)..... 160

Figure 4.41 Effect of reaction temperature on CO conversion at P= 1 atm., H₂/CO = 2, where GHSV= (◇)370, (□) 520 , (Δ) 670 and (x) 820 h⁻¹, and 5gm of catalyst..... 163

Figure 4.42 Effect of reaction temperature on H ₂ conversion at P=1 atm., H ₂ /CO = 2, where GHSV= (◇)370, (□) 520 , (Δ) 670 and (x) 820 h ⁻¹ , and 5gm of catalyst.....	163
Figure 4.43 Effect of GHSV on CO conversion at P=1 atm., H ₂ /CO = 2, where T = (◇)220, (□)235 and (Δ) 250 °C , and 5gm of catalyst.....	164
Figure 4.44 Effect of GHSV on H ₂ conversion at P = 1 atm., H ₂ /CO = 2, where T = (◇)220, (□)235 and (Δ) 250 °C , and 5gm of catalyst.....	165
Figure 4.45 Effect of reaction temperature on light hydrocarbon (C ₁ -C ₄) selectivity at P = 1 atm., H ₂ /CO = 2, where GHSV = (◇)370, (□) 520 , (Δ) 670 and (x) 820 h ⁻¹ , and 5gm of catalyst.....	167
Figure 4.46 Effect of reaction temperature on CO ₂ selectivity at P = 1 atm., H ₂ /CO = 2, where GHSV = (◇)370, (□) 520 , (Δ) 670 and (x) 820 h ⁻¹ , and 5gm of catalyst	168
Figure 4.47 Effect of GHSV on light hydrocarbons (C ₁ -C ₄) selectivity at P = 1 atm., H ₂ /CO= 2, where T = (◇)220, (□)235 and (Δ) 250 °C, and 5gm of catalyst.....	169
Figure 4.48 Effect of GHSV on CO ₂ selectivity at P = 1 atm., H ₂ /CO = 2, where T = (◇)220, (□)235 and (Δ) 250 °C, and 5gm of catalyst.....	170
Figure 4.49 Effect of reaction temperature on liquid hydrocarbon (C ₅₊) selectivity at P = 1 atm., H ₂ /CO =2 , where GHSV= (◇)370, (□) 520 , (Δ) 670 and (x) 820 hr ⁻¹ , and 5gm of catalyst.	172
Figure 4.50 Effect of GHSV on Liquid hydrocarbon (C ₅₊) selectivity at P = 1 atm., H ₂ /CO = 2, where T = (◇)220, (□)235 and (Δ) 250 °C, and 5gm of catalyst.....	173
Figure A.1 Calibration line Assay by Nelson-Somogyi for measuring reducing sugars.	ii
Figure A.2 Calibration curve for biomass growth.	ii
Figure B.1 Calibration curve for ethanol.	iii
Figure B.2 Calibration curve for butyric acid.	iii
Figure B.3 Calibration curve for acetic acid.	iii
Figure B.4 Calibration curve for propionic acid.	iv
Figure B.5 Calibration curve for methane.....	iv
Figure B.6 Calibration curve for hydrogen.	iv

Figure B.7 Calibration curve for carbone dioxide.v
Figure B.8 Calibration curve for hydrogen feed to FT reaction.v
Figure B.9 Calibration curve for carbone monoxide feed to FT reaction.....v

List of Abbreviations and Nomenclature

AD	Anaerobic digestion
ATR	Autothermal reforming
BSIR	Bench scale Inconel reactor
BTL	Biomass-To-Liquid
CNG	Compressed natural gas
°C	Degrees Celsius (Centigrade)
C/N	Carbon/Nitrogen
COD	Chemical oxygen demand.
CODH	Carbon monoxide dehydrogenase
CTL	Coal-To-Liquid
CSTR	Continuous stirred-tank reactor
cat.	Catalyst
CE	Concentration of desired elements (mg/L).
Conc.	Concentration (gm/ml,g/L,mg/L)
cm ³	Cubic centimeters
d.	Day
dm ³	Cubic decimeter
DR	Dry reforming
et al.	et al.ii (and others)
FTS	Fischer-Tropsch Synthesis
F ₄₃₀	F factor 430
FDH	Formate dehydrogenase
FID	Flame ionization detector
g or gm	Gram

List of Abbreviations and Nomenclature

GHSV	Gas hourly space velocity (h^{-1})
GR	Giant reed
GC	Gas chromatography
GTL	Gas-To-Liquid
HRT	Hydraulic retention time (day)
ΔH°	Standard enthalpy changes (kJ/mol)
HTFT	High Temperature Fischer-Tropsch
kJ	Kilojoules
kPa	Kilo Pascale
K	Kelvin
L	Liter
L-AD	Liquid-State anaerobic digestion
LCFAs	Long chain fatty acids
LTFT	Low Temperature Fischer-Tropsch
mg	Milligram
mol	Mole
ml or mL	Milliliter
m'	Mass flow rate of feed (Kg /h)
m_{cat}	Mass of catalyst (g)
mm	Millimeter
m	Meter
M	Molarity (mol/L)
MPB	Methane producing bacteria
MPa	Mega Pascal
MSW	Municipal Solid Wastes
Mi	Molecular weight of the element (g/mole)

List of Abbreviations and Nomenclature

Mc	Molecular weight of the compound (g/mole)
Nm	Nanometer
nCO _{in}	Mole flow rate of Carbone monoxide entering the reactor (mole/h)
nCO _{out}	Mole flow rate of Carbone monoxide leaving the reactor (mole/h)
nCH _{4out}	Mole of producing methane (mole/h)
nCO ₂	Mole of producing Carbone dioxide (mole/h)
NL	Normal liter
OD	Optical density
pH	Power of Hydrogen
POX	Partial oxidation
PFR	Plug flow reactor
PTR	Packed tubular reactor
rpm	Revolutions per minute (1/min)
RT	Retention time (day)
SMR	Steam methane reforming
SS-AD	Solid-State anaerobic digestion
SRB	Sulfate reducing bacteria
SR	Steam reforming
SBO	Semi-batch operation
SBCR	Slurry bubble column reactor
SLR	Slurry reactor
SSR	Stainless-steel reactor
STP	Standard temperature and pressure
SL	Standard liter
SV	Space velocity (h ⁻¹)
SEM	Scanning electron microscopy

List of Abbreviations and Nomenclature

S %	Selectivity percent.
T	Temperature (K and °C)
TBR	Tubular reactor
TPR	Temperature programmed reduction
TPD	Temperature programmed desorption
TGA	Thermo-gravimetric analysis
TCD	Thermal conductivity detector
TS %	Total solid percent
TVS%	Total volatile solids percent
V_r	Reactor Volume (m^3 , L)
$V \cdot$	Volumetric flow rate of feed (m^3/h , L/h, m^3/d)
$V_{Cat.}$	Volume of reactor or catalyst (m^3 , cm^3)
V	Working volume (L)
Vs.	Versus
wt. %	Weight percentage
WGS	Water gas shift
W/F	Weight of catalyst /molar flow rate (g.h/mol)
W_n	Weight fraction of the products
WC	Required weight of compound (mg)
x, y, n, m	Stoichiometric coefficient (mol)
X_i %	Conversion percentage
Y%	Yield percentage
α	Chain growth probability or growth factor
μg	Microgram
μl	Microliters

Chapter One: Introduction

1.1 General Introduction.

The increase of emissions of greenhouse gases derived from fossil fuel combustion processes is leading to global warming. Consequently, this problem raises public health issues, and is a topic of concern for scientists and governments.

Currently, a large part of the world's energy is satisfied by traditional fossil fuels (petroleum and natural gas), and it has been forecasted that the global energy requirement will continue to grow because of the world's increasing population (Kaygusuz K.,2012) and the expansion of emerging countries. It is well known that the supply of traditional fossil fuels will be exhausted in the near future and this stimulates the search for alternative energy sources. Moreover, the use of traditional fossil fuels also leads to the emission of greenhouse gases into the environment and induces serious environmental issues (Alaswad A. et al., 2015). In particular, the transportation sector consumes a high amount of energy (e.g., gasoline and diesel) and is the main responsible for the CO₂ and other pollutants emissions. In order to satisfy the increased energy needs, ensure energy security and assist with environmental protection, many attempts have been done to produce renewable biofuels (Hammond G.P. et al., 2008).

Biofuels include many types of fuels prevalently delivered from waste and biomass by biological or thermochemical processing approach, both liquid (ethanol, methanol, biodiesel and Fischer-Tropsch diesel) or gaseous

(biomethane and biohydrogen), that can be used in vehicles and in different industrial processes (Demirbas A., 2008, Nigam and Singh, 2011).

Organic wastes from agricultural and industrial sectors, animal manure, sewage sludge, as well as the biodegradable fraction of municipal solid waste (MSW), represent an important source of biomass for the production of biofuels (Naik S.N. et al., 2010, Campuzano and González-Martínez, 2016).

In this contest, Fischer-Tropsch synthesis is gaining great interest for production of biofuels starting from biogas obtained by gasification or digestion of renewable sources. The present study focuses the attention on the overall process that converts wastes and cheap biomass to liquid for the production of green fuels. A way to produce liquid fuels such as diesel and gasoline could consist of an anaerobic digestion of biomass for the production of methane, a reforming step to obtain H₂ and CO, and a Fischer-Tropsch (FT) synthesis (Galadima and Muraza, 2015, Park M.H. et al., 2015).

Fischer-Tropsch synthesis is a catalytic process that includes a great number of simultaneous reactions and a wide spectrum of products consisting of a complex multi component mixture of linear and branched hydrocarbons and oxygenated products (Choudhury and Moholkar, 2013). The products composition depends on the reaction conditions, such as reactor temperature, pressure, feed gas composition (H₂ to CO ratio), space velocity and the types of catalysts and promoters used (Dry M. E., 1996).

1.2 Objective of Thesis.

The Fischer–Tropsch (FT) process converts syngas (i.e. a mixture of CO and H₂, usually derived from coal, natural gas and biomass), into a range of hydrocarbons. FT offers an alternative to crude oil for the production of liquid fuels (gasoline and diesel) and chemicals (in particular, 1-alkenes).

The aim of this Ph.D. thesis is the production of liquid fuel by integration of anaerobic digestion for Municipal solid waste and Fischer-Tropsch process, as summarized in **Figure 1.1**.

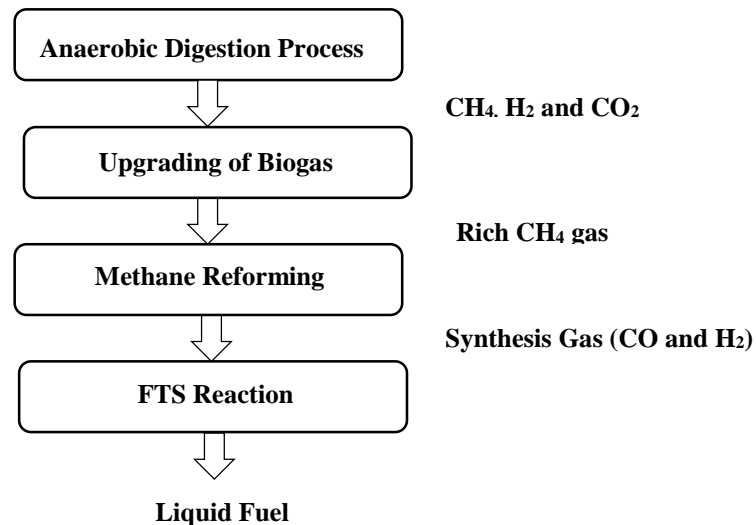


Figure 1.1 Short flow chart of experimental activity.

Specific objectives of this thesis are as follows:

1-Optimization of anaerobic digestion processes for biogas production (methane) as follows:

- a) Optimization of a total solid percentage.
- b) Optimization of the inoculum percentage.
- c) Optimization of anaerobic co-digestion of Municipal Solid Wastes (MSW) with lignocellulosic biomasses from Giant reed (GR).

- d) Study the effect mineral solution "M9 10x" and 400x Salts addition on a performance of anaerobic digestion process.
- e) Optimization of trace metals addition on anaerobic digestion process.

2-Optimization of Fischer-Tropsch synthesis reaction for liquid fuel production as follows:

- a) Preparation and characterization of cobalt-based catalyst.
- b) Analysis of the main parameters of the FT reaction (such as temperature and space velocity) for liquid fuel production.

1.3 Thesis Outline.

Chapter one is a general introduction and describes the objectives of this thesis. **Chapter two** is focused on a literature review of main techniques or methods used for the production of gaseous and liquid fuels (Clean fuel) in this Ph.D. thesis. **Chapter three** describes the experimental equipments as well as the analytical methods and procedures used. **Chapter four** describes the results obtained from the laboratory scale experiments of anaerobic digestion, catalyst characterization and FT reaction. Lastly, **Chapter five** highlights the most important conclusions and findings obtained from the experiment activity.

Chapter Two: Literature Review

2 Introduction.

Fischer-Tropsch reaction is a conversion of synthesis gas (CO and H₂) that was produced from the methane reforming into a broad range of hydrocarbons, in this chapter the literature review reports the theoretical background of main processes included in this approach related to this thesis such as anaerobic digestion processes for creating biogas with main product is a methane, Upgrading of Biogas, production of Synthesis gas and Fischer-Tropsch technology.

2.1 Anaerobic Digestion.

Anaerobic digestion (AD) is a synergistic process carried out by a consortium of microbes in an oxygen free environment to generate methane (CH₄), hydrogen(H₂) and carbon dioxide (CO₂), called biogas(Macias-Corral M. et al.,2008, Mudhoo and Kumar,2013). The AD process involves the steps of hydrolysis, acidogenesis, acetogenesis and methanogenesis as explain by the details below (Borja R. et al., 2005). A scheme of the AD process is shown in **Figure 2.1**. Many types of biomass can be used as substrates for the production of biogas from anaerobic digestion such as organic fraction municipal solid waste, sewage sludge, cow manure and energy crops (Mata-Alvarez et al., 2011). If the substrate for anaerobic digestion is a mix of two or more types of biomass, the process is called “Co-digestion” is a most common applications for biogas production(Cuetos et al.,2011), biogas is an alternative source of energy that can be used in different applications (Levis J.W. et al., 2010). It can be compressed to be used as a source of car fuel

similar to that of compressed natural gas (CNG). Alternatively, it can be burned to generate heat or electricity, or liquefied to produce methanol. It can also be used as feedstock for the catalytic steam methane reforming (SMR) to produce Syngas (H_2 and CO). Refined biogas can be fed into gas distribution grids. (Roubaud and Favrat, 2005, Ghosh S. et al., 2000).

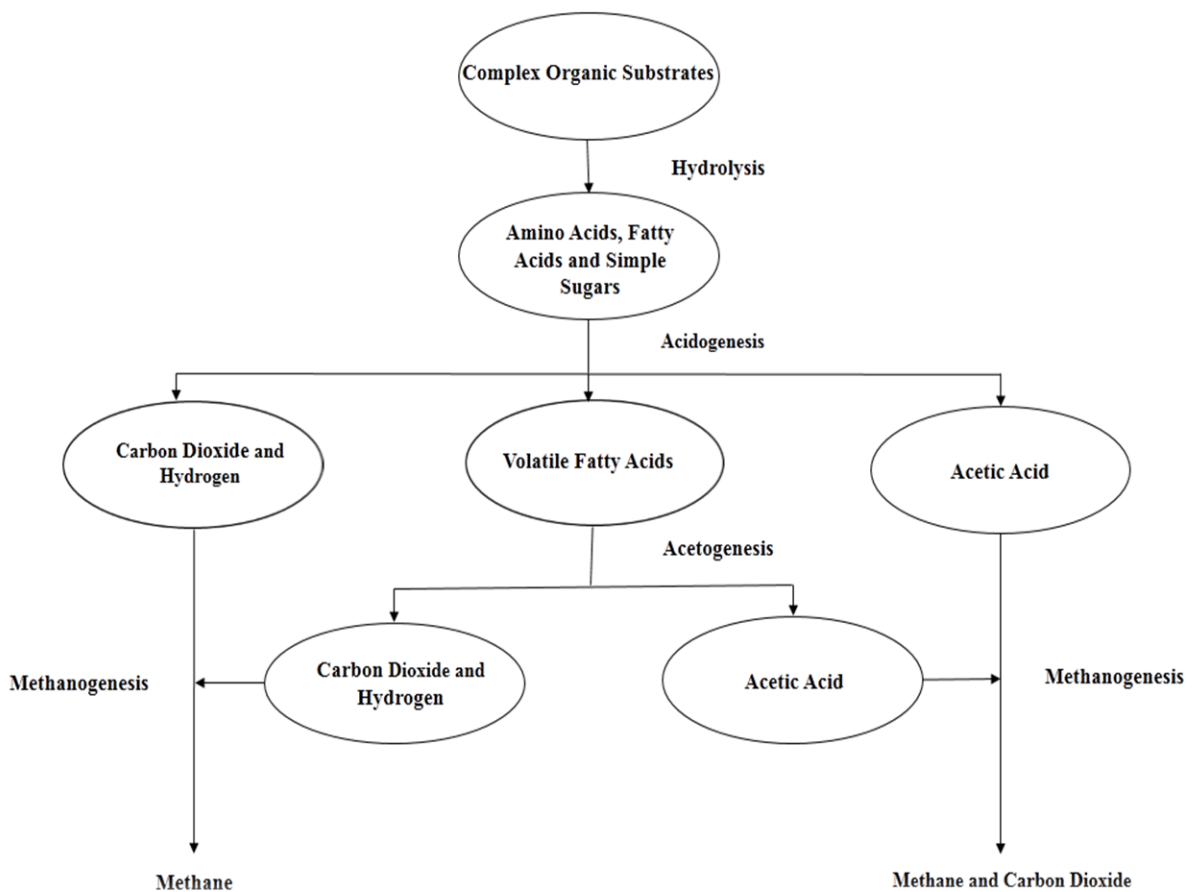


Figure 2.1 Anaerobic Digestion Flow Scheme.

2.1.1 Hydrolysis.

At the beginning of the process, extracellular enzymes catalyze the hydrolysis of the complex organic substrates (carbohydrates, lipids and proteins), that are degraded and split into simpler products such as amino acids, fatty acids and simple sugars as shown in equations (2.1 and 2.2) (Michael H.,2003, Demirel and Scherer,2008). These products are soluble and consequently more accessible to the bacteria involved in the following steps. Hydrolysis have been often the rate-limiting step of the whole process, in particular when lignocellulosic materials are used as feedstock. In this case, cellulolytic bacteria, such as *Cellulomonas*, *Clostridium*, *Bacillus*, *Thermomonospora*, *Ruminococcus*, *Bacteriodes*, *Erwinia*, *Acetovibrio*, *Microbispora*, and *Streptomyces* can produce cellulose enzymes that are able to hydrolyze cellulolytic biomass (Lo Y.C. et al., 2009).



The hydrolysis rate is a function of many parameters, such as pH, temperature, culture sources, hydraulic retention time (HRT) and particle size (Borja R. et al., 2005, Vavilin V.A. et al., 2008).

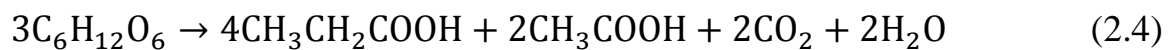
2.1.2 Acidogenesis.

Acidogenesis is the subsequent step. During this phase, a further division of the products is carried out, to obtain volatile fatty acids (VFAs) (with a consequent pH decrease) and other minor products such as carbon dioxide, hydrogen and acetic acid as shown in equations (2.3,2.4,2.5,2.6 and 2.7) (Batstone D. J. et al.,2002). Fermentative bacteria involved in this step may follow different metabolic pathways. The major pathways lead to are acetate (*Acetobacterium*, *Clostridium*, and *Sporomusa*), alcohols (*Saccharomyces*), butyrate (*Butyribacterium*, *Clostridium*), lactate (*Lactobacillus*, *Streptococcus*), propionate (*Clostridium*) (Michael H., 2003).

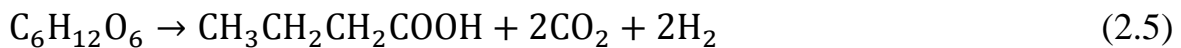
Acetate:



Propionate + Acetate:



Butyrate:



Lactate:



Ethanol:



2.1.3 Acetogenesis.

Acetogenesis is the transformation of Volatile Fatty Acids (VFAs) by acetogenic bacteria into acetic acid by the Wood-Ljungdahl pathway (Ragsdale S.W., 2008). Bacteria as *Acetobacterium* and *Sporomusa* are exclusively acetogenic, even though some among these can be both acetogenic and nonacetogenic (*Clostridium*, *Ruminococcus*, and *Eubacterium*). In this phase CO₂, H₂S and H₂ are also produced. High hydrogen concentrations inhibit acetogenic bacteria. Typical reaction equations in acetogenesis are shown in equations (2.8, 2.9 and 2.10) (Deublein and Steinhauser, 2008).

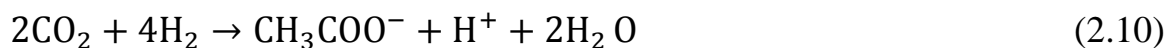
Propionic acid:



Butyric acid:



CO₂ and H₂ :



2.1.4 Methanogenesis.

Methanogenesis is the final step of AD, leading to the transformation of acetate, carbon dioxide, and hydrogen into methane. A fast removal of the produced hydrogen is essential to reduce the inhibition of acetogenic bacteria. Consequently, it results that methanogenic bacteria act in symbiosis with acetogenic bacteria (Shankaranand V.S. et al., 1992).

Methane can be produced by two different pathways:

- ❖ Hydrogenotrophic bacteria produce methane in anaerobic condition by hydrogen oxidation and using the CO₂ as final electron acceptor (Kral T.A. et al.,1998):



- ❖ Degradation of acetic acid into methane and carbon dioxide by the acetoclastic pathway (Ho N. C. et al.,2010):



2.2 Parameters Effect on Anaerobic Digestion Process.

Several Parameters have been seen that effect on the carrying out of AD process such as pH value, Temperature, Substrate Characteristics, Mixing, Carbon/Nitrogen ratio, Volatile Fatty Acids and Retention time. AS describe below.

2.2.1 pH value.

Anaerobic digestion reactions are highly pH dependent. A suitable range of pH values for anaerobic digestion has been stated by many studies, but the optimal value for methanogenesis has been found to be about 7.0 (Yang and Okos,1987). (Ward A. et al., 2008) reported that a pH range of 6.8–7.2 was perfect for anaerobic digestion. (Kim J. et al., 2003) found the appropriate pH range for thermophilic acidogens was 6-7 From the batch experiments (Lee D. et al., 2009) showed that methanogenesis in an anaerobic digester occurs efficiently at pH 6.5– 8.2, while (Park et al., 2008) reported the hydrolysis and acidogenesis happens at pH 5.5 and 6.5, respectively. (Liu C. et al., 2008) found that the best range of pH to achieve maximal biogas production in anaerobic digestion is 6.5–7.5.

Therefore, the pH value of an anaerobic digestion system is normally kept between methanogenic limits to ensure the continued operation of the digestion process to avoid the triumph of the acid-forming bacteria, which may cause Volatile Fatty Acids accumulation (Agdag and Sponza, 2007).

2.2.2 Temperature.

One of the most main parameters affecting microbial activity in an anaerobic digester and methane production is a temperature. There are three ranges of temperature operation in digestion process: psychrophilic (15-20°C), Mesophilic (30-40°C) and thermophilic (50-60°C) (Zupancic and Jemec, 2010). (Trzcinski and Stuckey, 2010) founds the lower temperatures through the process will decrease microbial growth, substrate consumption rates, and biogas yield. (Kashyap D.R. et al., 2003) showed the lower temperatures may also effect in an exhaustion of cell energy, a leakage of intracellular substances or complete hydrolysis. While, (Fezzani and Cheikh, 2010) found high temperatures will cause lower biogas production due to the increasing of volatile gas production such as ammonia which destroys methanogenic activities.

Usually, anaerobic digestion is carried out at Mesophilic temperatures (El-Mashad et al., 2003). The AD process at Mesophilic condition is more stable and needs a reduced energy cost (Zaher U. et al., 2007).

2.2.3 Substrate Characteristics.

The AD process is powerfully affected by the kind, accessibility and complexity of the substrate (Ghaniyari-Benis et al., 2009). (Fernandez et al., 2008) showed the initial concentration and total solid content of the substrate in the bioreactor can be effect on the performance of the digestion process and the amount of methane produced during the process. Many kinds of carbon source support many groups of microbes. Before the beginning of the digestion process, the substrate must be categorized for carbohydrate, lipid, protein and fiber contents (Lesteur et al., 2010). In addition, the substrate

should also be categorized for the amount of methane that can possibly be produced under anaerobic conditions. Carbohydrates are considered the greatest essential organic component of municipal solid waste for biogas production (Dong et al., 2009).

2.2.4 Mixing (Agitation).

Mixing generates a homogeneous substrate avoiding stratification and the formation of a surface crust, and confirms solids remain in suspension. An Addition, prevents the development of localized pockets of temperature variation, particle size reduction in digesting and release the produced gas (Michael H., 2003). Mixing and stirring equipment, and the way it is performed, varies according to reactor type and total solid content in the digester (Deublein and Steinhauser, 2011). (Gomez et al., 2006) shown the low speed mixing conditions permitted a digester to better absorb the disturbance of shock loading than did high speed mixing conditions. The effect of three mixing strategies(continuous, minimal and intermittent) on methane production from anaerobic digestion of manures was investigated in lab-scale and Pilot-scale continuously stirred tank reactors at thermophilic conditions by (Kaparaju P. et al., 2008), they founded , intermittent and minimal mixing strategies improved methane productions compared to continuous mixing.

2.2.5 Carbon/Nitrogen ratio.

The C/N ratio in the organic material plays a critical part in anaerobic digestion process. The unstable nutrients are observed as an important factor limiting anaerobic digestion of organic wastes. Where carbon constitutes the energy source for the microorganisms, nitrogen assists to improve microbial growth (Yadvika et al., 2004, Hong and David, 2007). For the enhancement of nutrition and Carbon/Nitrogen ratio, co-digestion of organic mixtures is used (Cuetos et al., 2008). (Zhang P. et al, 2008) studied the effect of Addition of organic fraction of municipal solid waste to improved carbon-to-nitrogen (C/N) ratio from 8.10 to 20.55 in the feedstock, they found a biogas yield increased by increased (C/N) ratio in feedstock. (Bouallagui et al., 2009a) reported the C/N ratio between 22/1 and 25/1 appeared to be best for anaerobic digestion of fruit and vegetable waste, while, (Lee et al., 2009) reported the optimum C/N ratio for anaerobic degradation of organic waste was 20-35.

2.2.6 Volatile Fatty Acids (VFAs).

Volatile Fatty Acids are important intermediary compounds in the production of methane (Cabbai V. et al., 2013). The major intermediate of anaerobic digestion products are acetic acid, propionic acid and butyric acid. Formulae and Structure as shown in table (2.1) (Wang Q. et al., 1999). However, two VFAs (acetic acid and butyric acid) are among the most favorite for methane formation, whereas, acetic acid contributes more than 70% to the methane formation (Wijekoon K. et al., 2011). If the present high concentrations of volatile fatty acid (VFA) in the system cause leads to a decrease of the pH. Non-methanogenic microorganisms responsible for

hydrolysis and fermentation adapt to low pH. On the contrary methanogens can be inhibited significantly at low pH (Mrafkova et al., 2003, Agdag and Sponza, 2007). (Lee D. et al.,2015) investigated the effect of volatile fatty acid concentration on the anaerobic degradation rate of food waste leachate, they showed the concentrations of VFAs should remain below 4,000mg/L, while (Siegert and Banks ,2005) reported the concentrations of VFAs above 2000 mg /L led to inhibition of cellulose degradation. (Wang Y. et al., 2009) studied the effects of different concentration of VFAs (acetic acid, propionic acid and butyric acid) and ethanol on the efficiency of fermentation, they found the highest concentrations of ethanol, acetic acid and butyric acid were 2400, 2400 and 1800 mg/L, respectively, there was no significant inhibition of the activity of methanogenic bacteria. However, when the propionic acid concentration was increased to 900 mg/L, significant inhibition appeared.

Table (2.1): Formulae and structure of major AD intermediate products.

Compound	Formulae	Structure
Acetic Acid	CH ₃ COOH	
Propionic acid	CH ₃ CH ₂ COOH	
Butyric acid	CH ₃ CH ₂ CH ₂ COOH	

2.2.7 Retention time (RT).

Retention time (RT) is an important parameter for dimensioning a plant for biogas production. The (RT) can be accurately set in batch operation mode. While, for continuously operated it expressed as a hydraulic retention time (HRT) is approximated estimated by dividing the digester volume by the daily influent rate as shown in equation (2.13) (Avraam K., 2012). The retention times are mainly dependent of operation temperature and type of substrates (Alexopoulos S., 2012).

$$\text{HRT} = \frac{V_r}{\dot{V}} \quad (2.13)$$

Where:

HRT= hydraulic retention time (d).

V_r = Reactor Volume (m^3).

\dot{V} = Daily volume flow rate (m^3/d).

2.3 Types or Operation Modes of Anaerobic Digestion Processes.

Many operation modes were used for AD processes that depend on substrate properties (Liquid or Solid State), treatment mode of substrate (Batch and Continuous) and process arrangement (Single or Two stage). AS describe below.

2.3.1 Liquid and Solid-State Anaerobic Digestion Processes.

Depend on the substrate properties, liquid and solid-state fermentation processes are convenient for anaerobic digestion (Weiland P., 2003). If a total solid concentration of 15 % wt. or more was adopted to carry out the so-called solid-state AD (Li Y. et al., 2011). This is usually done when the organic fractions of MSW and lignocellulosic biomass are processed. On the contrary, liquid AD (i.e. at a solid concentration lower than 15 % wt.) is preferred to treat animal manure and sewage sludge (Guendouz J. et al., 2010). Solid-state AD has several advantages over liquid AD, including higher volumetric organic loading rate, a smaller reactor volume for the same solids loading; fewer moving parts; lower energy requirements for heating and mixing; easier to handle end product and a greater acceptance of inputs containing glass, plastics, and grit (Jha A. K. et al., 2011, Li Y. et al., 2011)

A critical aspect of the solid-state AD stems from the heterogeneous nature of the substrate that generates different micro-environments, requiring different bacterial consortia for their degradation. Consequently, the dynamics of solid-state AD can be more complex in comparison to liquid AD (Shankaranand V.S. et al., 1992).

(Brown D. et al., 2012). Studied the effect of liquid (L-AD) and solid state (SSAD) on methane yields by using eight lignocellulosic feedstocks (switch

grass, corn Stover, wheat straw, yard waste, leaves, waste paper, maple, and pine), they founded no significant difference in methane yield between LAD and SS-AD, except for waste paper and pine. But, the volumetric productivity was two to seven times greater in the SS-AD system compared with the L-AD system.

(Lianhua L. et al., 2010). Investigated the effects of solid concentration in different temperatures on AD for rice straw conversion to biogas, they showed that higher biogas production was achieved in the dry mesophilic conditions.

(Fernandez J. et al., 2008). Reported when the total solid concentration of organic fraction of municipal solid waste (OFMSW) increased from 20% to 30%, the COD removal of the SS-AD decreased from 80.69% to 69.05%. Then methane yield was less by 17%.

2.3.2 Batch and Continuous Anaerobic Digestion Processes.

Depending on the substrate being treated, AD process can be done as a batch process or a continuous process (Forster-Carneiro T. et al., 2008). During batch operation the reactors are filled just the once with feedstock, and closed for the complete retention time, after which it is opened and the effluent removed and recharged. The advantage of batch reactor is uncomplicated, inexpensive and less equipment requirement. However, batch reactors need a larger volume due to longer retention time than continuously fed reactors. Where, the continuous digestion reactor is continuously fed feedstock, allowing a steady state to be reached in the reactor with a constant gas production. But, it has higher operating costs due to pumping requests (El-Mashad and Zhang, 2010, Nalo T. et al., 2014). Both batch and

continuous anaerobic digestion processes are in use to treat organic fractions of municipal solid waste (OFMSW) (Li Y. et al., 2011).

2.3.3 Single and Two Stages Anaerobic Digestion Process.

The arrangement of anaerobic digestion process is too essential for the efficiency of the methane production. A single-stage anaerobic digestion process has been commonly utilized for municipal solid waste treatment. As all AD steps (hydrolysis, acidogenesis, acetogenesis, and methanogenesis) happen with each other in a single reactor(Forster-Carneiro T. et al., 2008). However, the two-stage anaerobic digestion process has been developed based on the separation of hydrolysis/acidogenesis and acetogenesis/methanogenesis in two separate reactors (Chu C. et al., 2008), in such a system, fast-growing acidogens and hydrogen producing microorganisms are enriched for the production of hydrogen and volatile fatty acids (VFAs) in the first reactor, then, A slow-growing acetogens and methanogens are built-up in the second reactor, where VFAs are converted to methane and carbon dioxide(Kongjan P. et al ,2013).

2.4 Inhibition /toxicity of anaerobic digestion process.

A broad variety of inhibitory substances are the main reason of the anaerobic process upset or failure since they are present in significant concentrations in wastes. The inhibitors, usually present in anaerobic digesters include ammonia, sulfide, light metal ions, heavy metals, and organics (Chen Y. et al., 2008).

2.4.1 Ammonia.

Ammonia is one of the hydrolysis products formed during biological degradation of the nitrogenous matter, commonly in the form of proteins and urea that are present in significant concentrations in wastes (Kayhanian M., 1999), the free ammonia may be inhibit of anaerobic fermentation and toxic the methanogenic bacteria (Gallert and Winter,1997, Chiu S. et al.,2013.). The free ammonia concentration depends mainly on three parameters: the total ammonia concentration, temperature and pH. The wastes containing a high ammonia concentration are more easily inhibited at thermophilic conditions than at Mesophilic conditions (Hansen K.H. et al., 1998). In general, if the concentrations of ammonia less than 200 mg/L are useful to the fermentation process since nitrogen is a necessary nutrient for anaerobic microorganisms (Liu and Sung, 2002, Yenigün and Demirel, 2013).

2.4.2 Sulfide.

Sulfate is a common element of many waste stream industries (Cai J. et al., 2008), that will be converted into hydrogen sulfide (H₂S) by sulfate reducing bacteria (SRB). The Sulfate reducing bacteria produce sulfides which perhaps inhibitory and/or toxic to SRB and methane producing bacteria

(MPB), reduce the rate of methanogenesis and decrease the amount of methane produced by competing for the available carbon and/or H₂ (Chen J. L. et al., 2014). The decrease is done by two main combination of Sulfate reducing bacteria, including incomplete oxidizers, which oxidize compounds such as lactate to acetate and CO₂ and complete oxidizers (acetoclastic SRB), which quite convert acetate to CO₂ and HCO³⁻, together combination use hydrogen for sulfate reduction. Inhibition produced by sulfate reduction can be separated into two phases. Prime inhibition is specified by lower methane production by reason of competition of SRB and methanogenic bacteria to find communal organic and inorganic substrates. Secondary inhibition results from the toxicity of sulfide to numerous anaerobic bacteria combination. The hydrogen sulfide formed has an inhibitory effect on methanogens even at low concentrations (Chen Y. et al., 2008, Michael H., 2003).

2.4.3 Light metals ions.

Light metal ions are sodium (Na), potassium (K), calcium (Ca) magnesium (Mg) and aluminum (Al) are normally existing in influents of anaerobic digesters (Grady J. et al., 1999). They may be brought forth by the degradation of organic matter in the feeding substrate or by chemical adding for pH correction (Nayono S. E. et al., 2010). At moderate concentrations, light metal ions are necessary for the growth bacteria. However, immoderate concentrations will slow down a bacterial growth and the inhibition or toxicity will be accorded (Soto M. et al., 1993). The optimum concentration of (Na and Mg) is (350 and 720 mg/L), respectively, where the concentration of (K, Ca and Al) must be less than (400 , 7000 and 2500 mg/L), respectively to avoid process inhibition (Appels L. et al., 2008, Chen Y. et al., 2008).

2.4.4 Heavy metals.

The term of heavy metals denotes to metals and metalloids having densities more than 5 g /cm³ are predominantly existing in industrial wastewaters and municipal sludge in significant concentrations such as copper (Cu), zinc (Zn), lead (Pb), mercury (Hg), chromium (Cr), cadmium(Cd), iron (Fe), nickel (Ni), cobalt (Co) and molybdenum (Mo) and is commonly correlating with contamination and toxicity (Peng K. et al.,2006, Altaş L.,2009). Heavy metals may be stimulatory, inhibitory, or even toxic to anaerobic reactions and the range of these effects relies on the metal species and its concentration (Mudhoo and Kumar, 2013), some of these elements are needed by microorganisms at low concentrations. However, excessive quantities of heavy metals can lead to inhibition or toxicity (Li and Fang, 2007).

2.4.5 Organics.

An extensive kind of organic chemicals were mentioned can inhibit anaerobic bacteria, such as halogenated benzenes, halogenated phenols, phenol and alkyl phenols, halogenated aliphatic and long chain fatty acids (LCFAs) (Chen J. L. et al., 2014).

2.5 Improvement of AD process.

There are many way can be follow to improve the efficiency of AD process as describe below.

2.5.1 Co-digestion.

The co-digestion technology can be defined as the simultaneous treatment of two or more organic biodegradable waste streams by anaerobic digestion display considerable possibility for the suitable behavior of the organic fraction of solid waste advent from a source or separate gathering systems such as organic fraction municipal solid waste, sewage sludge, cow manure and energy crops (Mata-Alvarez J. et al., 2011, Alvarez and Liden, 2008). Co-digestion of different organic component is a popular practice to improve the performance of anaerobic digestion yields and requires accurate selection of substrates to improve the efficiency of the process (Alvarez J.A., et al., 2010, Cuetos M.J. et al., 2011). The main advantages of this technology are: enhanced balance nutrient and digestion, dilution of inhibitory and/or toxic compounds, well utilization of the digested volume, synergistic effects of microorganisms, improved load of biodegradable organic matter and better biogas produce (Hong-Wei and David, 2007, Sosnowski P. et al., 2003, Zhang L. et al., 2011). It has been found (Kaparaju P. et al., 2008) that biogas production is increased by co-digestion because of the more balanced nutritional composition and the increased buffering capability that improves the stability of the overall AD process. Consequently, the co-digestion permits the use of current installations increasing significantly the biogas yields and the global efficiency (Converti A., 1999, Poggi-Varaldo H.M., 1999).

2.5.2 Pretreatment of substrates.

Many types of substrates used for biogas production by anaerobic digestion process such as industrial waste, agricultural waste, organic fraction of municipal solid wastes (OFMSW) and energy crops. While, the hydrolysis is the rate-limiting step during the whole anaerobic process. Therefore, it is important to enhance hydrolysis for improving the performance of AD some substrates can be very slow to break down for several reasons, molecular structure is poorly accessible to microorganisms and their enzymes due to it has highly crystalline structure or low surface area in addition they have chemicals material that inhibit the growth and activity of the microorganisms (Carlsson M. et al, 2012). Various pretreatment technologies include mechanical, thermal, chemical, biological and Physicochemical pretreatment (He W.Z., et al., 2008, Shahriari H., et al., 2012, Masse L., 2003, Nah I. W. et al., 2000, Menardo S. et al., 2015, Lo Y.C. et al., 2009) have been developed to overcome some of these problems to cause one or more of these changes in biomass (size reduction, degradation of one or more of the main components of biomass (cellulose, hemicellulose, or lignin), increase in surface area and porosity of biomass, change in crystallinity and degree of polymerization of cellulose and prevent processing problems such as high electricity requirements for mixing or the formation of floating layers (Zhang C. et al., 2014).

2.5.2.1 Mechanical pretreatment.

Mechanical pretreatment is executed by mills, shredding, screening, sorting, squeezes and separation of ferrous components are some of the most commonly available processes which reduce the size of material and degree of crystallinity of lignocelluloses as a result greater possibility for enzymatic degradation of these materials towards biogas production (Leikam and Stegmann, 1999, Heo N.H. et al., 2003), additionally the size reduction eases mixing in digesters because of reducing the viscosity also can reduce the problems of floating layers (Schell and Harwood, 1994).

2.5.2.2 Thermal pretreatment.

In the thermal pretreatment, the substrate is heated under pressure and applied at that temperature for up to one hour (Garrote G. et al., 1999). The effects of thermal pretreatment depend on the substrate type and temperature range (Ariunbaatar J. et al., 2014). The general advantages of thermal treatment are particle size reduction, to increase the porosity of the materials, break down lignin and hemicellulose, to increase the bioavailability of organic matter, as well as improving dewatering performance and reduces viscosity of the digestive and an increase in pathogen reduction (Rincon B. et al., 2013, Tampio E. et al., 2014).

2.5.2.3 Chemical Pretreatment.

Chemical pretreatment has been accomplished by utilizing a scope of different chemicals, mainly acids, alkalis or oxidants under different conditions to modify the physical and chemical characteristics of lignocellulosic (Zheng Y. et al., 2014). In comparing acidic with alkaline

treatment, the second is the more favored chemical method because of during the anaerobic digestion process pH should an adjustment by the alkalinity addition (Li H. et al.,2012), the first reactions that happen during alkali treatment are solvation and saponification, which motivate the swelling of substrates, under those circumstances the specific surface area is increased and the substrates are readily attainable to anaerobic microbes(Kong F. et al., 1992), otherwise the main reaction that happens through acid treatment is the hydrolysis of hemicellulose into perspective monosaccharaides, whilst the lignin condensates and precipitates(Ariunbaatar J. et al.,2014). Oxidative pretreatment such as ozonation are also utilized to enhance the biogas production and improve the hydrolysis rate (Zheng Y. et al., 2014).

2.5.2.4 Biological pretreatment.

Biological pretreatment for improvement of anaerobic digestion process have been predominately associated with the act of fungi capable of producing enzymes that can degrade lignin, hemicellulose, and polyphenols or by enzyme addition to enhance the break down biomass that are already existent in digesters (Parawira W. et al.,2005). By comparison with other pretreatment methods, biological pretreatment, not simply less energy requirement and without chemical addition but also it is conducted under moderate environmental conditions consequently that few inhibitors, which could negatively effect on anaerobic digestion (Taherzadeh and Karimi, 2008). The main advantages of biological treatment are: enhancing the hydrolysis process, minimize the loss of carbohydrates and maximize the lignin removal for AD feedstocks with high digestibility (Carrere H. et al., 2010, Zheng Y. et al., 2014). Fungi such as (white, brown and soft-rot fungi) are practiced in this treatment to degrade lignin and hemicellulose in waste

materials (Galbe and Zacchi, 2007). White and soft rots have been reported to degrade cellulose and lignin, while brown rots generally attack cellulose, white-rot being the most effective at biological pretreatment of biomass (Sun and Cheng, 2002).

2.5.2.5 Physicochemical pretreatment.

Steam explosion is physicochemical pretreatment the most common technology used for the pretreatment of lignocellulosic materials, a method that opens up the fibers, and makes the biomass polymers more accessible for successive treatment (Fengel and Wegner, 1983). Generally in the steam explosion process the biomass are treated by hot steam (from 180 to 240 °C) at pressure (from 1 to 3.5 MPa) then followed by an explosive decompression of the biomass leading to a rift of the rigid structure of biomass fibers. The rapid pressure relief fraying the cellulose bundles and this results in an improved accessibility of the cellulose for enzymatic hydrolysis and fermentation (Tanahashi M., 1990).

Pre-treatments of lignocellulose by steam explosion offer different advantages (Garrote G. et al, 1999):

- No chemical materials are used except water;
- A low amount of unwanted byproducts is generated;
- No acid handling and recycling and consequently a reduced corrosion tank to the mild pH of reaction media.

2.5.3 Trace Metals Addition.

The influence of the adding of trace metals on the performance of bioreactors has been an important subject area field in anaerobic processes, as metals are required in the enzymatic activities of acidogenesis and methanogenesis (Qing-Hao H. et al., 2008). Minuscule quantities of the trace elements such as zinc, nickel, cobalt, copper, selenium, chromium, tungsten, molybdenum, manganese are required in anaerobic digestion processes were labeled essential trace elements (Franzle and Markert, 2002). Positive effects have been obtained mainly by the addition of single or more trace elements in anaerobic digestion processes because the trace components are an essential co-factor of the enzymes involved in the biochemical pathway of methane production (Zandvoort M.H. et al., 2006, Feroso F.G. et al., 2009, Karlsson A. et al., 2012). Table (2.2) shows a functions of elements was used in AD experiment adapted from (Kayhanian and Rich, 1995).

Table (2.2): Functions of elements.

Element	Functions	Remarks
Cobalt, Co	Corrinoids, CODH	Cobalt is present in specific enzymes and corrinoids. The common enzyme carbon monoxide dehydrogenase (CODH) uses cobalt. CODH plays an essential role in Acetogenic (acetate-forming) activity.
Nickel, Ni	CODH, synthesis of F ₄₃₀ , essential for sulfate reducing bacteria, aids CO ₂ /H ₂ conversion.	Many anaerobic bacteria are dependent on nickel when carbon dioxide (CO ₂) and hydrogen (H ₂) are the sole sources of energy. Most nickel is taken up by cells in a compound named F factor 430 (F ₄₃₀). F ₄₃₀ has been found in every methanogenic bacterium ever examined. In addition, CODH is a nickel protein and may aid sulfur-reducing bacteria.
Zinc, Zn	FDH, CODH, hydrogenase	Zinc is present in relatively large concentrations in many methanogens. It may be part of formate dehydrogenase (FDH), super dismutase (SODH) and hydrogenase.

2.6 Composition of Biogas.

Biogas produced by anaerobic degradation through bacterial reactions of organic material consisting mainly of two major components methane (CH_4) and carbon dioxide (CO_2). Additionally, small traces of other gases, including hydrogen sulfide (H_2S), water vapor (H_2O), ammonia (NH_3), hydrogen (H_2), oxygen (O_2) and nitrogen (N_2) (Yadvika S. et al., 2004, Geo J. et al., 2014) . Typical composition of biogas in volume fractions as obtained from various sources as shown in table (2.3), the great variation happens in the composition of biogas, predominantly caused by differences in feedstocks and operating conditions (Massoud K. et al., 2007, Alexopoulos S., 2012).

Table (2.3): Typical Composition of biogas in volume fraction.

Component	Symbol	Volume Fraction
Methane	CH_4	50-75 %
Carbon dioxide	CO_2	25-45%
Hydrogen	H_2	0-1%
Hydrogen sulfide	H_2S	20-20,000ppm (2%)
Ammonia	NH_3	0-0.05%
Water vapor	H_2O	2-7%
Oxygen	O_2	0-2%
Nitrogen	N_2	0-2%

2.7 Upgrading of Biogas.

To achieve a biogas enriched in a methane (CH_4) the upgrading technologies are required to eliminate the percentage of carbon dioxide (CO_2), hydrogen sulphide (H_2S) and water vapor to allowed value be used in many application (Harasimowicz M. et al., 2007). There are four main technologies used for upgrading a biogas such as adsorption, absorption, cryogenic separation and membrane separation (Starr K. et al., 2012).

2.7.1 Adsorption technology.

Adsorption technology accomplished by feeding the biogas on the surface of molecular sieves at high temperature and pressure such as , silica, alumina, activated carbon or silicates, the CO_2 , H_2S , moisture and other impurities simultaneously removed from biogas by transfer it to surface of molecular sieves as a result of physical or Vander wall forces (Kapdi S.S. et al., 2005).

2.7.2 Absorption technology.

Absorption technology is classified to physical and chemical absorption, the easiest and cheapest method in physical absorption is the feeding the compressed biogas to bottom of packed bed column and pressurized water used as an absorbent is sprayed from the top, the CO_2 as well as H_2S are dissolved in water and collected at the bottom of the column, whilst, chemical absorption based on used chemical solvents such as aqueous solutions of amines or alkaline salts (Kapdi S.S. et al., 2005).

2.7.3 Cryogenic separation technology.

Cryogenic separation includes separation of biogas composition by fractional condensations and distillations at low temperatures, the biogas is cooled until the CO₂ changes to a liquid or solid phase while the methane remains in multiple stages compression to high pressure with drying to avoid freezing in inter-cooling, and the CO₂ will condensate and removed by a separator (Ryckebosch E. et al., 2011).

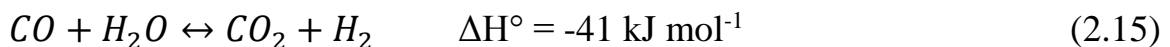
2.7.4 Membrane separation technology.

Membrane separation technology have been known as one of the most efficient methods for upgrading biogas from the carbon dioxide and hydrogen sulfide by using gas permeation membranes (Favre E. et al.,2009).

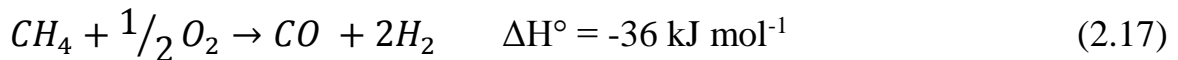
2.8 Production of Synthesis gas.

For the application of Fischer - Tropsch synthesis reaction to liquid fuel production the gas mix is required as the main reactant material called synthesis gas, the synthesis gas is a mix of hydrogen (H₂) and carbon monoxide (CO), may be created by reforming, partial oxidation or autothermal reforming of methane gas generated from many types of material such as natural gas, petroleum coke, coal, and biomass (Wilhelm D.J. et al., 2001, Lavoie JM., 2014).

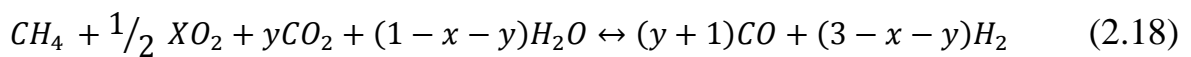
The reforming process is classified to steam and dry reforming, the steam reforming (SR) is a highly endothermic reaction as shown in equation (2.14), in this process the methane gas is mix with excess amount of steam in presence of metal based catalysts in the reformer at temperature about 900 °C and pressure 30 bar to generate a high ratio of syngas (H₂/CO = 3), appropriate for ammonia production, the produced carbon monoxide (CO) have additional reaction with steam to generate further hydrogen and carbon dioxide by the water gas shift (WGS) reaction as shown in equation (2.15) (Gangadharan P. et al., 2012). While, the dry reforming (DR) is performed by mix of CH₄ with CO₂ as shown in equation (2.16) the reaction also is a highly endothermic like steam reforming and accorded in existence of metal based catalysts at high temperature more than 750°C, the produced syngas ratio (H₂/CO =1) appropriate for Fischer–Tropsch synthesis reaction. (Goula M. A. et al. 2015, Charisiou N.D. et al, 2016).



In general, the partial oxidation reaction is a slightly exothermic reaction carried out by reacting a methane and oxygen with or without presence of metal catalyst as shown in equation (2.17), the reaction temperatures more than 1127 °C for the reaction without catalyst, whilst 727-927°C with catalysts the product synthesis ratio ($H_2/CO= 2$) appropriate for Fischer–Tropsch synthesis reaction (Kleinert A. et al, 2006).



The integration of steam and dry methane reforming with partial oxidation (POX) of methane in a single reactor to produce a syngas as shown in equation (2.18) the processes is known as autothermal reforming (ATR), the partial oxidation happens in an upper zone at the inlet of the reactor for providing heat to the steam reforming reaction that happening in a lower zone packed with metal catalyst, the product synthesis ratio (H_2/CO) in the range from about 2 to 3.5 appropriate for Fischer–Tropsch synthesis reaction (Araki S., et al, 2010).



2.9 Fischer-Tropsch Synthesis (FTS).

Fischer–Tropsch synthesis was developed in the 1920s by Franz Fischer and Hans Tropsch, is a set of catalytic processes that can be used to produce fuels and chemicals from synthesis gas (syngas) which is a mixture of carbon monoxide (CO) and hydrogen (H₂) (Iglesia E., 1997). Syngas can be derived from natural gas, coal, or biomass, the raw material is converted first into syngas, then subsequently reacted to form hydrocarbons via Fischer-Tropsch synthesis as shown scheme diagram in **Figure 2.2**, the process is named according to the feedstock: Gas-To-Liquid (GTL), Biomass-To-Liquid (BTL) and Coal-To-Liquid (CTL) (Dry E. M., 2002, Rostrup-Nielsen J.R., 2000, Vliet O.P.R. et al., 2009).

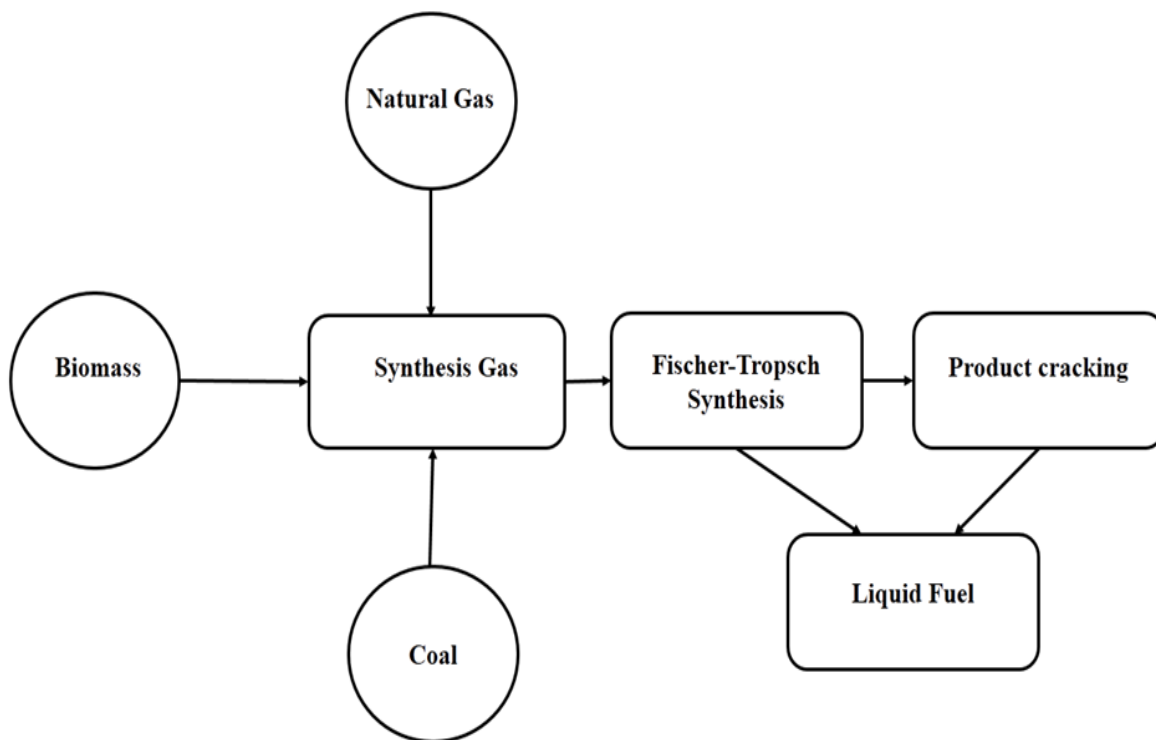


Figure 2.2 Scheme diagram of overall Fischer-Tropsch Synthesis process.

The fuels and chemical feedstock produced from Fischer-Tropsch synthesis not produce environmentally destructive compounds encountered in direct hydrogenation (Rofer-Depoorter C.K., 1981).

A various types of reactors (multi-tubular fixed-bed reactor; bubble column slurry reactor; bubbling fluidized-bed reactor; three-phase fluidized bed reactor; and circulating fluidized-bed reactor), have been considered in the history of FTS process development. (Rahimpour and Elekaei, 2009a, Rahimpour and Elekaei, 2009b).

Fischer-Tropsch synthesis is technically classified into two categories, the High Temperature Fischer-Tropsch (HTFT) and the Low Temperature Fischer-Tropsch (LTFT) processes. The standard for this categorization is the operating temperature of the synthesis (Leckel D., 2009, Dry M.E., 1999).

2.9.1 Fischer-Tropsch Synthesis reactions.

Fischer-Tropsch synthesis process includes a simultaneous great number of reactions and the product spectrum involving of a complex multi component mixture of linear and branched hydrocarbons and oxygenated products (Choudhury and Moholkar, 2013a). These products can be a mixture of alkanes, alkenes, aromatics, ring compounds and the oxygenated compounds are comprised of mainly alcohols as well as some acids, ketones and aldehydes (Liu Y. et al., 2007a) the general reactions of FTS are summarized as follows:

Paraffins:



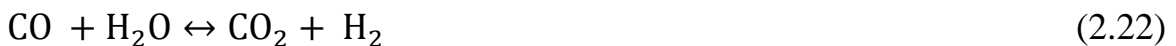
Olefins:



Oxygenates:



Water gas shift reaction (WGS) as a side reaction:



A simplified represent for overall stoichiometry F-T synthesis reaction is:



The mixture of products depends on the reaction and operating conditions, such as reactor temperature, pressure, feed gas composition (H_2 to CO ratio), space velocity and the types of catalysts and promoters used (Dry M. E., 1996).

2.9.2 Catalysts for Fischer-Tropsch synthesis.

The most common Fischer-Tropsch catalysts are Co, Fe, Ru, and Ni (Rafiq M. H. et al., 2011). Mainly iron- and cobalt-base catalyst are employed in industrial applications. Iron catalyst is inexpensive, has a high water-gas shift (WGS) activity and so it is best suitable for CO rich syngas. Though, it is prone to exhaustion and the water produced by the F-T synthesis may decrease its activity, whilst, the cobalt-based catalyst has more activity and longer life than iron catalyst due to it is not inhibited by water more resistant to exhaustion as well as has a little WGS activity and so it is best suitable for H₂-rich syngas (Dry E. M., 2002).

Nickel is the typical FT catalyst for producing higher molecular weight hydrocarbons, but at high pressure it tends to form nickel carbonyl, and with increasing the reaction temperature the selectivity changes mostly to methane. This trend is found also with Cobalt and Ruthenium but less immoderate, Ruthenium shows the highest catalytic activity for producing long chain hydrocarbons at low reaction temperature, but, it is very expensive and a limited world resource and so it is not considered a sustainable option for use in industrial (Schulz H., 1999).

The most common supports used for cobalt and Iron based catalyst were alumina (Al₂O₃), zeolites, silica (SiO₂), titanium (TiO₂), activated carbon (C) and magnesia (MgO) (Zhang J. et al., 2002).

Iron catalysts are used for High Temperature Fischer-Tropsch (HTFT) processes, whereas both Fe and Co are appropriate for Low Temperature Fischer-Tropsch (LTFT) processes (Dry E. M., 2002). Tables (2.4 and 2.5) summarizing parameter studies by using Iron and Cobalt based catalyst.

Table (2.4): Summary Parameter studies by using Iron –based catalysts.

Catalyst	Reactor	T	P	H ₂ /CO	Flow Rate	Reference
Fe–Cu–K	FBR	493–542 K	10.9–30.9 bar	0.98-2.99	SV= 4000 –10 000 h ⁻¹	Wang Y.N. et al.,2003
Fe/Cu/K/SiO ₂	FBR	250°C	1.48Mpa	0.67	2NL/g _{cat.} h	Bukur D. B. et al.,2005
Fe/Mn/Cu/K/SiO ₂ Fe/Mn/K/SiO ₂ Fe/Mn/SiO ₂	CSTR	543K	1.5Mpa	0.67	2000-4000 h ⁻¹	Zhang C.H. et al., 2006
Fe/Cu/K/SiO ₂	SBO	240-270 °C	20-30 atm.	1	-	Farias F.E.M. et al., 2007
Fe/SiO ₂	CSTR	513-553 K	1-2.85Mpa	0.4-2	W/F=7.5 g _{cat.} h/mol	Hayakawa H. et al., 2007
100Fe,FeCr,,FeMn,FeMo ,FeTa ,FeV ,FeW, FeZr	FBR	280 °C	1.8 atm.	2	60 cm ³ /min (STP)	Lohitharn N. et al., 2008a

100Fe,100Fe1.5K ,100Fe2.5K,100Fe4K ,100Fe9K,FeMn, FeMn2.5K,FeMn4K FeMn6.5KFeMn9K	FBR	280 °C	1.8 atm.	2	60 cm ³ /min (STP)	Lohitharn N. et al., 2008b
Fe-Cu-La/SiO ₂	FBR	290 °C	17 bar	1	GHSV = 4.0 NL·h ⁻¹ ·g ⁻¹ _{Fe} .	Pour A. N. et al., 2008 b
Fe/Cu/SiO ₂ Fe/Cu/La/SiO ₂ Fe/Cu/Mg/SiO ₂ Fe/Cu/Ca/SiO ₂	FBR	563K	1.7Mpa	1	4.86&13.28 NLh ⁻¹ _{g_{cat.}}	Pour A. N. et al.,2008 c
Fe/K-free Fe/K-ZSM-5 Fe/K-SiO ₂ Fe/K-Al ₂ O ₃	FBR	250 °C	1.50MPa	2	GHSV= 4000 h ⁻¹	Zhao G. et al., 2008
Fe100/K1.4/Si4.6/Cu2.0	CSTR	270 °C	1.3 MPa	0.7	5.0 SL/(h g _{-Fe})	Luo M. et al., 2009
Fe-Cu-K/SiO ₂	FBR	553 K	1.0 MPa	1.15	W/F = 5 g h/mol.	Zhang Y. et al., 2009
Fe/K/Al ₂ O ₃	CSTR	240-270 °C	20-30 atm.	1	50Nml/min.	Farias F.E.M. et al., 2010

Fe/K ₂ O/SiO ₂ Fe/K ₂ O/In/SiO ₂	FBR	275°C	10 bar	2	2ml/min	Wonga and Coville, 2010
Fe, Fe/Cu , Fe/Ca ,Fe/Mg, Fe/K	FBR	533-573 K	3Mpa	1-2	SV(W/F)=13-20gm h/mol.	Kumabe K. et al., 2010
Fe/Cu/K/SiO ₂	SBCR	265°C	2.5Mpa	1	2.61-3.92L/h g _{cat} .	Jung H. et al., 2010
Fe/Co/Zn/Ru, Fe/Co/Zn, Fe /Zn/K, Fe/Co/Zn/K	FBR	275-300-350°C	250-350 Psig	2	10-50 ml/min	Dasgupta and Wiltowski, 2011
Fe/Mn with promoter (Zn, Rb ,Cs, K and Ce)	FBR	230 ,240, 250, 260 ,270, 280, 290 and 300	1, 3, 5, 7, 9 ,11, 13, 15 and 20 atm.	2	GHSV = 1000, 1100 ,1200 ,1300 ,1400, 1500 and 1600(h ⁻¹)	Feyzi M. et al., 2011
(Fe, Mn)/SiO ₂	FBR	250 and 260 °C	1 bar	1.5 and 2	GHSV = 1000 and 1100 h ⁻¹	Feyzi M. et al., 2013
Fe	FBR	593 K	1 ,1.5 and 2 MPa	2	GHSV = 1800 - 3600 h ⁻¹	Choudhury and Moholkar, 2013b

Table (2.5): Summary Parameter studies by using cobalt-based catalysts.

Catalyst	Reactor	T	P	H ₂ /CO	Flow Rate	Reference
Co/Rurchemie	SLR	220-240 °C	0.5-1.5 MPa	1.5 to 3.5	SV=0.085 and 0.008 L (STP)/min/g _{cat.}	Yates and Satterfield, 1992
Co-Ni-ZrO ₂	FBR	513-533 K	1-31 atm	1	CO(WHSV)=5-25 h ⁻¹	Sethuraman R. et al., 2001
Co/Al ₂ O ₃ Pt/ Co/Al ₂ O ₃ Ru/Co/Al ₂ O ₃	CSTR	493 K	1.8MPa	2	-	Jacobs G. et al.,2002
CoN373, CoN423 ,CoN673, CoAc443 ,CoAc493,CoAc673	FBR	463 K	1 atm.	2	-	Girardon J.S. et al.,2005a
CoAc673 CoAc443 CoN673 CoN423 RuCoN673 RuCoAc673 RuCoAc443 ReCoAc673	FBR	-	1 atm.	2	-	GirardonJ. S. et al., 2005b

Co/TiO ₂ Co/Mn/TiO ₂	SSR	220 °C	1,4, 8, and 18 bars	2	Flow rate=1, 4, 8, and 18 ml/min	Morales F. et al., 2005
CoPtZrO ₂ /Al ₂ O ₃	FBR	473-493 K	0.5-2.5 MPa	2	GHSV = 200, 500 and 1000 mL.h ⁻¹ .g ⁻¹	Xu D. et al., 2006
Co/Al ₂ O ₃ -473 CoPt/Al ₂ O ₃ -473 Co/Al ₂ O ₃ -473 Co/Al ₂ O ₃ -613 CoPt/Al ₂ O ₃ -613 Co/Al ₂ O ₃ -673 Co/Al ₂ O ₃ -CoPt/Al ₂ O ₃ -773	FBR	443–483 K	1 bar	2	GHSV = 1800 cm ³ /g/h	Chu W. et al.,2007
CoRu673(S),CoRe673(S) , CoRu373, CoRu673 , CoRe373, CoRe673	FBR	463 K	1 atm.	2	-	Girardon J. S. et al., 2007
Co/γ-Al ₂ O ₃ Co–Re/γ-Al ₂ O ₃	FBR	483K	20 bar	1 to 2.1	(GHSV)=3 , 6.3 and 12Ndm ³ /g _{cat} . h	Tristantini D. et al.,2007
Co/TiO ₂ Co/Mn/TiO ₂	FBR	220 °C	1 bar	2	(GHSV)=3010 h ⁻¹	Morales F. et al.,2007
Co/SiO ₂	FBR	503K	0.2 to2 Mpa	2	2	Zheng S. et al., 2007

Co/SiO ₂	TBR	230 °C	2.1 MPa	2	W/F (CO+H ₂) = 5.0 g _{cat} . h. mol ⁻¹	Liu X. et al., 2007
Co/SiO ₂	CSTR FBR	230°C	10bars	2	2SL h ⁻¹ g ⁻¹	Liu Y. et al., 2007b
Co/Zn/TiO ₂	FBR	220 °C	8 bar	2	GHSV= 400 h ⁻¹	Mnqanqeni and Coville, 2008
Co/Al ₂ O ₃ Co/Al ₂ O ₃ (SiO ₂)	FBR	212 °C	20 bars	2	GHSV= 5000 h ⁻¹	Marie A. J. et al., 2009
25Co/0.1Pt/Al ₂ O ₃	FBR	220 °C	20 bars	2	-	Karaca H.et al., 2009
30%Co/SBA-15 30%Co/0.05Ru/SBA-15 30%Co/0.1Ru/SBA-15 30%Co/0.5Ru/SBA-15	FBR	210 °C	2.0 MPa	2	GHSV= 8000 h ⁻¹	Xiong H. et al., 2009
CoSi1 CoRuSi1 CoSi2 CoRuSi2 CoSi3 CoRuSi3	FBR	190 °C	1 atm.	2	GHSV = 1800 ml/g _{cat} .h	Hong J. et al., 2009

CoMCM-41 CoZr ₂ MCM-41 CoZr ₅ MCM-41 CoZr ₁₀ MCM-41 CoSBA-15 CoZr ₂ SBA-15 CoZr ₅ SBA-15 CoZr ₁₀ SBA-15	FBR	473K	1 bar	2	GHSV=1800ml/g h	Hong J. et al., 2010
Co/ γ -Al ₂ O ₃	FBR	488, 492, 494 and 513K	2000 kPa	2	100 mL min ⁻¹	Yang J. H. et al., 2010
Co/ γ -Al ₂ O ₃ Co-foam	FBR	203, 217,223 and 240 °C	-	2	W/F = 15 &45 g _{cat} min L ⁻¹	Jung I.Y. et al., 2010
Co/Al ₂ O ₃ Ca-Co/Al ₂ O ₃ Mg-Co/Al ₂ O ₃ K-Co/Al ₂ O ₃ Na-Co/Al ₂ O ₃	FBR	210–300 °C	20 bar	2	GHSV = 6000 h ⁻¹	Osa A.R. et al., 2011a
CoPt/Al ₂ O ₃ –N1 CoPt/Al ₂ O ₃ –N2 CoPt/Al ₂ O ₃ –A	FBR	493 K	20 bar	2	GHSV= 14,000 mol g ⁻¹ h ⁻¹ GHSV= 25,000 mol g ⁻¹ h ⁻¹	Karaca H. et al., 2011
Co/Al ₂ O ₃ Co/bentonite Co/TiO ₂ Co/SiC	FBR	210–300 °C	20 bars	2	GHSV = 6000 h ⁻¹	Osa A.R. et al., 2011b

CoPt/Al ₂ O ₃	FBR	493 K	20 bar	0.5,2,4	GHSV= 25 000 ml g ⁻¹ h ⁻¹	Sadeqzadeh M. et al., 2011
Co-Sorb(2)/SiO ₂ Co-Sorb(5)/SiO ₂ Co-Sorb(10)/SiO ₂ Co/SiO ₂	FBR	190 °C	1 bar	2	GHSV = 1800 ml/g _{cat} .h	Hong J. et al., 2011
Al ₂ O ₃ Co/Al ₂ O ₃ Ca-Co/Al ₂ O ₃	FBR	210–300 °C	20 bars	0.5 to 2	4000 h ⁻¹ and 12,000 h ⁻¹	OsaA.R. et al., 2011 c
Co/Al ₂ O ₃	FBR	473 K	20 bars	2	GHSV= 37 to 180 NmL.g _{cat} ⁻¹ .h ⁻¹	Rafiq M.H. et al., 2011
CuO/CoO/Cr ₂ O ₃ (+ MFI Zeolite)	FBR	225–325 °C	28–38 atm	1 to 2	GHSV= 457 to 850 h ⁻¹	Mohanty P. et al., 2011
5Co/SiC 5Co/2Ca/SiC 20Co/SiC 20Co/2Ca/SiC	BSI R	220–250 °C	20 bar	2	GHSV= 6000 N cm ³ /g _{cat} . h	Osa A.R. et al., 2012

Co/Al ₂ O ₃	CSTR	220°C	2.2 MPa	2	-	Ma W. et al., 2014
Co/γ-Al ₂ O ₃	FPR	220–240 °C	25 bar	1.73	GHSV = 6410 cm ³ (STP)/g _{cat} h	Fratolocchi L. et al., 2015
10Co/ TiO ₂	TPR	220°C	25 bar	2	75 (NTP) ml/min	Muleja A.A., 2016
0.5% Pt–25% Co/Al ₂ O ₃ 0.2% Pt–10% Co/TiO ₂ 20% Co/SiO ₂	CSTR	220°C	1.9 MPa	2	3&4 SL/g _{cat} . h	PendyalaV.R.R. et al., 2016
CoPt/C-SiO ₂	PFR	220°C	20 bar	2	3 - 12 L/g _{cat} . h	Cheng K., 2016
Co/γ-Al ₂ O ₃	PTR	220°C	1bar	2	1800 & 2520 mL/g _{cat} . h	Najafabadi A.T. et al., 2016

2.9.3 Mechanisms of Fischer –Tropsch Synthesis.

Fischer- Tropsch synthesis mechanisms of different types of catalysts have been the primary aim of many studies for the formation of the products, the Fischer-Tropsch synthesis is a polymerization reaction with the following steps (Adesina A.A., 1997, Rofer-Depoorter C.K., 1981).

- 1- Reactant adsorption.
- 2- Chain initiation.
- 3- Chain growth.
- 4- Chain termination.
- 5- Product desorption.
- 6- Readsorption and further reaction.

In general, four mechanistic (Alkyl , Alkenyl, Enol mechanism and CO-insertion mechanism)were established for the Fischer-Tropsch synthesis, which differs in their path to demonstrate activation of CO, formation of monomer species, and adding of monomers to growing chains (Overett M.J. et al., 2000, Davis B.H., 2001, Gaube and Klein, 2008, Teng B. et al., 2005).

2.9.3.1 Alkyl mechanism.

The most common mechanism accepted for chain growth in Fischer-Tropsch synthesis reaction is a Alkyl mechanism as shown in the **Figure 2.3**, in this mechanism the chain initiation occurs by dissociation of adsorbed CO to surface C and O atoms, Surface C hydrogenate by adsorbed H₂ to yielding in a successive reaction CH₂ and CH₃ surface species, Where the chain initiator is CH₃ surface species and the monomer for reaction scheme is CH₂ surface species, Then the Chain growth is thought to take place by consecutive combination of methylene surface species (CH₂), then, α-olefins is generate by elimination of β-hydride, or alkanes generation by reduction of surface hydride at termination (Overett M.J. et al., 2000).

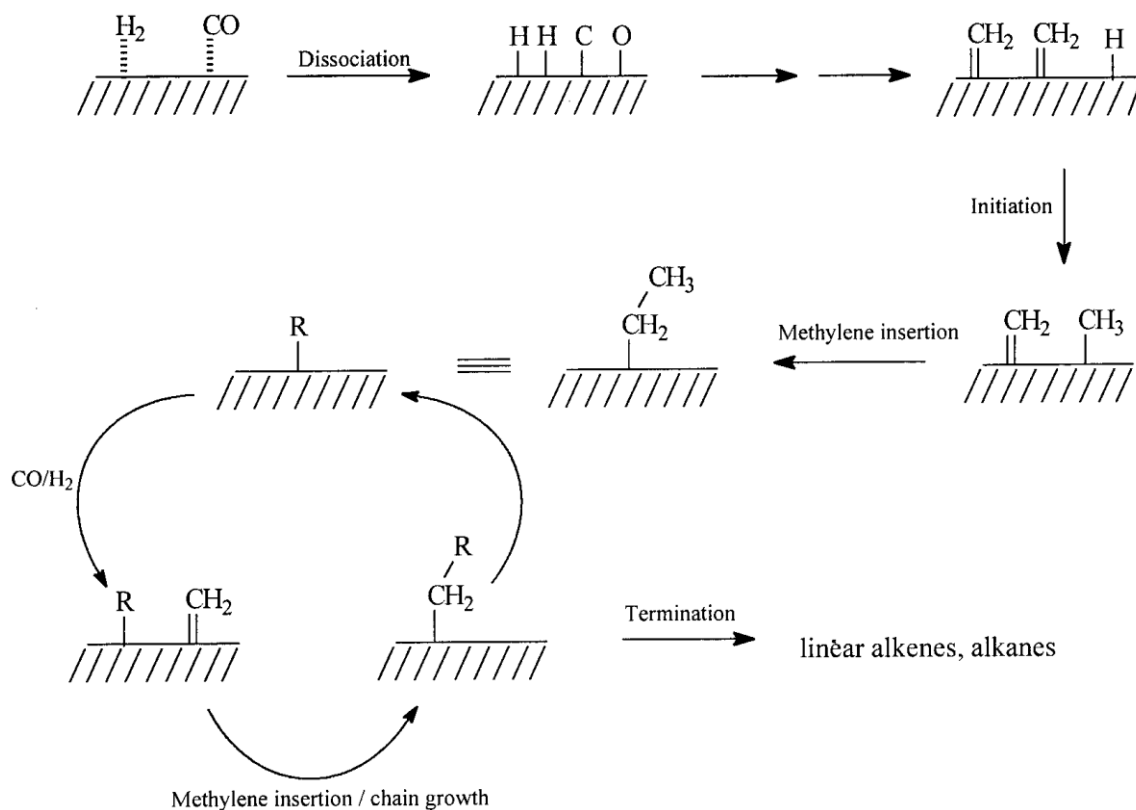


Figure 2.3 Alkyl mechanism.

2.9.3.2 Alkenyl mechanism.

In the alkenyl mechanism as shown in **Figure 2.4**, the surface methylene species is taken into account as a monomer unit which reacts with surface methyne to generate surface vinyl species ($-\text{CH}=\text{CH}_2$) by reaction initiated, then the chain growth occurs by reaction of vinyl species with the monomer unit ($=\text{CH}_2$) to generate an allyl species ($-\text{CH}_2\text{CH}=\text{CH}_2$), then Alkenyl species ($-\text{CH}=\text{CHCH}_3$) formed as a results of allyl species Isomerization, Sequentially the reaction between surface hydrogen and the surface alkenyl species generating α -olefins at Chain termination (Ail and Dasappa, 2016).

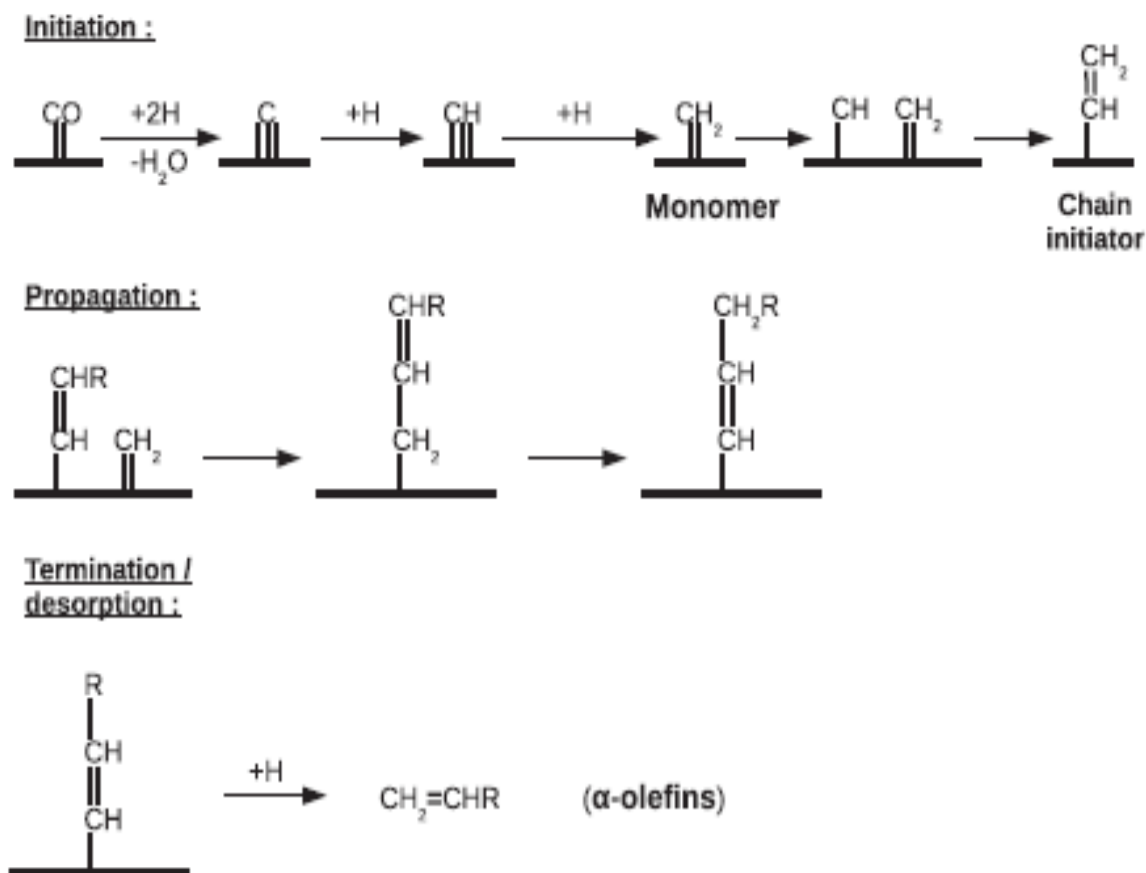


Figure 2.4 Alkenyl mechanism.

2.9.3.4 CO-insertion mechanism.

In this CO-insertion mechanism as shown in **Figure 2.6**, the adsorbed CO is proposition as the monomer and the surface methyl species as a chain initiator, as a result insertion of CO in the metal-alkyl bond the surface acyl species is formed and lead to growth of chain, enlarged alkyl species are formed will causing removal of O₂ from the surface species, the chain termination is occur, and the aldehydes and alcohols were formed due to existence of oxygenated compounds in this step (Teng B. et al., 2005, Ail and Dasappa, 2016).

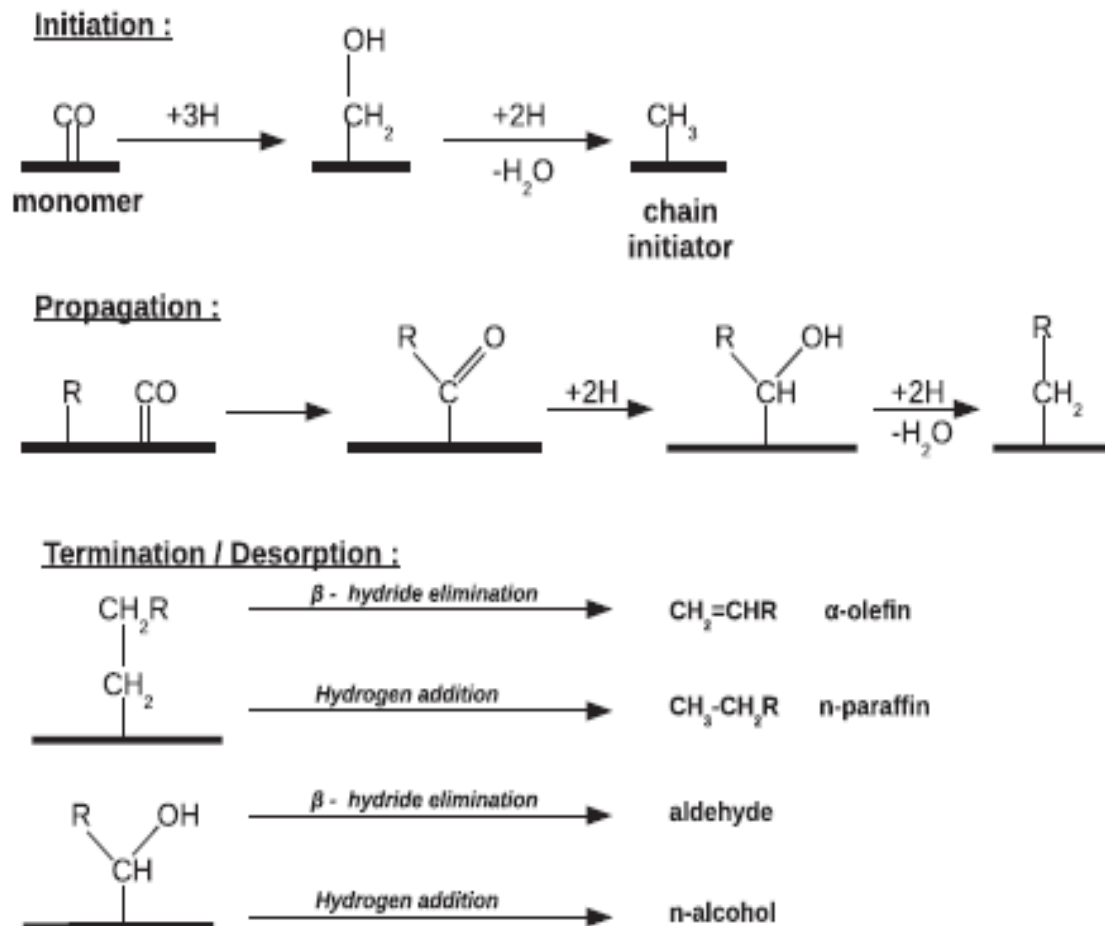


Figure 2.6 CO-insertion mechanism.

2.9.4 Product distribution or (product selectivity).

The distribution of the resultant carbon containing products in FT synthesis is usually denoted to as the product selectivity (Steynberg and Dry, 2004). In the latest period, several studies on FTS were focused on the dependence of the chain length distribution of hydrocarbons on catalyst type and reaction conditions. If the hydrocarbon chain is formed stepwise by insertion or addition of C_1 intermediates with constant growth probability, then the chain length distribution is given by the ASF distribution equation (2.24) (Patzlaff J. et al., 1999). The products can be described by a single parameter, the chain growth probability or growth factor or α (Rafiq M.H. et al., 2011, Schulz and Claeys, 1999):

$$W_n = (\ln^2 \alpha) n \alpha \quad (2.24)$$

Where:

W_n = weight fraction of the products.

n = carbon number.

α = chain growth probability or growth factor.

The logarithmic form of this kinetic expression is shown below in equation (2.25):

$$\log W_n/n = \log(\ln^2 \alpha) + n \log \alpha \quad (2.25)$$

Where:

W_n/n = mole fraction.

According to the equation (2.25), a plot of $\log W_n/n$ versus n should give a straight line (ASF plot). Nevertheless, in practice, the “ideal” molecular weight distributions were ever detected. The common studies on ASF plots showed a nearly straight line only in the C_4 – C_{12} region (Rafiq M.H. et al., 2011). The most common parameter effect on product distribution are temperature, pressure, GHSV or WHSV and H_2/CO as describes below (Pour A. N. et al., 2008a).

2.9.4.1 Parameter Effect on the catalyst activity and product selectivity of F-T Reaction.

The catalyst activity (CO conversion) and product selectivity of Fischer - Tropsch reaction are influenced by the process conditions, such as reactor temperature, space velocity, feed gas composition (H₂ to CO ratio), and pressure (Dry M. E., 1996). These parameters are discussed below.

2.9.4.1.1 Temperature.

One of the most significant parameters influenced on Fischer – Tropsch process is temperature because of the exothermic nature of its reaction. In this way, the temperature should be deliberately controlled and kept up within a constant range in order to stay away from temperature runaways that can prompt the transcendent arrangement of methane and fast catalyst deactivation (Steynberg A. and Dry M., 2004). It has been reported the conversion of Carbone monoxide (CO) was increased as a result reaction temperature was increased, which will lead to growth of reaction rate. As well as, the composition product shifts towards the production of methane and low molecular weight compounds, i.e. the average chain length of the products decreases (Osa A.R. et al., 2011c, Osa A.R. et al., 2012, Najafabadi A., 2016).

2.9.4.1.2 Pressure.

Pressure is an important parameter as it delivers a significant effect on product selection, increase of reaction pressure, leading to an increase in the CO conversion and the long chain hydrocarbons is likely to form that could possibly condense and saturate the catalyst pores by liquid product

(Choudhury and Moholkar, 2013b). The increase in pressure preferred to the formation of C₈₊ to C₁₁₊, while methane and other gaseous hydrocarbons decreased with an increase in pressure (Mohanty P. et al., 2011). In general, C⁵⁺ hydrocarbon selectivity increases obviously with increasing reaction pressure (Hayakawa H. et al., 2007, Farias F.E.M. et al., 2010).

2.9.4.1.3 H₂/CO Feed Ratio.

The H₂/CO ratio plays a vital role in higher hydrocarbon synthesis, it can affect both reaction rates and activity (Mohanty P. et al., 2011). At high H₂/CO ratio lead to decreases the yield of high molecular-weight hydrocarbons and low-molecular-weight hydrocarbons are increasing, chiefly methane (Yates and Satterfield, 1992).though, at lower ratio the conversion and the CH₄ selectivity decreased, however the C⁵⁺ selectivity and the olefin/paraffin ratio for C₂–C₄ increased. (Tristantini D. et al., 2007, Najafabadi A., 2016), the H₂/CO equal 2 is most commonly used for cobalt based catalysts in order to reach a good activity in the Fischer-Tropsch reaction, while, the much lower than 2 used iron based catalysts due to their high WGS activity (Steynberg and Dry, 2004).

2.9.4.1.4 Space velocity.

Space velocity (SV) one of the main process conditions in Fisher-Tropsch reaction was focused about its influence by many studies, space velocity can be specified in terms of gas hourly space velocity (GHSV) or weight hourly space velocity (WHSV), which can be calculated as follows.

$$GHSV = \frac{\dot{V}}{V_r \text{ or } V_{cat.}} \quad \text{Unit is } (h^{-1}) \quad (2.26)$$

Where:

\dot{V} = Volumetric flow rate of feed (m^3/h).

V_r or $V_{\text{Cat.}}$ = Volume of reactor or catalyst (m^3).

$$WHSV = \frac{\dot{m}}{m_{\text{cat.}}} \quad \text{Unit is } (\text{h}^{-1}) \quad (2.27)$$

Where:

\dot{m} = mass flow rate of feed (Kg /h).

$m_{\text{cat.}}$ = mass of catalyst.

Since, space velocity has inverse proportionality with a residence time of reaction, conversion of carbon monoxide was decreased at increased GHSV, where, the selectivity to $\text{C}_1\text{--C}_4$ light hydrocarbons were increased and the selectivity to C_{5+} decrease (Osa A.R. et al., 2011 c), while (Rafiq M.H. et al., 2011) described the conversion of synthesis gas, selectivity of methane and $\text{C}_1\text{--C}_4$ light decreased, while the selectivity and productivity to C_{5+} increased with an increase of GHSV. On the other hand, (Mohanty P. et al., 2011) who noted carbon monoxide conversion decreases and hydrocarbon selectivity increased as result space velocity was increased at a specific value, then liquid hydrocarbon fraction (C_{8+}) decreased as the space velocity was further increases in space velocity.

2.9.5 Fischer-Tropsch Reactors.

A various types of commercial scale reactors (multi-tubular fixed-bed reactor; bubble column slurry reactor; bubbling fluidized-bed reactor; three-phase fluidized bed reactor; and circulating fluidized-bed reactor), have been considered in the history of FTS process development. (Rahimpour and Elekaei, 2009a, b). These early reactor types are the following (Sie and Krishna, 1999).

- ❖ A fixed-bed reactor with internal cooling operated at high conversion in a once-through mode. The catalyst was packed in a rectangular box and water-cooled tubes fitted with cooling plates at short distances were installed in the bed to remove the reaction heat. This type of reactor was applied in the atmospheric synthesis process.
- ❖ A multitubular reactor with sets of double concentric tubes, in which the catalyst occupied the annular space, surrounded by boiling water. This type of reactor was applied to gas at medium pressure.
- ❖ Adiabatic fixed-bed reactor with a single bed, large recycle of hot gas which was cooled externally.
- ❖ A fixed-bed reactor with multiple adiabatic beds, inter-bed quenching with cold feed gas, recycle of hot gas and external cooling.
- ❖ Adiabatic fixed-bed reactor with large recycle of heavy condensate passing in up flow through the bed. The liquid recycles stream was cooled externally.
- ❖ Slurry reactor with entrained solid catalyst, large recycle of hot oil and external cooling.

2.9.6 Catalyst Preparation Methods.

The Catalyst can be prepared by numerous sequential steps. Different supported metal and oxide catalysts are prepared by the sequence of impregnation, drying, calcination and activation. A solid catalysts can be prepared by the following methods (Haber J. et al., 1995, Perego and Villa, 1997, Regalbuto J., 2007, Schwarz J.A. et al., 1995).

2.9.6.1 Impregnation.

Impregnation is the most common methods involves in contacting a solid with a liquid containing the components to be deposited on the surface. During impregnation many different processes occur with different rates.

- Selective adsorption of species (charged or not) by coulomb force, van der Waals forces or H-bonds;
- Ion exchange between the charged surface and the electrolyte;
- Polymersation/depolymerisation of the species (molecules, ions) attached to the surface;
- Partial dissolution of the surface of the solid.

Impregnation can be ended by at least 8 different ways.

1-Impregnation by soaking, or with an excess of solution, 2-Dry or pore volume impregnation, 3-Incipient wetness impregnation, 4-Deposition by selective reaction with the surface of the support, 5-Impregnation by percolation, 6-Co-impregnation, 7-Succcessive impregnation and 8-Precipitation-deposition.

2.9.6.2 Precipitation and co-precipitation.

In all precipitations it is essential to wisely control all the details of the process including:

- The order and rate of addition of one solution into the other.
- The mixing procedure.
- The pH and variant of pH during the process.
- The ripening process.

Precipitation includes two distinctive processes, namely nucleation and growth.

In the co-precipitation of a phase connecting two (or several) elements, if one of them is contained in an anion and the second in a cation, the precipitate will have a fixed or at least very inflexible compositions. If both are cations (or both anions) the characteristics of the reactions with a common anion (or cation) of the solution, the solubility constants, and the super saturation values will all be different, and the properties of the precipitate will change with time.

2.9.6.3 Gel formation and related processes.

The gel can be done by a variety of different methods as follow as:

- Chemical reaction, e.g. formation of a tridimensional polymer by alkoxide hydrolysis (sol-gel process) and, more generally, by polymerisation (of an anion, such as molybdate);
- complexation, e.g. with an acid-alcohol such as citric acid ;
- Freeze drying;
- Addition of a gum or a gelling agent (hydroxymethyl cellulose, etc.).

2.9.6.4 Selective removal.

Selective removal is a method used for very few, but important catalysts. Raney Ni is a representative of this group. Starting from a relatively coarse powder of an alloy (e.g. NiAl_x, constituted of several phases in the present practice), one component (Al) is removed by a leaching agent (NaOH) leaving the active agent (Ni) in a relatively highly dispersed form.

2.9.7 Catalyst Characterization.

The characterization of catalyst is carried out to determine catalyst properties such as the surface area and pore size, active phase in the catalyst, moisture retention, and suitable reduction temperatures for the catalyst activation procedures, extent of coke and wax deposition during reaction, etc. Many techniques are used to studied the characterization of catalyst, such as BET surface area, pore diameter and volume determination, and scanning electron microscopy (SEM), X-ray diffraction (XRD), temperature programmed reduction (TPR), temperature programmed desorption (TPD) and thermo-gravimetric analysis (TGA) (Fei J.H. et al., 2004).

2.9.8 Operating Modes.

As mentioned, FTS is technically classified into two categories: HTFT and LTFT processes. The standard for this categorization is the operating temperature of the deduction, which runs between 310-340 °C for the HTFT process and 210-260 °C for the LTFT process (Leckel D., 2009). The mode of FT operation has a significant influence on the nature and composition of the products obtained from the synthesis reaction. LTFT' products are mainly diesel and waxes, whereas HTFT products are mainly alkenes and gasoline (Dry M. E., 1999, 2001).

Chapter Three: Materials and Methods

This chapter describes the strategy that was planned for the experimental work, experiment and analysis laboratory equipment, analytical methods and procedures that are followed for optimization of biogas production by anaerobic digestion process, catalyst preparation and Fischer-Tropsch synthesis reaction.

3.1 Raw materials, experimental and analysis equipment, analytical methods and procedures for biogas production anaerobic digestion Process.

3.1.1 Municipal Solid Wastes (MSW).

MSW typically consists of food waste, garden waste, paper products, plastics, textiles, wood, metals, construction demolition waste and soils. The composition of MSW varies from region to region as it depends upon lifestyle, demographic features and legislation. Table (3.1) shows the different types of materials and their proportions selected to simulate a MSW for laboratory applications at reference percentage 60% and corrected percentage to 100 % degradable material . The MSW was prepared weighting the required amount of the fresh individual, adding a volume of deionized water equals to 24 %wt. of the total amount, and mixing until the moisture distribution appears homogenous (Krishna et al., 2009).

Table (3.1): Materials used for simulating the MSW and its composition.

Material	60 % by Weight	100 % by Weight	Specifications
Garden waste	20	33	Branch and leaves size less than 1 mm wide and 12 mm long
Vegetable Waste	10	17	Greens (approximately cut into 6.33 mm size)
Meat	5	8.5	Ground beef
Cellulose Non-paper Material	5	8.5	White wheat bread (size less than 7-10 mm)
Paper Waste	20	33	Plain paper shredded (Approximately less than 3 mm wide by 25 mm long)

3.1.2 Giant reed (GR).

Giant reed (*Arundo donax*) was collected from Torre Lama (Campania, Italy) agro-land. The leaves were separated from stems, washed, dried overnight at 80⁰C and minced with a chopper. The powder was perpetrated in by steam explosion at 210 °C for 6 min in the ENEA Research Center of Trisaia (Matera, Italy).

3.1.3 Inoculum.

Sewage sludge was obtained from a primary sludge digester of a municipal wastewater treatment plant of Nola (NA), Italy. Firstly, the anaerobic consortium was adapted to a synthetic medium containing D-glucose 10 g/L as sole carbon source, supplemented with (Na_2HPO_4 7.0 g/L, KH_2PO_4 3.0 g/L, NaCl 0.5 g/L, NH_4Cl 1.0 g/L), the two phosphate salts Na_2HPO_4 and KH_2PO_4 , in addition to being a source of phosphorus, acting as a buffer for pH fluctuations to maintain the values close to neutrality, while sodium chloride instead serves to adjust the osmotic pressure to maintaining the solution isotonic and the ammonium chloride is the source of nitrogen, then the saline solution ($\text{CuSO}_4 \cdot 5\text{H}_2\text{O}$ 0.125 g/L, $\text{ZnSO}_4 \cdot 7\text{H}_2\text{O}$ 0.72 g/L, $\text{MnCl}_2 \cdot 4\text{H}_2\text{O}$ 0.50 g/L, CaCO_3 1.0 g/L, MgSO_4 62.09 g/L, $\text{FeSO}_4 \cdot 7\text{H}_2\text{O}$ 4.75 g/L, $\text{CoSO}_4 \cdot 7\text{H}_2\text{O}$ 0.14 g/L, H_3BO_3 0.03 g/L and 37% HCl 25.6 mL) provides the trace elements were added that is necessary for microbial growth. Resazurin (0.025% w/v) was also added as anaerobiosis indicator (Toscano et al, 2013). The microbiological consortium obtained was used as inoculum.

3.1.4 Trace elements.

Metal compounds (NiCl₂.6H₂O, ZnSO₄.2H₂O and CoSO₄.7H₂O) were weighted and added directly into the batch bioreactors, according to the desired amount of elements Ni, Zn and Co, the weight of each compound was calculated based on the following equation:

$$CE = \frac{WC \times \left(\frac{Mi}{Mc}\right)}{V} \quad (3.1)$$

Where:

CE= Concentration of desired elements (mg/L).

WC = Required weight of compound (mg).

Mi = Molecular weight of the element (g /mole).

Mc = Molecular weight of the compound (g /mole).

V = Working volume (L).

3.1.5 Chemical analysis of the liquid phase producing from anaerobic digestion processes.

The chemical analysis for the liquid phase production from anaerobic digestion after the sample centrifugation at 2200 RPM for 10 minutes and filtration with 0.2 μm cut-off filters, concerns on the estimation of biomass growth (microbial biomass), reducing sugars (colorimetric method) or glucose (enzymatic) and volatile fatty acids and alcohols.

3.1.5.1 Measurement of biomass growth (microbial biomass).

The concentration of biomass is monitored by measuring the optical absorbance of liquid samples at wavelength 600 nm. The concentration of microbial biomass in culture medium, after measurement of the optical absorbance, is calculated in terms of dry biomass (mg/mL) by using a calibration curve relating dried biomass to absorbance at 600 nm as shown in (Appendix C).

3.1.5.2 Measurement of reducing sugars (colorimetric method) or glucose (enzymatic).

The concentration of glucose was measured following a modified Nelson-Somogyi method for reducing sugars (Pirozzi et al., 2013). In the first a standard glucose solution (Stock solution) was prepared by dissolving 100 mg glucose in 100 mL of distilled water in a volumetric flask (to obtaining a concentration of 1 mg / mL). Then 10 mL of a Stock solution diluted by adding 90 mL of water (to obtaining a concentration of 0.1 mg / mL or 100 $\mu\text{g}/\text{mL}$). Subsequently, 0.1, 0.2, 0.3, 0.4 and 0.5 mL of this solution were taken and placed in test tubes, and in each was added distilled water to obtain

a final volume of 2 mL. Then, after adding 1 mL of alkaline copper tartrate solution (see composition in appendix A), the tubes were vortex and placed in a boiling water bath for 10 min. After the tubes were cooling down it was added 1 mL of arsenomolybdate reagent (see composition in appendix A) and then distilled water added to obtain a final volume of 10 mL. Finally, for each sample it was measured the optical density at 620 nm. Then plot a standard calibration curve of OD at 620nm vs. glucose concentration ($\mu\text{g}/\mu\text{l}$) as shown in (Appendix A).

In each test, 0.1 mL sample from the batch reactor was taken and diluted 10 times. Then, 0.2 mL of the diluted sample was placed in a test tube, then distilled water was added to obtain a final volume of 2 mL. Subsequently, after adding 1 mL of alkaline copper tartrate solution, the tube was vortex and placed in a boiling water bath for 10 min. After cooling down it was added 1 mL of arsenomolybdate reagent and then distilled water added to obtain a final volume of 10 mL. Finally, the optical density was measured at 620 nm.

3.1.5.3 Analysis of Volatile Fatty Acids (VFAs) and Alcohols.

The concentration of VFAs (acetic acid, butyric acid, and propionic acid), ethanol and liquid phase composition produced from Fischer-Tropsch synthesis reactions, were determined by GC analysis, using a Shimadzu GC-17A equipped with a FID detector and a capillary column with a PEG stationary phase (BP20, 30 m by 0.32 mm i.d., 0.25 μm film thickness, from SGE). Samples of 1 μL were injected with a split-ratio of 1:10. Helium was fed as carrier gas with a flow rate of 6.5 mL/min. Injector and detector temperatures have been set to 320 $^{\circ}\text{C}$ and 250 $^{\circ}\text{C}$, respectively. The initial column temperature was set to 30 $^{\circ}\text{C}$, kept for 3 min, following a ramp of 10 $^{\circ}\text{C}/\text{min}$ till 140 $^{\circ}\text{C}$, and kept constant for 1 min. The calibration (see in appendix B) of each species we were made by analyzing of different concentration solutions (mg / mL). Each solution was prepared by mixing: 500 μL of sample and 50 μL standard solutions (3.6 mL of distilled water and 40 μL of 1-pentanol). For each sample three tests were carried out.

3.1.5.4 Power of Hydrogen (pH).

pH was measured by using a pH-meter (WTW, Germany). The probe of pH meter was calibrated before each days of pH measurement, by using buffer solutions of pH 4.0, 7.0 and 9.

3.1.6 Chemical analysis of the gas phase (Biogas) production anaerobic digestion processes and gas phase products from FT reaction.

The composition of the biogas (CH_4 , H_2 and CO_2), synthesis gas and produced gas phase from FTS reaction were determined by using gas chromatography analysis, using a HP 5890 (GC) equipped with a thermal conductivity detector (TCD), flame ionization detector (FID) and a molecular sieve capillary column. The calibration curves (see in appendix B) of each species were made by analyzing a different volume percentage (V/V).

3.1.7 Analysis of Total solid (TS), Total volatile solids (TVS), Moisture content and Ash percentage.

TS and TVS, Moisture and Ash percentage of raw material used as degradable material for anaerobic digestion process. Were measured by standard methods 2540B, 2540E (APHA, 2005) as follow as.

The characterization of raw materials (MSW and GR) is shown in table (3.2).

Table (3.2): Characterization of raw materials (MSW and GR).

Properties	Municipal Solid Waste	GR (<i>Arundo donax</i>)
Moisture %	51.4	60.1
Total solid (%)	48.6	39.9
Total Volatile solid (%)	30.5	18.0
Ash %	18.1	21.9

3.1.7.1 Total solid percent (%TS).

A well-mixed sample is evaporated in, a weighed dish and dried to constant weight in an oven at 103 to 105°C. The increase in weight over that of the empty dish represents the total solids. The total solids in percentage of wet samples are calculated as:

$$\% \text{ TS} = \frac{(A-B)}{(C-B)} \times 100 \quad (3.2)$$

Where:

A = weight of the dish (g) + weight of dried residue (g).

B = weight of the dish (g).

C = weight of the dish (g) + weight of wet sample (g).

3.1.7.2 Total volatile solids (%TVS).

The residue from the total solids determination is ignited to constant weight at 550°C. The remaining solids represent the fixed total, dissolved, or suspended solids while the weight lost on ignition is the volatile solids. Total volatile solids are determined as per calculation below. Its determination is useful in the control of biological treatment plant operation because it offers a rough approximation of the amount of organic matter present in the solid fraction of wastes.

$$\% \text{ TVS} = \frac{(A-D)}{(A-B)} \times 100 \quad (3.3)$$

Where:

D = weight of residue (g) + dish after ignition (g).

3.1.7.3 Moisture content.

The moisture content is the loss of weight after drying a sample to a constant value in an oven at 103°C to 105°C. The expression for calculating moisture content as per below is on a wet basis.

$$\% \text{ Moisture} = \frac{(w-d)}{(w)} \times 100 \quad (3.4)$$

Where:

w = initial (wet) weight of sample (g).

d = final (dry) weight of sample (g).

3.1.7.4 Ash.

Its represent the amount of remaining solids percentage in dish after ignited to constant weight at 550°C. The Ash percentage of dry samples are calculated as deference between total solid and total volatile solids percentage as show below:

$$\text{Ash \%} = \%TS - \%TVS \quad (3.5)$$

3.1.8 Batch anaerobic digestion experiments.

Crimped Pyrex bottles with preferable butyl rubber septa, with a working volume of 100 mL, were used as batch reactors. The reactors were filled with substrate, inoculated with specific volume amount of inoculum, then distilled water was added to obtain a total liquid volume of 100 mL. **Figure 3.1** shows a view of the experimental apparatus of the batch anaerobic digester. Anaerobic conditions were ensured by flushing the medium with nitrogen for 20 min, after that the reactors were placed in an electrical furnace at 37°C and 150 rpm.



Figure 3.1 Experimental apparatus of the batch anaerobic digester.

3.1.9 Collection of Producing Biogas.

Each anaerobic digester was connected by a capillary tube to an inverted 125 mL glass bottle, filled with (100mL) water and sealed in the same way as the digesters. To enable gas transfer through the two connected bottles, the capillary tube was equipped at both ends with a needle. **Figure 3.2** shows a view of the experimental apparatus, while, **Figure 3.3** shows the schematic diagram of a biogas collection unit. The biogas volume was measured by weighing the water displaced through a second needle from the inverted glass bottle, the collection glass bottle that was periodically replaced.



Figure 3.2 View of experimental equipment used to measure of biogas production by anaerobic fermentation.

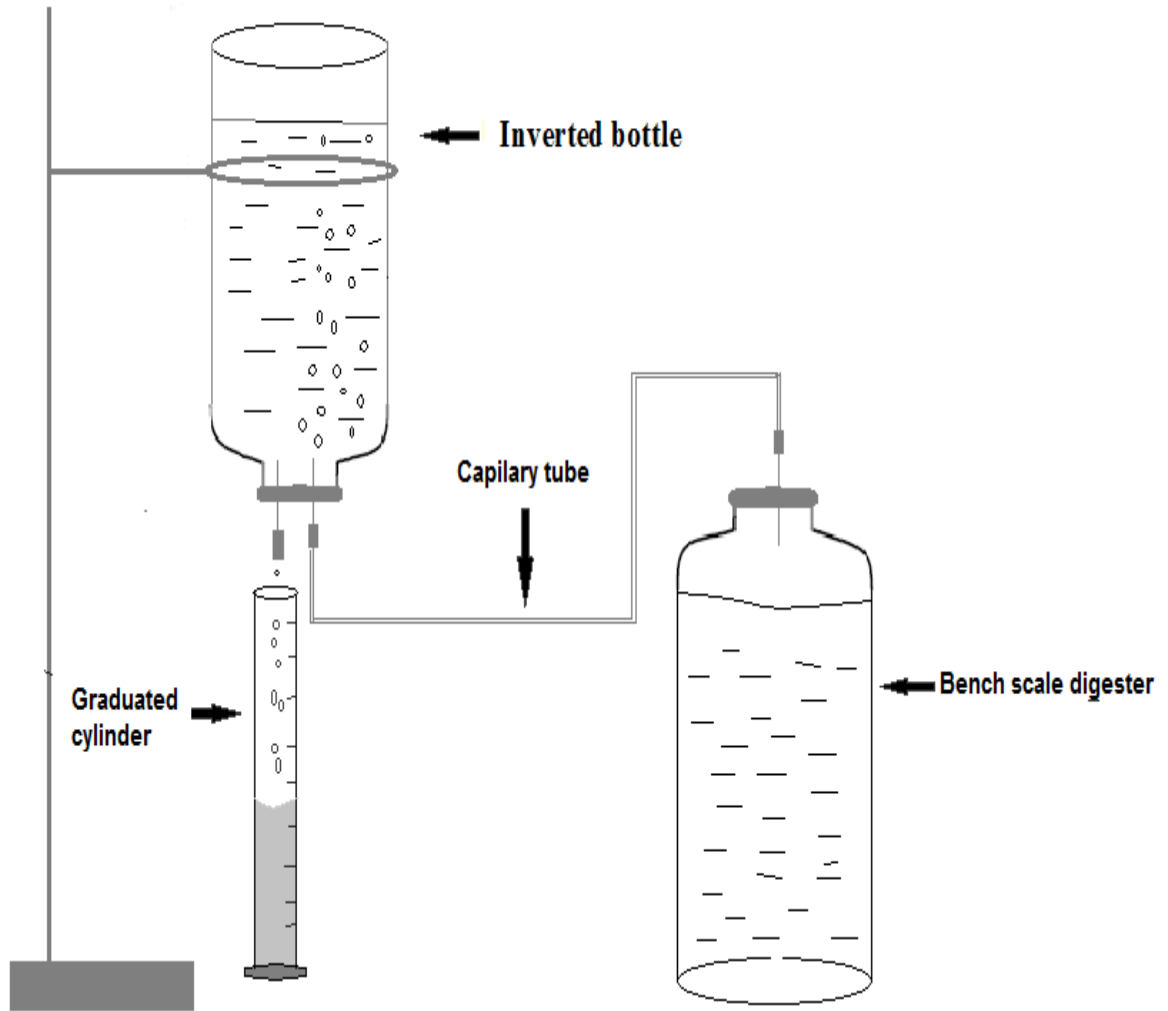


Figure 3.3 Schematic diagram of experimental equipment used to measure of biogas production by anaerobic fermentation.

3.2 Catalyst preparation, experimental and analysis equipment, analytical methods and procedures for Fisher-Tropsch Process.

3.2.1 Fischer –Tropsch catalyst preparation method.

Catalyst is made by 15% wt. of Cobalt dispersed on Alumina support (Yang J. H., et al., 2010) and it was prepared by impregnation technique under vacuum condition according to the following procedure. About 5 g of extruded cylindrical pellets ($d = 2$ mm) of Al_2O_3 were thermal treated in 100 mL/min helium flow at 250 °C for 2 h, then cooled to room temperature and followed by dynamic vacuum for 15 min in a flask of 100 mL. The impregnation was carried out under vacuum to favor the solution penetration into the Alumina pores and to obtain a more uniform dispersion (Micoli L. et al., 2013). After that, an aqueous 4 M Cobalt (II) nitrate hexahydrate ($\text{Co}(\text{NO}_3)_2 \cdot 6\text{H}_2\text{O}$) solution at $T = 40$ °C, was dripped up to complete wetting of the support, with no excess solution as shown in **Figure 3.4**. Afterwards the impregnated support was dried at 120 °C for 12 h and then heated at 400 °C in air flow (6 L/h) for 4 h (Jung I. Y. et al., 2010) favoring the Cobalt oxidation. Then the catalyst was reduced in situ using 6 NL/h of diluted H_2/Ar (2 and 98 % v/v) at 400 °C for 10 h heating rate of 10°C /min and atmospheric pressure.

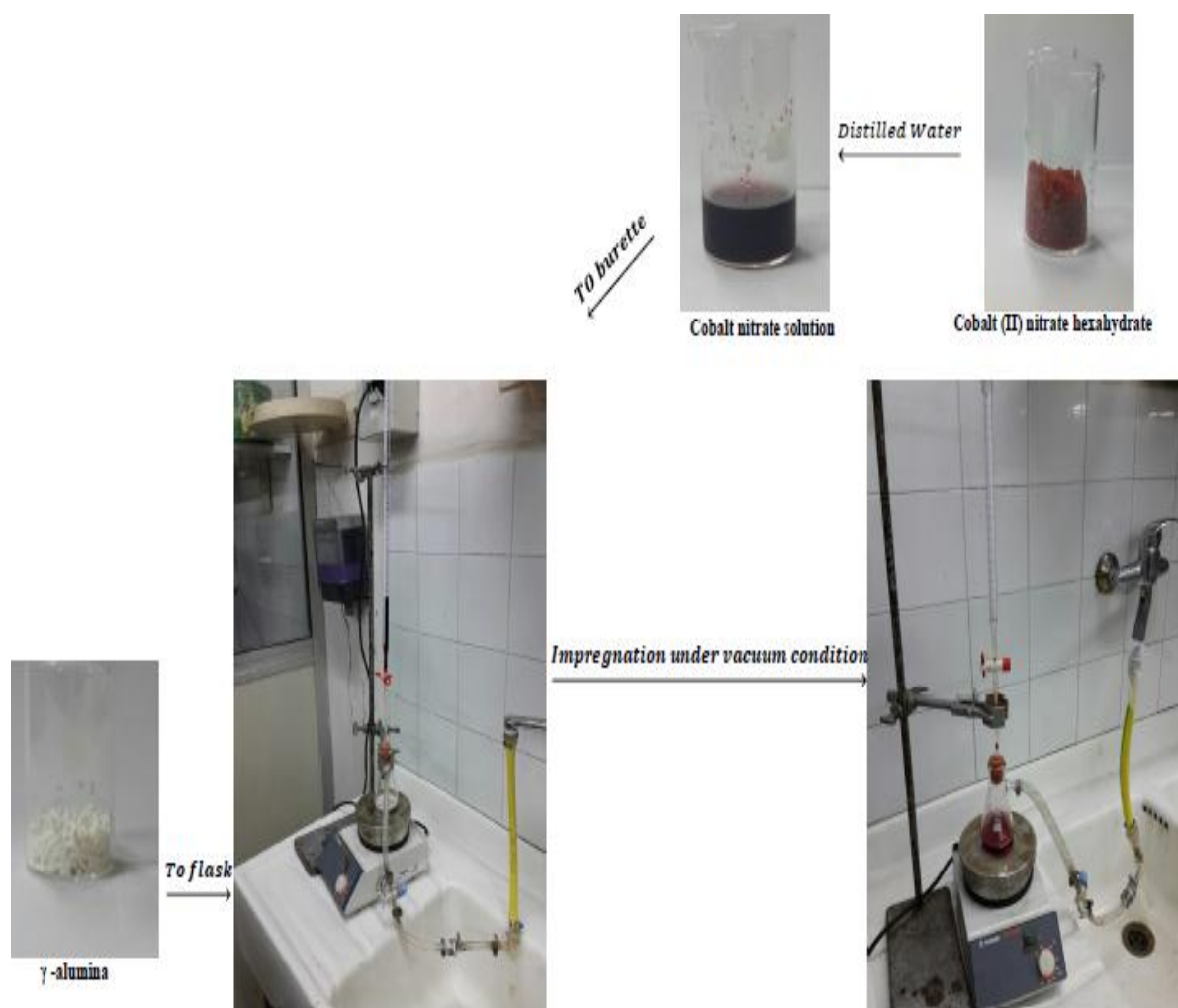


Figure 3.4 Experimental apparatus and procedure for catalyst preparation by vacuum impregnation.

3.2.2 Catalyst characterization techniques.

The characterization of catalyst is carried out to determine catalyst properties such as the surface area and pore size, active phase in the catalyst, moisture retention, suitable reduction temperatures for the catalyst activation procedures, extent of coke and wax deposition during reaction, etc. Many techniques are used to study the characterization of catalyst, such as BET surface area, pore diameter and volume determination, and scanning electron microscopy (SEM), X-ray diffraction (XRD), temperature programmed reduction (TPR), temperature programmed desorption (TPD) and thermogravimetric analysis (TGA) (Fei J.H. et al., 2004).

3.2.2.1 Temperature Programmed Reduction (TPR).

Average Co oxidation state was evaluated by Temperature Programmed Reduction (TPR) measurement using a flow apparatus equipped with a TCD detector (Turco et al., 2011) and a quartz down-flow cell that contained about 100 mg of powder sample (size 90-125 μ m), using 2 % H₂/Ar flow (100 mL/min) and heating rate of 10 °C / min up to 850 °C.

3.2.2.2 Nitrogen adsorption measurement.

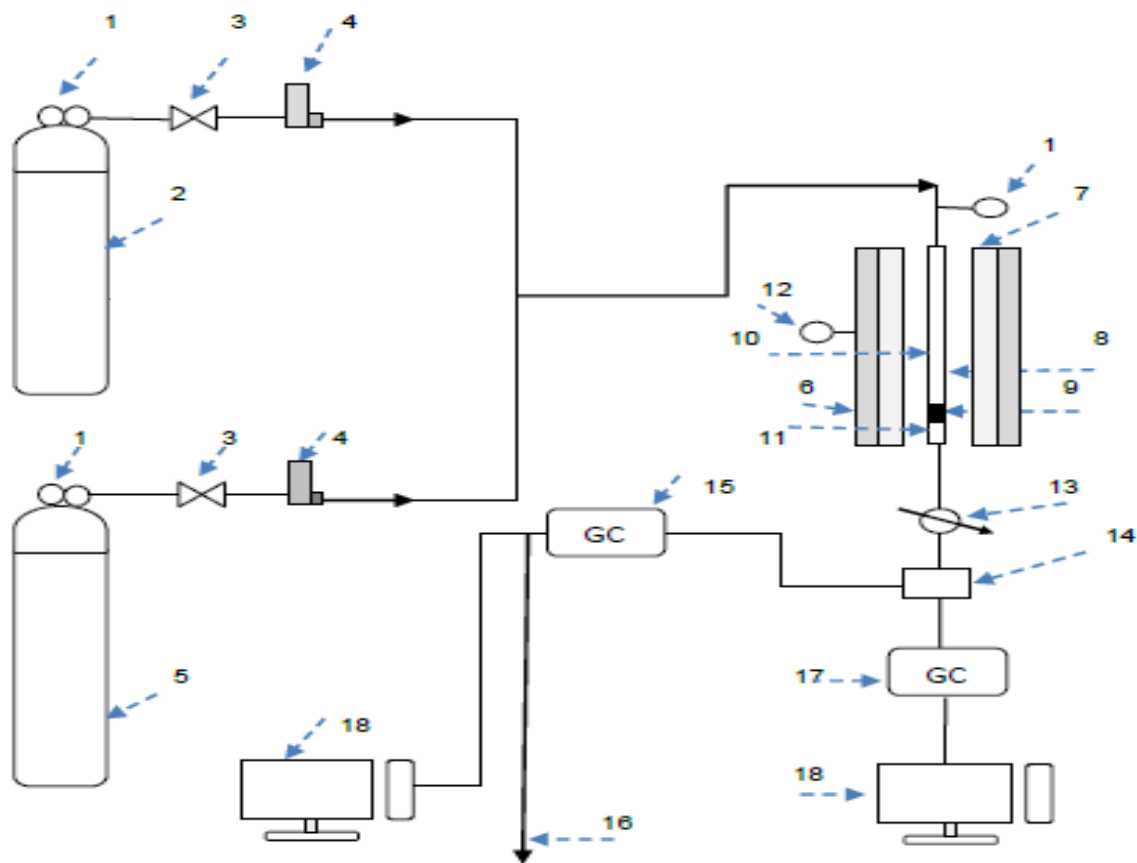
The BET surface area and pore volume for the support and the catalysts were measured by N₂ adsorption at -196 °C by using Micromeritics ASAP 2020 instrument through BET equation. The N₂ adsorption isotherm has been obtained using 50 mg of samples treated at 250 °C under vacuum condition for 2 hours.

3.2.3 Fischer-Tropsch Experimental setup.

The Fischer-Tropsch reaction is carried out in a single fixed-bed reactor (FBR) (pyrex glass pipe, 15 mm internal diameter) as shown a schematic diagram in **Figure 3.5**. The reactor has one gas supply that was used for fed of reduction gas, synthesis gas mixture (CO and H₂) and inert gas (helium) were fed separately and controlled with mass flow controllers (Brooks Instruments Model 5850S), reactor was heated by electrical furnace (Carbolite Furnaces), and the temperature was regulated by a cascade temperature controller, the oven is placed inside an aluminum jacket. The vapor phase products and unreacted reactant gases exit the reactor at the undermost, and go through a cooled trap, the heavy hydrocarbons (C₅₊) and the water were condensed and collected in a condenser working at 0 °C. Since the FT produces a large variety of products, such as paraffins, olefins, alcohols and aldehydes (Liu Y., et al., 2007), a detailed analysis of liquid products results a difficult task. Therefore the liquid phase has been analyzed considering the range C₅-C₁₁, C₁₂-C₂₀, >C₂₀ according to the number of C atoms in the chains (Bukur D. B., et al.,1989, Bukur D. B., et al.,1990, Bukur D. B., et al.,2005, Zimmerman and Bukur, 1990). The uncondensed (Light hydrocarbons) and unreacted gases were leaving the trap and periodically analyzed by on-line gas chromatograph (GC) HP 5890 equipped with a thermal conductivity detector (TCD) and flame ionization detector (FID) (see section 3.1.6), while the condensed liquid in a cooled trap were collected in every end of each test and analyzed through off-line gas chromatograph (GC) Shimadzu GC-17A equipped with flame ionization detector (FID) (see section 3.1.5.3). A sample (five grams) of 15 % calcined Co/AL₂O₃ catalyst were loaded inside the reactor and enclosed between two layers. One of it is glass wool was put at end of the catalyst bed

to prevent the loss of the catalyst and the either is quartz sphere's (D: 1.5 mm) on top of the catalyst bed for preheating a gas reactant mixture and kept isothermal zone; the height of quartz sphere layer is about (5 cm). Before the reduction and Fischer-Tropsch reaction testing, the reactor was pressed with helium gas to test for leaks. Therefore, the system was decompressed to atmospheric and the catalyst was reduced in situ by 2% of the (H₂/Ar) gas at a flow rate 6 NL/h., at 400 °C for 10 hours with heating ramp of 10°C /min and atmospheric pressure. Later on in situ reduction the temperature was depressed to the room temperature in the same gas mixture and with the same flow rate as during the reduction. The helium (He) gas was flow through the reactor at flow rate 2.5 NL/h, prior every Fischer-Tropsch reaction test to set the catalyst bed to the desired reaction temperature(220, 235 and 250 °C) at heating ramp of 10°C /min. Then Synthesis gas mixture was introduced into the reactor at a specified space velocity (GHSV from 370 to 820 h⁻¹) and at a constant H₂: CO ratio of 2:1 with a concentration (4% H₂, 2% CO, 94% He). Diluted feeding conditions were employed in order to guarantee isothermal profile in the reactor.

Thermal treatment was made for the catalyst bed before every change of reaction condition under helium flow rate 2.5 NL/ h at temperature 400 °C for 3 hours, to remove any deposited of carbone atoms on catalyst surface that causes deactivation of catalyst.



- | | | | |
|----|--|-----|----------------------------------|
| 1. | Pressure indicator | 10. | Glass balls |
| 2. | Helium gas cylinder | 11. | Glass wool |
| 3. | Valve | 12. | Temperature indicator controller |
| 4. | Mass flow controller | 13. | Condenser |
| 5. | Gas mixture (H ₂ and CO) cylinder | 14. | Trap |
| 6. | Aluminum jacketing | 15. | Online gas chromatography |
| 7. | Furnace | 16. | Vent |
| 8. | Reactor | 17. | Offline gas chromatography |
| 9. | Catalyst bed | 18. | Computer |

Figure 3.5 Schematic diagram of Fischer – Tropsch reaction System on fixed bed reactor.

3.2.4 Calculation of Fischer-Tropsch Synthesis reactor.

The calculation for Fischer-Tropsch Synthesis reactor include reactant conversion, yield and Selectivity of producing light (C₁-C₄) and heavy hydrocarbon (C₅₊) and yield and Selectivity of producing Carbene dioxide, . These can be calculated from the analysis of inlet and outlet flow rates.

3.2.4.1 Reactant conversion.

The reactant conversion is estimated by the conversion of carbon monoxide and hydrogen according to the stoichiometry of the reaction equations (3.6 and 3.7).

$$\%X_{CO} = \frac{n_{CO_{in}} - n_{CO_{out}}}{n_{CO_{in}}} \times 100 \quad (3.6)$$

Where:

%= Percent.

XCO= Conversion percent of Carbene monoxide towards products.

nCO_{in}=Mole flow rate of Carbene monoxide entering the reactor (mole/h).

nCO_{out}=Mole flow rate of Carbene monoxide leaving the reactor (mole/h).

$$\%XH_2 = \frac{n_{H_2_{in}} - n_{H_2_{out}}}{n_{H_2_{in}}} \times 100 \quad (3.7)$$

Where:

XH₂ = Conversion percent of Hydrogen towards products.

nH_{2in}=Mole flow rate of Hydrogen entering the reactor (mole/h).

nH_{2out}=Mole flow rate of Hydrogen leaving the reactor (mole/h).

3.2.4.2 Product yield.

Yield of producing carbons from Fischer-Tropsch synthesis can be estimated from main reaction products and carbon monoxide entering the reactor as follows.

$$\%YCH_4 = \frac{nCH_4}{nCO_{in}} \times 100 \quad (3.8)$$

$$\%YCO_2 = \frac{nCO_2}{nCO_{in}} \times 100 \quad (3.9)$$

$$\%YC_{2-4} = \frac{\sum nC_{2-4}}{nCO_{in}} \times 100 \quad (3.10)$$

$$\%YC^{5+} = \frac{nC^{5+}}{nCO_{in}} \times 100 \text{ or } = 100 - YCH_4 - YCO_2 - YC_{2-4} \quad (3.11)$$

Where:

YCH_4 = Yield of producing methane.

nCH_4 = Mole of producing methane (mole/h).

YCO_2 = Yield of producing Carbone dioxide.

nCO_2 = Mole of producing Carbone dioxide (mole/h).

YC_{2-4} = Yield of producing hydrocarbon from two to four atoms.

$\sum C_{2-4}$ = mole summation of producing hydrocarbon from two to four atoms

YC^{5+} = Yield of producing hydrocarbon from five and more than atoms.

3.2.4.3 Product selectivity.

Selectivity of producing carbons from Fischer-Tropsch synthesis can be estimated from main reaction products and carbon monoxide conversion as follows.

$$\%SCH_4 = \frac{nCH_4}{nCO_{in} - nCO_{out}} \times 100 \quad (3.12)$$

$$\%SCO_2 = \frac{nCO_2}{nCO_{in} - nCO_{out}} \times 100 \quad (3.13)$$

$$\%SC_{2-4} = \frac{\sum nC_{2-4}}{nCO_{in} - nCO_{out}} \times 100 \quad (3.14)$$

$$SC^{5+} = 100 - SCH_4 - SCO_2 - SC_{2-4} \quad (3.15)$$

Where:

SCH_4 = Selectivity of producing methane.

SCO_2 = Selectivity of producing Carbene dioxide.

SC_{2-4} = Selectivity of producing hydrocarbon from two to four atoms.

$\sum C_{2-4}$ = mole summation of producing hydrocarbon from two to four atoms

SC^{5+} = Selectivity of producing hydrocarbon from five and more than atoms.

Chapter Four: Results and Discussion

This chapter describes the results obtained from laboratory scale experiments of biogas production from MSW by a series of sequential operations: anaerobic digestion under mesophilic conditions and conversion of biogas to hydrocarbons by Fisher-Tropsch synthesis.

The first part of the chapter describes the optimization of anaerobic digestion processes in terms of substrate percentage, inoculum percentage, a percentage of co-digestion of MSW with lignocellulosic biomass, the effect of salt solution addition and trace metals addition. The second part describes the results obtained from catalyst characterization such as (Temperature Programmed Reduction, Nitrogen adsorption measurement) and the effect of two operating parameters such as (Temperature and Gas Hourly Space Velocity) on the performance of Fisher-Tropsch synthesis reaction.

4.1 Optimization of Anaerobic Digestion Process.

4.1.1 Optimization of a total solid percentage for biogas production by anaerobic digestion process form Municipal Solid Waste (MSW).

The effect of Total Solid percentage (TS %) to biogas production was studied by performing a series of biodigestion tests at different values of Total Solid percentage in feed. Total solids content is defined as the weight fraction of solids in the digester. In this study, three batch stirred reactors (125 mL glass bottle with a working volume of 100mL) were filled with different amounts of MSW, in order to obtain different values of TS %. Each reactor was inoculated with 5 mL of inoculum and distilled water to obtain a total liquid volume of 100mL, and sealed by rubber stoppers. Anaerobic conditions were ensured by flushing nitrogen for 20 min. Subsequently, the reactors were placed in electrical furnace at 37°C and 150 rpm for 192 hours. The experimental conditions adopted for the batch tests are summarized in table (4.1).

Table (4.1): Batch tests conditions for the effect of a total solid percentage.

No.	MSW (gm of TS%)	Inoculum (mL)	Distilled water (mL)	Total volume (mL)	Temp. (°C)
1	5	5	90	100	37
2	10	5	85	100	37
3	15	5	80	100	37

4.1.1.1 VFAs production and pH variation.

Figures 4.1a-b-c present volatile fatty acid (acetic, butyric and propionic) and ethanol concentrations as a function of time for the three different amounts of MSW. The production of alcohol, acetic and butyric acid indicates that acetic and butyric fermentations are occurring, causing a decreasing of the biogas yield. The concentrations of butyric acid and acetic acid increase as higher initial amounts of MSW are adopted, due to more organic matter was hydrolyzed and transformed to VFA in the reactors (Yi J. et al., 2014).

The pH decrease observed during the digestion period was corresponding to an increase of VFA concentration in reactors. Suitable amounts of 1 M Na_2HCO_3 solution were added to the digester to keep the pH value within the optimum limit (6.5-7.5) (Liu C. et al., 2008), to avoid the inhibition of methanogenesis occurring under acidic conditions. **Figure 4.2** shows that the pH variations during the digestion period are not significant, though the VFA concentration progressively increases.

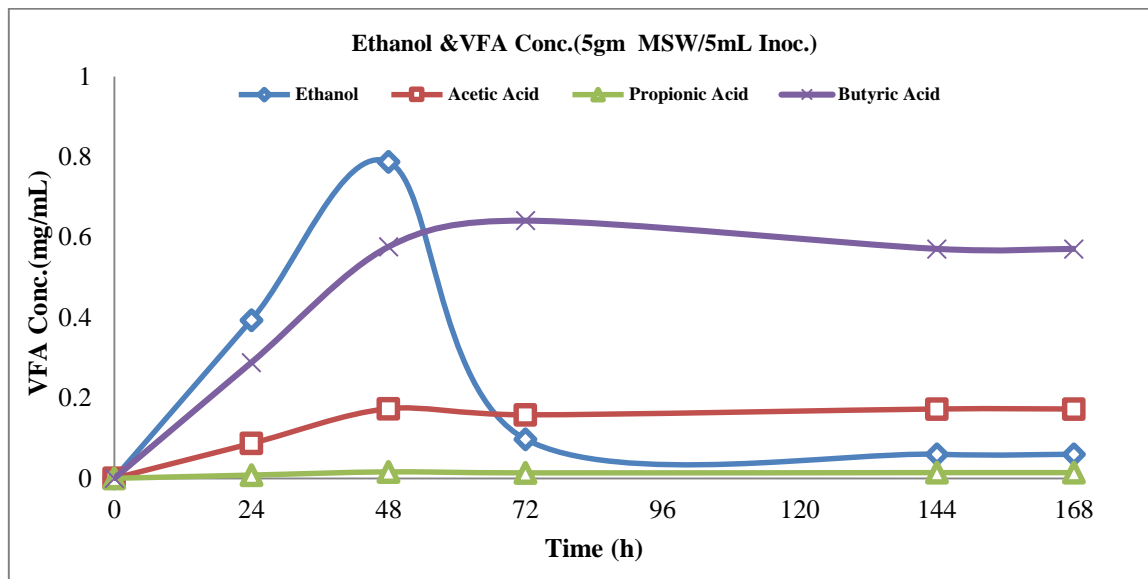


Figure 4.1a VFA variation during digestion at $T = 37^{\circ}\text{C}$, 150 rpm and MSW: 5gm. Products: Ethanol (\diamond), Acetic Acid (\square), Propionic Acid (\triangle) and Butyric Acid (\times), the composition of liquid phase was analysis by GC-17A equipped with a FID detector (see section 3.1.5.3).

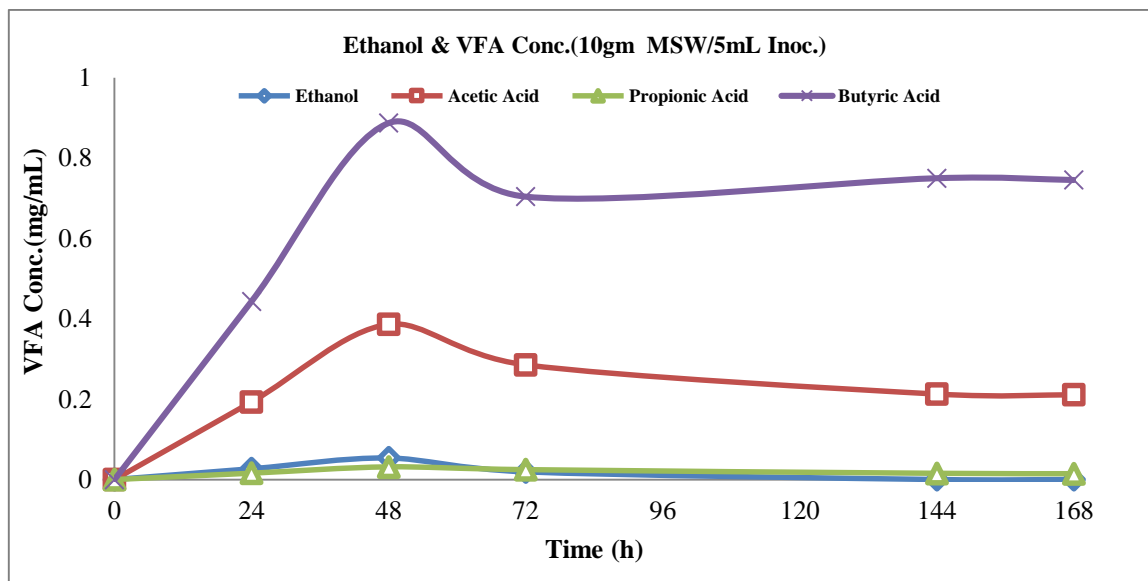


Figure 4.1b VFA variation during digestion at $T = 37^{\circ}\text{C}$, 150 rpm and MSW: 10gm. Products: Ethanol (\diamond), Acetic Acid (\square), Propionic Acid (\triangle) and Butyric Acid (\times), the composition of liquid phase was analysis by GC-17A equipped with a FID detector (see section 3.1.5.3).

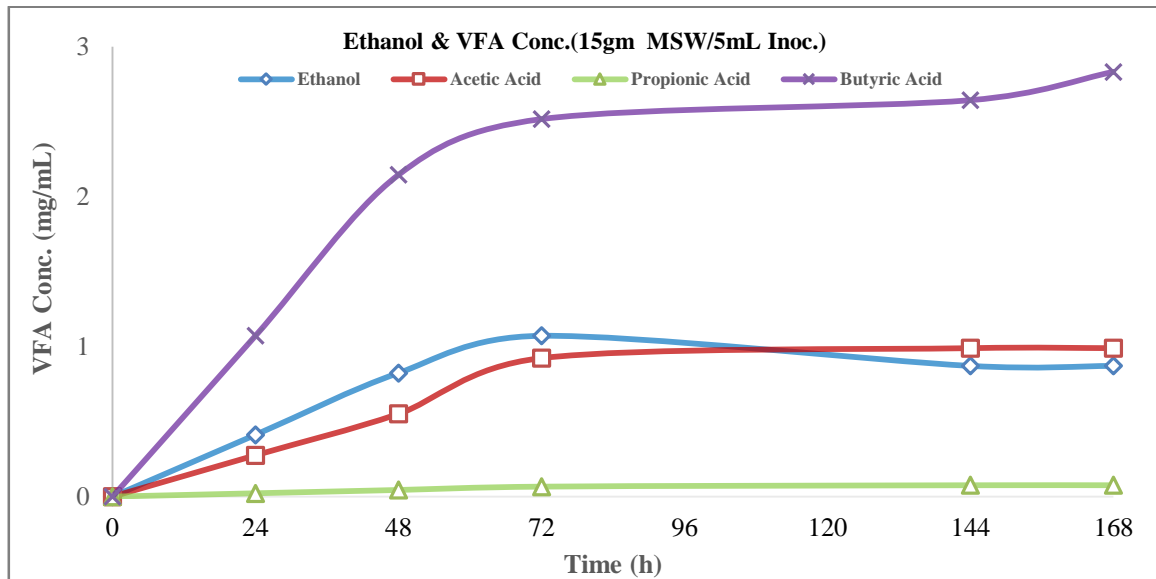


Figure 4.1c VFA variation during digestion at $T= 37^{\circ}\text{C}$, 150 rpm and MSW: 15gm. Products: Ethanol (\diamond), Acetic Acid (\square), Propionic Acid (\triangle) and Butyric Acid (\times), the composition of liquid phase was analysis by GC-17A equipped with a FID detector (see section 3.1.5.3).

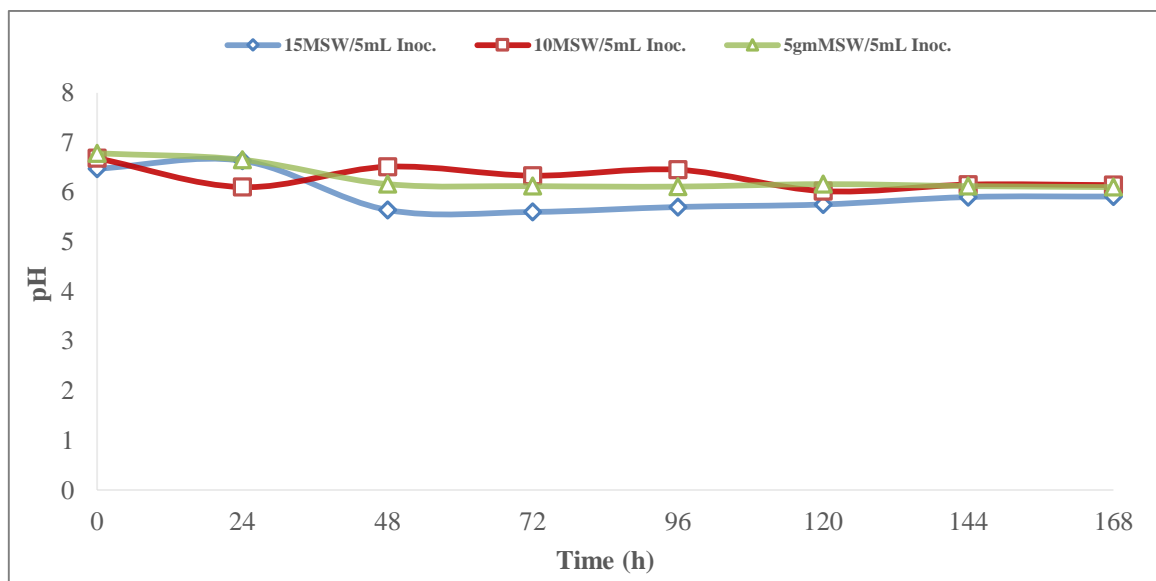


Figure 4.2 pH variation during AD tests at $T= 37^{\circ}\text{C}$, 150 rpm and Feed load: 15 gm. (\diamond), 10 gm. (\square) and 5 gm. (\triangle).

4.1.1.2 Biogas yield.

The effect of TS percentage on biogas production is shown in **Figure 4.3**. Gas production can be significantly affected by the TS content in feedstock and on the biological activity in the anaerobic digester. The best performance for biogas production was obtained when adopting the highest amount of TS (15 %). This behavior is in agreement with the results reported in the Literature, and is likely due to the conversion of accumulative VFAs to biogas (Igoni A.H. et al., 2008, Duan N. et al., 2012). The highest biogas yield was 272 mL after 192 hrs. While the lowest values were 144 and 155 mL attained when the percentage of TS were 5 and 10 respectively. In order to clarify this result, the composition of biogas (CH_4 , H_2 and CO_2) was measured daily as shown in the **Figures 4.4a-b-c**. The maximum fraction of biomethane was obtained during the intermediate phase of the test made with 15% TS percentage.

In the first part of each test, significant volumes of biohydrogen were produced, probably due to the action of the hydrogen-producing bacteria (especially *Clostridium*) contained in the inoculum. While the CO_2 was continued in produced over a digested period on account of the significant production of VFAs, which are converted to CO_2 by fermentation steps.

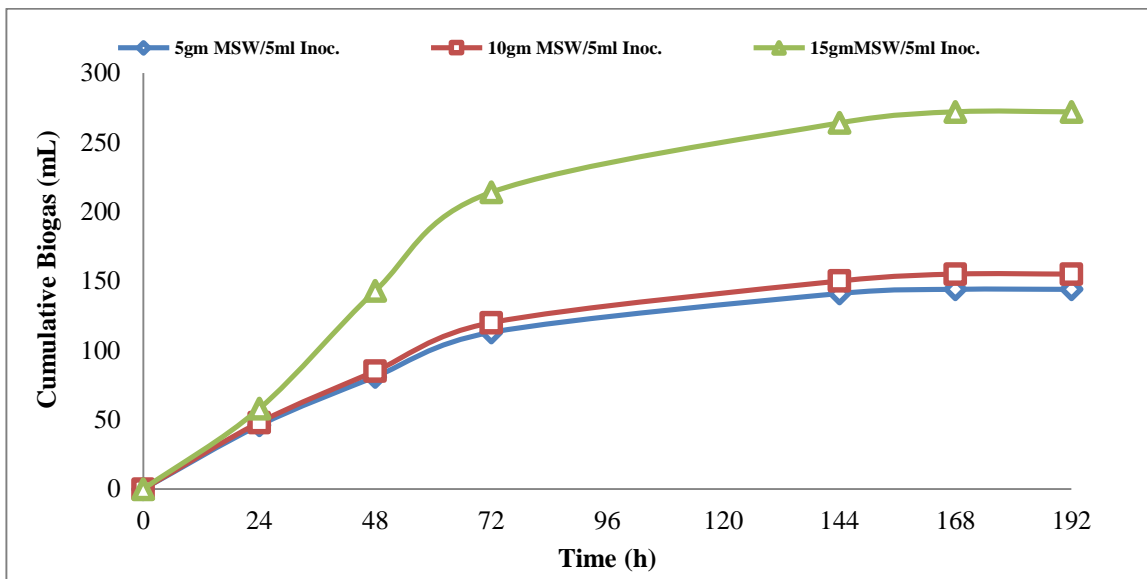


Figure 4.3 Cumulative biogas yield during AD tests at $T= 37^{\circ}\text{C}$, 150 rpm. Feed load: 5gm. (\diamond), 10 gm. (\square), and 15gm. (\triangle).

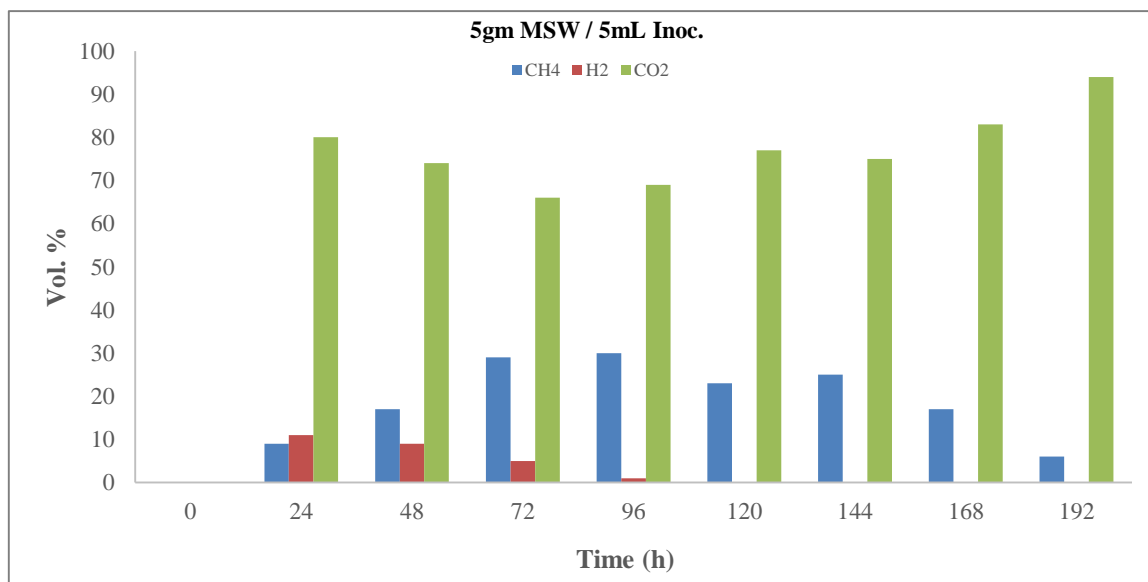


Figure 4.4a Biogas composition during digestion at $T= 37^{\circ}\text{C}$, 150 rpm and MSW: 5 gm., the composition of biogas was analysis by GC-HP 5890 equipped with a TCD detector (see section 3.1.6).

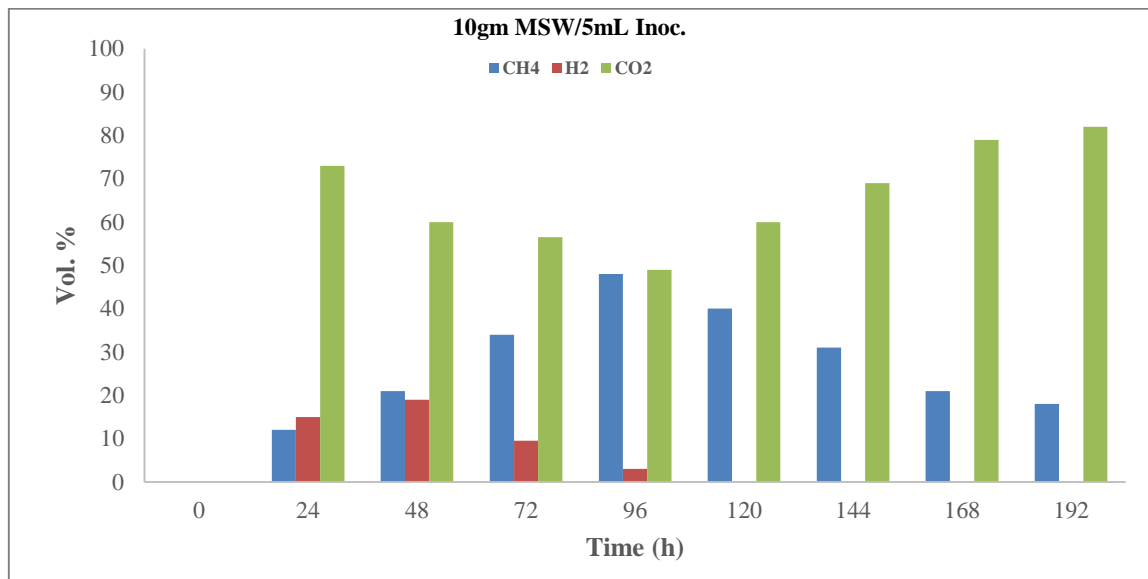


Figure 4.4b Biogas composition during digestion at T= 37°C, 150 rpm and MSW: 10 gm., the composition of biogas was analysis by GC-HP 5890 equipped with a TCD detector (see section 3.1.6).

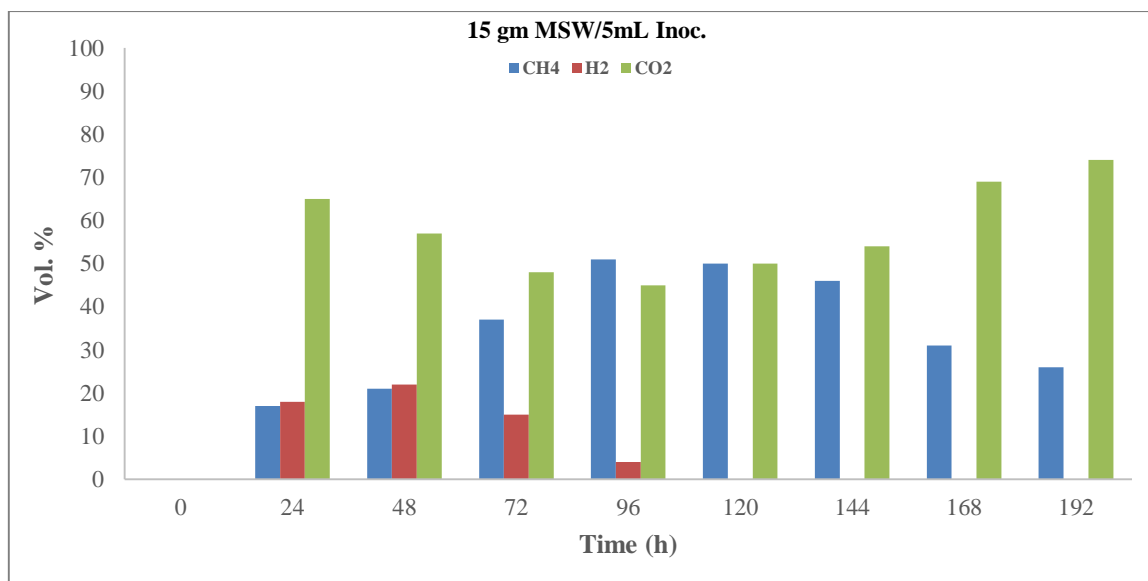


Figure 4.4c Biogas composition during digestion at T= 37°C, 150 rpm and MSW: 15 gm., the composition of biogas was analysis by GC-HP 5890 equipped with a TCD detector (see section 3.1.6).

4.1.1.3 Biomass growth and glucose concentration.

To enhance the efficiency of anaerobic digestion of MSW, it is necessary to grasp the role of the TS contents on the conduct of the microbial community involved in the anaerobic digestion. **Figure 4.5** shows the fluctuations in the biomass concentration during the growth, stationary and decline phases of the digestion period. Throughout the growth process the initial biomass concentration were measured to be about (7.13, 6.74 and 9.41 mg/mL) for 5, 10 and 15 % feed load respectively. The stationary phase and maximum biomass concentration was varied with different feed load. In all instances, the biomass concentration arrived near to zero after about 170 hrs.

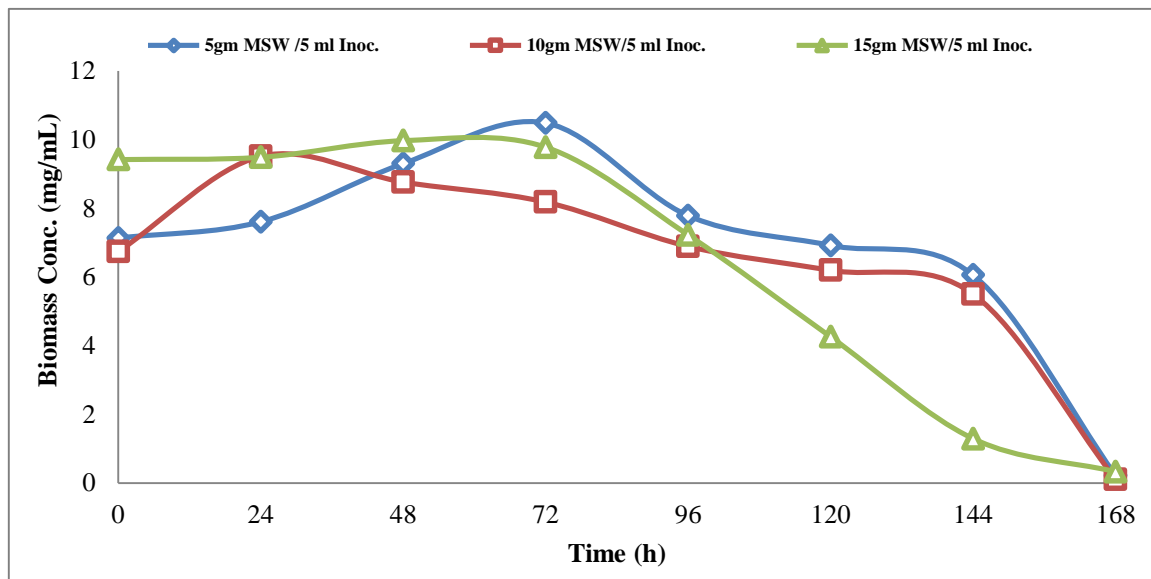


Figure 4.5 Biomass growth during digestion period at $T = 37\text{ }^{\circ}\text{C}$, 150 rpm and feeds load: 5gm. (\diamond), 10gm. (\square) and 15gm. (\triangle).

Figure 4.6 describes the profile of glucose concentration during the anaerobic digestion period. Initial glucose concentrations were (6.67, 7.18 and 8.69 g/L) for 5, 10 and 15 TS%, respectively. In all cases the profiles decrease at the beginning the growth cycle, when an increase of the biomass concentration is observed.

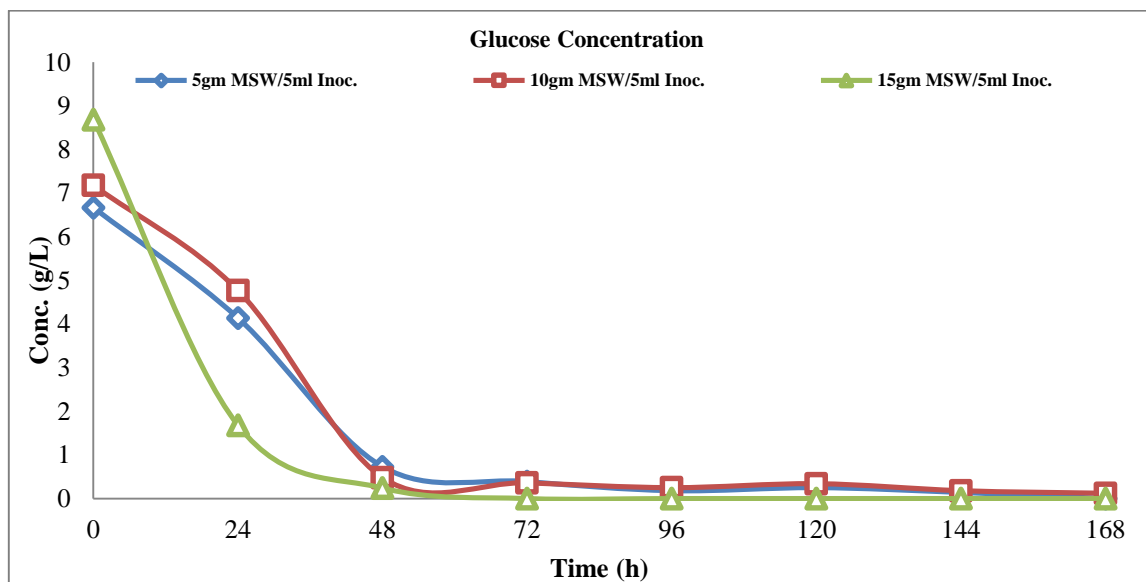


Figure 4.6 Concentration of glucose during digestion period at $T= 37^{\circ}\text{C}$, 150 rpm and feeds load: 5gm. (\diamond), 10gm. (\square) and 15gm. (\triangle).

4.1.2 Optimization of the inoculum for biogas production by solid-state anaerobic digestion of Municipal Solid Waste (MSW).

For this study, three batch stirred reactors (125 ml glass bottle with a working volume of 100ml) were filled with MSW to obtain a 15 % fraction of total solids, using different volumes of inoculum (10, 15, and 20 mL respectively). Distilled water was added to produce a total liquid volume of 100 mL. Anaerobic conditions were ensured by flushing nitrogen for 20 min. Subsequently, the reactors were placed in an electrical furnace at 37°C and 150 rpm for 192 hrs. The conditions of the batch tests are summarized in table 4.2.

Table (4.2): Batch tests conditions for effect of different percentage of Inoculum.

No.	MSW (gm of TS%)	Inoculum (mL)	Distilled water (mL)	Total volume (mL)	Temp (°C)
1	15	10	75	100	37
2	15	15	70	100	37
3	15	20	65	100	37

4.1.2.1 VFAs production and pH variation.

In the **Figures 4.7-a-b-c** the acetic, butyric and propionic acid and the ethanol profiles are shown as a function of time for three different concentrations of inoculum. The production of ethanol, acetic acid and butyric acid indicates that acetic and butyric fermentations are ongoing, causing a reduction of the biogas yield. The high values of the final concentration of butyric acid contributes to inhibit the bacteria that are responsible of the subsequent stages of the process (Mata-Alvarez J., 2003). The sample obtained using a higher amount of inoculum resulted in higher concentrations of VFA.

The pH variations during the digestion period are shown in the **Figure 4.8**. A decreasing behavior of the pH was observed in each test, due to the increase of VFA concentration. Consequently, at regular intervals (24 h), a suitable amount of 1 M Na_2HCO_3 solution was added into the reactor to restore the initial value of pH (7,0), to avoid the inhibition of methanogenesis occurring under acidic conditions.

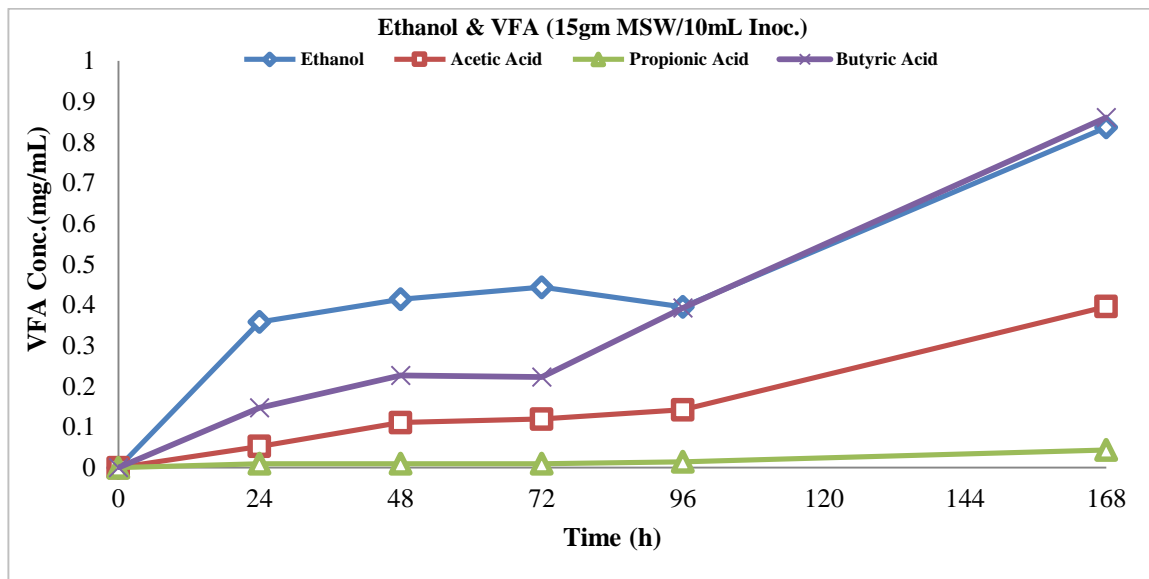


Figure 4.7a VFA variation during digestion at $T= 37^{\circ}\text{C}$, 150 rpm and Inoculum: 10 mL. Products: Ethanol (\diamond), Acetic Acid (\square), Propionic Acid (\triangle) and Butyric Acid (\times), the composition of liquid phase was analysis by GC-17A equipped with a FID detector (see section 3.1.5.3).

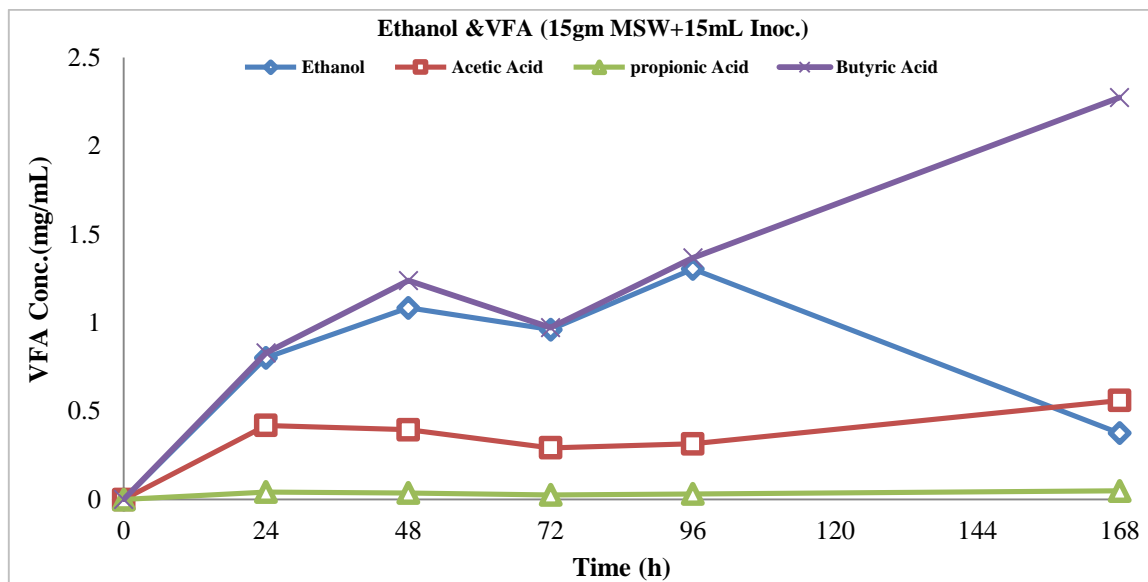


Figure 4.7b VFA variation during digestion at $T= 37^{\circ}\text{C}$, 150 rpm and inoculum: 15 mL. Products: Ethanol (\diamond), Acetic Acid (\square), Propionic Acid (\triangle) and Butyric Acid (\times), the composition of liquid phase was analysis by GC-17A equipped with a FID detector (see section 3.1.5.3).

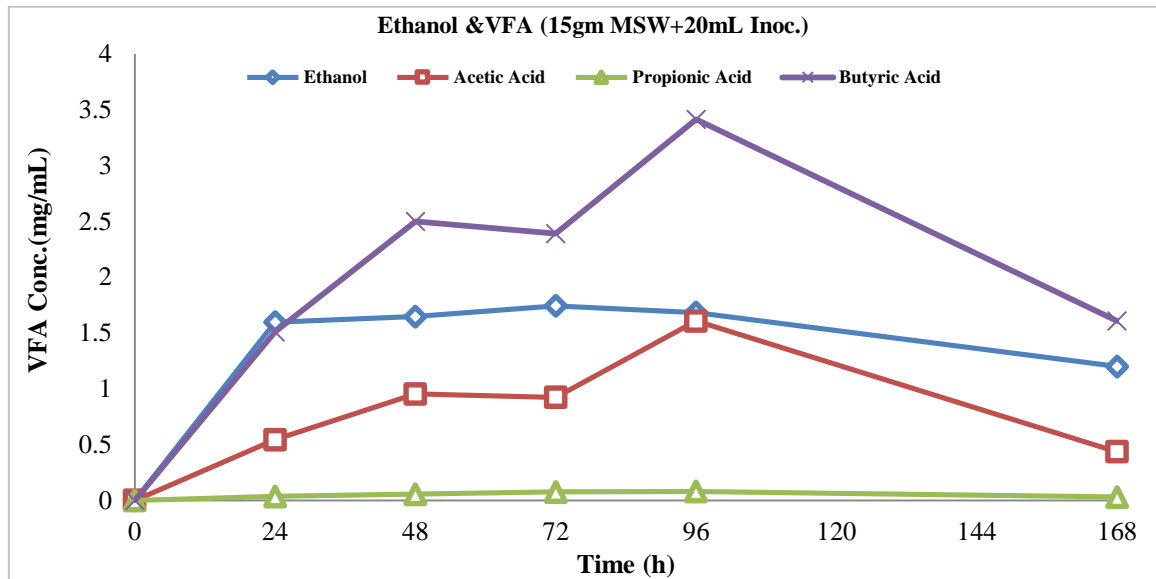


Figure 4.7c VFA variation during digestion at $T = 37^{\circ}\text{C}$, 150 rpm and Inoculum: 20 mL. Products: Ethanol (\diamond), Acetic Acid (\square), Propionic Acid (\triangle) and Butyric Acid (\times), the composition of liquid phase was analysis by GC-17A equipped with a FID detector (see section 3.1.5.3).

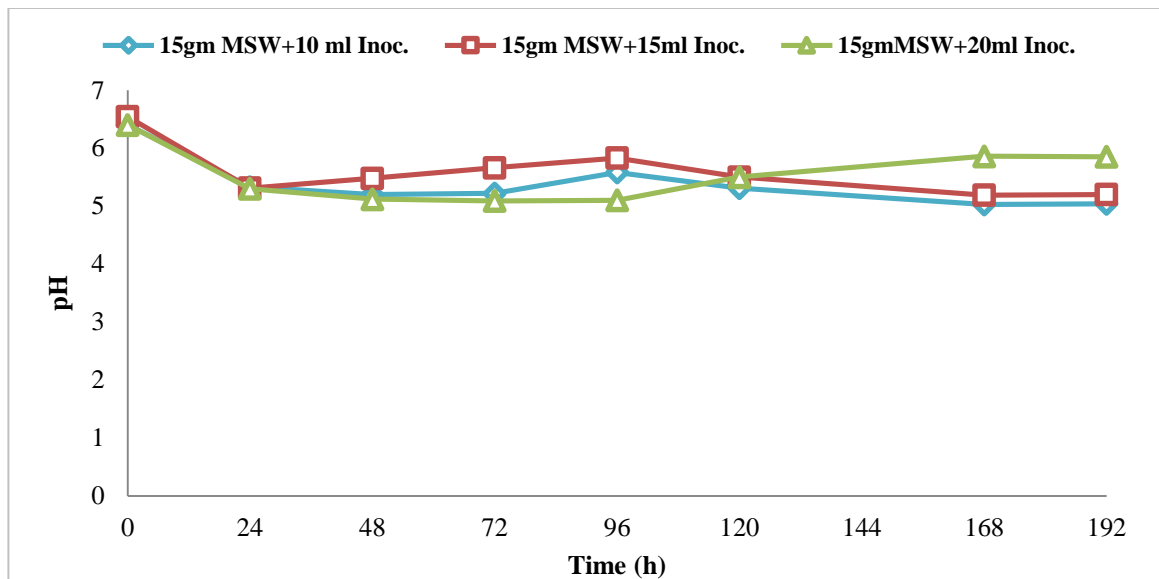


Figure 4.8 pH variation during AD tests at $T = 37^{\circ}\text{C}$, 150 rpm and volumes of inoculum: 10 mL (\diamond), 15 mL (\square) and 20 mL (\triangle).

4.1.2.2 Biogas yield.

The cumulative volumes of biogas are presented in the **Figure 4.9a** whereas the cumulative biogas production per total VS added (specific biogas production) is presented in **Figure 4.9b**. The maximum cumulative volumes of biogas were obtained using the minimum amount of inoculum (10mL). The trends observed are in agreement with the results obtained in another study (Kalloum S. et al., 2014), they found the biogas production from an anaerobic digestion of slaughterhouse waste increased at values of the inoculum-substrate (I/S) ratio decreased. In order to explain this result, we measured the concentration-time profiles of biogas (CH₄, H₂ and CO₂) at different volumes of inoculum (10, 15, 20 mL). The results, shown in the **Figures 4.10a-b-c**, demonstrate that a higher fraction of methane is obtained as the inoculum volume is lower, the trends observed are in agreement with the results obtained in another study (Fernandez B. et al., 2001), they found greatest values of the specific methane produced from an anaerobic digestion for an organic fraction of municipal solid waste (OFMSW) at the lowest values of the inoculum-substrate (I/S) ratio.

A similar tendency was obtained by (Raposo F. et al., 2006) for the maize fermentation under anaerobic conditions, the tests carried out using a range of inoculum to substrate (I/S) the maximum methane production rate was obtained at lower values of the inoculum-substrate (I/S) ratio.

On the basis of the experimental results obtained, it can be said that higher volumes of inoculum do not represent the best choice, as they produce a higher production of VFA (see Figures 4.7a-b-c), and then higher inhibition effects.

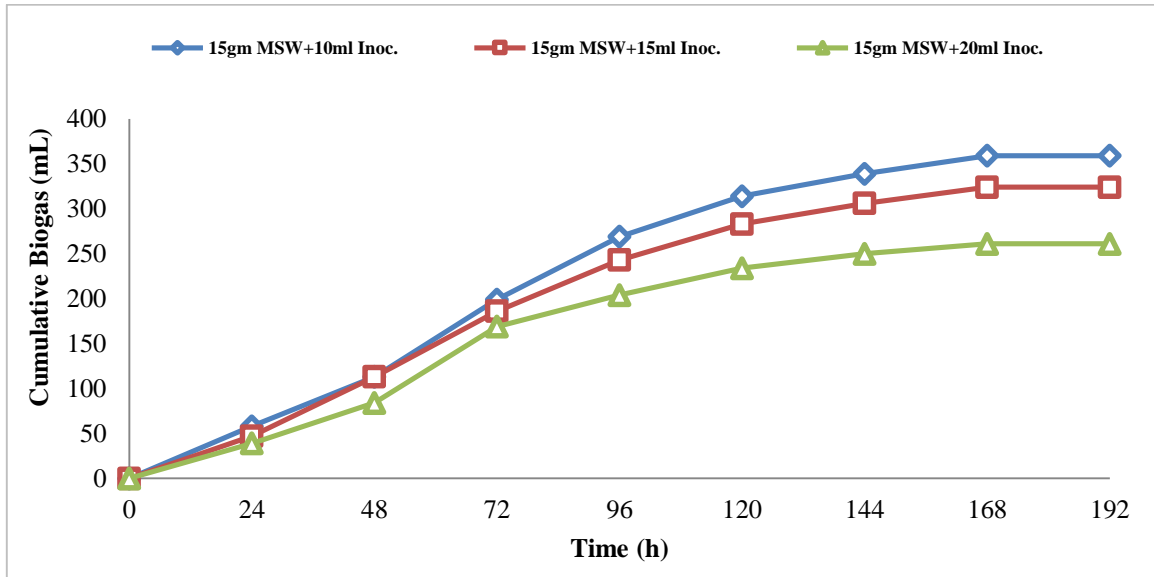


Figure 4.9a Cumulative biogas yield during AD tests at $T= 37^{\circ}\text{C}$, 150 rpm and volumes of inoculum: 10 mL (\diamond), 15 mL (\square) and 20 mL (\triangle).

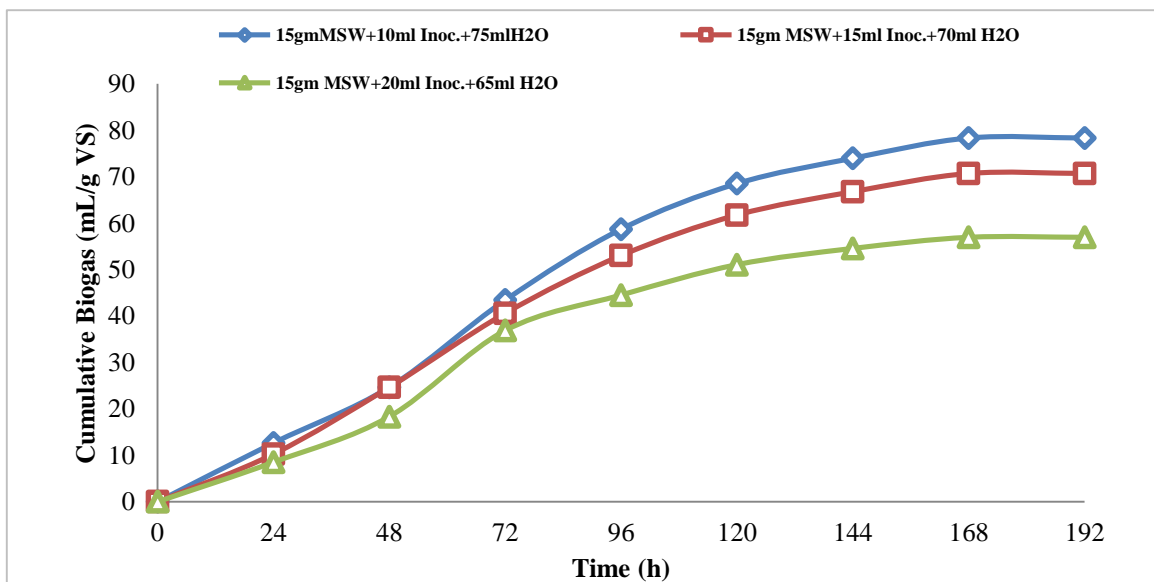


Figure 4.9b Cumulative biogas/gm VS yield during AD tests at $T= 37^{\circ}\text{C}$, 150 rpm and volumes of inoculum: 10 mL (\diamond), 15 mL (\square) and 20 mL (\triangle).

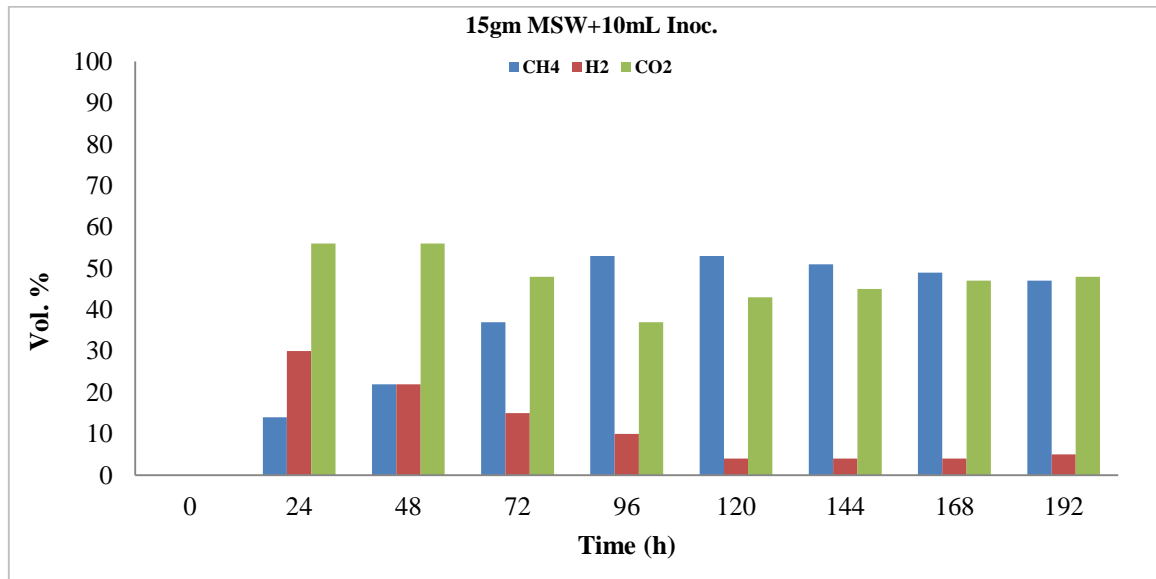


Figure 4.10a Biogas composition during digestion at $T= 37^{\circ}\text{C}$, 150 rpm and inoculum: 10 mL, the composition of biogas was analysis by GC-HP 5890 equipped with a TCD detector (see section 3.1.6).

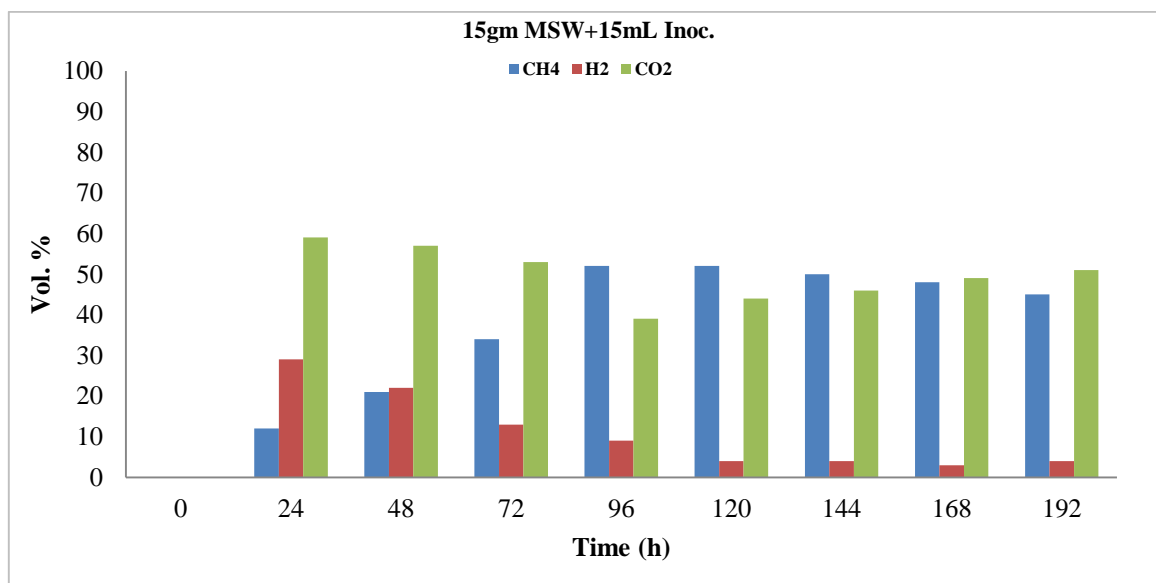


Figure 4.10b Biogas composition during digestion at $T= 37^{\circ}\text{C}$, 150 rpm and inoculum: 15 mL, the composition of biogas was analysis by GC-HP 5890 equipped with a TCD detector (see section 3.1.6).

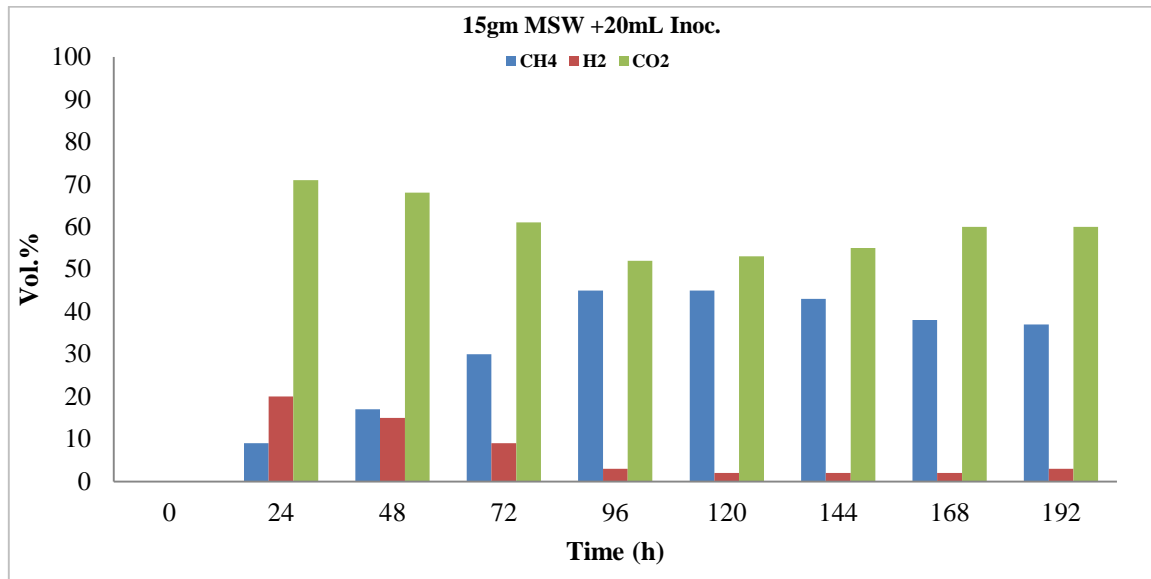


Figure 4.10c Biogas composition during digestion at $T=37^{\circ}\text{C}$, 150 rpm and inoculum: 20 mL, the composition of biogas was analysis by GC-HP 5890 equipped with a TCD detector (see section 3.1.6).

4.1.2.3 Biomass growth and glucose concentration.

The data in **Figure 4.11** describe the growth of biomass during digestion. Firstly the biomass has a rapid increase in the intermediate stage of the digestion (24-96 hours), however, the biomass decreases until it reaches a constant value in the final phase.

The concentration profile of glucose during the digestion is shown in the **Figure 4.12**. The glucose at time zero is partially derived from the synthetic medium used to prepare the inoculum, so the initial concentration of glucose increases when the quantity of inoculum is higher.

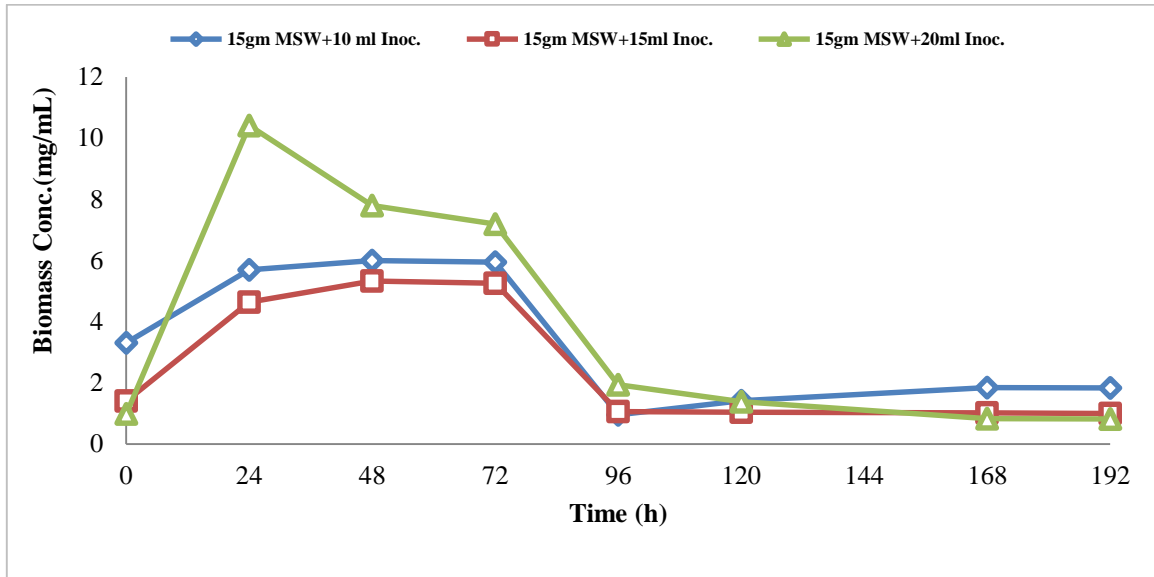


Figure 4.11 Biomass growth during digestion period at $T = 37^{\circ}\text{C}$, 150 rpm and volumes of inoculum: 10 mL (\diamond), 15 mL (\square) and 20 mL (\triangle).

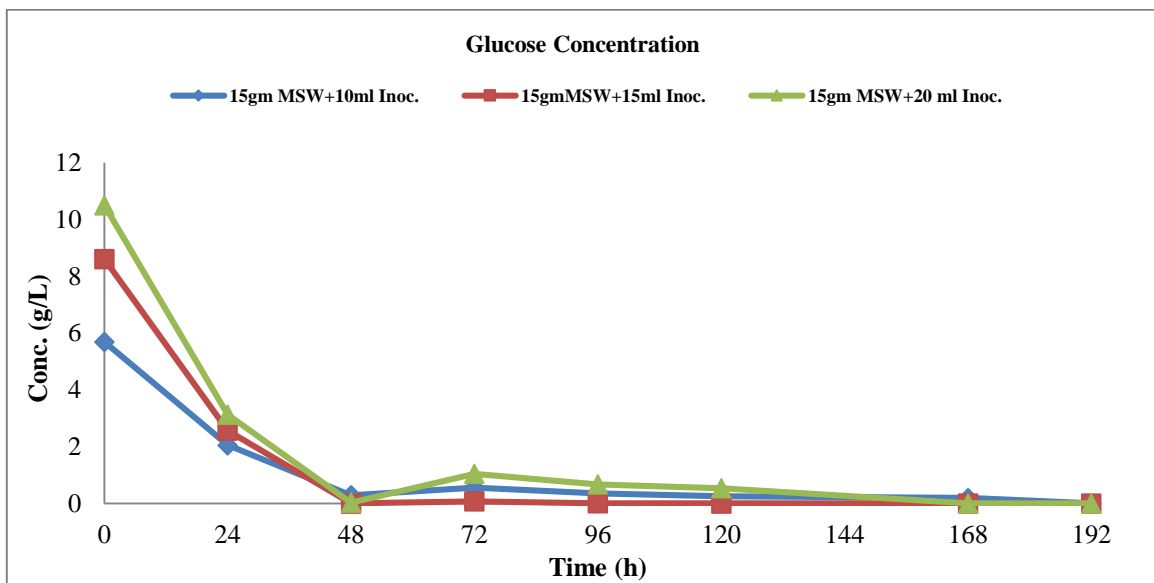


Figure 4.12 Concentration of glucose during digestion period at $T = 37^{\circ}\text{C}$, 150 rpm and volumes of inoculum: 10 mL (\diamond), 15 mL (\square) and 20 mL (\triangle).

4.1.3 Optimization of anaerobic co-digestion of Municipal Solid Wastes (MSW) with lignocellulosic biomasses from Giant reed (GR) under mesophilic conditions.

For this study, five batch stirred reactors (125 mL serum bottles). were filled with 7.5 g TS of a mixture of MSW and GR and inoculated with 5 mL of inoculum, 37.5 mL of distilled water, and finally closed by butyl rubber stoppers with crimped metal seals. Anaerobic conditions were ensured by flushing nitrogen for 20 min. Subsequently, the reactors were placed in an electrical furnace at 37°C and 150 rpm for 384 hrs. (16 days of anaerobic digestion). Mixture compositions adopted for the batch tests are summarized in table (4.3). Final TS content of digestion mixture was 15 % by weight.

Table (4.3): Batch tests conditions for anaerobic co-digestion of Municipal Solid Wastes (MSW) with lignocellulosic biomasses from Giant reed (GR).

No.	Feed load (TS %)	GR%	MSW%
1	15	0	100
2	15	100	0
3	15	25	75
4	15	50	50
5	15	75	25

4.1.3.1 VFAs production and pH variation.

The concentration-time profiles of ethanol and the most abundantly produced VFAs (acetic acid, butyric acid, propionic acid) were analyzed (**Figures 4.13a-b-c-d-e**). The VFA concentrations showed a maximum that was reached in about 24 hrs. Subsequently, a progressive decrease was observed, that was quite fast when using a lower amount of lignocellulosic material (i.e. 25% GR). On the contrary, as the initial fraction of lignocellulosic material was increased, the concentrations of VFAs kept on a higher level for a prolonged time period. This period was as longer as higher amounts of lignocellulosic material were used.

In all instances, acetic acid and butyric acid were the most abundant VFAs. The maximum concentrations of acetic acid (3.6 g/L) and butyric acid (5.6 g/L) were obtained using 75% GR+25% MSW.

During each AD test, a tendency to pH decrease due to VFA production was observed. In order to avoid pH values out optimum limits (6.5-7.5), potentially leading to the inhibition of methanogenesis (Agdag and Sponza, 2007), 1M Na₂HCO₃ of a basic solution was added daily to the reactors. The pH profiles observed in the reactors are described in the **Figure 4.14**. In all instances, the observed pH were in the range 5-8.

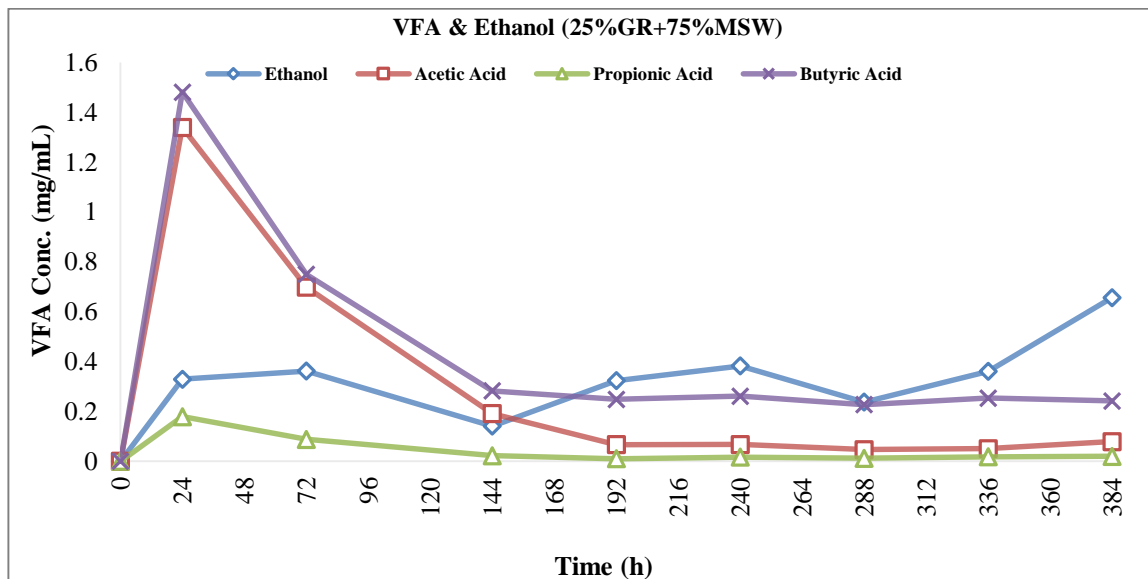


Figure 4.13a VFA variation during digestion period at $T = 37\text{ }^{\circ}\text{C}$, 150 rpm, 15% TS (25% GR+75% MSW) and 10 mL inoculum, where (\diamond) Ethanol, (\square) Acetic Acid, (\triangle) Propionic Acid and (\times) Butyric Acid, the composition of liquid phase was analysis by GC-17A equipped with a FID detector (see section 3.1.5.3).

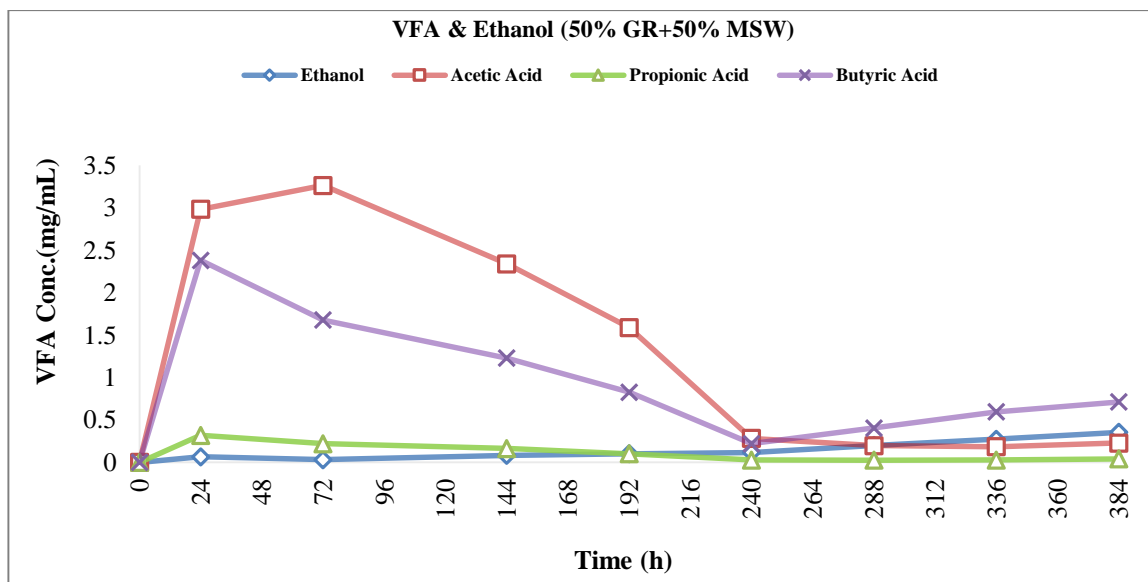


Figure 4.13b VFA variation during digestion period at $T = 37\text{ }^{\circ}\text{C}$, 150 rpm, 15% TS (50% GR+50% MSW) and 10 mL inoculum, where (\diamond) Ethanol, (\square) Acetic Acid, (\triangle) Propionic Acid and (\times) Butyric Acid, the composition of liquid phase was analysis by GC-17A equipped with a FID detector (see section 3.1.5.3).

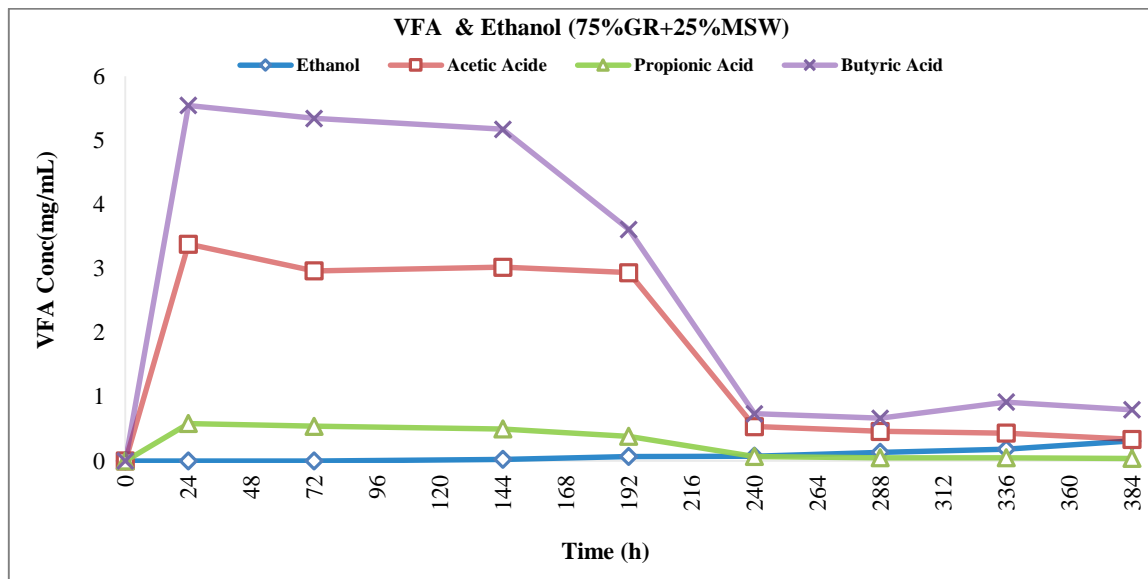


Figure 4.13c VFA variation during digestion period at $T = 37\text{ }^{\circ}\text{C}$, 150 rpm, 15% TS (75% GR+25% MSW) and 10mL inoculum, where (\diamond) Ethanol, (\square) Acetic Acid, (\triangle) Propionic Acid and (\times) Butyric Acid, the composition of liquid phase was analysis by GC-17A equipped with a FID detector (see section 3.1.5.3).

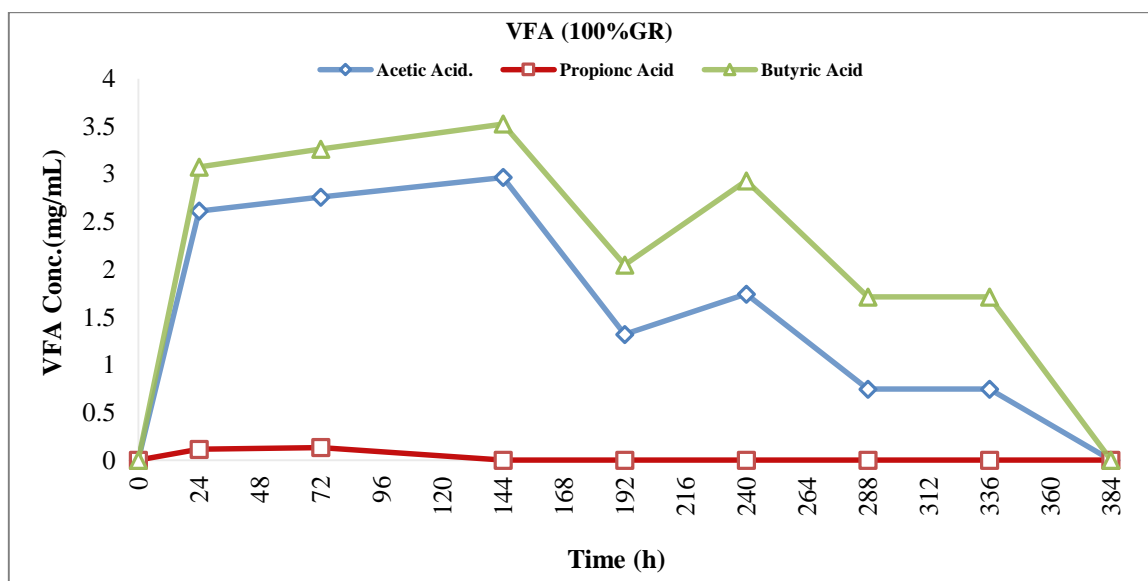


Figure 4.13d VFA variation during digestion period at $T = 37\text{ }^{\circ}\text{C}$, 150 rpm, 15% TS (100% GR) and 10 mL inoculum, where (\diamond) Acetic Acid, (\square) Propionic Acid and (\triangle) Butyric Acid, the composition of liquid phase was analysis by GC-17A equipped with a FID detector (see section 3.1.5.3).

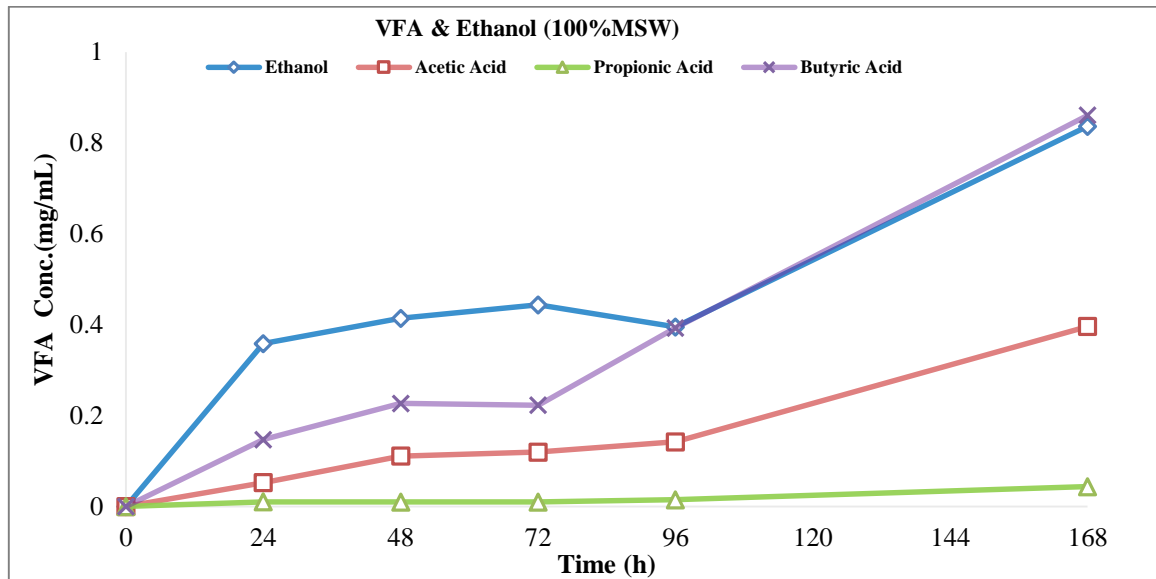


Figure 4.13e VFA variation during digestion period at $T = 37^\circ\text{C}$, 150 rpm, 15%TS (15gm MSW) and 10 mL inoculum, where (\diamond) Ethanol, (\square) Acetic Acid, (\triangle) Propionic Acid and (\times) Butyric Acid, the composition of liquid phase was analysis by GC-17A equipped with a FID detector (see section 3.1.5.3).

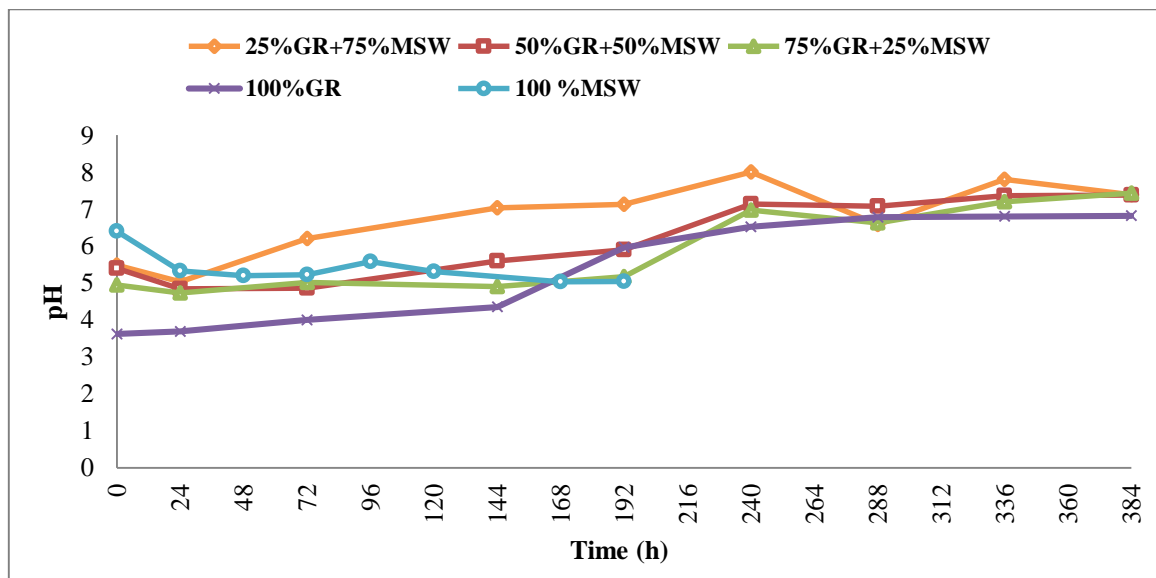


Figure 4.14 pH variation n during digestion period at $T = 37^\circ\text{C}$, 150 rpm, 10mL Inoc. and 15%TS, where (\circ) 100%MSW, (\diamond) 25%GR+75%MSW, (\square) 50%GR+50%MSW, (\triangle) 75%GR+25%MSW and (\times) 100%GR.

4.1.3.2 Biogas yield.

The **Figure 4.15** describes the effect of the initial composition of the feedstock on the specific biogas production. The highest cumulative specific volume of biogas (about 276.1 mL/gVS) was obtained when using a 75% fraction of the lignocellulosic material, due to a higher glucose concentration was producing during the hydrolysis step (see Figure 4.19). Lower values were obtained when the fraction of pre-treated GR was 50% (219 mL of biogas /g VS of biogas) and 25% (202 mL of biogas/gVS). A poor biogas production (42.1 and 78.4 mL/g VS) was obtained in the presence of 100% GR and 100% MSW. This result confirms that co-digestion of different wastes is effective for the optimization of the digestion efficiency. Because of the co-digestion technology, diluted of potentially toxic compounds, enhanced balance of nutrients, synergistic effects of microorganisms, increased load biodegradable organic matter and increased digestion rate, will lead to better biogas yield (Sosnowski P. et al., 2003, Nielfa A. et al., 2015).

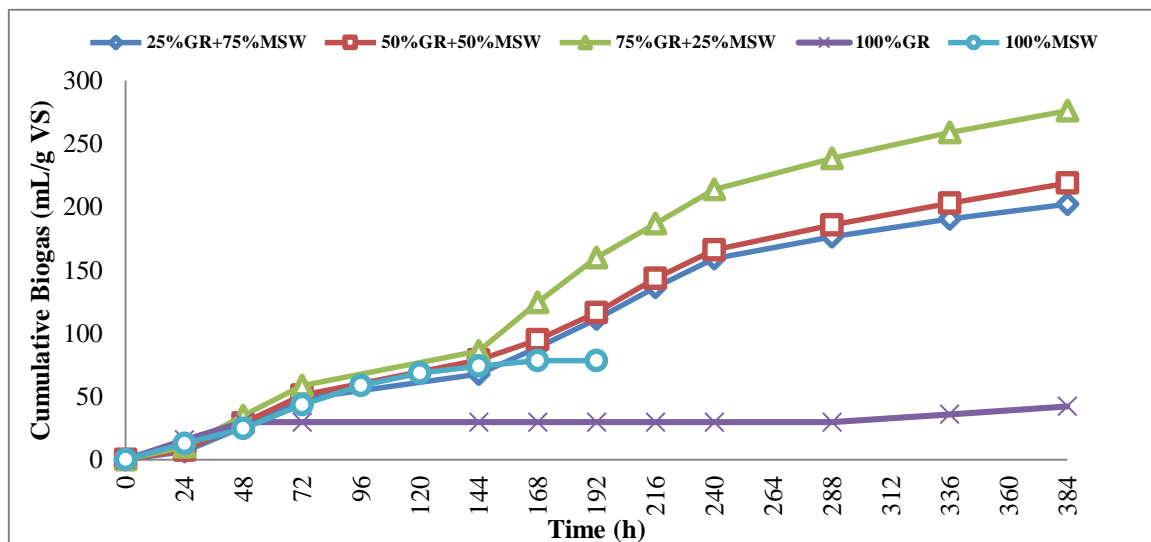


Figure 4.15 Specific cumulative biogas yield during digestion period at T =37°C, 150 rpm, 10mLInoc. and 15%TS, where (○) 100 % MSW (◇) 25%GR+75%MSW, (□) 50%GR+50%MSW, (△) 75%GR+25%MSW and (x) 100%GR.

The **Figures (4.16a-b-c-d-e)** show the variation in the composition of biogas (CH_4 , H_2 and CO_2) as a function of the initial composition of the feedstock. The test with 100% of MSW, the biogas production was stopped after 192hrs, due to the reduced availability of easily biodegradable organics that is provided by lignocellulosic material in other digesters.

In all tests, an initial rise of the methane concentration was observed, followed by a progressive decrease. The highest fraction of methane was obtained when using a feedstock composition (75%GR - 25%MSW). Under these conditions, the highest amount of biogas was also obtained.

The fraction of biomethane produced is in agreement with the data presented in the literature (Bolzonella et al., 2006, Baoning et al., 2009, Ingrid et al., 2014). The maximum fraction of biomethane occurring during the intermediate phase of the process has been observed in previous works, as well (Liew L.N. et al., 2012).

In the first part of each test, significant volumes of biohydrogen were produced, due to the action of the hydrogen-producing bacteria (especially *Clostridium*) contained in the inoculum, as explained in the **Figure 4.17** the growth to biohydrogen gas yield was limited during batch digestion test for municipal solid wastes (MSW), was done at same condition of digestion for other tests and same composition of MSW and inoculated with an inoculum prepared from adapted *Clostridium* bacteria to a synthetic medium at same procedure was followed for sewage sludge.

Compared to data from the literature (Vindis P. et al., 2009, Ingrid H. et al., 2014), the fractions of CO_2 were higher. This is due to the significant production of VFAs, which are converted to CO_2 by fermentation, as confirmed by the formation of bioethanol.

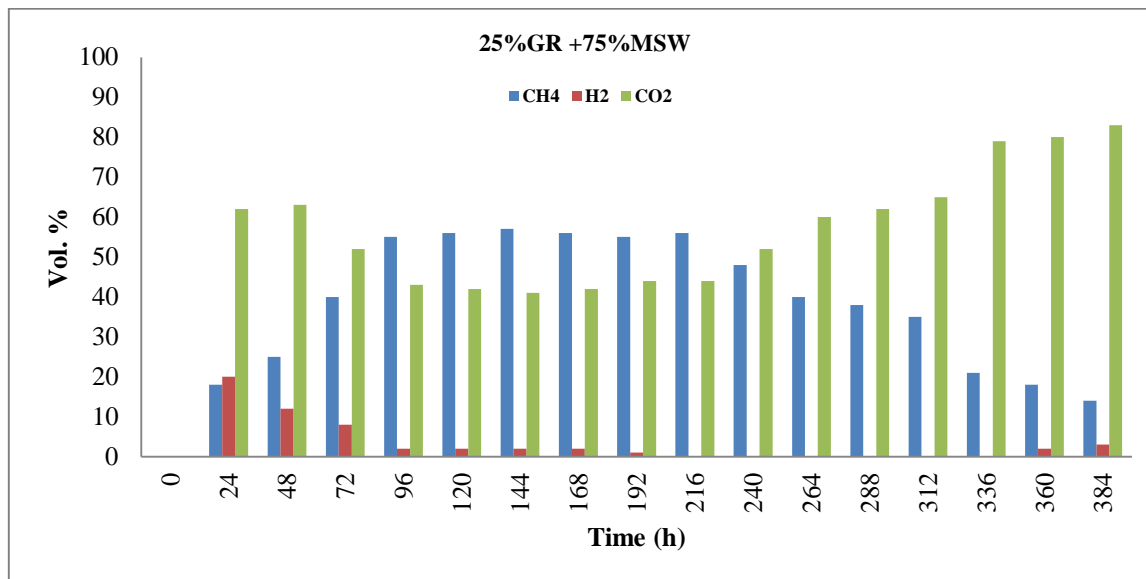


Figure 4.16a Composition of biogas for the sample 25%GR + 75% MSW at T = 37°C, 150 rpm, 10mL Inoc. and 15%TS, the composition of biogas was analysis by GC-HP 5890 equipped with a TCD detector (see section 3.1.6).

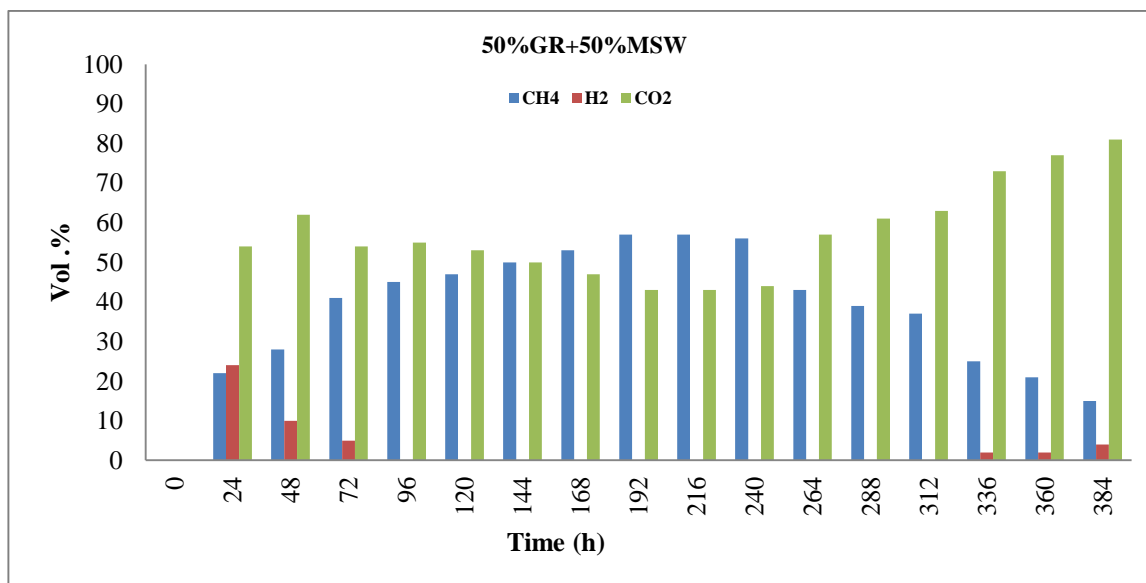


Figure 4.16b Composition of biogas for the sample 50%GR + 50% MSW at T = 37 °C, 150 rpm, 10mL Inoc. and 15%TS, the composition of biogas was analysis by GC-HP 5890 equipped with a TCD detector (see section 3.1.6).

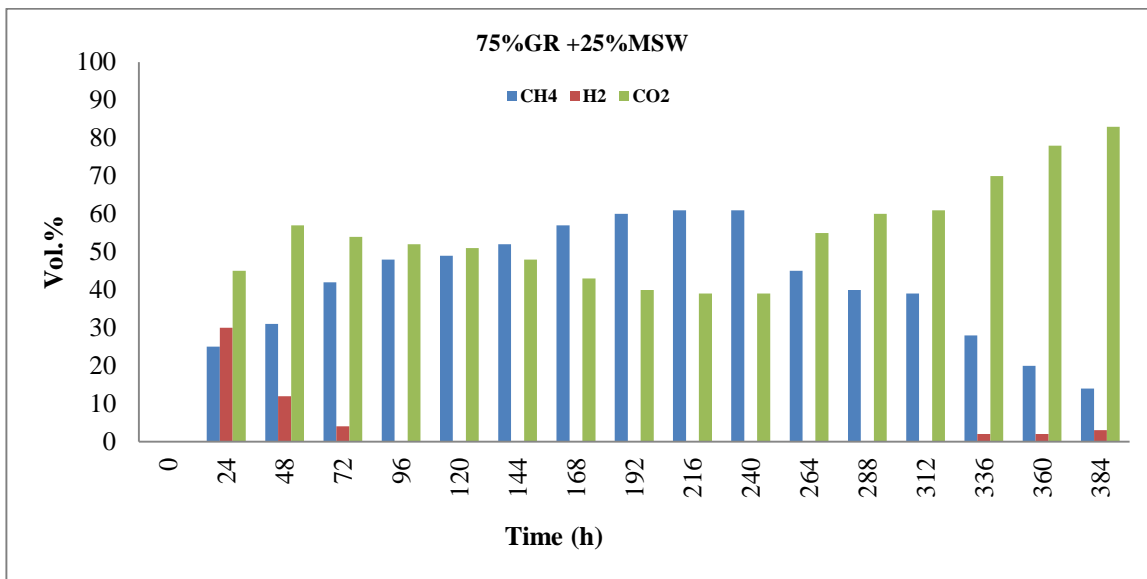


Figure 4.16c Composition of biogas for the sample 75%GR + 25% MSW at T = 37 °C, 150 rpm, 10mL Inoc. and 15%TS, the composition of biogas was analysis by GC-HP 5890 equipped with a TCD detector (see section 3.1.6).

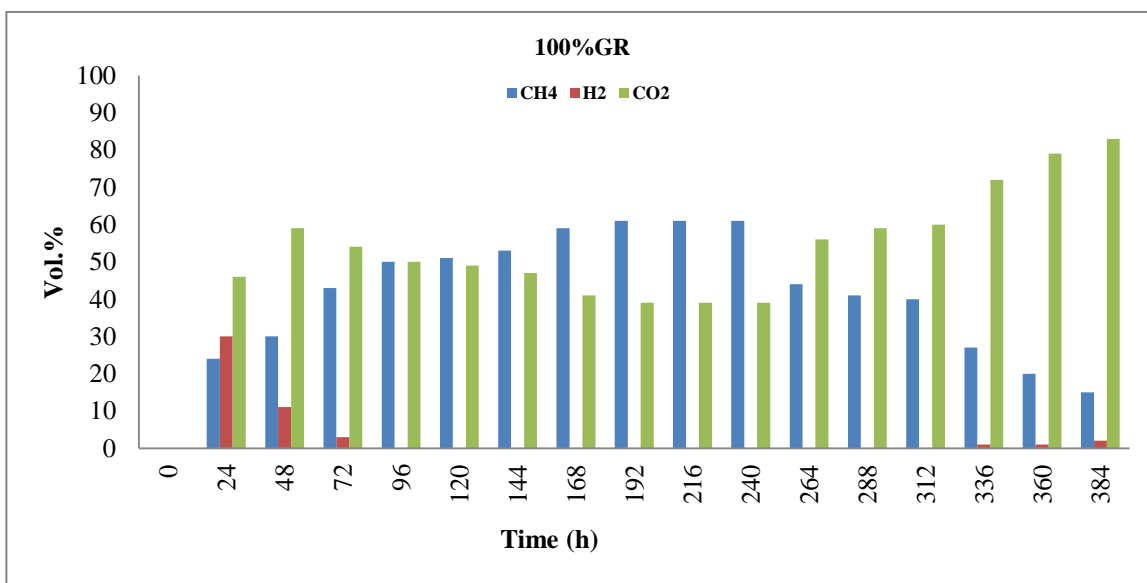


Figure 4.16d Composition of biogas for the sample 100% GR at T = 37 °C, 150 rpm, 10mL Inoc. and 15%TS, the composition of biogas was analysis by GC-HP 5890 equipped with a TCD detector (see section 3.1.6).

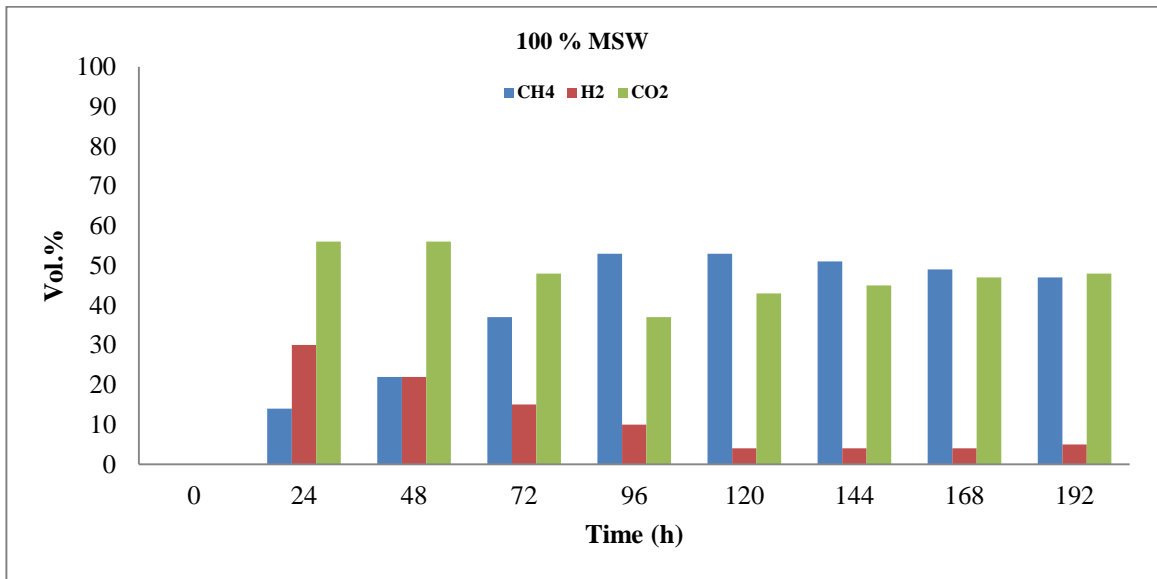


Figure 4.16e Composition of biogas for the sample 100% MSW at $T = 37^{\circ}\text{C}$, 150 rpm, 10mL Inoc. and 15% TS, the composition of biogas was analysis by GC-HP 5890 equipped with a TCD detector (see section 3.1.6).

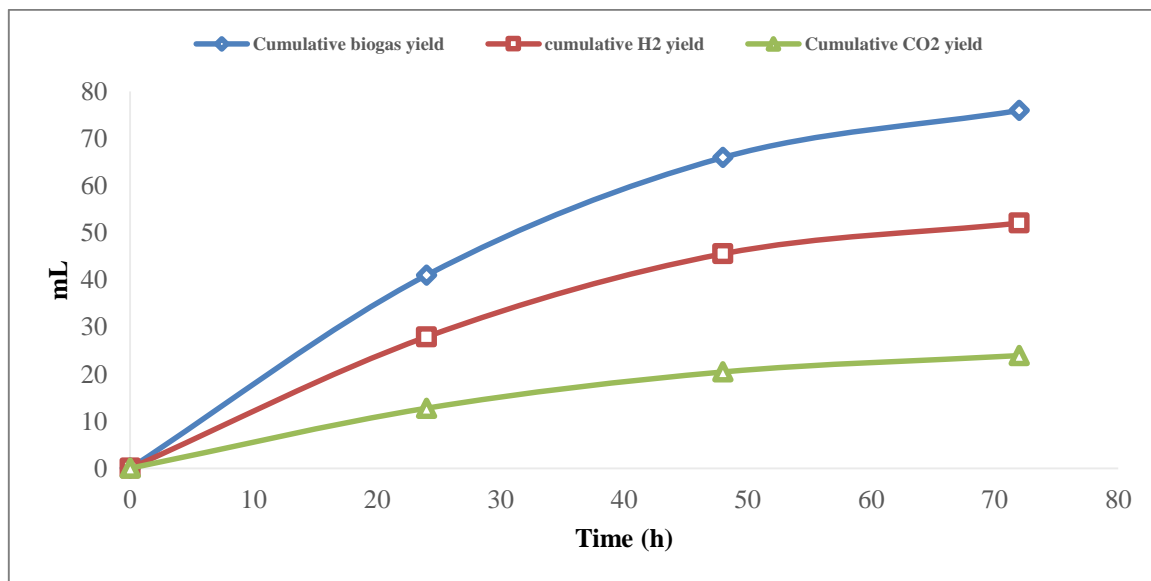


Figure 4.17 Cumulative biogas , H₂ and CO₂ yield during digestion period for MSW at $T = 37^{\circ}\text{C}$, 150 rpm, 10mL of inoculum from synthetic medium prepared by adapted Clostridium bacteria and 15% TS, where Cumulative biogas (\diamond), Cumulative H₂ (\square) and Cumulative CO₂ (\triangle), the composition of biogas was analysis by GC-HP 5890 equipped with a TCD detector (see section 3.1.6).

4.1.3.3 Biomass growth and glucose concentration.

The **Figure 4.18** shows the growth of biomass during digestion period. When using mixtures of GR and MSW, similar behaviors were observed, whatever the initial composition adopted. In all cases, a maximum biomass concentration of about 4.9, 5.23 and 5.33 (mg/mL) for 25% ,50% and 75% GR, respectively was observed after about 144 hrs. Subsequently, a progressive reduction of the biomass concentration was observed.

On the contrary, when using 100% GR, no significant increases of the biomass concentration were observed. A possible explanation of this result is that there is no availability of nutrients for microorganisms.

When using 100% MSW, a significant increase of biomass concentration was observed (5.7 -5.9 mg/mL) from 24 to 72 hrs, though the biogas production stopped after 192 hours. Again, this result could be due to the poor immediate of easily biodegradable organics that is provided by lignocellulosic material in other digesters.

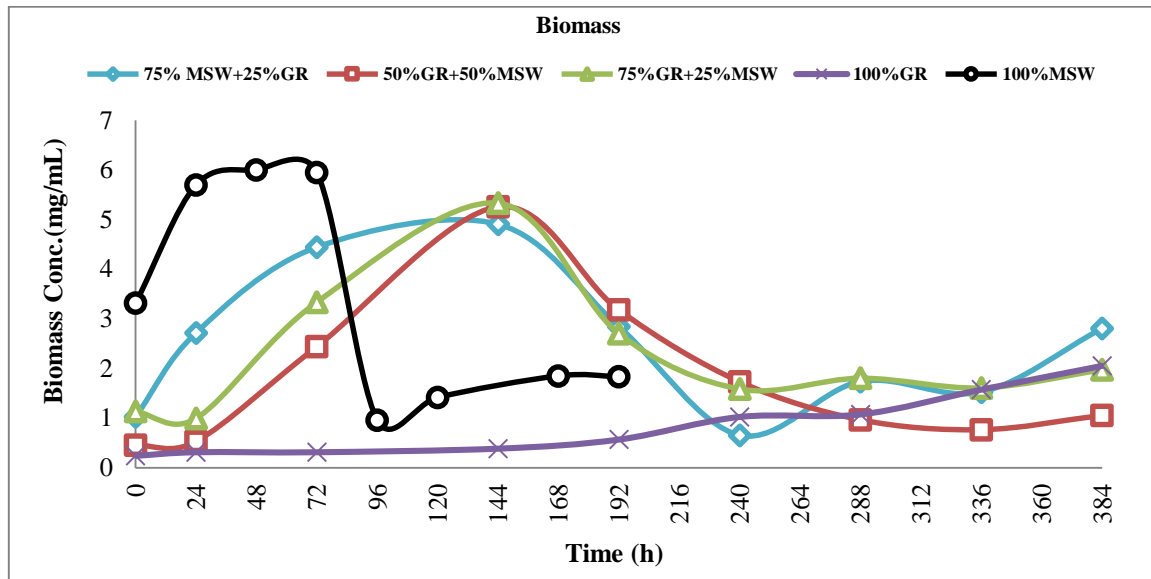


Figure 4.18 Biomass growth during digestion period at $T= 37^{\circ}\text{C}$, 150 rpm, 10mL Inoc.and15% TS(100%MSW,25%GR+75%MSW,50%GR+50%MSW,75%GR+25%MSWand100%GRrespectively),where(o)100%MSW,(◇)25%GR+75%MSW,(□)50%GR+50%MSW,(△)75%GR+25%MSW and (x) 100%GR.

The **Figure 4.19** describes the profile of the glucose concentration during the anaerobic digestion. When using mixtures of GR and MSW, significant increases of glucose concentration were initially observed, due to the hydrolysis of the cellulose/hemicellulose feedstock.

The results indicate that the hydrolysis rate is affected by the initial concentration of cellulose/hemicellulose feedstock. The maximum concentrations of glucose were obtained when adopting higher concentrations of GR (29.75g/L, 17.06 and 10.81 g/L in the presence of 75%, 50% and 25% GR, respectively).

In the test with 100%GR, only a slight increase of glucose concentration was observed. This confirms that, in the absence of MSW, there are not immediately available nutrients to digest.

In the test with 100%MSW the glucose concentration started from 5.96 g/L to decrease progressively. No increases due to the hydrolysis step were observed.

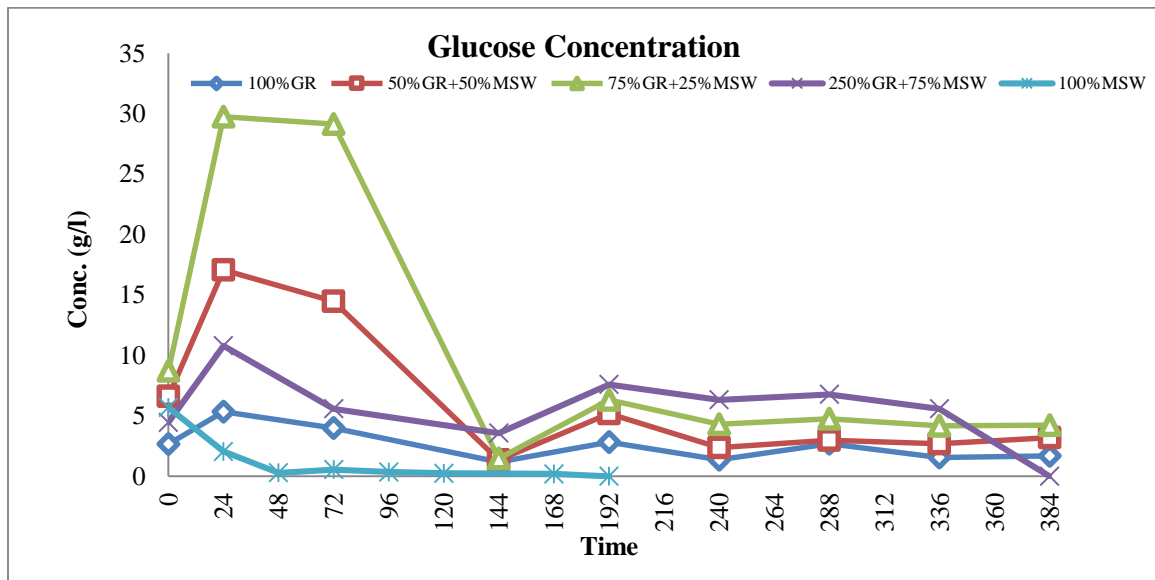


Figure 4.19 Concentration of glucose during digestion period at $T=37^{\circ}\text{C}$, 150 rpm, 10mLInoc.and15% TS(100% MSW,25% GR+75%MSW,50%GR+50%MSW ,75% GR+25%MSWand100%GRrespectively),where(*)100%MSW,(×)25% GR+75%MSW, (□) 50%GR+50%MSW, (△) 75%GR+25%MSW and (◇) 100%GR.

4.1.4 Effect mineral solution "M9 10x" and 400x salts addition on a performance of anaerobic digestion for Municipal Solid Waste (MSW).

For this study, a batch reactor (125 mL glass bottle with a working volume of 100mL) was filled with 15 % of total solid from MSW, inoculum (10 v/v%), 1.5 mL of M9 salts (Na_2HPO_4 7.0 g/L, KH_2PO_4 3.0 g/L, NaCl 0.5 g/L, NH_4Cl 1.0 g/L) and 40 μL of 400x salts ($\text{CuSO}_4 \cdot 5\text{H}_2\text{O}$ 0.125g/L, $\text{ZnSO}_4 \cdot 7\text{H}_2\text{O}$ 0.72g/L, $\text{MnCl}_2 \cdot \text{H}_2\text{O}$ 0.50g/L, CaCO_3 1g/L, MgSO_4 62.09g/L, $\text{FeSO}_4 \cdot 7\text{H}_2\text{O}$ 4.75g/L, $\text{CoSO}_4 \cdot 7\text{H}_2\text{O}$ 0.14g/L, H_3BO_3 0.03g/L, HCL 25.6mL/L). Distilled water was added to obtain a total liquid volume of 100 mL. Anaerobic conditions were ensured by flushing the medium with nitrogen for 20 min, after that the vial is placed in electrical furnace at 37°C and 150 rpm for 192 hrs.

4.1.4.1 VFAs production and pH variation.

The **Figure 4.20** shows VFA (acetic acid, butyric acid, Propionic Acid) and ethanol variation during the digestion period. The VFA concentration increased and decreases gradually with time. The organic fraction of municipal solid waste (OFMSW) is degradable organic matters, which is easily converted into VFA. As VFA concentration cases increased, a corresponding decrease of pH was observed, as shown in **Figure 4.21**. The pH was corrected to optimal average values between 6.5 and 7.5 by addition of 1M of Na_2HCO_3 solution to avoid the inhibition of methanogenesis at low pH. By comparing this result with that obtained under the same conditions (par. 4.1.2.1, Figure 4.7a) in the absence of mineral and salts, we can observe a little increase in the VFAs production.

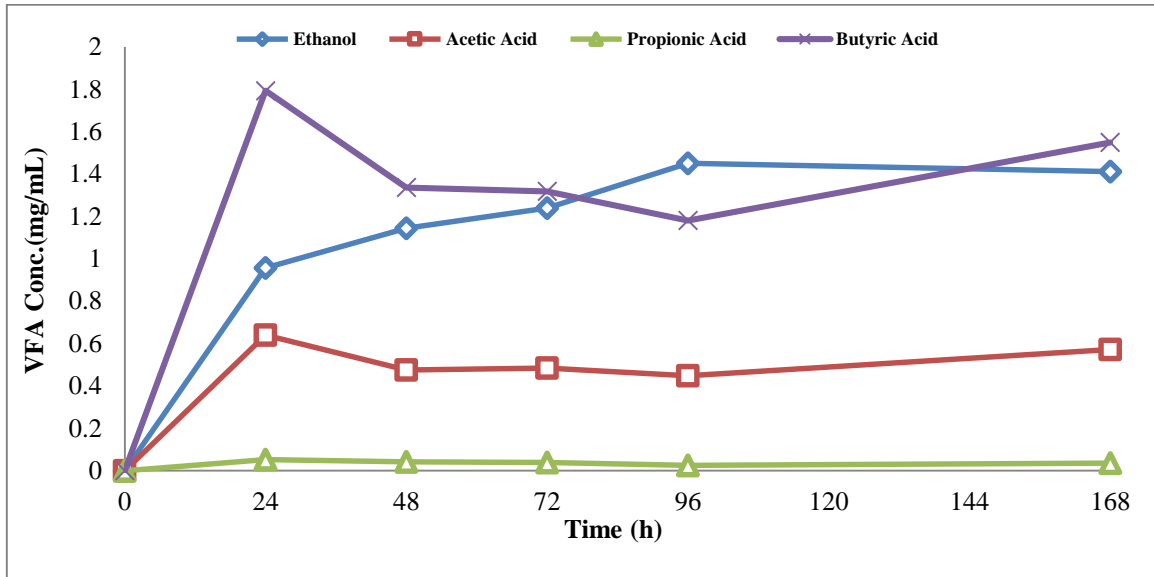


Figure 4.20 VFA variation during digestion period at $T= 37^{\circ}\text{C}$, 150 rpm, 15%TS and 10 mL Inoculum for effect of mineral and salts solution addition , where (\diamond) Ethanol, (\square)Acetic Acid, (\triangle) Propionic Acid and (\times) Butyric Acid, the composition of liquid phase was analysis by GC-17A equipped with a FID detector (see section 3.1.5.3).

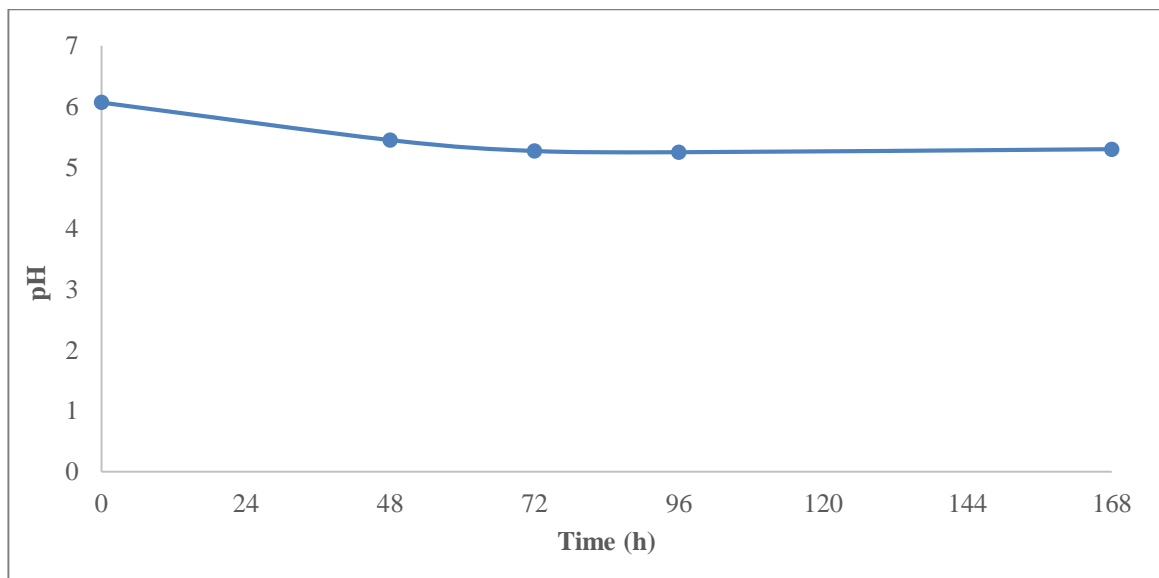


Figure 4.21 pH variation during digestion period at $T= 37^{\circ}\text{C}$, 150 rpm, 15%TS and 10 mL Inoculum for effect of mineral and salts solution addition.

4.1.4.2 Biogas yield.

The effect of mineral and salts solution addition on anaerobic digestion of MSW was studied adopting a TS content of 15%. The **Figure 4.22** shows that the maximum cumulative volume biogas yield was about 386ml. By comparing this result with that obtained under the same conditions in the absence of mineral and salts (par. 4.1.2.2, Figure 4.9a), we can observe that a higher amount of biogas was produced (386 mL versus 359 mL) regardless a little increase in the produce VFAs that explained above. In addition, a higher fraction of methane was obtained, as shown in the **Figure 4.23**, by comparing with that obtained in (par. 4.1.2.2, Figure 4.10a). Consequently, it can be said that the addition of the salts solution improvise the efficiency of the methanogenesis step.

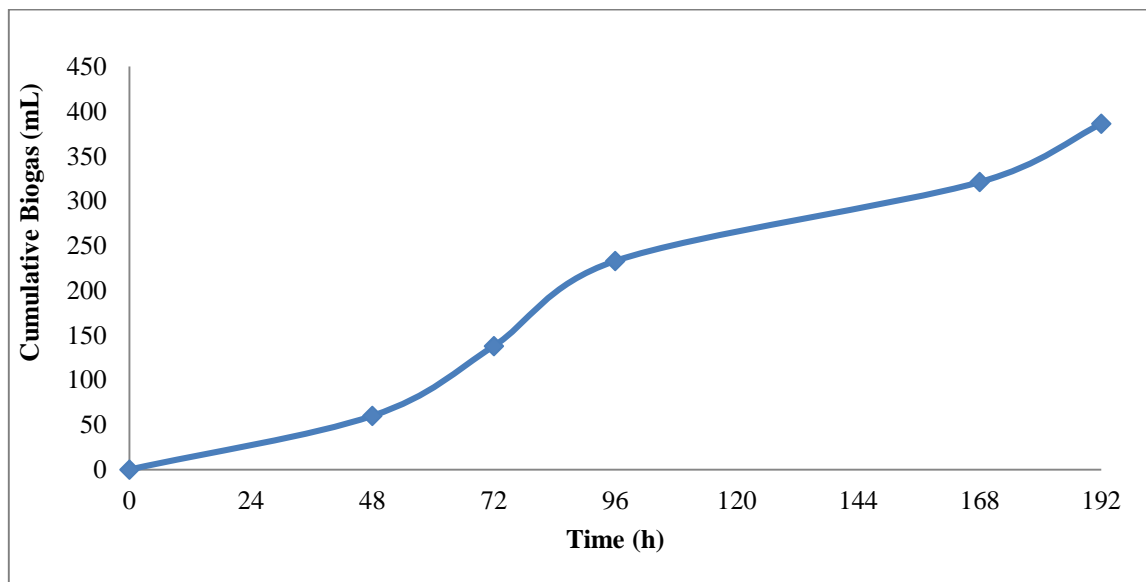


Figure 4.22 Cumulative biogas yield during digestion period with mineral and salts solution addition at T= 37 °C, 150rpm, 10v/v Inoc. and 15%TS.

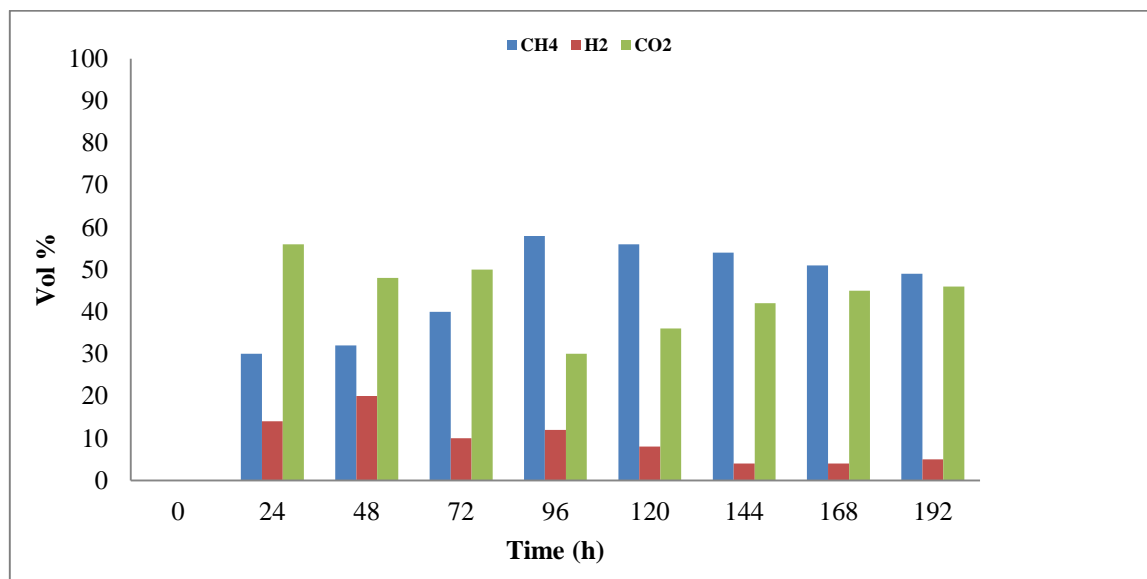


Figure 4.23 Composition of biogas for the test with mineral and salts solution addition at $T= 37\text{ }^{\circ}\text{C}$, 150rpm, 10v/v Inoc. and 15% TS , the composition of biogas was analysis by GC-HP 5890 equipped with a TCD detector (see section 3.1.6).

4.1.4.3 Biomass growth and glucose concentration.

The **Figure 4.24** shows the growth of biomass and glucose concentration during the digestion period. Firstly the biomass concentration increased rapidly, reaching a maximum concentration after 72 hours. Subsequently, a progressive reduction of the biomass concentration was observed, tending to zero. The concentrations of glucose at zero time was 5.7 g/L, then decreases to zero due to increasing growth of microorganisms.

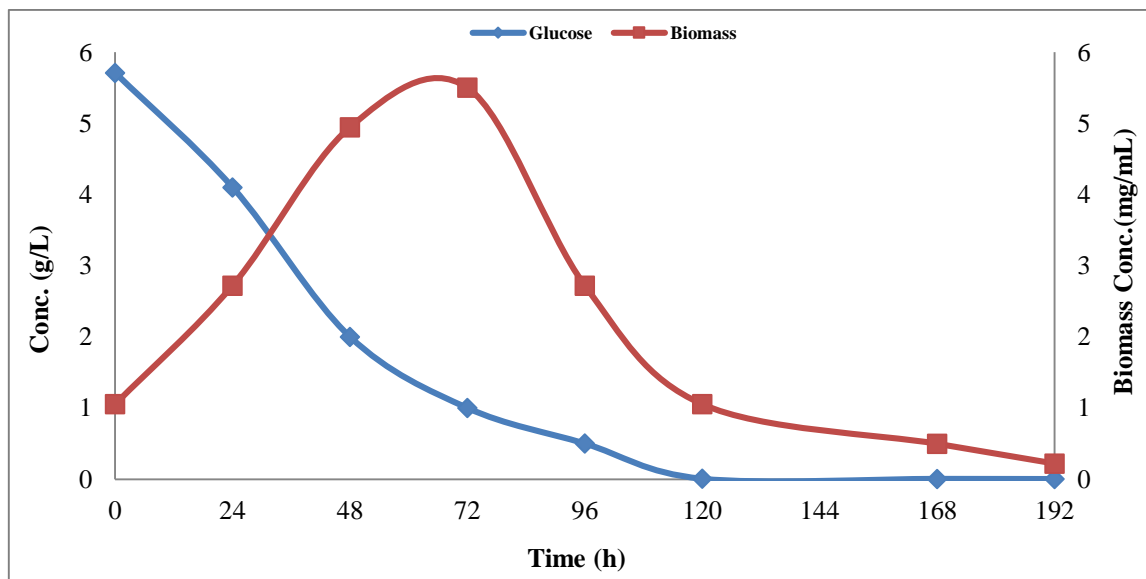


Figure 4.24 Biomass growth and glucose concentration during digestion period at T= 37°C, 150 rpm, 15% TS and mineral and salts solution addition.

4.1.5 Optimization of trace metals addition for biogas production from solid-state anaerobic digestion process of Municipal Solid Waste (MSW).

In this study, fourteen batch stirred reactors (125 mL glass bottle with a working volume of 100 mL) were filled with MSW (15 % wt.) and inoculum (10 mL), then distilled water was added to obtain a liquid volume of 100mL. Each bioreactor was dosed with the desired concentration of single or mixed trace elements, and sealed by rubber stoppers. Anaerobic conditions were ensured by flushing nitrogen for 20 min. Subsequently, the reactor was placed in an electrical furnace at 37°C and 150 rpm for 288 hrs. The conditions adopted for the batch tests are summarized in table (4.4).

Table (4.4): Batch tests conditions for the effect of trace metals addition.

No.	Feed load (g)	Ni Conc. (mg/L)	Zn Conc. (mg/L)	Co Conc. (mg/L)	Inoculum (mL)	Distilled water (mL)	Total volume (mL)	Test temp. (°C)
1	15	-	-	-	10	75	100	37
2	15	5	-	-	10	75	100	37
3	15	50	-	-	10	75	100	37
4	15	100	-	-	10	75	100	37
5	15	-	5	-	10	75	100	37
6	15	-	50	-	10	75	100	37
7	15	-	100	-	10	75	100	37
8	15	-	-	5	10	75	100	37
9	15	-	-	50	10	75	100	37
10	15	-	-	100	10	75	100	37
11	15	5	5	5	10	75	100	37
12	15	5	5	-	10	75	100	37
13	15	5	-	5	10	75	100	37
14	15	-	5	5	10	75	100	37

4.1.5.1 VFA and pH variation during (AD).

4.1.5.1.1 VFA and pH variation during (AD) for individual trace element.

The **Figures 4.25a-b-c-d-e-f-g-h-i-j** show the produced VFAs (acetic acid, butyric acid, propionic acid) and ethanol concentration profiles as a function of time. Three different concentrations (5, 50 and 100 mg/L) were adopted for each trace element (Ni, Zn and Co). A control test with MSW in the absence of trace elements was also carried out.

The final concentrations of VFAs and ethanol obtained in each experimental test are reported in the table (4.5).

Table (4.5): Final concentrations of VFAs and ethanol obtained in each experimental test for the effect of trace metals addition.

No.	Feed load (g)	Ni Conc. (mg/l)	Zn Conc. (mg/l)	Co Conc. (mg/l)	Eth. Conc. (mg/ml)	Ac.Ac. Conc. (mg/ml)	Pr.Ac. Conc. (mg/ml)	Bu. Ac. Conc. (mg/ml)
1	15	-	-	-	1.16263286	0.37594093	1.04217477	11.8396156
2	15	5	-	-	1.03519155	1.14151031	1.1742664	5.67745807
3	15	50	-	-	9.85927063	0.59363293	4.97693198	12.3576966
4	15	100	-	-	8.96888684	1.28763319	6.25846247	21.4425244
5	15	-	5	-	1.15877701	0.9315939	1.41904648	13.3381798
6	15	-	50	-	9.75016495	0.55030256	2.3505797	18.5342096
7	15	-	100	-	14.407508	0.29891511	1.78393113	26.4890812
8	15	-	-	5	1.36210613	0.99698225	1.01316519	6.43470437
9	15	-	-	50	6.06917247	0.69574184	2.4780791	15.8992825
10	15	-	-	100	15.5661026	0.76556233	2.64183418	31.4835773
11	15	5	5	5	1.16838152	0.10259954	0.11939709	0.42111724
12	15	5	5	-	4.62411385	0.63897586	0.47054711	5.26690066
13	15	5	-	5	2.09376594	0.23121232	0.01321978	1.99751781
14	15	-	5	5	2.44373134	0.35336288	1.97604511	6.92426447

In all cases, higher values of the final concentration chiefly (Butyric acid) and alcohol (Ethanol), was obtained when higher amounts of trace element were used. On the contrary, as the initial concentration of trace elements was decreased, the concentrations of VFA and alcohol kept at a low level. The higher concentration of butyric acid contributes to inhibit the bacteria that are responsible of the subsequent stages of the fermentation process.

The pH variations during the digestion period are shown in the **Figures 4.26a-b and c**. The pH was tended to decrease during the anaerobic digestion process due to VFA production. In order to avoid pH values out optimum limits (6.5-7.5), potentially leading to the inhibition of methanogenesis under acidic conditions (Agdag and Sponza, 2007), 1M Na_2HCO_3 solution was added daily to the reactors.

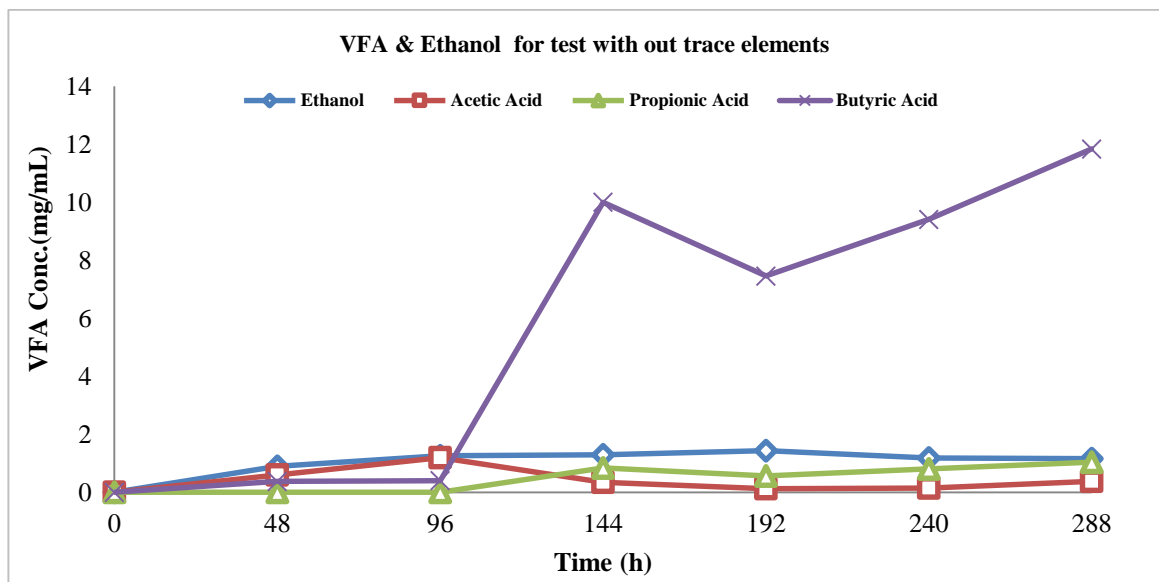


Figure 4.25a VFA variation during digestion period at $T=37\text{ }^{\circ}\text{C}$, 150 rpm, 15%TS MSW ,10 mL Inoculum and Zero trace elements Conc., where (\diamond) Ethanol, (\square) Acetic Acid (\triangle) Propionic Acid and (\times) Butyric Acid, the composition of liquid phase was analysis by GC-17A equipped with a FID detector (see section 3.1.5.3).

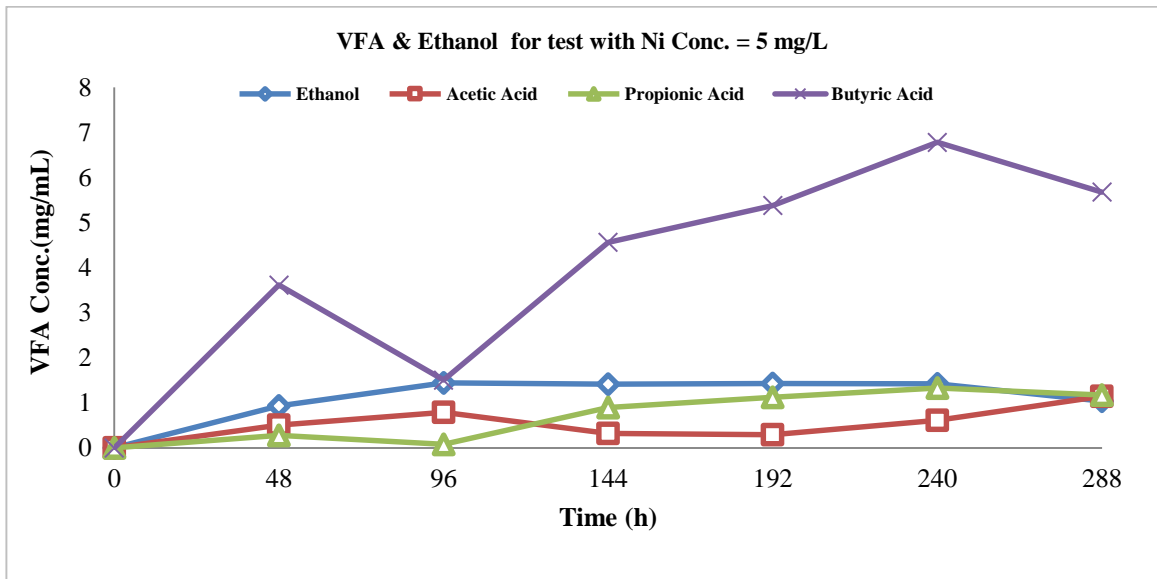


Figure 4.25b VFA variation during digestion period at $T = 37\text{ }^{\circ}\text{C}$, 150 rpm, 15%TS MSW, 10 mL Inoculum and 5mg/L Ni Conc., where (\diamond) Ethanol, (\square) Acetic Acid, (\triangle) Propionic Acid and (\times) Butyric Acid, the composition of liquid phase was analysis by GC-17A equipped with a FID detector (see section 3.1.5.3).

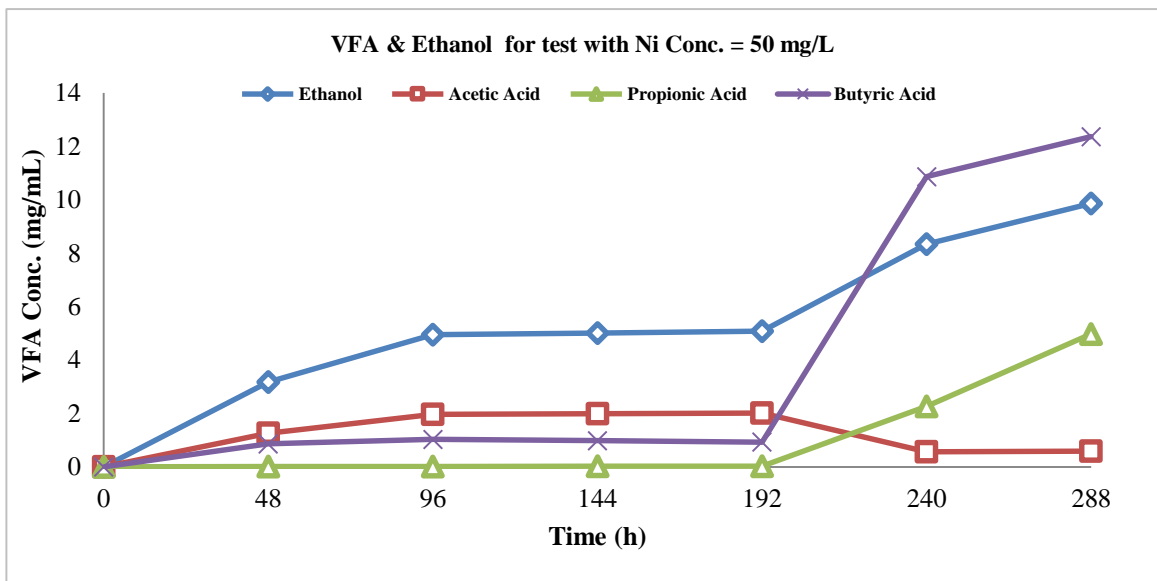


Figure 4.25c VFA variation during digestion period at $T = 37\text{ }^{\circ}\text{C}$, 150 rpm, 15%TS MSW, 10 mL Inoculum and 50mg/L Ni Conc., where (\diamond) Ethanol, (\square) Acetic Acid, (\triangle) Propionic Acid and (\times) Butyric Acid, the composition of liquid phase was analysis by GC-17A equipped with a FID detector (see section 3.1.5.3).

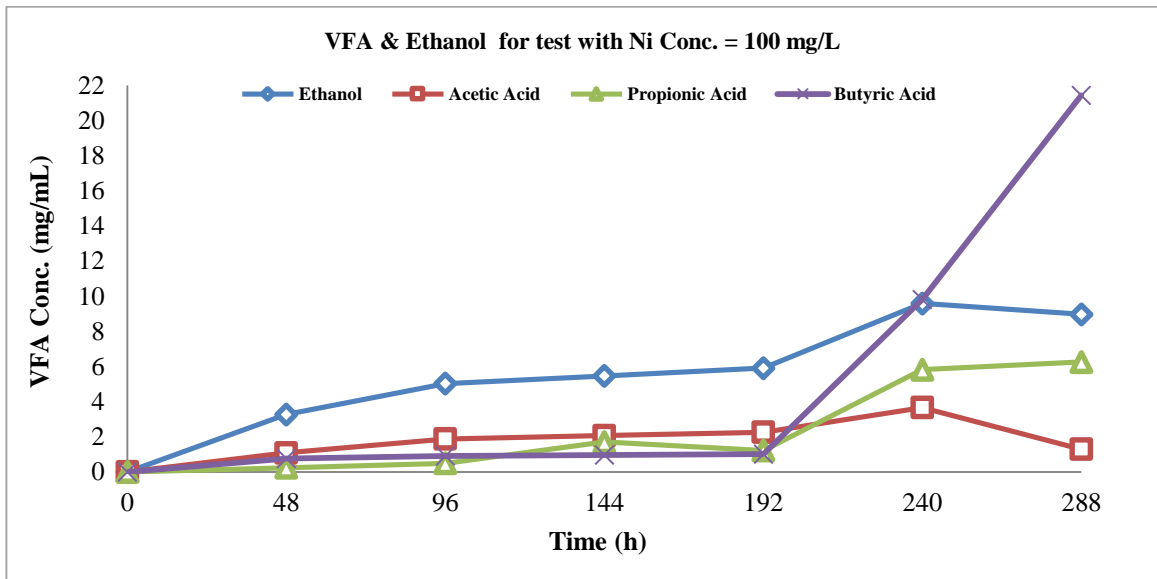


Figure 4.25d VFA variation during digestion period at T= 37 °C, 150 rpm, 15%TS MSW, 10 mL Inoculum and 100 mg/L Ni Conc., where (◇) Ethanol, (□) Acetic Acid, (△) Propionic Acid and (×) Butyric Acid, the composition of liquid phase was analysis by GC-17A equipped with a FID detector (see section 3.1.5.3).

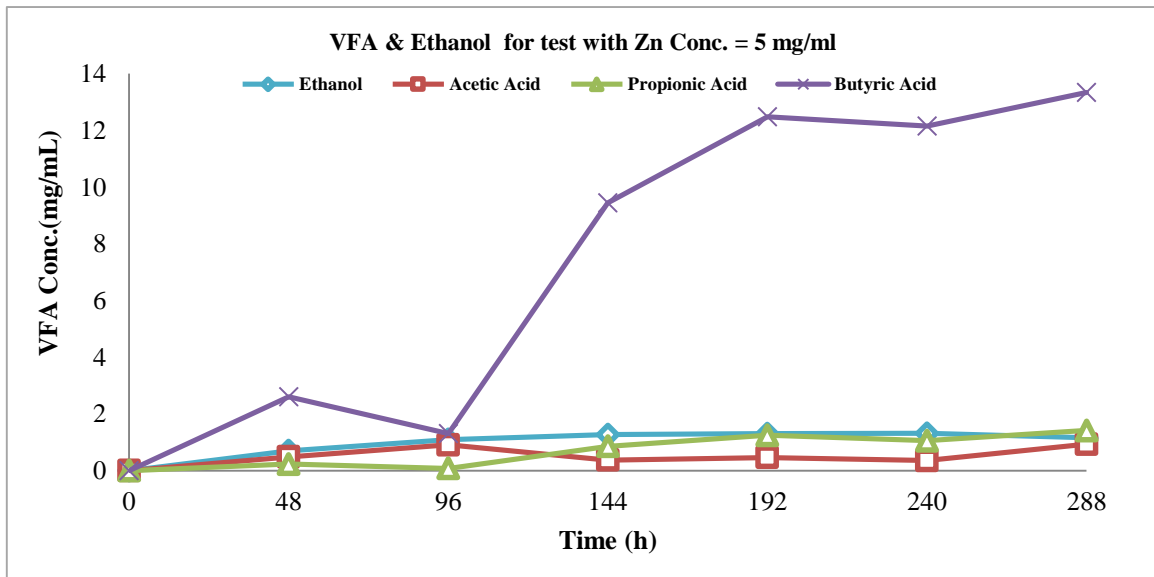


Figure 4.25e VFA variation during digestion period at T= 37 °C, 150 rpm, 15%TS MSW, 10 mL Inoculum and 5 mg/L Zn Conc., where (◇) Ethanol, (□) Acetic Acid, (△) Propionic Acid and (×) Butyric Acid, the composition of liquid phase was analysis by GC-17A equipped with a FID detector (see section 3.1.5.3).

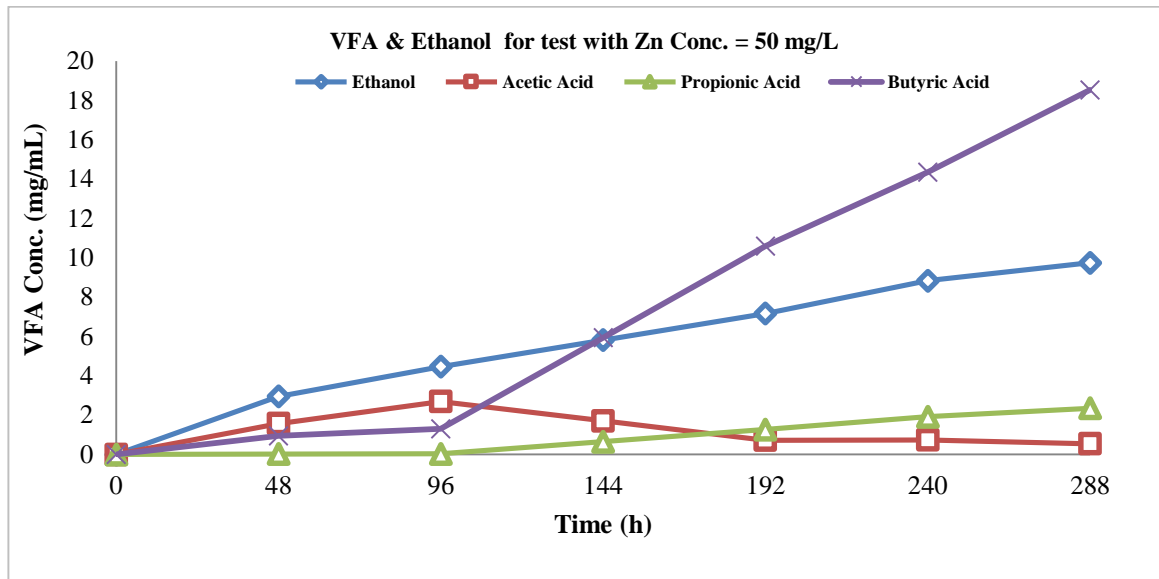


Figure 4.25f VFA variation during digestion period at $T= 37\text{ }^{\circ}\text{C}$, 150 rpm, 15%TS MSW ,10 mL Inoculum and 50mg/L Zn Conc., where (\diamond) Ethanol, (\square) Acetic Acid., (\triangle) Propionic Acid and (\times) Butyric Acid, the composition of liquid phase was analysis by GC-17A equipped with a FID detector (see section 3.1.5.3).

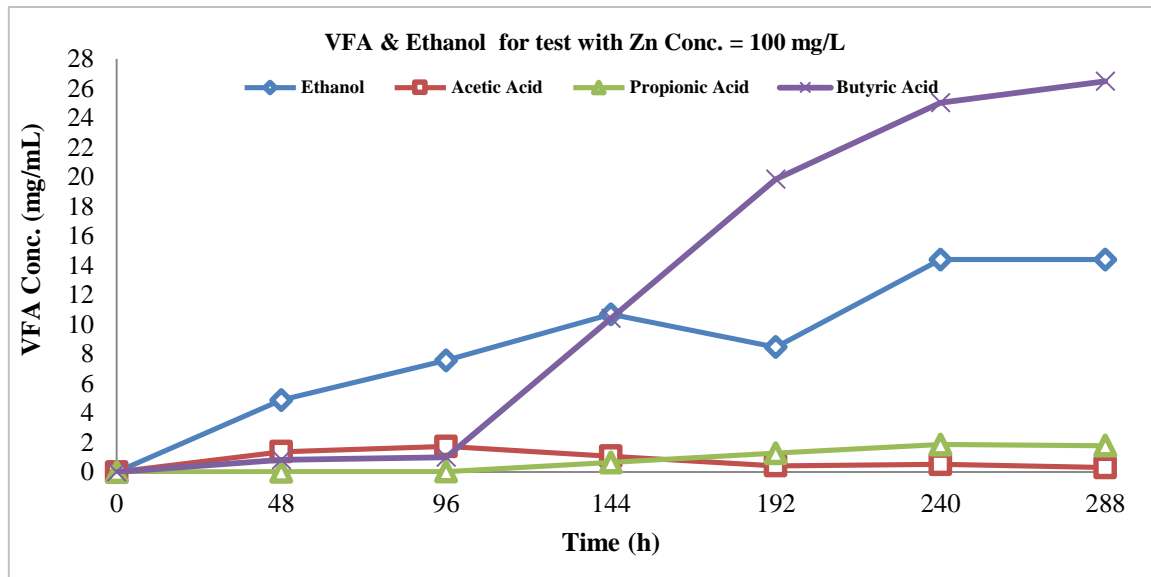


Figure 4.25g VFA variation during digestion period at $T= 37\text{ }^{\circ}\text{C}$, 150 rpm, 15%TS MSW, 10 mL Inoculum and 100 mg/L Ni Conc., where (\diamond) Ethanol, (\square) Acetic Acid, (\triangle) Propionic Acid and (\times) Butyric Acid, the composition of liquid phase was analysis by GC-17A equipped with a FID detector (see section 3.1.5.3).

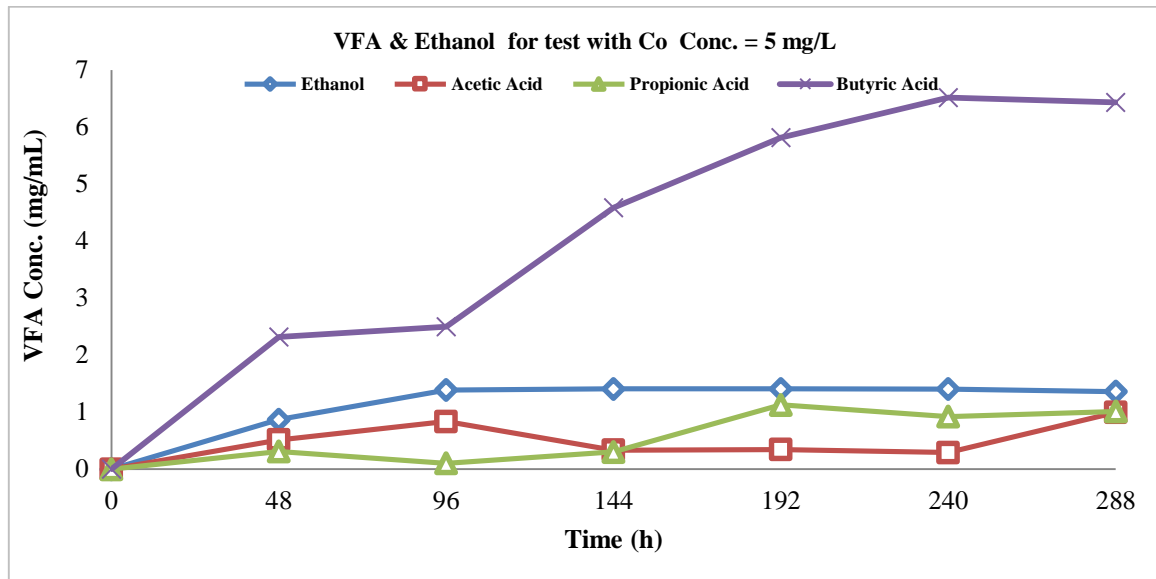


Figure 4.25h VFA variation during digestion period at $T= 37\text{ }^{\circ}\text{C}$, 150 rpm, 15%TS MSW, 10 mL Inoculum and 5 mg/L Co Conc., where (\diamond) Ethanol, (\square) Acetic Acid, (\triangle) Propionic Acid and (\times) Butyric Acid, the composition of liquid phase was analysis by GC-17A equipped with a FID detector (see section 3.1.5.3).

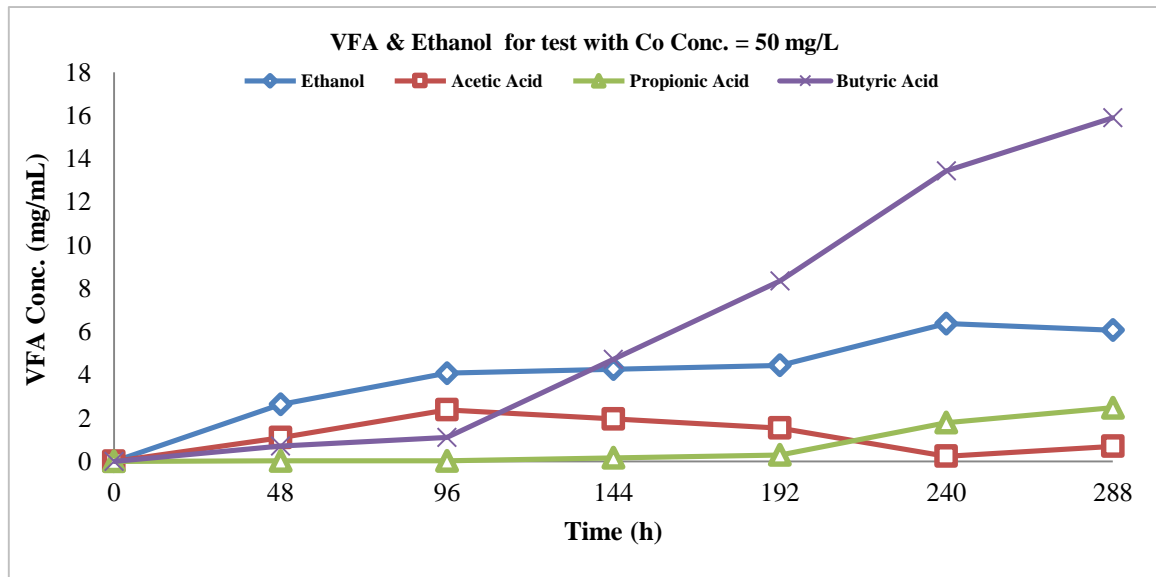


Figure 4.25i VFA variation during digestion period at $T= 37\text{ }^{\circ}\text{C}$, 150 rpm, 15%TS MSW, 10 mL Inoculum and 50mg/L Co Conc., where (\diamond) Ethanol, (\square) Acetic Acid, (\triangle) Propionic Acid and (\times) Butyric Acid, the composition of liquid phase was analysis by GC-17A equipped with a FID detector (see section 3.1.5.3).

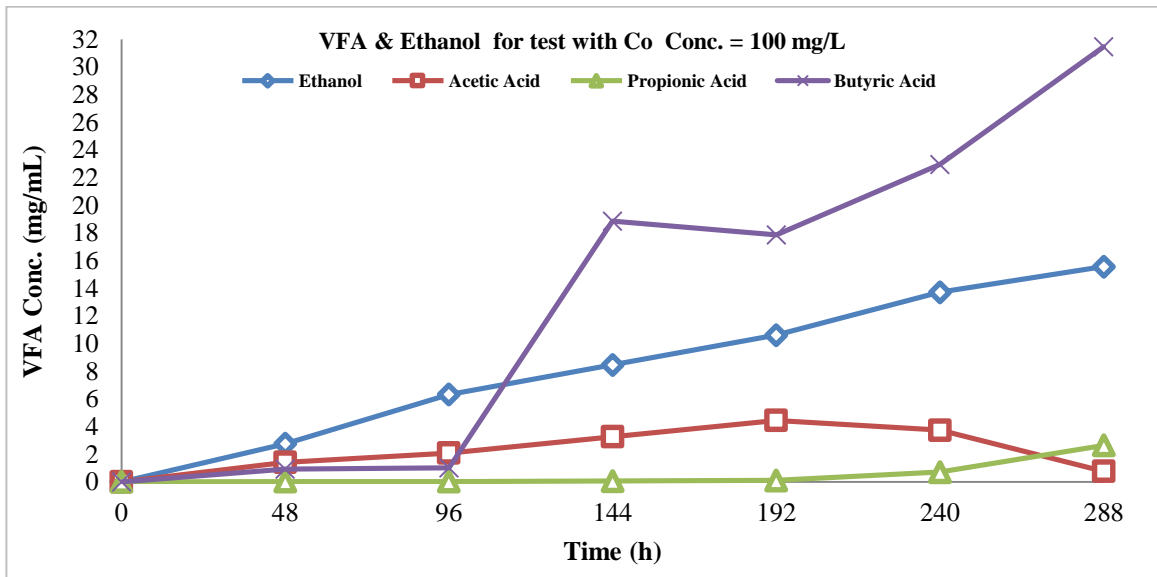


Figure 4.25j VFA variation during digestion period at T= 37 °C, 150 rpm, 15% TS MSW, 10 mL Inoculum and 100 mg/L Co Conc., where (◇) Ethanol, (□) Acetic Acid, (△) Propionic Acid and (×) Butyric Acid, the composition of liquid phase was analysis by GC-17A equipped with a FID detector (see section 3.1.5.3).

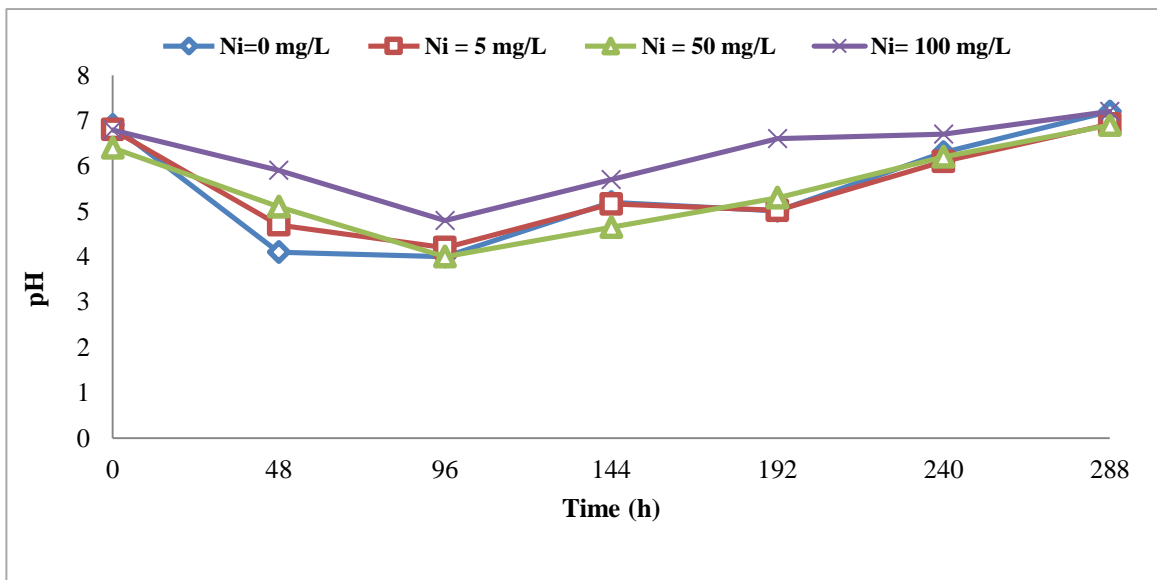


Figure 4.26a pH variation during digestion period at T= 37 °C, 150 rpm, 10mL Inoculum, 15% TS MSW and different Ni Concentration, where (◇) Zero, (□) 5mg/L, (△) 50mg/L and (×) 100mg/L.

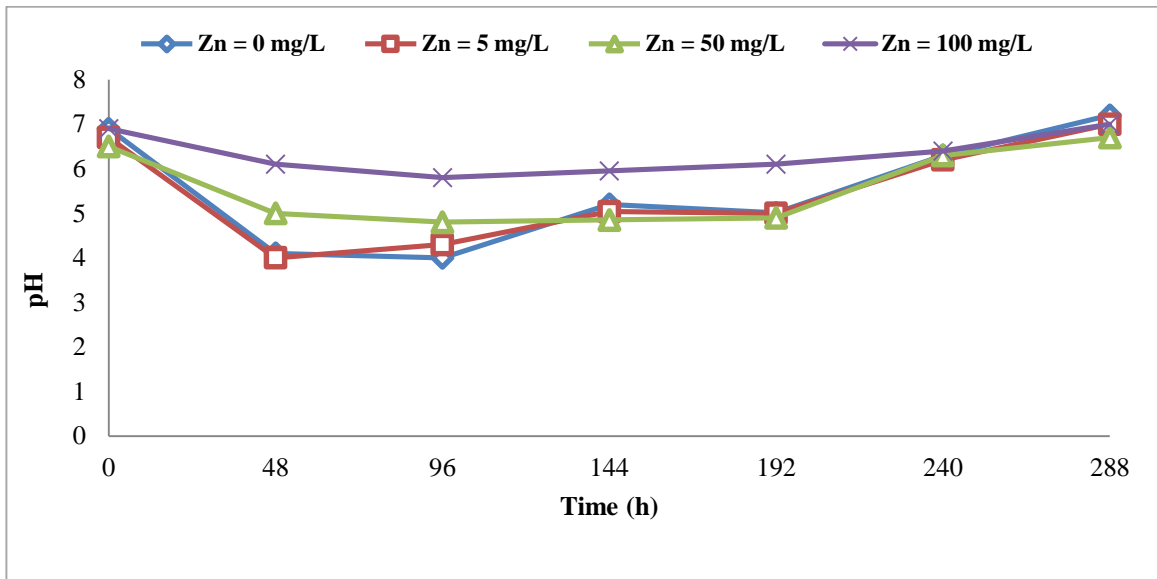


Figure 4.26b pH variation during digestion period at $T = 37\text{ }^{\circ}\text{C}$, 150 rpm, 10mL Inoculum, 15% TS MSW and different Zn Concentration, where (\diamond) Zero, (\square) 5mg/L, (\triangle) 50mg/L and (\times) 100mg/L.

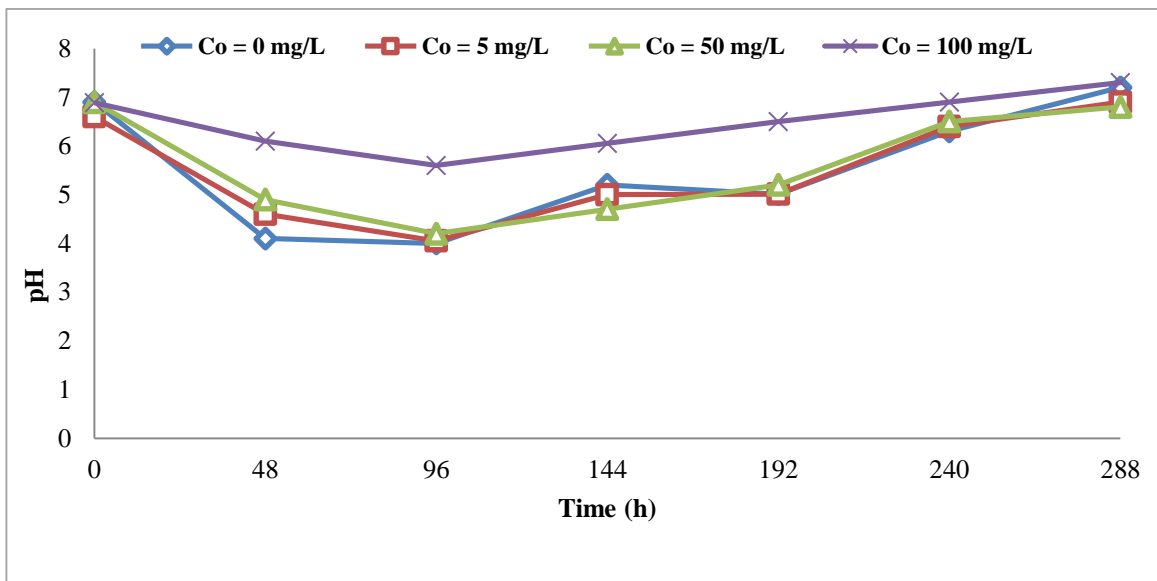


Figure 4.26c pH variation during digestion period at $T = 37\text{ }^{\circ}\text{C}$, 150 rpm, 10mL Inoculum, 15% TS MSW and different Co Concentration, where (\diamond) Zero, (\square) 5mg/L, (\triangle) 50mg/L and (\times) 100mg/L.

4.1.5.1.2 VFA and pH variation during (AD) for mixed trace element.

In this part we were studying the effect of different mixed essential trace elements (Ni, Zn and Co) with optimum concentration 5mg/L were obtained in the first part of this study.

Figures 4.27 a-b-c and d. Show the concentration-time profiles of ethanol and the most abundantly produced VFAs (acetic acid, butyric acid, propionic acid) were analyzed. The VFA and ethanol accumulations show a maximum when a mixed from two essential trace elements (Ni/Co, Ni/Zn and Zn/Co) were used. While, the lowest accumulations were observed when mixed from three trace elements (Ni/Co/Zn) was used. The final concentrations of VFAs and ethanol obtained in each experimental test are reported above in the Table (4.5).

The pH variations during the digestion period are presented in the **Figure 4.28**. The pH was tended to decrease during the anaerobic digestion process due to VFA production. a few drops from Sodium bicarbonate solution at concentration (1M), was added daily to the bioreactors to avoid pH values out optimum limits (6.5-7.5), that cause inhibition of methanogenesis step. The pH profiles detected in each test was corresponding to the profiles of the VFA concentration.

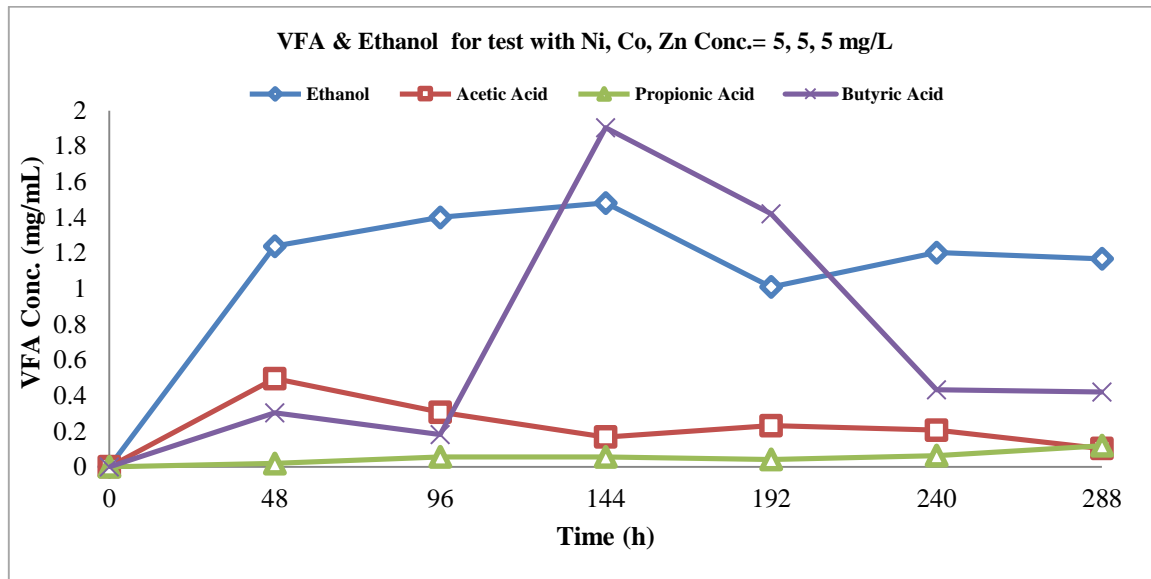


Figure 4.27a VFA and ethanol variation during digestion period at $T= 37\text{ }^{\circ}\text{C}$, 150 rpm, 15%TS MSW ,10 mL Inoculum and mix of three trace elements (Ni, Zn and Co) with concentration 5mg/L For each one , where (\diamond) Ethanol, (\square) Acetic Acid , (\triangle) Propionic Acid and (\times) Butyric Acid, the composition of liquid phase was analysis by GC-17A equipped with a FID detector (see section 3.1.5.3).

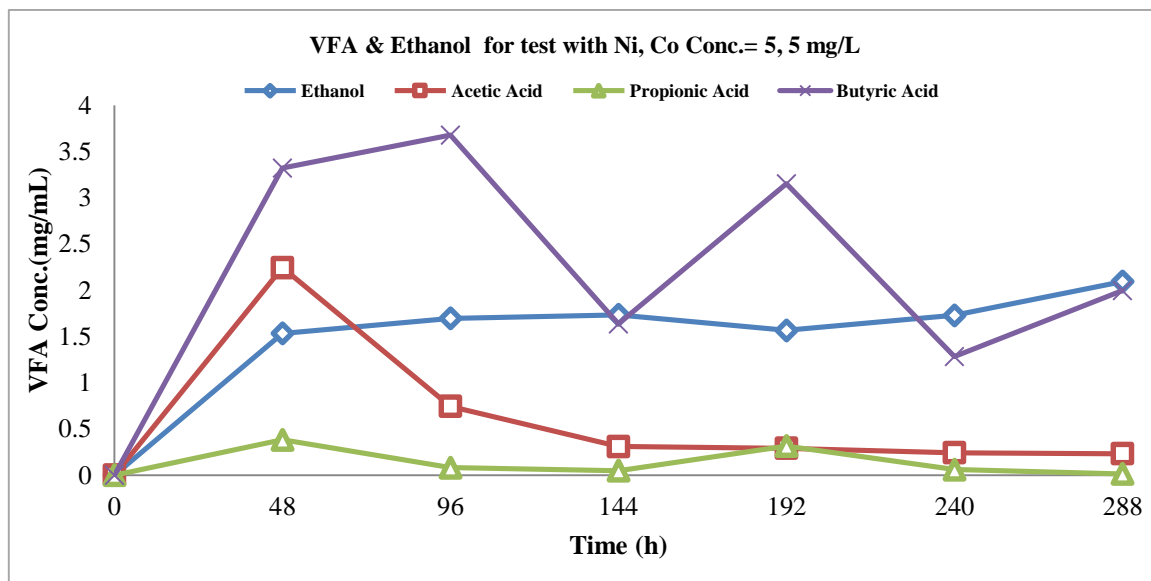


Figure 4.27b VFA and ethanol variation during digestion period at $T= 37\text{ }^{\circ}\text{C}$, 150 rpm, 15%TS MSW, 10 mL Inoculum and mix of two trace elements (Ni and Co) with concentration 5mg/L For each one, where (\diamond) Ethanol, (\square) Acetic Acid., (\triangle) Propionic Acid and (\times) Butyric Acid, the composition of liquid phase was analysis by GC-17A equipped with a FID detector (see section 3.1.5.3).

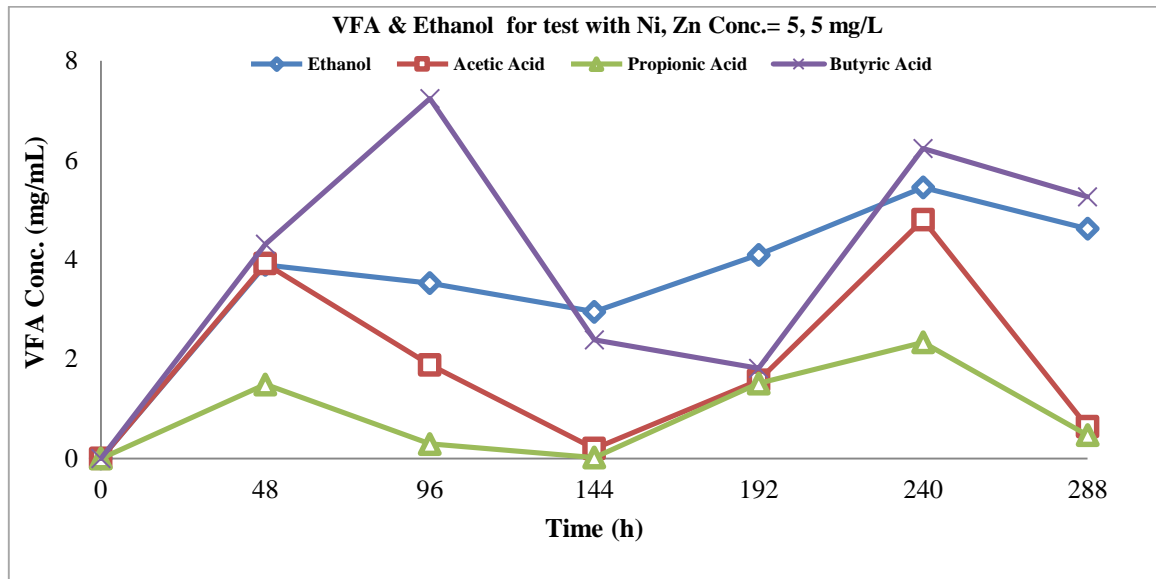


Figure 4.27c VFA and ethanol variation during digestion period at $T= 37\text{ }^{\circ}\text{C}$, 150 rpm, 15%TS MSW, 10 mL Inoculum and mix of two trace elements (Ni and Zn) with concentration 5mg/L. For each one, where (\diamond) Ethanol, (\square) Acetic Acid, (\triangle) Propionic Acid and (\times) Butyric Acid, the composition of liquid phase was analysis by GC-17A equipped with a FID detector (see section 3.1.5.3).

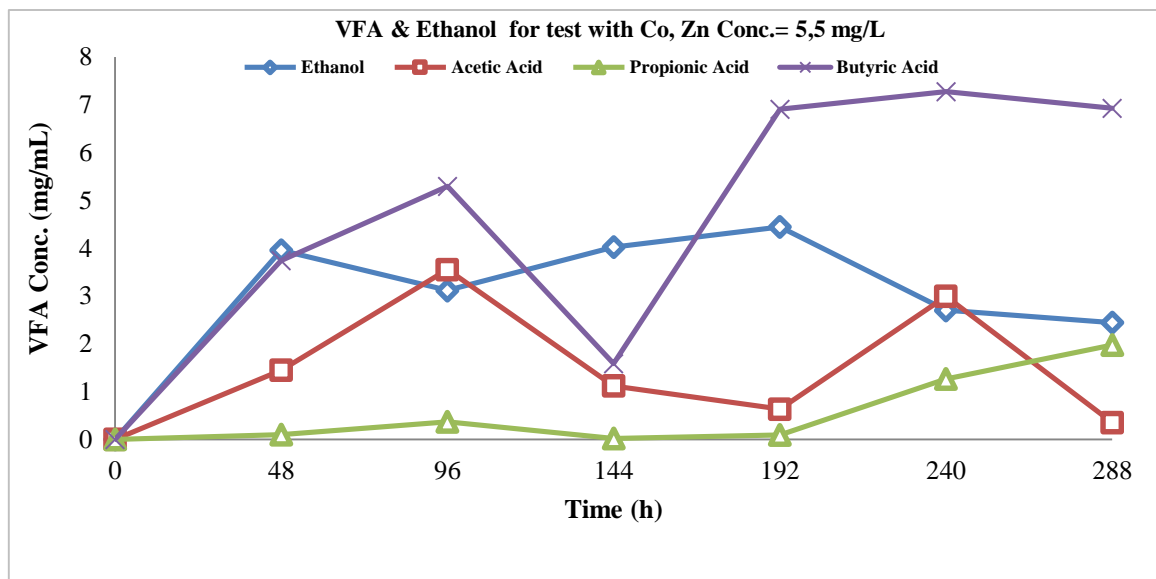


Figure 4.27d VFA and ethanol variation during digestion period at $T= 37\text{ }^{\circ}\text{C}$, 150 rpm, 15%TS MSW, 10 mL Inoculum and mix of trace elements (Zn and Co) with concentration 5mg/L. For each one, where (\diamond) Ethanol, (\square) Acetic Acid, (\triangle) Propionic Acid and (\times) Butyric Acid, the composition of liquid phase was analysis by GC-17A equipped with a FID detector (see section 3.1.5.3).

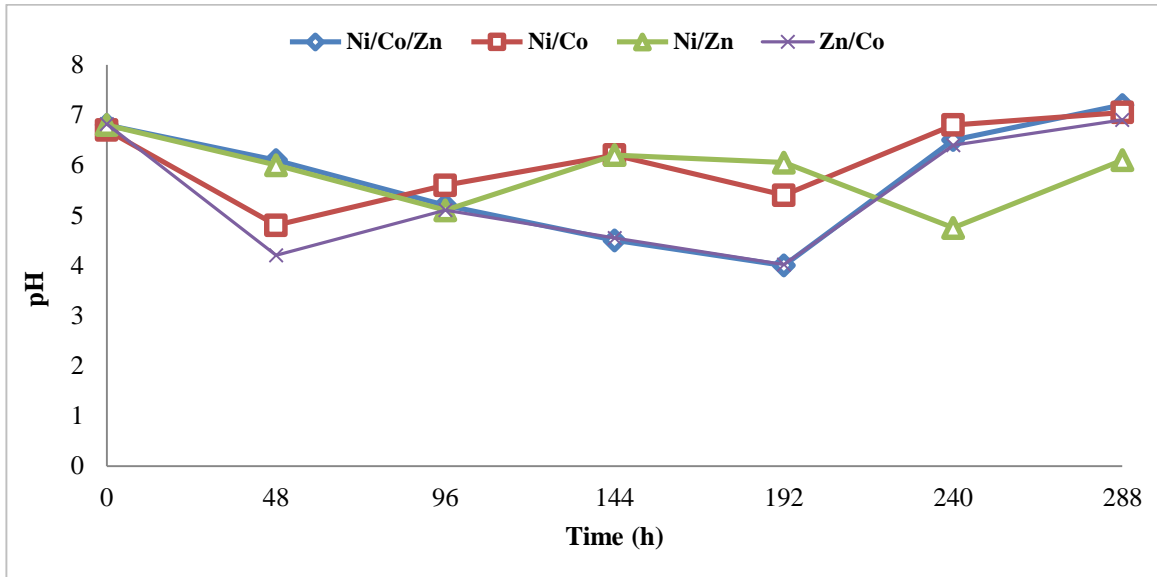


Figure 4.28 pH variation during digestion period at $T=37\text{ }^{\circ}\text{C}$, 150 rpm, 10mL Inoculum, 15% TS MSW and different mix of trace elements, where (\diamond)Ni/Co/Zn, (\square) Ni/Co, (Δ) Ni/Zn and (\times) Zn/Co.

4.1.5.2 Biogas yield.

4.1.5.2.1 Effect of individual trace element addition on biogas yield.

The cumulative volumes of biogas production for with and without individual trace element addition are presented in **Figures 4.29a-b and c**. The highest values were obtained about (768, 733 and 800 mL) at 5mg/L addition for each Ni, Zn and Co respectively. Whereas, Lower values were about (246.5, 211.5 and 184.5 mL) for Ni, Zn and Co respectively, when the concentration of individual trace elements was 100mg/L. On the other hand, a little increasing was observed when a 50mg/L was used, they produced (507, 541.5 and 557 mL) for Ni, Zn and Co respectively. Whilst, the reactor without element addition it was produced (425mL).

This result suggests that the optimum biogas production at a concentration (5mg/L) from each individual trace element addition.

Figures (4.30a-b-c-d-e-f-g-h-i and j). Show the variation in the composition of biogas (CH_4 , H_2 and CO_2) as a function of the individual trace element addition (Ni, Zn and Co). These results show an initial rise of the methane concentration, followed by a progressive decrease.

The highest fraction of methane was obtained when using 5mg/L, as the highest amount of biogas was produced under these additions. The results are agreement with the data presented in the literature (Lo H.M. et al., 2012, Altas L., 2009). The maximum production occurring approximately during the intermediate phase of the process has been observed in previous work, as well (Brulé M. et al., 2013).

In the first part of each test, significant volumes of biohydrogen were produced, probably due to the action of the hydrogen-producing bacteria (especially *Clostridium*) contained in the inoculum.

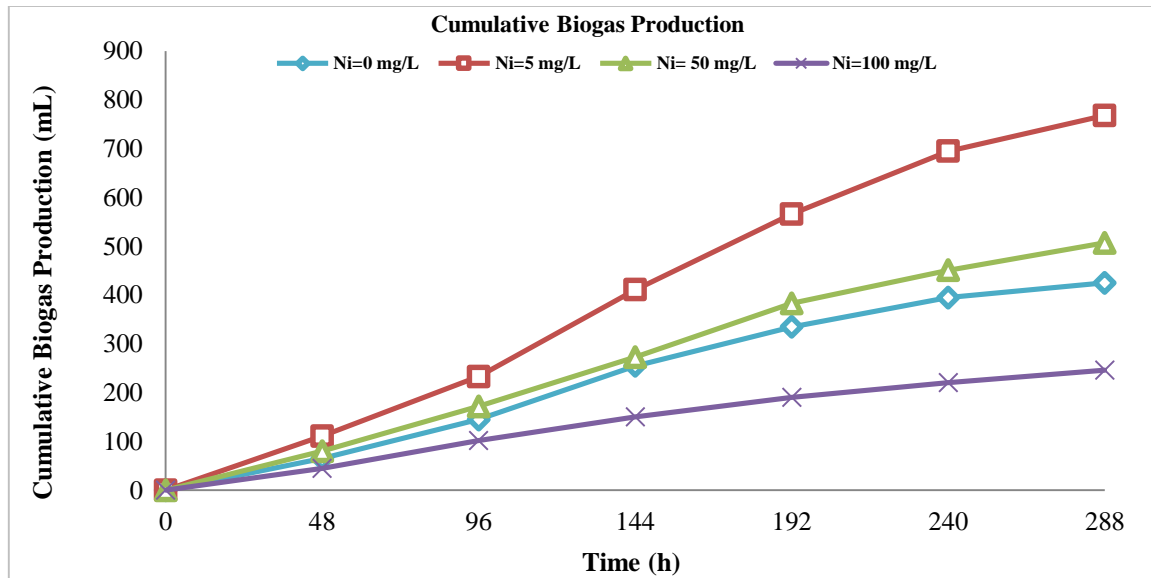


Figure 4.29a Cumulative biogas yield during digestion period at T= 37°C, 150 rpm, 10mL Inoculum, 15% TS MSW and different Ni concentration, where (◇) Zero, (□) 5mg/L, (△) 50mg/L and (x) 100mg/L.

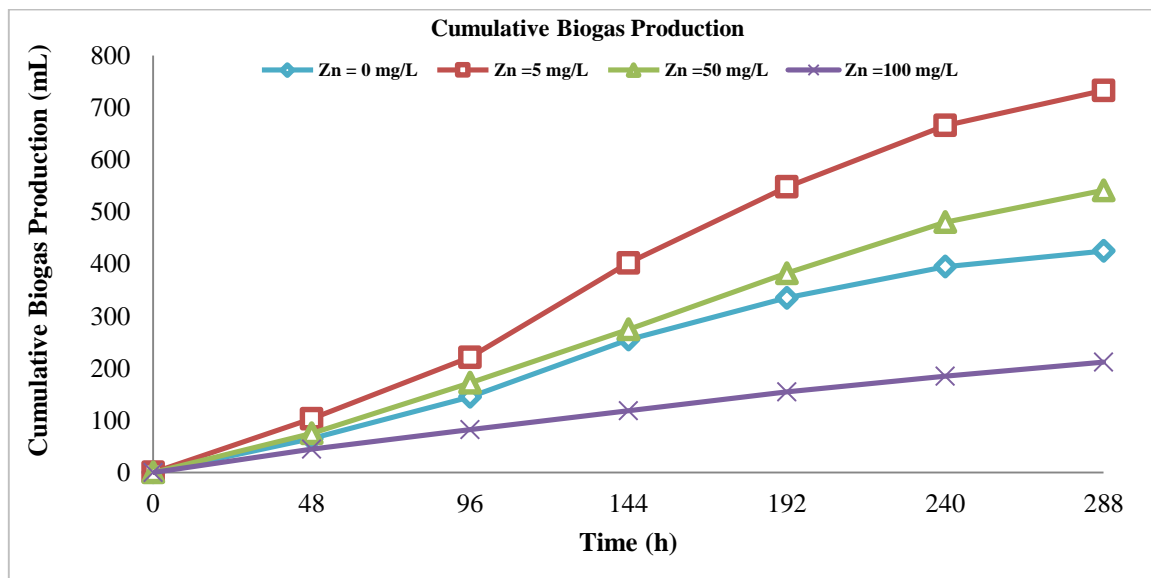


Figure 4.29b Cumulative biogas yield during digestion period at T= 37°C, 150 rpm, 10mL Inoculum, 15% TS MSW and different Zn concentration, where (◇) Zero, (□) 5mg/L, (△) 50mg/L and (x) 100mg/L.

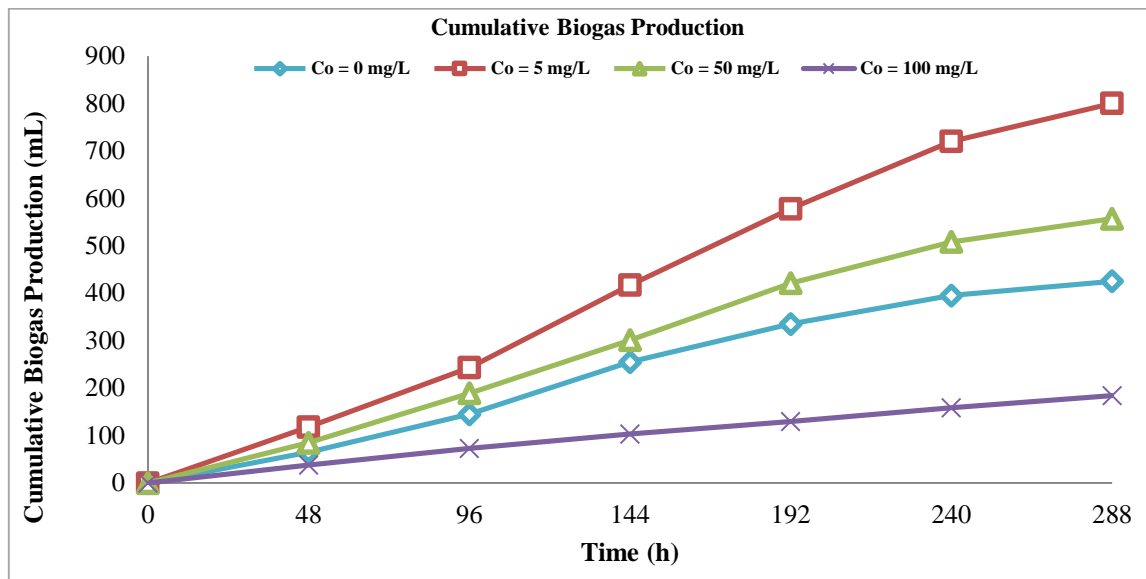


Figure 4.29c Cumulative biogas yield during digestion period at $T= 37^{\circ}\text{C}$, 150 rpm, 10mL Inoculum ,15%TS MSW and different Co concentration, where (\diamond) Zero, (\square) 5mg/L , (\triangle) 50mg/L and (\times) 100mg/L.

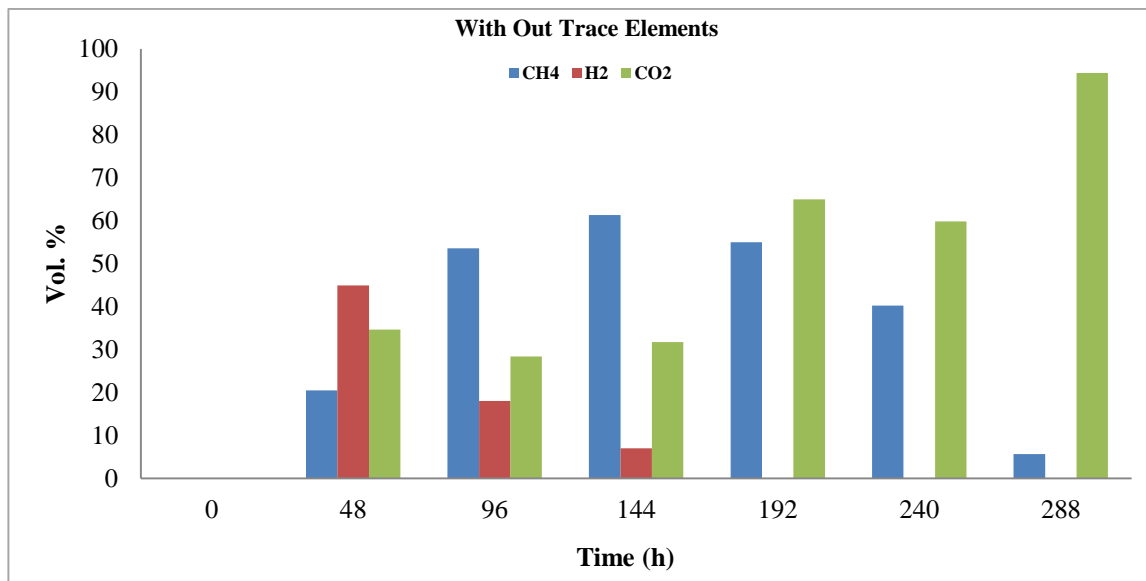


Figure 4. 30a Composition of biogas for the sample without trace element addition at $T= 37^{\circ}\text{C}$,15%TS, 150 rpm and 10mL Inoculum, the composition of biogas was analysis by GC-HP 5890 equipped with a TCD detector (see section 3.1.6).

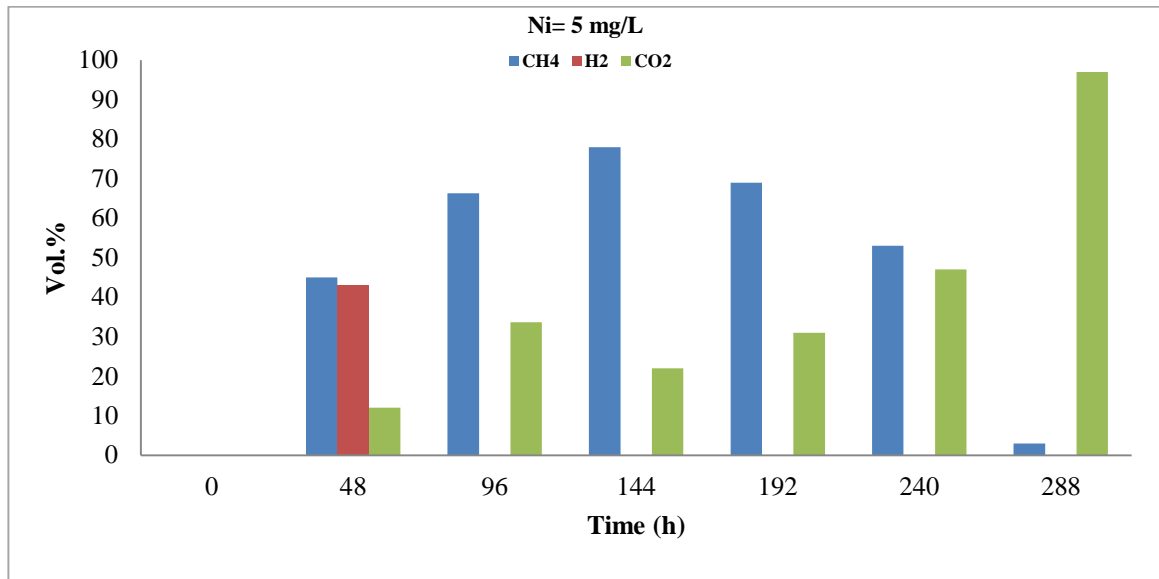


Figure 4.30b Composition of biogas for the sample with Ni concentration 5mg/L at T= 37 °C, 15 %TS, 150 rpm and 10mL Inoculum, the composition of biogas was analysis by GC-HP 5890 equipped with a TCD detector (see section 3.1.6).

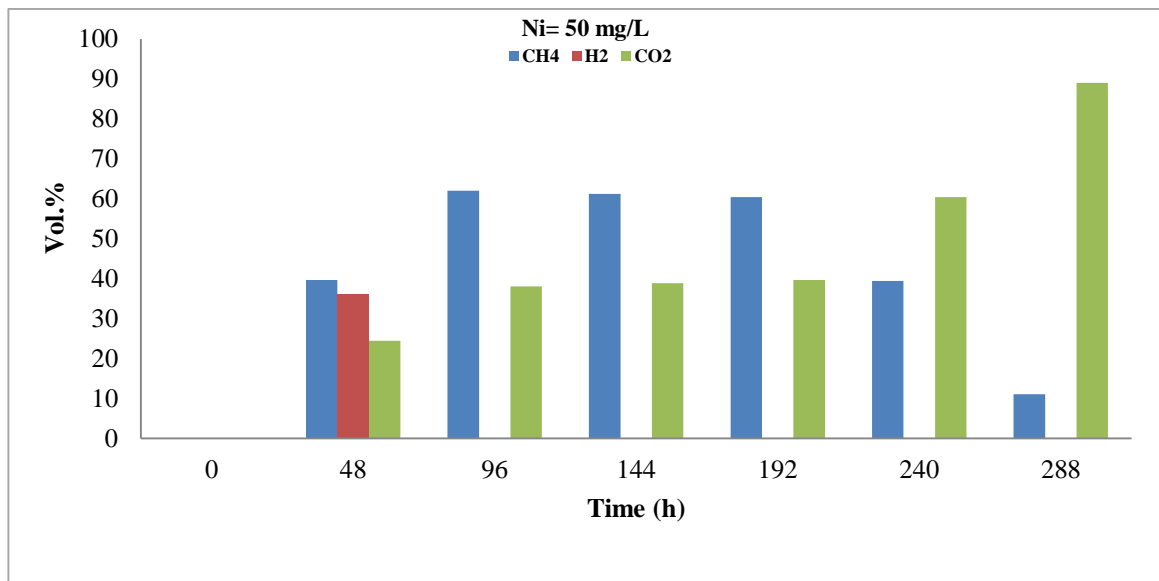


Figure 4.30c Composition of biogas for the sample with Ni concentration 50mg/L at T= 37°C, 15 %TS, 150 rpm and 10mL Inoculum, the composition of biogas was analysis by GC-HP 5890 equipped with a TCD detector (see section 3.1.6).

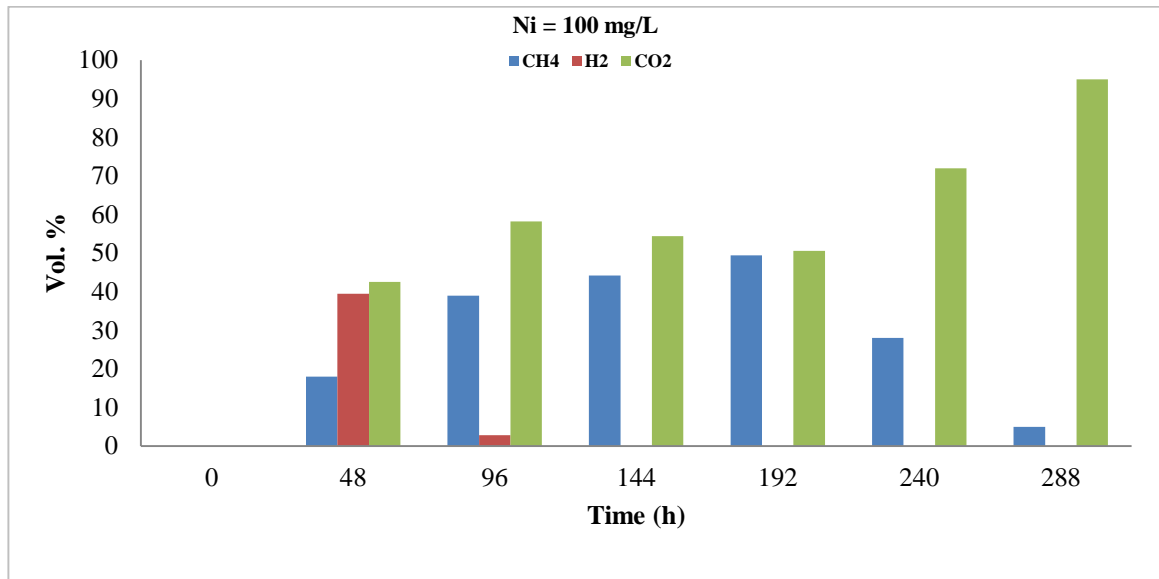


Figure 4.30d Composition of biogas for the sample with Ni concentration 100 mg/L at T= 37 °C, 15%TS, 150 rpm and 10mL Inoculum, the composition of biogas was analysis by GC-HP 5890 equipped with a TCD detector (see section 3.1.6).

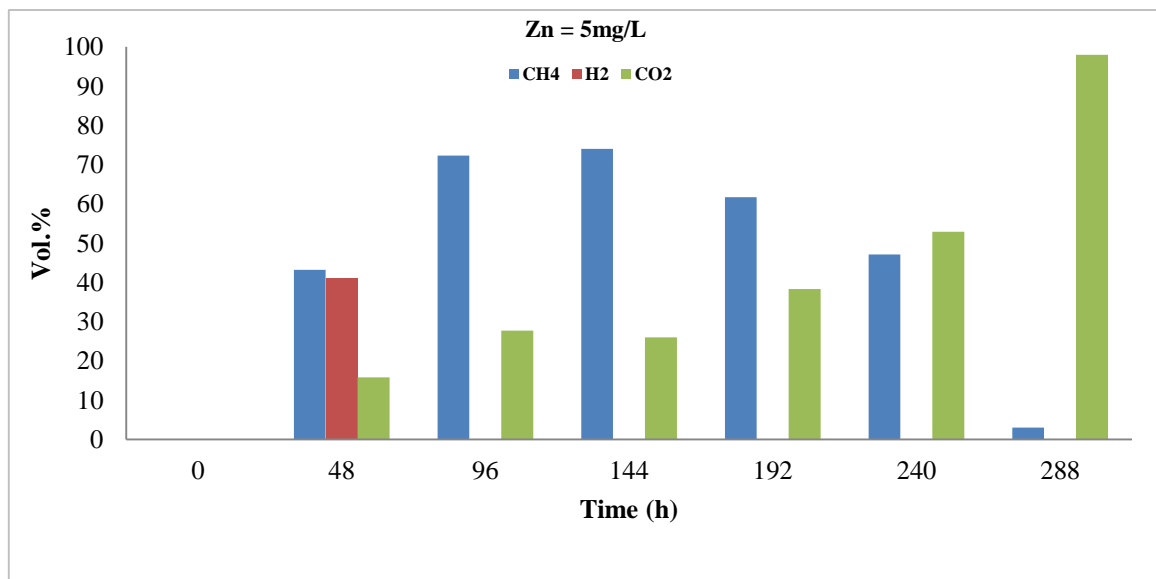


Figure 4.30e Composition of biogas for the sample with Zn concentration 5mg/L at T= 37 °C, 15%TS, 150 rpm and 10mL Inoculum, the composition of biogas was analysis by GC-HP 5890 equipped with a TCD detector (see section 3.1.6).

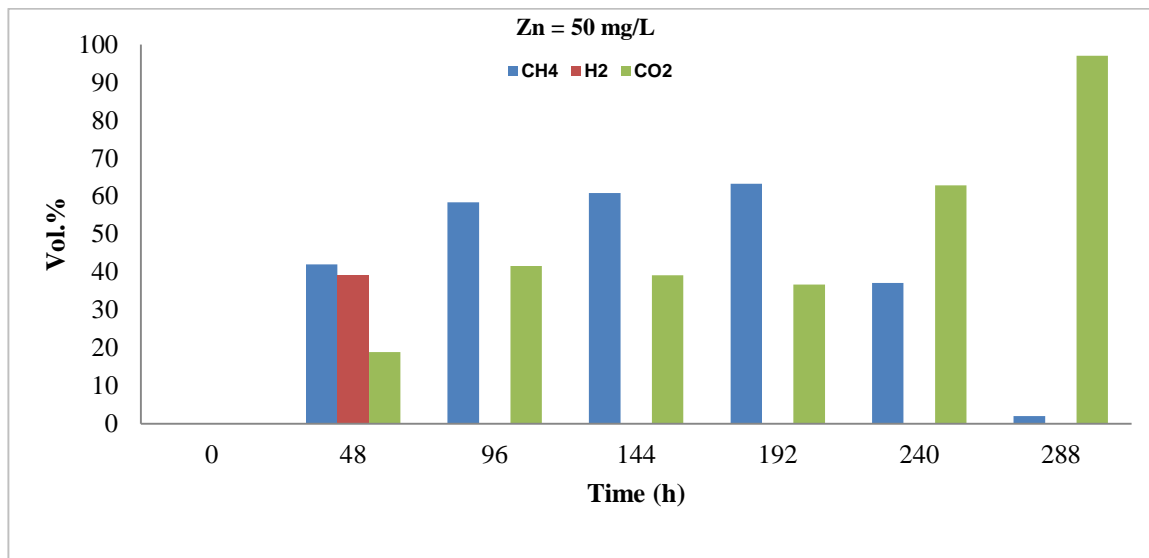


Figure 4.30f Composition of biogas for the sample with Zn concentration 50 mg/L at T= 37 °C, 15%TS, 150 rpm and 10mL Inoculum, the composition of biogas was analysis by GC-HP 5890 equipped with a TCD detector (see section 3.1.6).

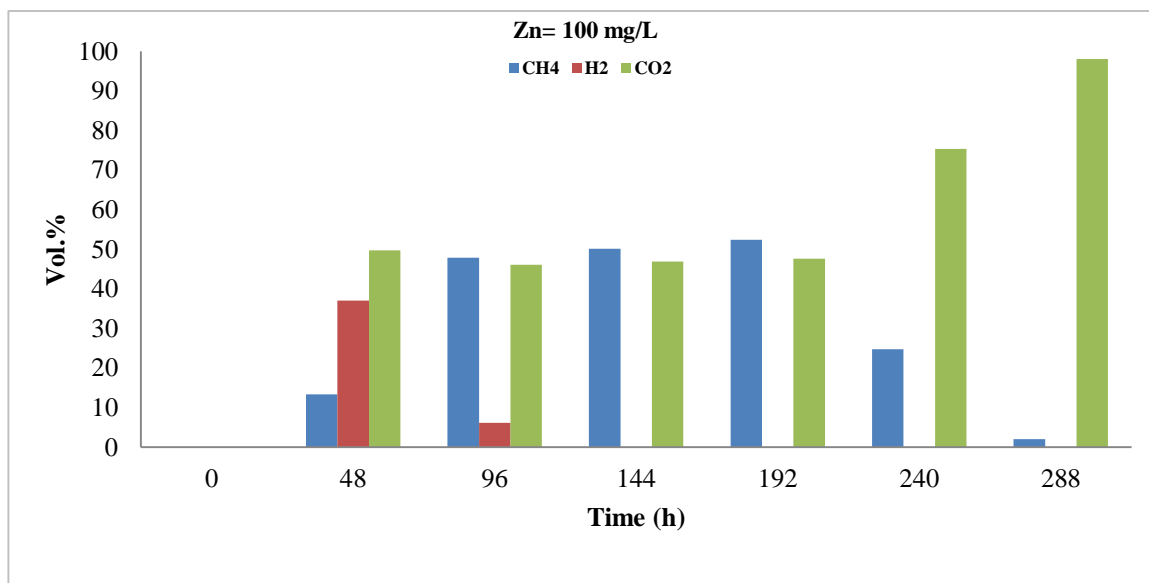


Figure 4.30g Composition of biogas for the sample with Zn concentration 100 mg/L at T= 37°C,15%TS, 150 rpm and 10mL Inoculum, the composition of biogas was analysis by GC-HP 5890 equipped with a TCD detector (see section 3.1.6).

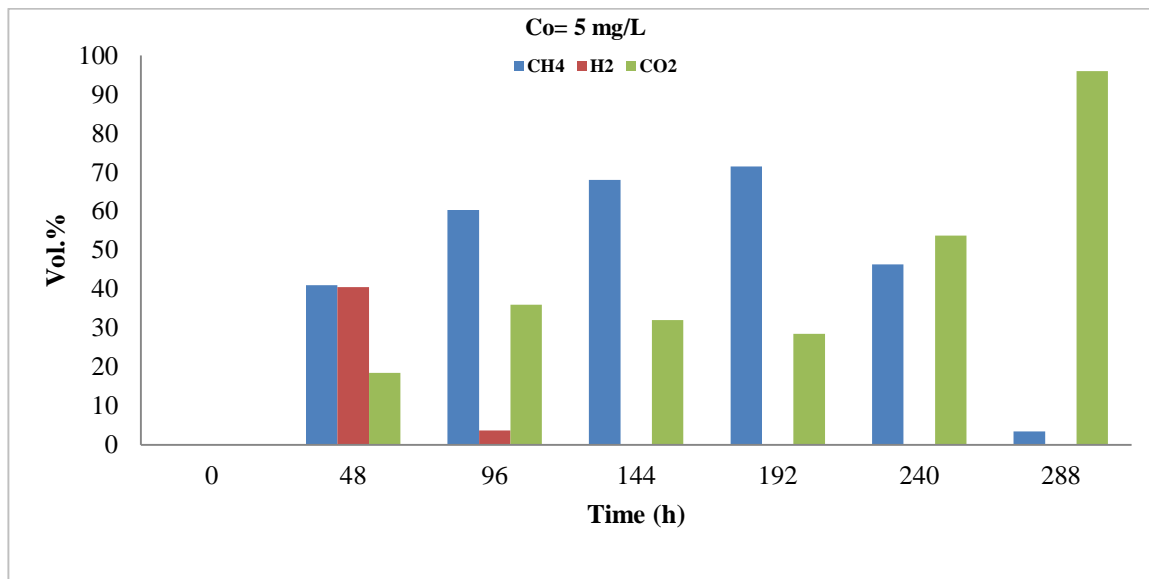


Figure 4.30h Composition of biogas for the sample with Co concentration 5mg/L at T= 37°C,15%TS, 150 rpm and 10mL Inoculum, the composition of biogas was analysis by GC-HP 5890 equipped with a TCD detector (see section 3.1.6).

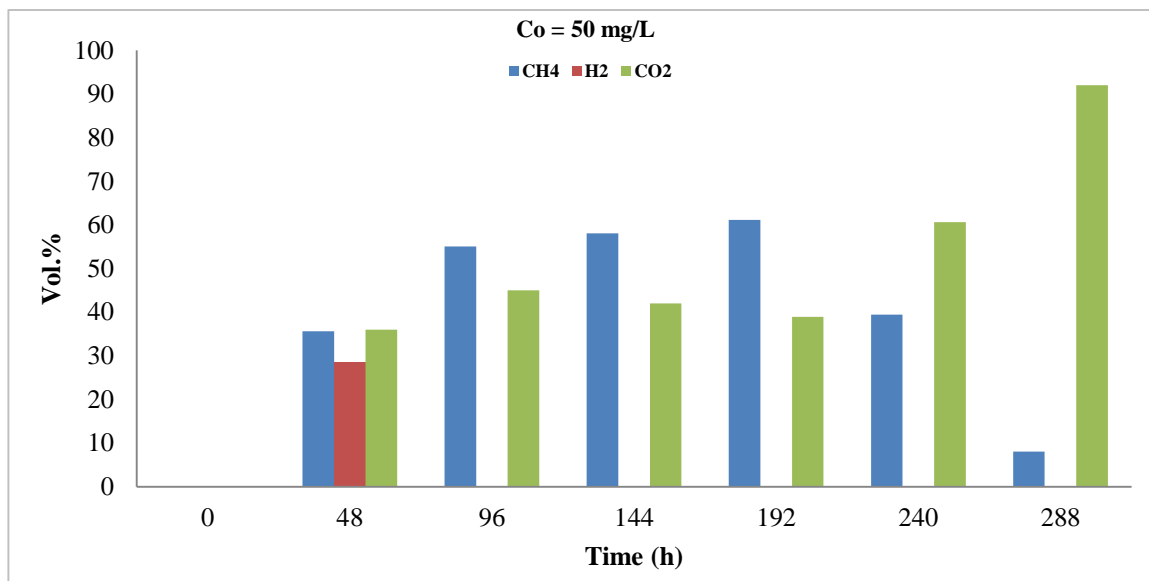


Figure 4.30i Composition of biogas for the sample with Co concentration 50 mg/L at T= 37°C,15%TS, 150 rpm and 10mL Inoculum, the composition of biogas was analysis by GC-HP 5890 equipped with a TCD detector (see section 3.1.6).

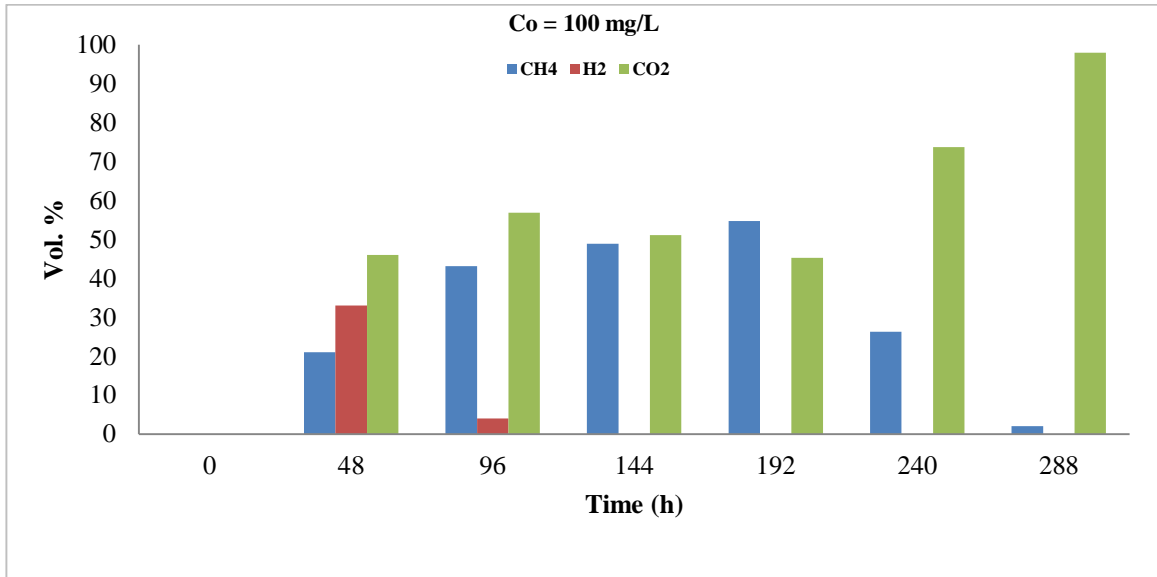


Figure 4.30j Composition of biogas for the sample with Co concentration 100 mg/L at $T = 37^{\circ}\text{C}$, 15% TS, 150 rpm and 10mL Inoculum, the composition of biogas was analysis by GC-HP 5890 equipped with a TCD detector (see section 3.1.6).

4.1.5.2.2 Effect mixed trace element addition on Biogas yield.

The effect of different mixed essential trace element addition (Ni, Zn and Co) concentration 5mg/L for each one, on cumulative volumes of biogas production are presented in **Figure 4.31**. The highest cumulative volume of biogas was about 1332.65 mL. This value was obtained by adding a mix from three trace elements to the reactor. Lower values were obtained when the mix of two trace elements were used, it was about (1113.08 mL) for Ni/Co and (974.36 mL) for Ni/Zn. While, the mix of two elements (Zn/Co) adding not have any significant effect above single trace element addition, we were studying in first part, it was produced (703.67 mL). This result suggests that the optimum biogas production at mix from three elements (Ni//Co/Zn) was added to the reactor.

Figures 4.32a-b-c and d. Show the variation in the composition of biogas (CH₄, H₂ and CO₂) as a function of the different mixture from trace element addition (Ni/Co/Zn, Ni/Co, Ni/Zn and Zn/Co) at the concentration 5mg/L for every element. In these results we were observing an initial rise of the biomethane fraction, followed by a progressive decrease. The maximum fraction of producing biomethane occurring in the period between (96 and 192 hrs.). This result are agreeing with the data presented in the literature (Qiang H. et al., 2012).

In the first test time for each sample, we can noting, significant volumes of biohydrogen were produced, probably due to the action of the hydrogen-producing bacteria (especially Clostridium) contained in the inoculum.

This result suggests, according to cumulative production of biogas the higher accumulative volume of biomethane produced when the mixture of trace elements were used, especially with three trace elements.

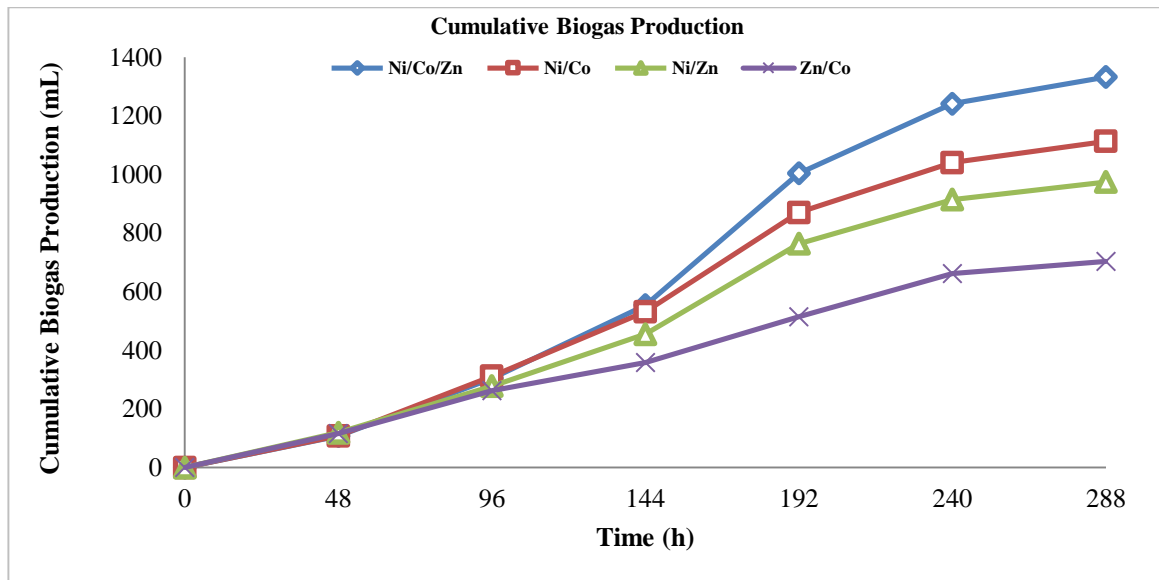


Figure 4.31 Cumulative biogas yield during digestion period at T= 37°C, 150 rpm, 10mL Inoculum, 15% TS MSW and different mix of trace elements, where (◇) Ni/Co/Zn, (□) Ni/Co, (△) Ni/Zn and (x) Zn/Co.

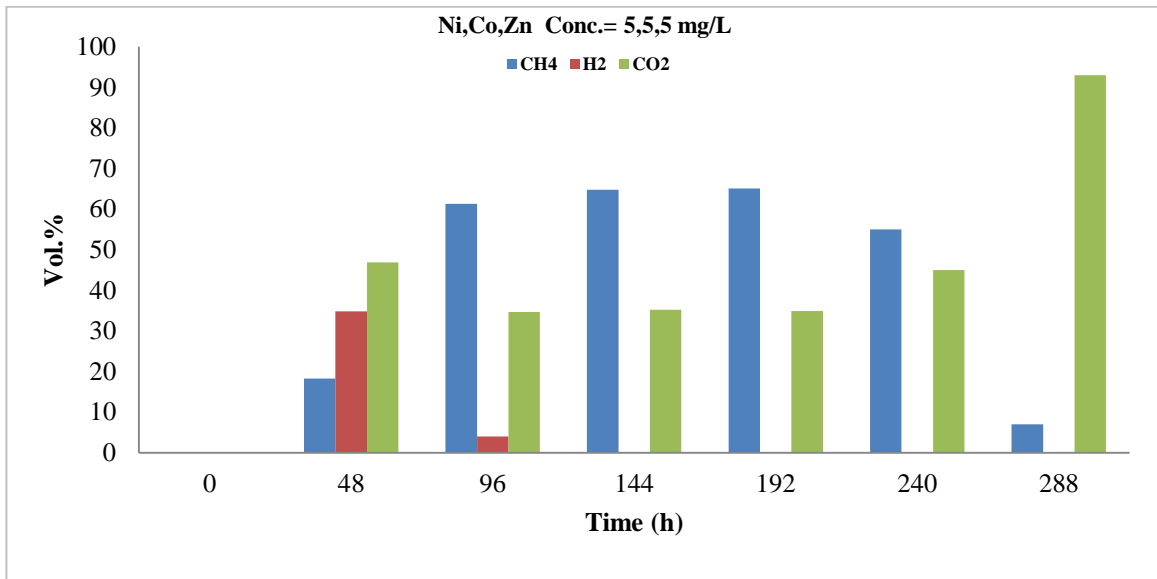


Figure 4.32a Composition of biogas for the sample with mix from three trace elements Ni/Co/Zn at T=37°C, 15%TS, 150 rpm and 10mL Inoculum, the composition of biogas was analysis by GC-HP 5890 equipped with a TCD detector (see section 3.1.6).

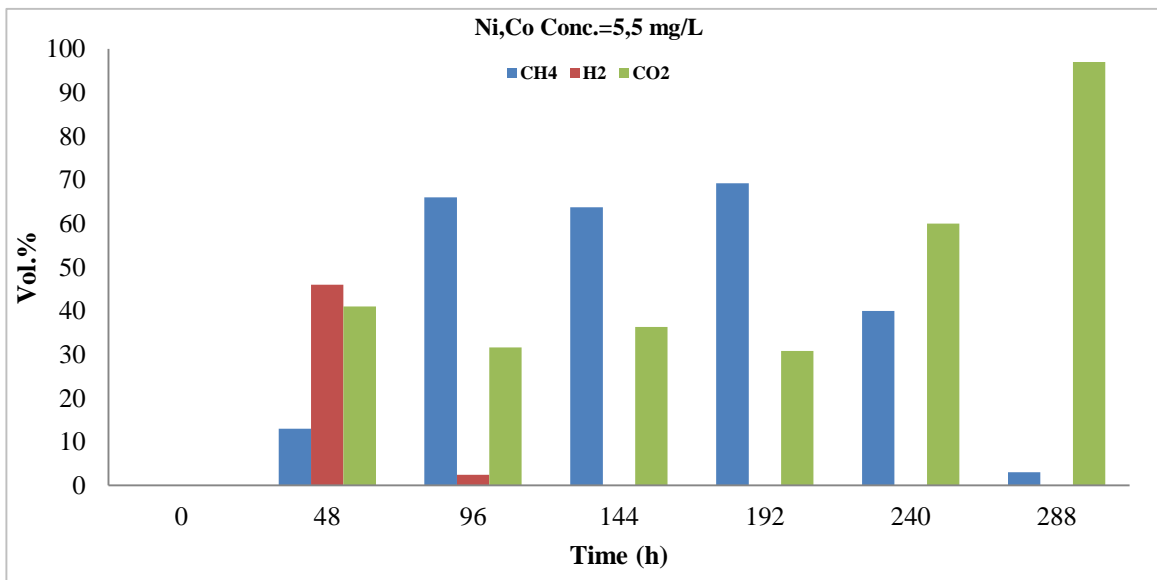


Figure 4.32b Composition of biogas for the sample with mix from two trace elements Ni/Co at T= 37°C,15%TS, 150 rpm and 10mL Inoculum, the composition of biogas was analysis by GC-HP 5890 equipped with a TCD detector (see section 3.1.6).

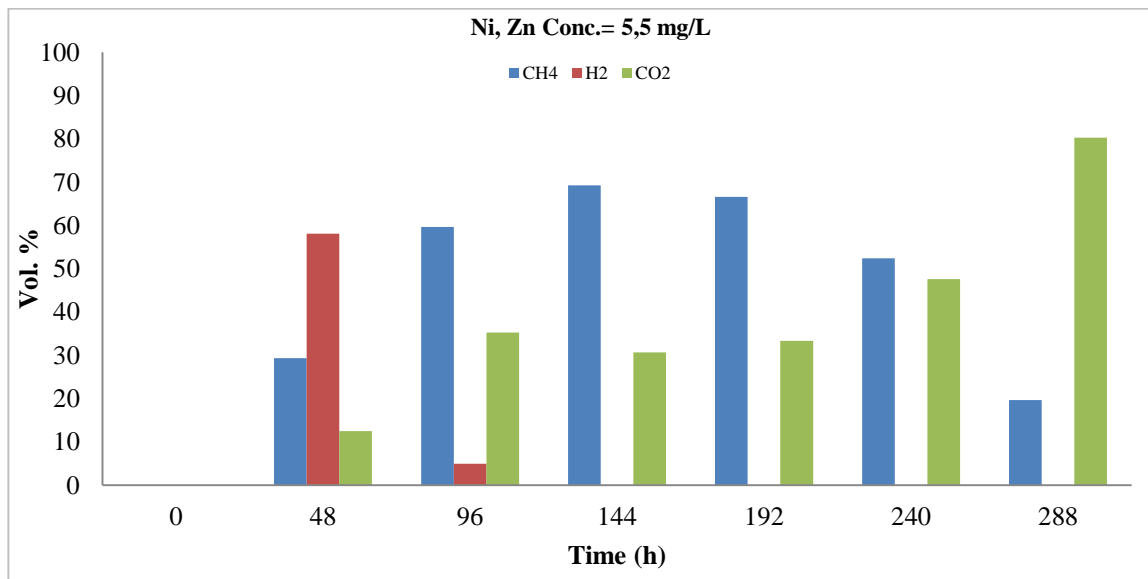


Figure 4.32c Composition of biogas for the sample with mix from two trace elements Ni/Zn at T=37°C, 15% TS, 150 rpm and 10mL Inoculum, the composition of biogas was analysis by GC-HP 5890 equipped with a TCD detector (see section 3.1.6).

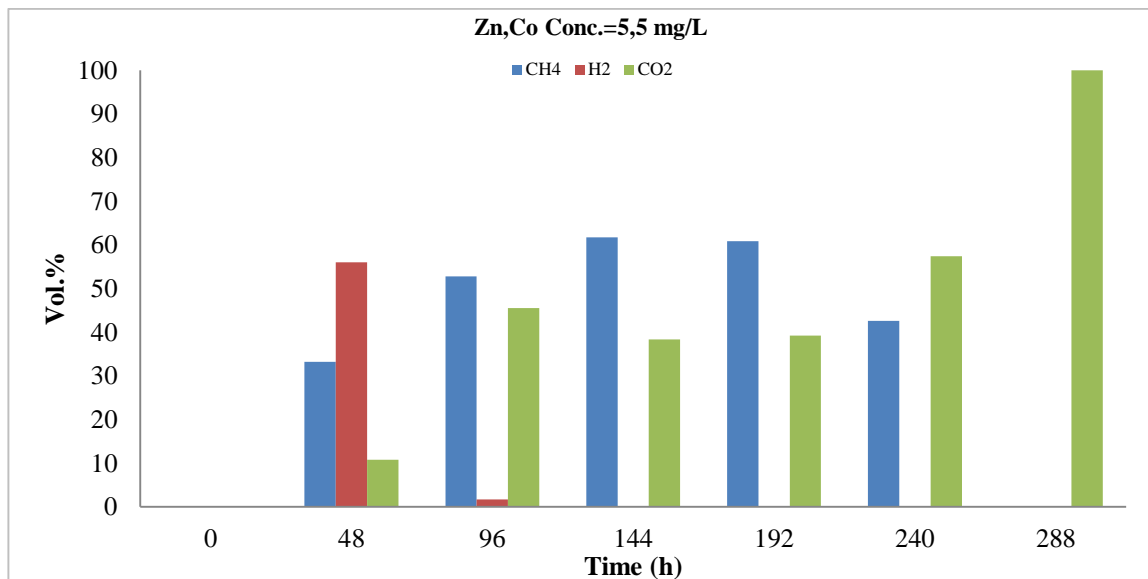


Figure 4.32d Composition of biogas for the sample with mix from two trace elements Zn/Co at T=37°C, 15% TS, 150 rpm and 10mL Inoculum, the composition of biogas was analysis by GC-HP 5890 equipped with a TCD detector (see section 3.1.6).

4.1.5.3 Biomass growth and glucose concentration.

4.1.5.3.1 Effect of individual trace element addition on biomass growth.

Figures 4.33a-b and c. Show the influence of individual trace element addition with three different concentrations (5, 50 and 100 mg/L) on the growth of biomass during the digestion period. In all cases, approximately similar behaviors of growth were observed, and the maximum concentration of biomass was (6.951, 6.72 and 7.01 mg/mL) at (144hrs.) for single element Ni, Zn and Co respectively at concentration 5mg/L was used. On the contrary, when using concentration 100mg/L of single elements, to little significant increases of the biomass concentration were observed. Due to processes inhabitation at this concentration.

Figures 4.34 a-b and c. describe the reduction of glucose Concentration during the digestion period. The concentration of glucose at zero time for the test without element addition, it was a bout (7g/L) and (7.24, 7.22 and 7.32), (7.19, 7.25 and 7.12), (7.27, 7.12 and 6.51) for Ni, Zn and Co at three individual different concentrations 5, 50 and 100 mg/ L respectively. A simple sugars formed at intermediate hydrolysis step are immediately biodegraded and indeed successive values tend to zero.

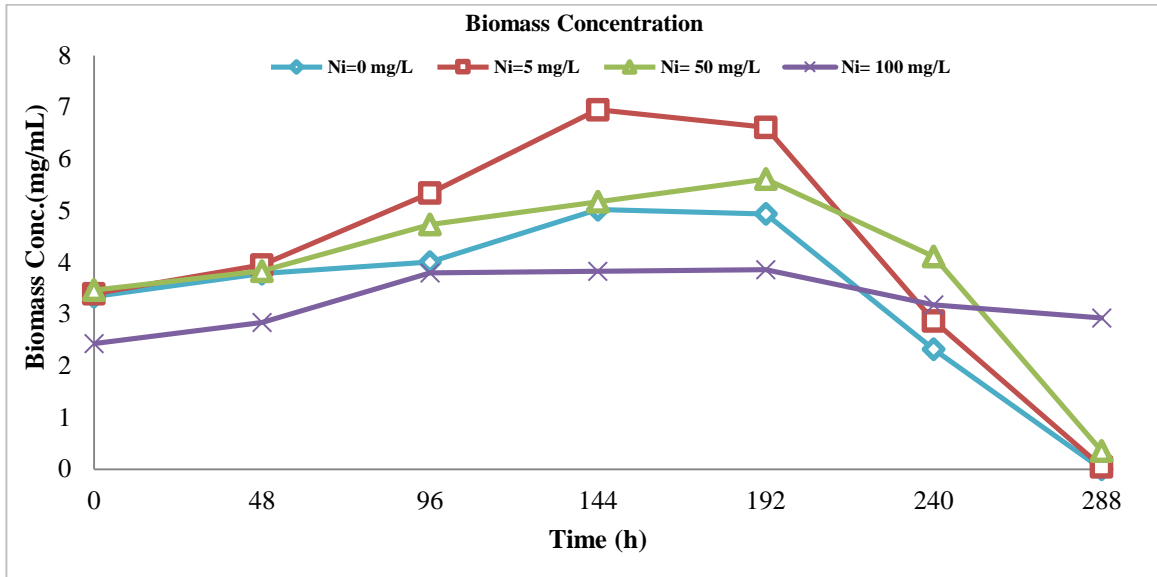


Figure 4.33a Biomass growth during digestion period at T= 37°C, 150 rpm, 10mL inoculum, 15%TS MSW and different Ni concentration where (◇) Zero, (□) 5mg/L, (△) 50mg/L and (x) 100mg/L.

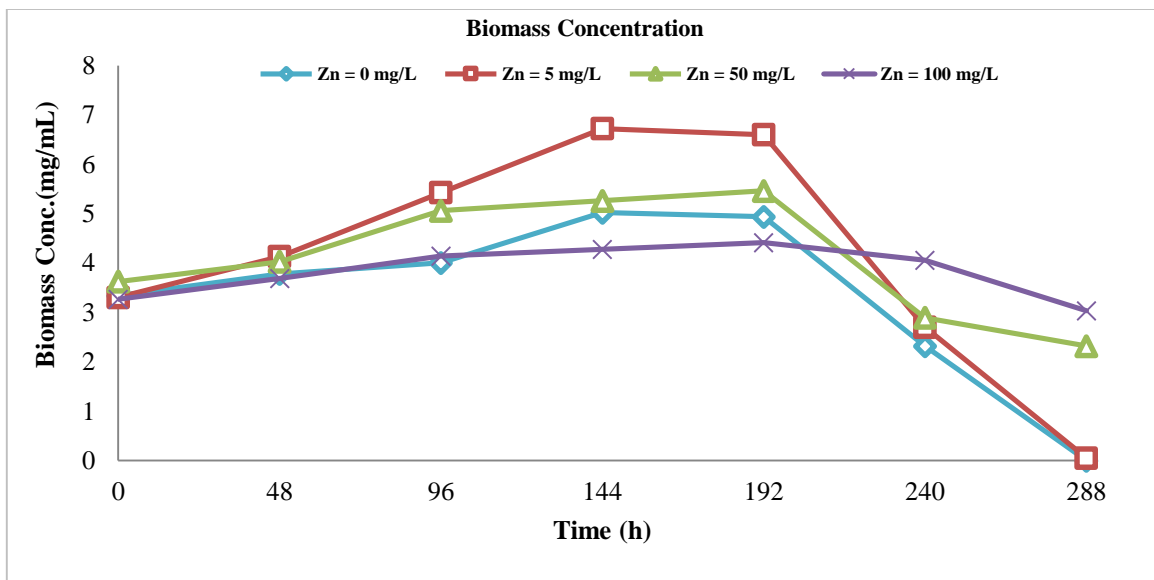


Figure 4.33b Biomass growth during digestion period at T= 37 °C, 150 rpm, 10mL Inoculum, 15%TS MSW and different Zn concentration ,where (◇) Zero, (□) 5mg/L , (△) 50mg/L and (x) 100mg/L.

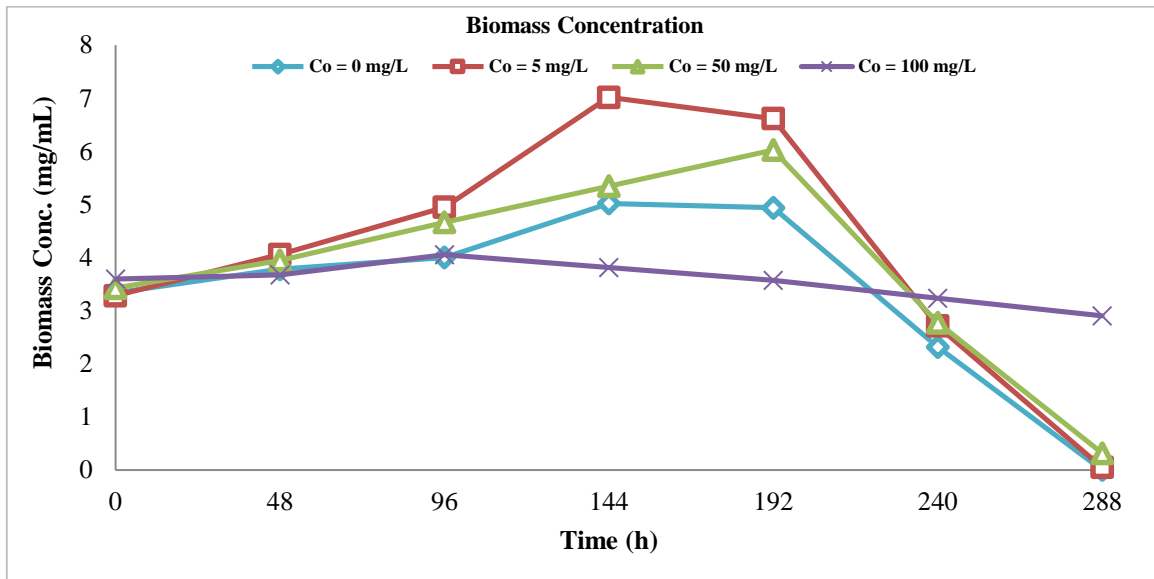


Figure 4.33c Biomass growth during digestion period at $T = 37^{\circ}\text{C}$, 150 rpm, 10mL Inoculum, 15%TS MSW and different Co concentration, where (\diamond) Zero, (\square) 5mg/L, (\triangle) 50mg/L and (\times) 100mg/L.

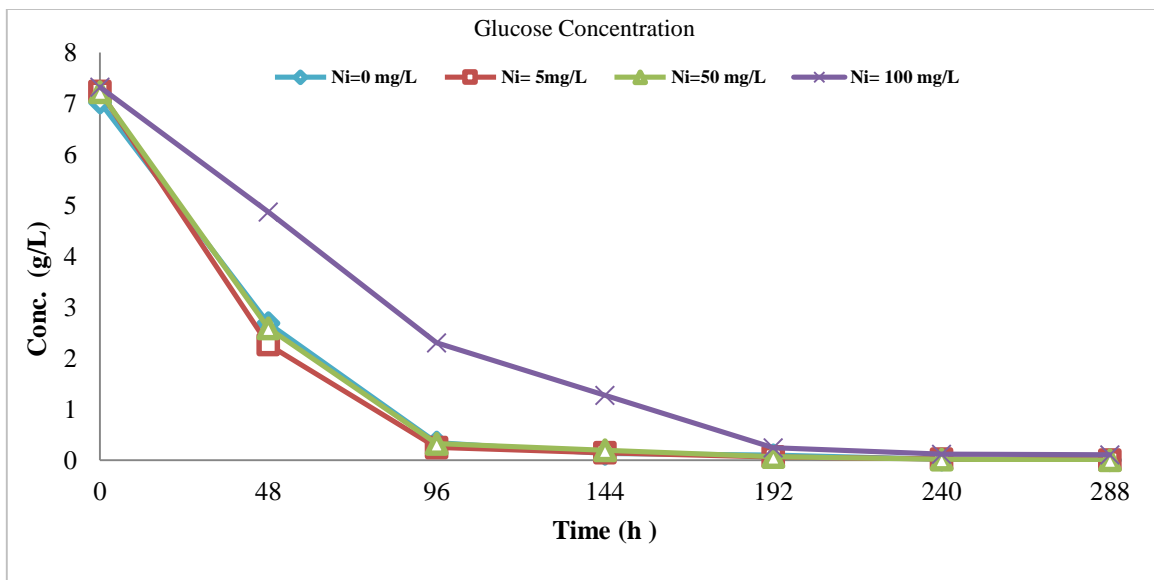


Figure 4.34a Concentration of glucose during digestion period at $T = 37^{\circ}\text{C}$, 150 rpm, 10mL Inoculum, 15%TS MSW and different Ni concentration, where (\diamond) Zero, (\square) 5mg/L, (\triangle) 50mg/L and (\times) 100mg/L.

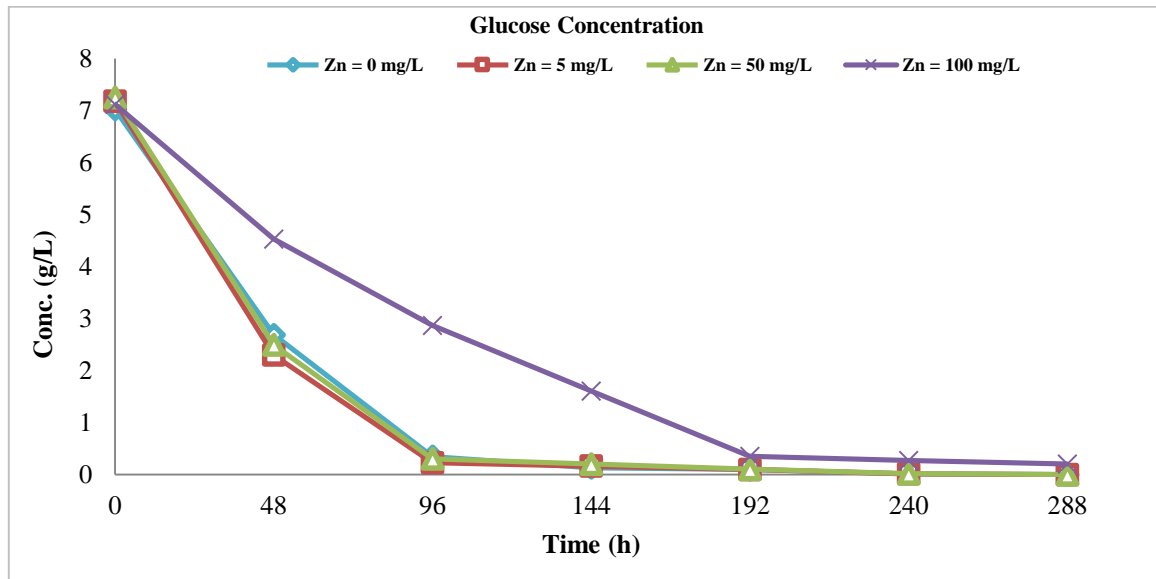


Figure 4.34b Concentration of glucose during digestion period at $T = 37^{\circ}\text{C}$, 150 rpm, 10mL Inoculum, 15%TS MSW and different Zn concentration, where (\diamond) Zero, (\square) 5mg/L, (Δ) 50mg/L and (\times) 100mg/L.

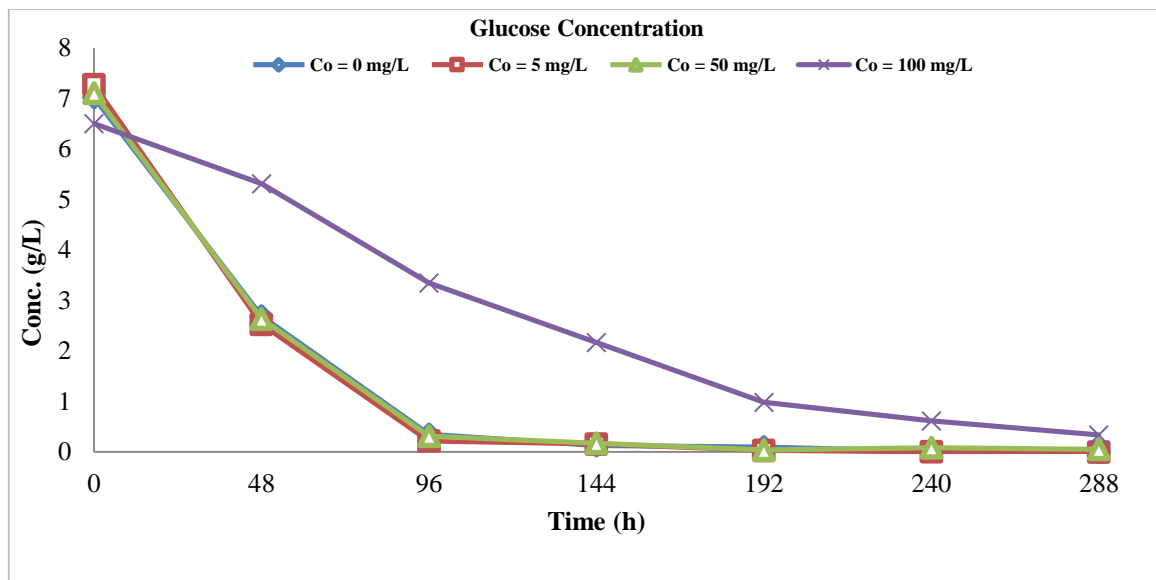


Figure 4.34c Concentration of glucose during digestion period at $T = 37^{\circ}\text{C}$, 150 rpm, 10mL Inoculum, 15%TS MSW and different Co concentration, where (\diamond) Zero, (\square) 5mg/L, (Δ) 50mg/L and (\times) 100mg/L.

4.1.5.3.2 Effect of mixed trace element addition biomass growth and glucose concentration.

Figure 4.35 shows the growth of biomass during the digestion period. When using different mixtures of trace elements with concentration 5mg/L for everyone, similar behaviors were observed, In all cases, a maximum biomass concentration about 8.27, 8.01,7.34 and 6.89 (mg/mL) for Ni/CO/Zn ,Ni/Co, Ni/Zn and Zn/Co Mixture addition, respectively was observed after about 144 hrs. Subsequently, a progressive reduction of the biomass concentration to zero value at the end of a testes were observed.

The reduction of glucose Concentration during the digestion period were analyzed as shows in **Figure 4. 36**. The concentration of glucose in the beginning, it was about (7.29, 7.2, 7.14 and 7.02 g/L) for Ni/Zn/Co, Ni/Co, Ni/Zn and Zn/Co mixture addition, respectively. A simple sugars formed at intermediate hydrolysis step are immediately biodegraded and indeed successive values tend to zero.

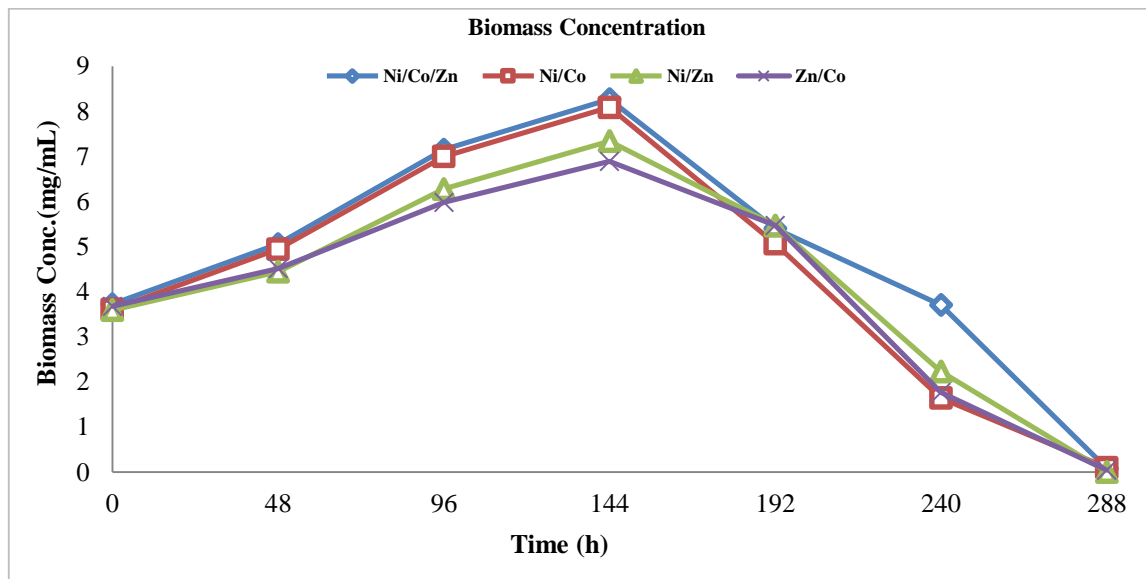


Figure 4.35 Biomass growth during digestion period at $T = 37^{\circ}\text{C}$, 150 rpm, 10mL Inoculum, 15% TS MSW and different mix of trace elements addition, where (\diamond) Ni/Co/Zn, (\square) Ni/Co, (\triangle) Ni/Zn and (\times) Zn/Co.

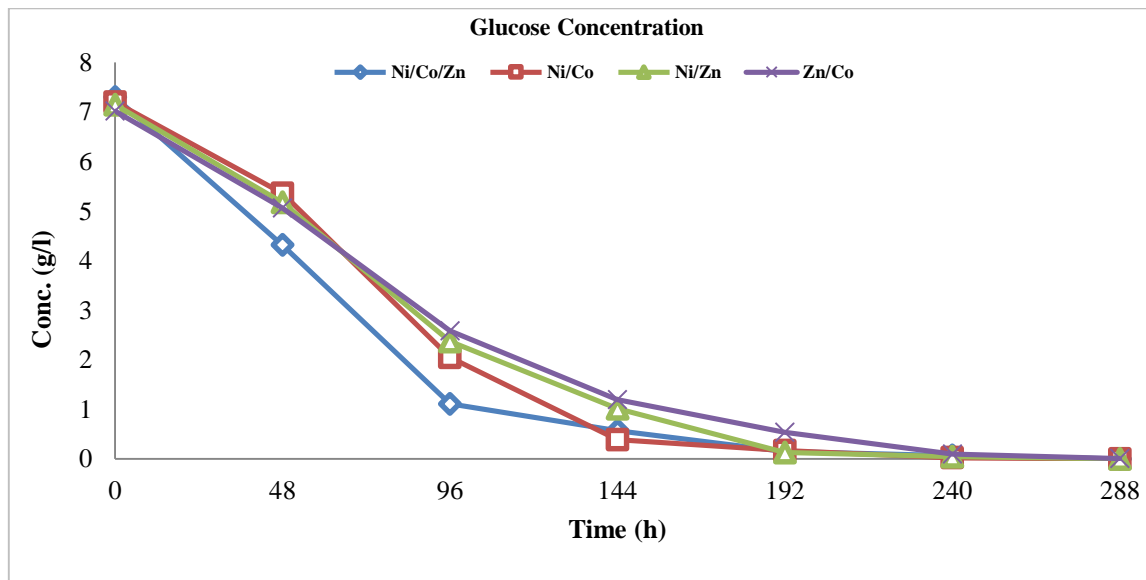


Figure 4.36 Concentration of glucose during digestion period at $T = 37^{\circ}\text{C}$, 150 rpm, 10mL Inoculum, 15% TS MSW and different mix of trace elements addition, where (\diamond) Ni/Co/Zn, (\square) Ni/Co, (\triangle) Ni/Zn and (\times) Zn/Co.

4.2 Catalyst Characterization.

4.2.1 Temperature-programmed reduction (TPR).

The reduction behavior of 15% Co/Al₂O₃ was studied by temperature-programmed reduction (TPR) as shown in **Figure 4.37**.

Four hydrogen consumption peaks were observed. The first peak at 167 °C was assigned to the reduction of incompletely decomposed of nitrate species Co(NO₃)₂ in hydrogen after calcination (Chu W. et al., 2007). The second and third peak, at 300°C and 373°C respectively, were assigned to the reduction of Co₃O₄ to CoO and CoO to Co⁰ according to equations (4.1 and 4.2) (Pendyala V.R.R. et al., 2016). Whilst, the fourth peak at (655 °C) represents the reduction of the cobalt aluminum mixed (e.g. Co₂AlO₄), formed during the TPR analysis as a result of the interaction of the highly dispersed CoO with the -Al₂O₃ support (Jalama K., 2011, Fratalocchi L., 2015). Hence, it was proven that 2% H₂/Ar flow of 6 NL/h at 400 °C for 10 hours was appropriate for reducing the cobalt oxides to metallic cobalt prior to the FTS reaction (Appendix C, C.1).



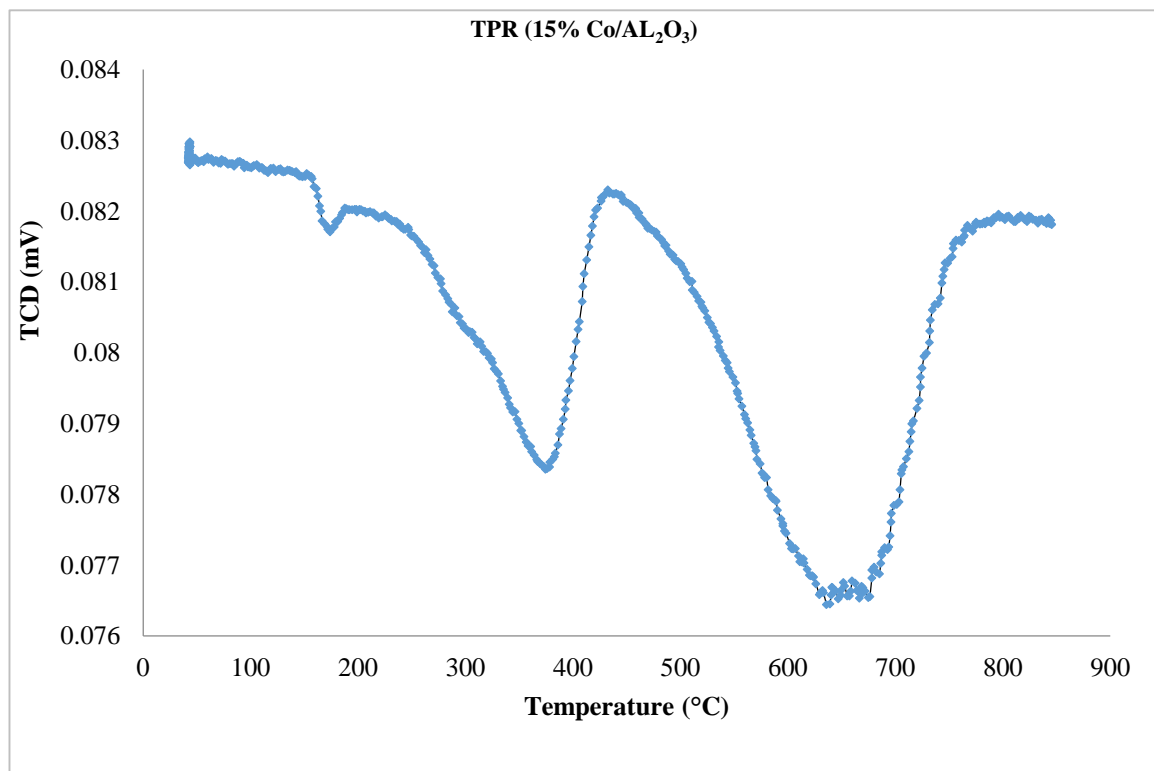


Figure 4.37 TPR profiles of the catalysts.

4.2.2 Nitrogen adsorption measurement.

BET surface area and pore volume for the catalyst, shown in the table (4.6), were measured by nitrogen adsorption at $-196\text{ }^{\circ}\text{C}$.

A percentage loading of 15 % Co is equivalent to 20.4% by weight of Co_3O_4 . The BET surface area of the $\text{Co}/\text{Al}_2\text{O}_3$ catalyst should be approximately $0.796 \times 220 = 175.12\text{ m}^2\text{g}^{-1}$ in theory (see Appendix C, C.2). The measured value ($120\text{ m}^2\text{g}^{-1}$), though, is observably lower than the calculated value, which indicates some pore blockage by cobalt oxide clusters.

Table (4.6): BET surface area and pore volume for the support and catalyst.

Catalyst/Support	BET surface area (m^2g^{-1})	Pore volume (cm^3g^{-1})
Al_2O_3	220	0.75
15% $\text{Co}/\text{Al}_2\text{O}_3$	120	0.15

4.3 Fischer –Tropsch Synthesis Parameter Study.

The FT Synthesis experiments were previously explained in chapter three. In general, the catalyst was activated under the following conditions: drying under helium flow at atmospheric pressure, followed by a reduction in (2% H₂/Ar) flow at 400 °C with a heating rate of 10°C/min.

After reduction, the temperature of the reactor was decreased gradually for the first test of FT reaction temperature (220 °C), then the first experiment was started.

Once the catalyst is activated, in all the subsequent tests the catalysts were heated to experiment temperature under helium flow at a flow rate of 2.5 NL/h, starting from room temperature.

The effect of two parameters (Temperature and Gas hourly space velocity) on the catalytic activity and product selectivity were studied and the results were recorded once the system reached steady-state conditions. All the experiments were done with diluted feeding conditions (4% H₂, 2% CO, He as balance) at ratio H₂/CO = 2, with 5 g of 15Co/AL₂O₃ catalyst and 1 atm of overpressure.

The experimental conditions and the results at steady-state conditions are summarized in table (4.7).

The discussion below will be including:

- a. Trends of reactants conversion and products as a function of the time on stream for a test achieved as an example from results as an optimum condition (T=220 °C and GHSV=370 h⁻¹) for the high selectivity liquid product.
- b. Effect of parameters (T and GHSV) on the conversion of reactants and products selectivity at steady-state conditions.

Table (4.7): F-T Synthesis experiments conditions and results at steady -state conditions.

Parameters		Conversion %		Selectivity %						Collected Product Selectivity %	
T (°C)	GHSV (h ⁻¹)	CO	H ₂	CH ₄	C ₂ -C ₄	CO ₂	C ₅ -C ₁₁	C ₁₂ -C ₂₀	C ₂₁₊	C ₁ -C ₄	C ₅₊
220	370	26.66	20.75	0.32	0.0126	1.36	40.303	47.184	10.82	0.3326	98.3
	520	26.65	13.64	2.23	0.0892	1.42	39.466928	46.205184	10.588688	2.3192	96.2608
	670	27.48	12.83	2.56	0.1024	1.52	39.285216	45.992448	10.539936	2.6624	95.8176
	820	23.92	12.36	3.2	0.128	1.91	38.85242	45.48576	10.42382	3.328	94.762
235	370	26.99	21.89	2.82	0.1128	2.16	38.911952	45.555456	10.439792	2.9328	94.9072
	520	22.5	18.31	3.31	0.1324	2.18	38.694816	45.301248	10.381536	3.4424	94.3776
	670	24.37	18.11	3.96	0.1584	2.2	38.409456	44.967168	10.304976	4.1184	93.6816
	820	24.62	17.94	5.02	0.2008	2.32	37.908272	44.380416	10.170512	5.2208	92.4592
250	370	22.64	22.96	5.17	0.2068	2.29	37.856612	44.319936	10.156652	5.3768	92.3332
	520	24.84	18.72	5.46	0.2184	2.27	37.741156	44.184768	10.125676	5.6784	92.0516
	670	23.27	18.57	5.63	0.2252	2.32	37.648168	44.075904	10.100728	5.8552	91.8248
	820	22.78	18.12	6.74	0.2696	2.95	36.916564	43.219392	9.904444	7.0096	90.0404

4.3.1 Description of transitory condition (Time on Stream) for single test as an example.

Results on FT tests at $T = 220\text{ }^{\circ}\text{C}$ and $\text{GHSV} = 370\text{ h}^{-1}$ are discussed as following. **Figures 4.38-4.40** show the trends of H_2 and CO conversion and the concentration of the most relevant products during the initial transitory phase.

According to the results showed in **Figure 4.38**, the reaction starts with a higher conversion of CO (X_{CO}) and lower conversion of H_2 (X_{H_2}), then X_{CO} decreases and X_{H_2} increases gradually up to values of 27 and 21% respectively at the steady-state conditions, that begins approximately after 600-800 min. These trends can be explained taking into account that the catalytic mechanism involves the initial absorption of CO whilst the increase of H_2 conversion is due to the chain propagation for the polymerization reaction, as described in literature data (Post M. F. M. et al., 1989, Cheng J. et al., 2008). Indeed, the pathway of this FT reaction can be explained according to alkyne mechanism. In this model, the chain initiation of reaction occurs by dissociation of adsorbed CO toward C and O atoms on the Co sites, then C is hydrogenated by adsorbed H_2 to yield in a successive reaction methyne ($-\text{CH}_3$) and methylene ($-\text{CH}_2$) groups. Because $-\text{CH}_3$ is chain initiator and $-\text{CH}_2$ is the monomer of polymerization reaction, then the chain growth is thought to take place by consecutive combination of methylene surface species (CH_2) to generate hydrocarbons (n-paraffins or α -olefins) by hydrogen addition or β -hydride elimination respectively (Overett M. J. et al., 2000, Ail and Dasappa, 2016). Moreover, the products of this polymerization reaction are saturated linear hydrocarbons with a broad range of carbon (Dry E. M., 2002).

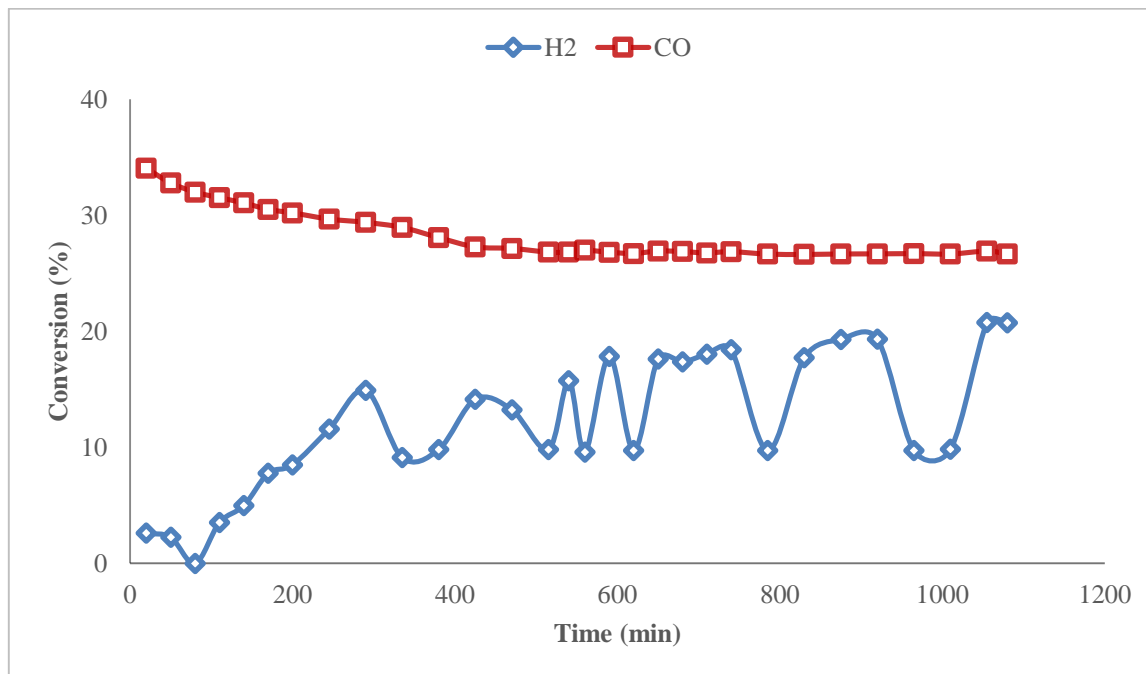


Figure 4.38 Conversion of CO and H₂ on time stream at P= 1 atm., H₂/CO = 2, T=220 °C , GHSV = 370 h⁻¹ and 5gm of catalyst, where (□) CO and (◇)H₂, the inlet and outlet amount of syngas was analysis by GC-HP 5890 equipped with a TCD detector (see section 3.1.6).

Figure 4.39 shows the trends of the most relevant gaseous product: CH₄, CO₂ and hydrocarbons in C₂-C₄ range, considering that hydrocarbons with more than four C atoms (C₅₊) are liquid. **Figure 4.40** shows trends of yields in liquid (C₅₊) and gaseous products (CH₄ + C₂-C₄) and CO₂ during the transitory phase.

According to literature data (Tristantini D. et al., 2007, Pendyala V. R. et al., 2016), the initial formation of light hydrocarbons products and CO₂ is preferred due to the water-gas shift reaction. Then they decrease gradually in favour of the formation of liquid products, which corresponds to an increase of the chain growth. Stable yield values are reached after 600 min, observing yields in liquid hydrocarbons of about 26 %.

The decrease in the production of light hydrocarbons (CH_4 and $\text{C}_2\text{-C}_4$) and CO_2 obtained should lead to an increase of the selectivity towards gasoline and diesel hydrocarbons, in the range of $\text{C}_5\text{-C}_{11}$ and $\text{C}_{12}\text{-C}_{20}$ respectively (Rytter E. et al., 2016, Galadima and Muraza, 2015, Zennaro R. et al., 2000).

The Table (4.7) above shows the selectivity to different products and the CO and H_2 conversions obtained at the steady-state condition (after 600 min). It can be observed that the selectivity of products of interest, gasoline and diesel hydrocarbons, is 40.30% and 47.18% respectively. An amount of heavy hydrocarbons, with a number of C atoms higher than 20 (C_{21+}) of about 10.82% has been found. It is important to note that such an increase of the liquid product selectivity is not caused by the lower degree of CO conversion, but is as a result of the decrease of the light hydrocarbons formation and of a side reaction (water-gas shift reaction), as explained in literature (Cheng K. et al., 2016).

The steady state condition has been kept for 10 days. The test has been repeated several times with no appreciable changes. As a consequence it can be hypothesized that no deactivation of the catalyst had occurred during these tests.

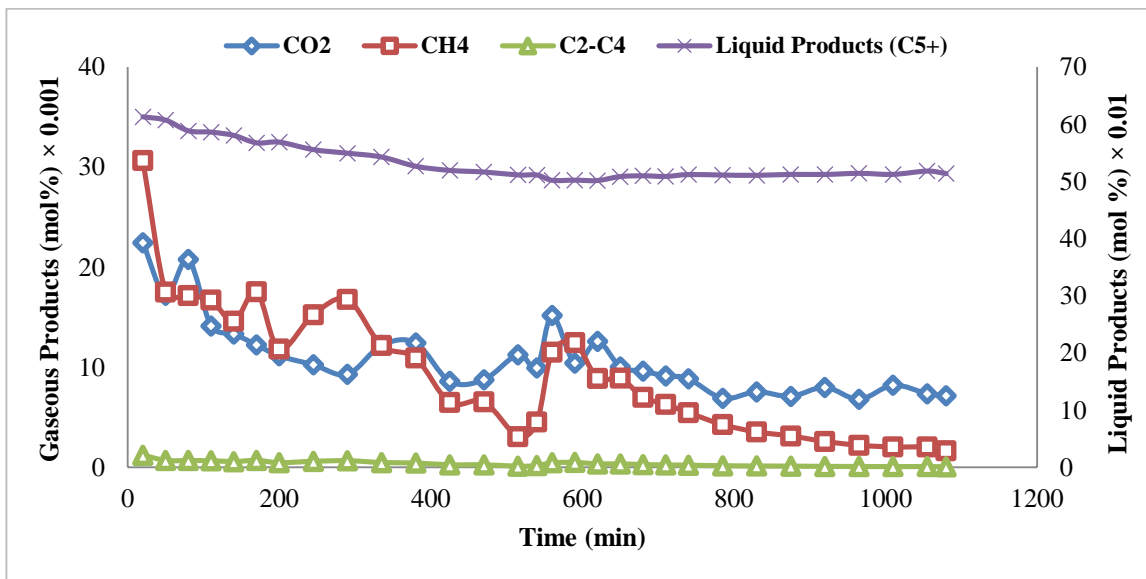


Figure 4.39 Mole percentage of products on time stream at $P = 1$ atm., $H_2/CO = 2$, $T = 220$ °C, $GHSV = 370$ h⁻¹ and 5gm of catalyst, where (x) Liquid products, (Δ) C₂-C₄, (\diamond) CH₄ and (\square) CO₂, the composition of produced liquid phase was analysis by GC-17A equipped with a FID detector (see section 3.1.5.3) and the composition of produced gas phase was analysis by GC- HP 5890 equipped with a TCD detector (see section 3.1.6).

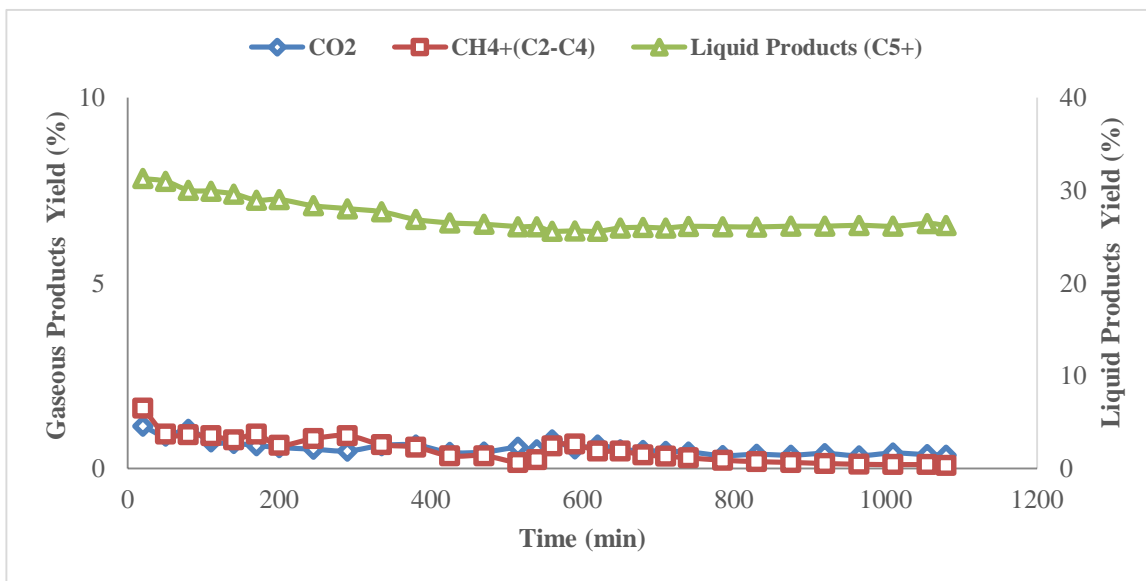


Figure 4.40 Yield percentage of products on time stream at $P = 1$ atm., $H_2/CO = 2$, $T = 220$ °C, $GHSV = 370$ h⁻¹ and 5gm of catalyst, where (Δ) Liquid products, (\diamond) CO₂ and (\square) CH₄+(C₂-C₄), the composition of produced liquid phase was analysis by GC-17A equipped with a FID detector (see section 3.1.5.3) and the composition of produced gas phase was analysis by GC-HP 5890 equipped with a TCD detector (see section 3.1.6).

4.3.2 Description the results at steady-state conditions.

In this section the discussion focuses on the synthesis gas conversion (CO and H₂) and product selectivity as a function of reaction temperature and GHSV. When the values reach a steady-state as shown above in table (4.7), the reaction accrues under atmospheric pressure, H₂/CO feed ratio equal 2, different gas hourly space velocity (370,520,670 and 820 h⁻¹) and the reaction temperatures (220, 235 and 250 °C).

4.3.2.1 Effect of reaction temperature and GHSV on the conversion of synthesis gas.

In this part, the discussion focuses on the effect of reaction temperature and gas hourly space velocity on synthesis gas conversion (CO and H₂).

4.3.2.1.1 Effect of reaction temperature on synthesis gas conversion (CO and H₂).

Figure 4.41 shows the CO conversion as a function of the reaction temperature. The CO conversion seems approximately constant with increasing the reaction temperature for all space velocities. This is probably due to the diluted concentration of CO (2%) and the operating pressure limitation (1atm) for the reaction system used in this study. On the other hand, the conversions at steady state for all tests at lower temperature (220 °C) are higher in comparison to the values reported by Marie A. J. et al., 2009 (15 wt.% Co/Al₂O₃, T=212 °C , P=20 bar and X_{CO}=22), Chu W. et al., 2007 (15 wt.% Co/Al₂O₃, T=453-483 K , P=1 bar and X_{CO}=2.2-7.9) and Nabaho D. et al., 2016 (20wt.% Co/Al₂O₃, T=220 °C , P=20 bar and X_{CO}=9.5).

The conversion of H₂ as a function of the reaction temperature as shown in **Figure 4.42**. The experimental results show that the H₂ conversion has a little increase with the increasing reaction temperature for all space velocities. Again, this is probably due to the diluted concentration of H₂ (4%) and the operating pressure limitation (1atm) for the reaction system used in this study. At steady state for all tests, the trends observed are in agreement with the results obtained in another study carried out using cobalt-based catalysts (Osa A.R. et al., 2011 c).

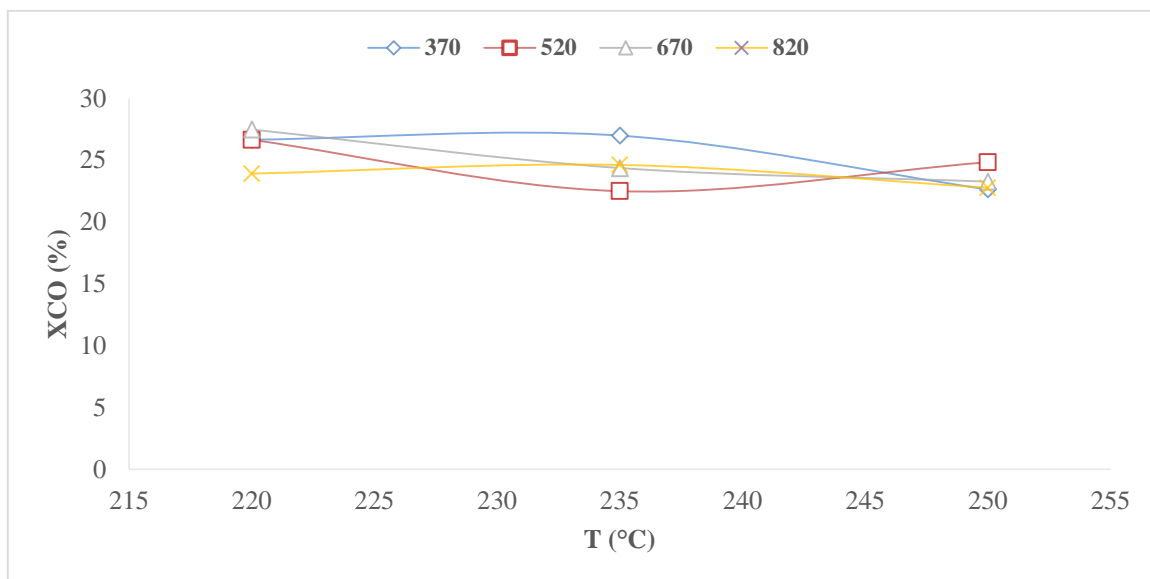


Figure 4.41 Effect of reaction temperature on CO conversion at $P=1$ atm., $H_2/CO = 2$, where $GHSV = (\diamond)370$, $(\square)520$, $(\Delta)670$ and $(x)820$ h^{-1} , and 5gm of catalyst, the outlet amount of CO was analysis by GC-HP 5890 equipped with a TCD detector (see section 3.1.6).

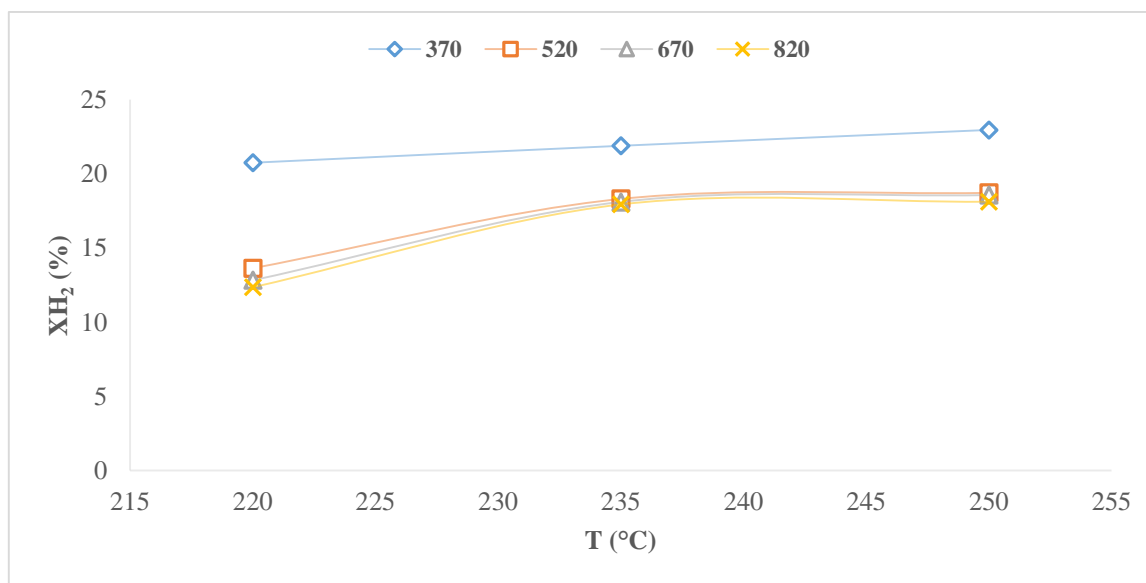


Figure 4.42 Effect of reaction temperature on H_2 conversion at $P=1$ atm., $H_2/CO = 2$, where $GHSV = (\diamond)370$, $(\square)520$, $(\Delta)670$ and $(x)820$ h^{-1} , and 5gm of catalyst, the outlet amount of H_2 was analysis by GC-HP 5890 equipped with a TCD detector (see section 3.1.6).

4.3.2.1.2 Effect of gas hourly space velocity (GHSV) on synthesis gas conversion (CO and H₂).

Figures 4.43 and 4.44 show the conversion of synthesis gas (CO and H₂) as a function of gas hourly space velocity. In all cases the conversion of CO, seems approximately constant, while H₂ conversion shows a little decrease with increasing the gas hourly space velocity. As explained above, the observed trends are probably due to the diluted concentration of the reactants CO (2%) and H₂ (4%) and to the operating pressure limitation (1atm) for the reaction system used in this study. At steady-state, for all tests, the trends observed for H₂ are in agreement with results obtained with other studies using cobalt-based catalysts (Tristantini D. et al., 2007, Osa A.R. et al., 2011 c).

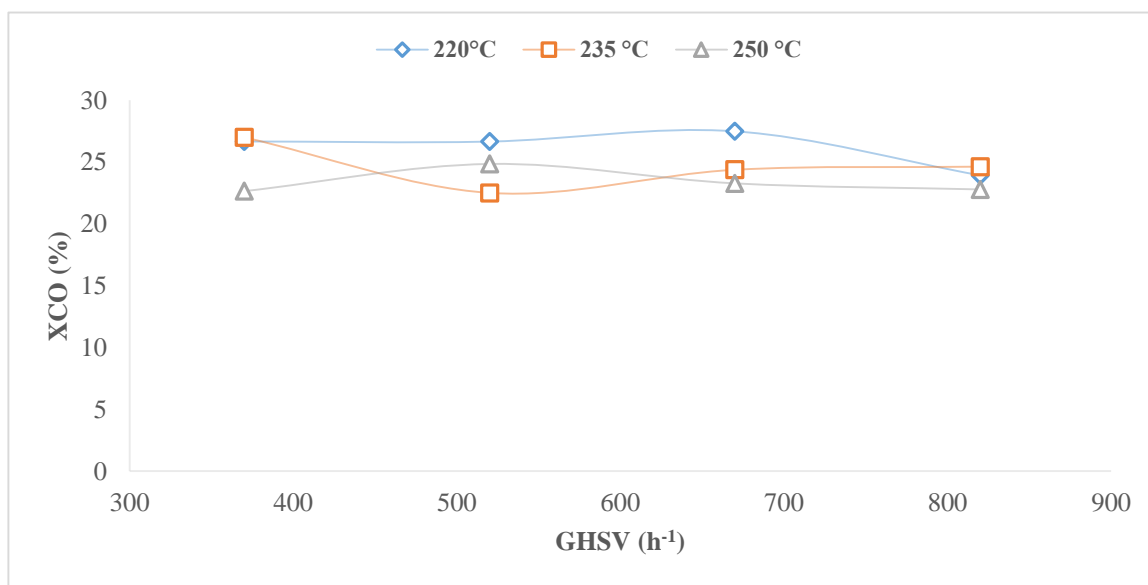


Figure 4.43 Effect of GHSV on CO conversion at P=1 atm., H₂/CO = 2, where T = (◇)220, (□)235 and (△) 250 °C, and 5gm of catalyst, the outlet amount of CO was analysis by GC-HP 5890 equipped with a TCD detector (see section 3.1.6).

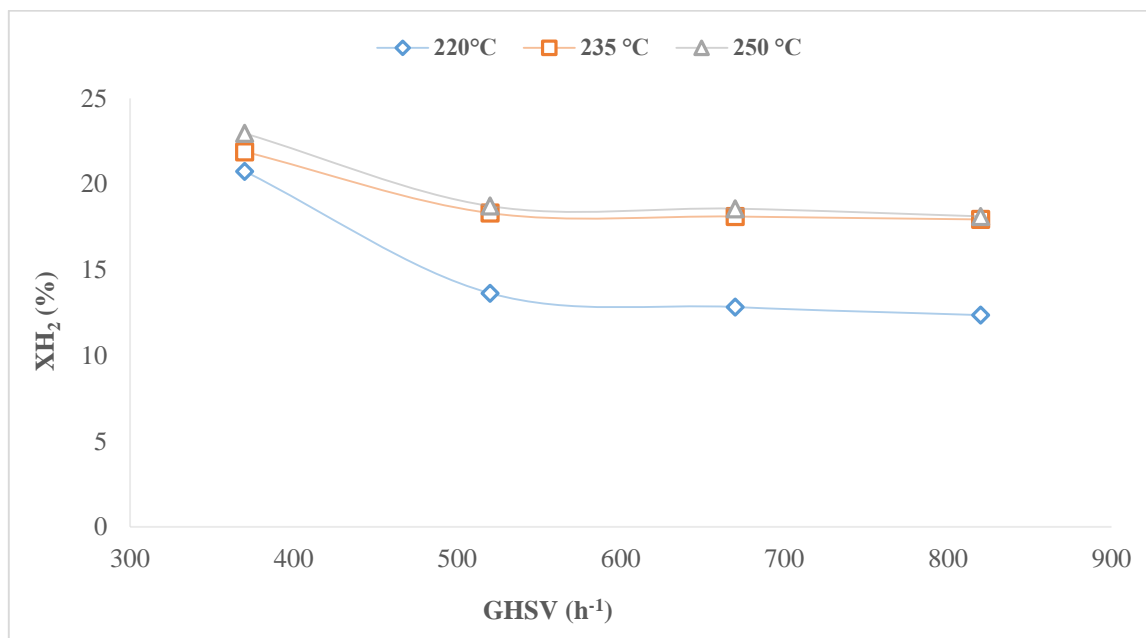


Figure 4.44 Effect of GHSV on H₂ conversion at P = 1 atm., H₂/CO = 2, where T = (◇)220, (□)235 and (△) 250 °C, and 5gm of catalyst, the outlet amount of H₂ was analysis by GC-HP 5890 equipped with a TCD detector (see section 3.1.6).

4.3.2.2 Effect of reaction temperature and GHSV on gases product selectivity.

In this part, the discussion focuses on the effect of reaction temperature and GHSV on Gases product selectivity.

4.3.2.2.1 Effect of reaction temperature on light hydrocarbon selectivity.

The selectivity of collected light hydrocarbon (C₁- C₄) reported in the table (4.7) above, is described as a function of reaction temperature in the **Figure 4.45**. An increase of the reaction temperature was caused by a gradual increase in selectivity of light hydrocarbons. Since the FT polymerization reaction is exothermic, an increase in reaction temperature leads to an increase of hydrogenation rate of 'CH₂' units, and consequently the products are shifted towards low molecular weight hydrocarbon (Dry M. E., 1996, Mansouri M. et al., 2014). At steady state for all tests, the trends are in agreement with results obtained in other studies using cobalt-based catalysts (Osa A.R. et al. 2011a, b and c, Najafabadi A.T.etal.,2016).

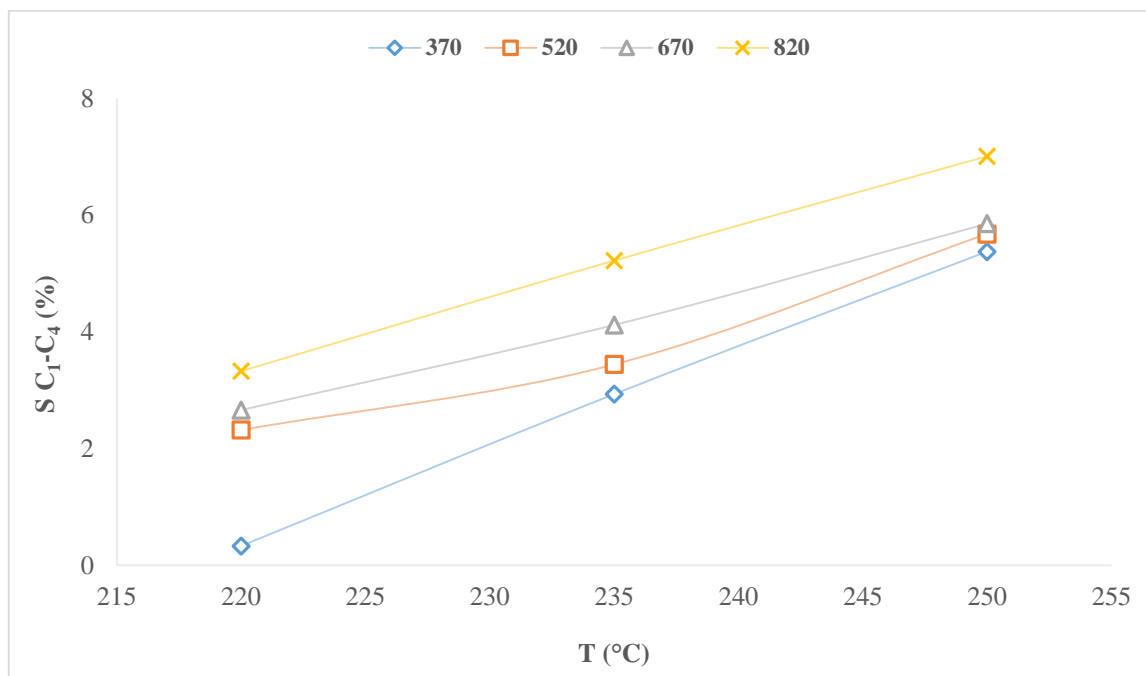


Figure 4.45 Effect of reaction temperature on light hydrocarbon (C₁- C₄) selectivity at P = 1 atm., H₂/CO = 2, where GHSV = (◇)370, (□) 520 , (△) 670 and (x) 820 h⁻¹, and 5gm of catalyst, the composition of produced gas phase was analysis by GC-HP 5890 equipped with a TCD detector (see section 3.1.6).

4.3.2.2.2 Effect of reaction temperature on Carbon dioxide selectivity.

The selectivity for Carbon dioxide (CO_2) as a function of reaction temperature is presented in **Figure 4.46**. An increase of the reaction temperature caused by a gradual increase in selectivity of CO_2 . The CO_2 production depends on the amount of water produced through water–gas shift (WGS) in FT reaction. Consequently, the little amount of CO_2 produced is in agreement with the little WGS activity normally shown by the cobalt catalyst (Osa A.R. et al., 2011 c; Pendyala V. R. R. et al., 2016). At steady state for all tests, the trends are in agreement with results obtained in other studies using cobalt-based catalysts (Xu D. et al., 2006, Jung I.Y. et al., 2010, Osa A.R. et al.2011a and b).

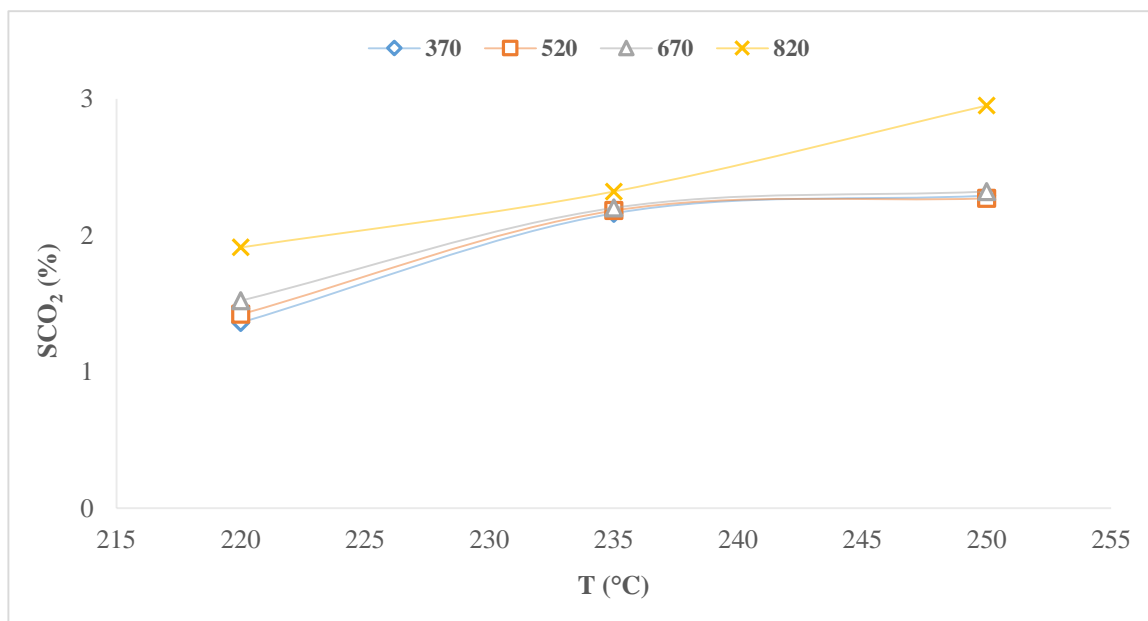


Figure 4.46 Effect of reaction temperature on CO_2 selectivity at $P = 1$ atm., $\text{H}_2/\text{CO} = 2$, where $\text{GHSV} = (\diamond)370$, $(\square) 520$, $(\Delta) 670$ and $(x) 820$ h^{-1} , and 5gm of catalyst, the amount of produced CO_2 was analysis by GC-HP 5890 equipped with a TCD detector (see section 3.1.6).

4.3.2.2.3 Effect of gas hourly space velocity (GHSV) on light hydrocarbon selectivity.

The selectivity of collecting Light hydrocarbon (C_1-C_4) reported in the table (4.7) as a function of gas hourly space velocity as shown in **Figure 4.47**. When increasing the gas hourly space velocity, the formation of CH_4 and light hydrocarbon (C_2-C_4) is increased. At steady state for all tests the trends found are in agreement with results obtained in other studies using cobalt-based catalysts (Tristantini D. et al., 2007 , Osa A.R. et al., 2011 c).

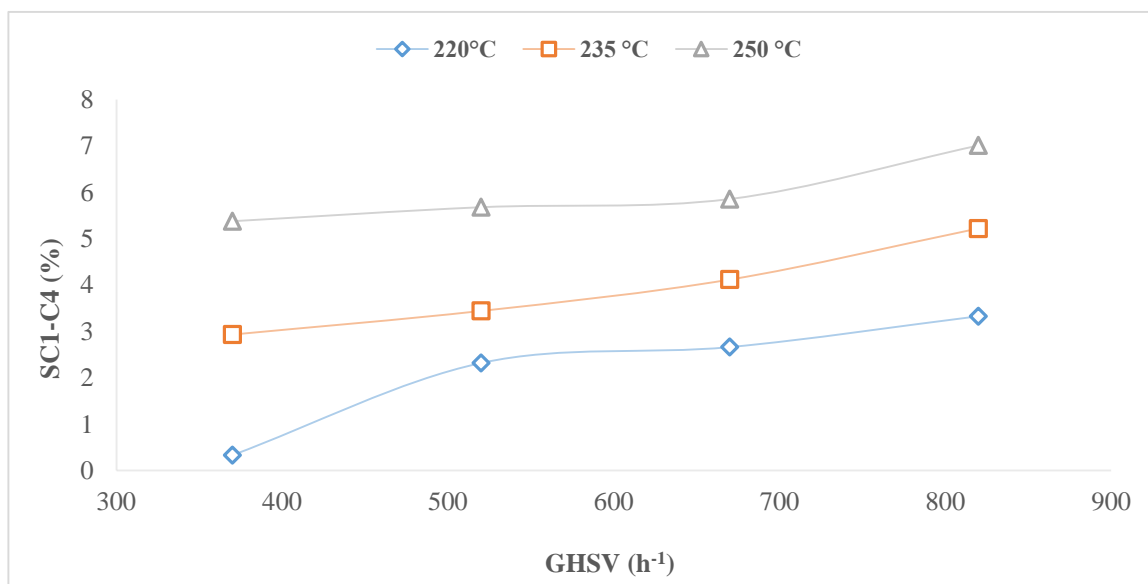


Figure 4.47 Effect of GHSV on light hydrocarbons (C_1-C_4) selectivity at $P = 1$ atm., $H_2/CO = 2$, where $T = (\diamond)220$, $(\square)235$ and $(\Delta) 250$ °C, and 5gm of catalyst, the composition of produced gas phase was analysis by GC-HP 5890 equipped with a TCD detector (see section 3.1.6).

4.3.2.2.4 Effect of gas hourly space velocity (GHSV) on Carbon dioxide (CO₂) selectivity.

The CO₂ selectivity is reported in **Figure 4.48** as a function of gas hourly space velocity. Increases in GHSV caused a moderate increase in the selectivity of CO₂. As a matter of facts, CO₂ production depends on the amount of water produced by water–gas shift (WGS) in FT reaction, and the WGS reaction is a side-reaction that cannot take place before the water has been produced in FT (Tristantini D. et al., 2007). The negligible amount of CO₂ produced is in agreement with the reduced WGS activity obtained in other studies using cobalt-based catalysts (Osa A.R. et al., 2011a, b and c).

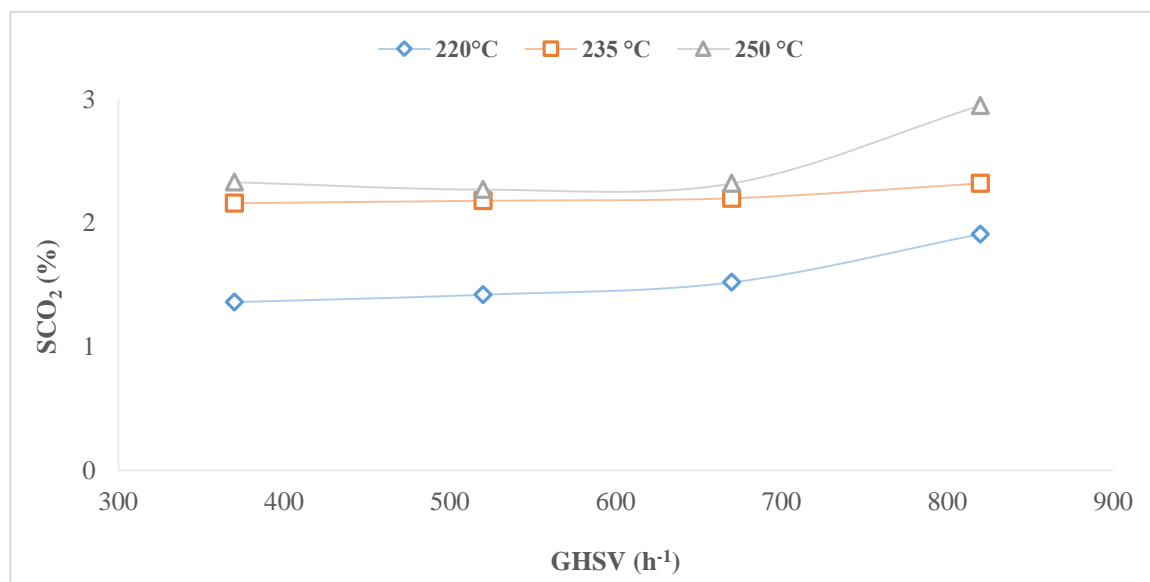


Figure 4.48 Effect of GHSV on CO₂ selectivity at P = 1 atm., H₂/CO = 2, where T = (◇)220, (□)235 and (△) 250 °C, and 5gm of catalyst the amount of produced CO₂ was analysis by GC-HP 5890 equipped with a TCD detector (see section 3.1.6).

4.3.2.3 Effect of reaction temperature and GHSV on liquid products selectivity.

In this part, the discussion focuses on the effect of reaction temperature and GHSV on Liquid products (C_{5+}) selectivity.

4.3.2.3.1 Effect of reaction temperature on liquid hydrocarbon selectivity.

The selectivity of in liquid hydrocarbons (C_5-C_{11} , $C_{12}-C_{20}$ and > 20) reported in the table (4.7) in terms of (C_{5+}) as a function of reaction temperature is described in **Figure 4.49**. The liquid hydrocarbon selectivity decreases when increasing the reaction temperature. As a matter of facts, increases in reaction temperature lead to an increase in the hydrogenation activity, thus producing a shift in the reaction towards light hydrocarbons, as explained in the section 4.3.2.2.1. In other words, the selectivity of desired products (e.g. gasoline and diesel hydrocarbons), in the range of C_5-C_{11} and $C_{12}-C_{20}$ respectively, can be achieved at a low reaction temperature. At steady state, for all tests the observed trends are in agreement with the results obtained in other carried out using cobalt-based catalysts (Chu W. et al., 2007, Osa A.R. et al., 2011 a, b and c, Rytter E.etal.,2016).

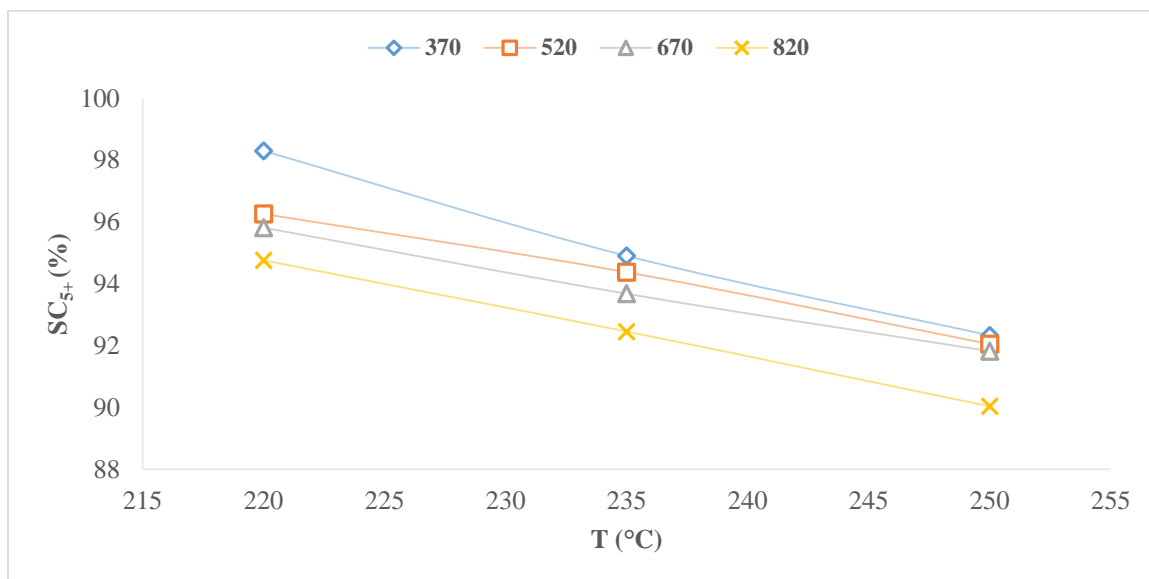


Figure 4.49 Effect of reaction temperature on liquid hydrocarbon (C_{5+}) selectivity at $P = 1$ atm., $H_2/CO = 2$, where $GHSV = (\diamond) 370$, $(\square) 520$, $(\triangle) 670$ and $(\times) 820$ hr^{-1} , and 5gm of catalyst, the composition of produced liquid phase was analysis by GC-17A equipped with a FID detector (see section 3.1.5.3).

4.5.2.3.2 Effect of gas hourly space velocity (GHSV) on liquid product selectivity.

The light hydrocarbon selectivity is increased when increasing the gas hourly space velocity, as shown in section 4.3.2.2.3. On the contrary, the selectivity in liquid hydrocarbons (C_5-C_{11} , $C_{12}-C_{20}$ and >20) decreases with the gas hourly space velocity, as shown in the table (4.7) in terms of (C_{5+}) and in **Figure 4.50**. For this reason, the desired products (e.g. gasoline and diesel hydrocarbons), in the range of C_5-C_{11} and $C_{12}-C_{20}$ respectively, can be achieved at a lower GHSV. At steady state, for all tests the trends observed are in agreement with results obtained in other studies carried out using cobalt-based catalysts (Tristantini D. et al., 2007 , Osa A.R. et al., 2011 c).

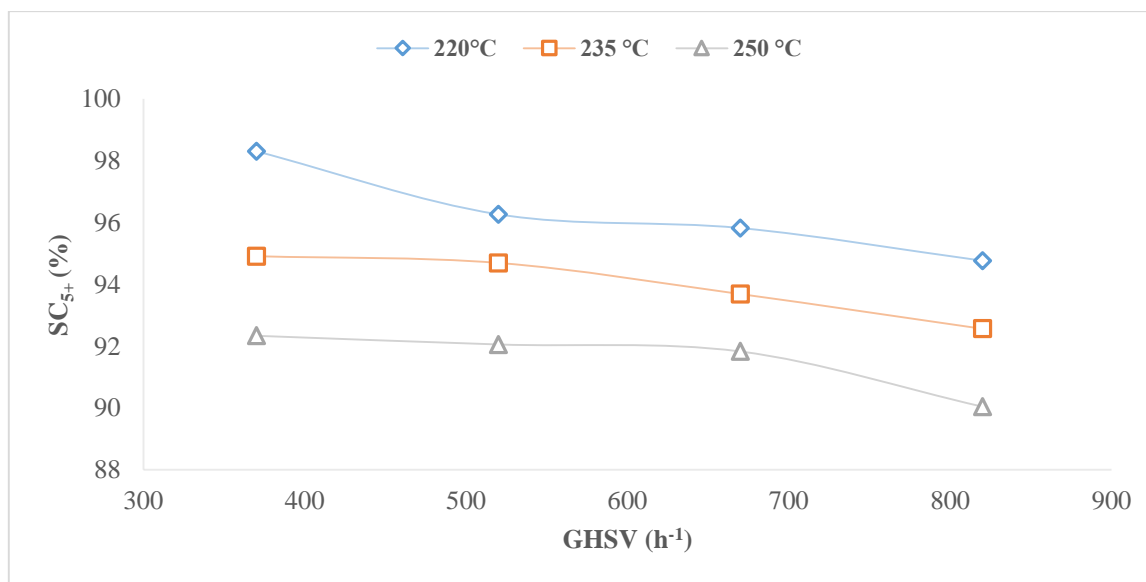


Figure 4.50 Effect of GHSV on Liquid hydrocarbon (C_{5+}) selectivity at $P = 1$ atm., $H_2/CO = 2$, where $T = (\diamond)220$, $(\square)235$ and $(\triangle) 250$ °C, and 5gm of catalyst, the composition of produced liquid phase was analysis by GC-17A equipped with a FID detector (see section 3.1.5.3).

Chapter Five: Conclusions

The following conclusions can be drawn from the results obtained:

5.1 Conclusions - optimization of an anaerobic digestion process.

- ❖ The effect of three different total solid fractions (TS %) from municipal solid waste on the biogas production was studied by performing a series of experiments using sewage sludge, adapted in a synthetic medium, as inoculum. The results show that the gas production is significantly affected by the TS content in feedstock. The best performance for biogas generation and methane fraction was obtained when adopting the highest amount of TS (15 %).
- ❖ The effect of three different volume fractions of inoculum on the biogas production was studied by performing a series of experiments using a synthetic medium. The best results in term of biogas generation and methane fraction were obtained adopting lower volume fractions of volume inoculum (10 v/v %). Higher volumes of inoculum produced a higher amounts of VFA, leading to higher inhibition effects.
- ❖ The effect of co-digestion with different fractions of MSW and GR on performances of digesters for biogas production were studied. The results show that:
 - The best performances of co-digestion were obtained in the presence of 75% GR and 25% MSW. This is because a large amount of GR provides an appropriate intake of carbon to balance the nitrogen content in the MSW.

- When using 100% GR, the biogas production was very low. This was due to the poor availability of nutrients, leading to a slow carbon hydrolysis. Similarly, when using 100% MSW, a poor biogas production was observed.
 - These results indicate that a synergic use of both MSW and GR may significantly improve the efficiency of the anaerobic digestion process.
 - The addition of mineral solution "M9 10x" and 400x salts had a positive effect on anaerobic digestion of MSW, increasing the biogas production as well as the fraction of methane. This is probably due to the improved efficiency of the methanogenesis step.
- ❖ The effects of addition Ni, Zn and Co, separately or in mixtures, on biogas production, composition of biogas and intermediate products of AD (acetic acid, butyric acid, propionic acid and ethanol), have been studied. The results show that:
- The biogas production and the methane fraction were increased by the separate addition of a single element in a concentration range from 5 to 50 mg/L. Whatever the element added, the best results were obtained at a concentration of 5 mg/L. Inhibition phenomena were observed at 100mg /L.
 - Whatever the element added, a minimum amount of VFAs was obtained at a concentration of 5mg/L.
 - The addition of trace elements (Ni, Zn and Co) is very important to improve the anaerobic digestion process, though the best growth of biomass was obtained at low concentrations of these elements.

- The best values of cumulative volume of biogas produced, biomass growth, and the minimum VFA production was obtained when adding any mixture of trace element containing Ni, with the concentration 5 mg/L for each one. And the best results were obtained when using all the three elements (Ni, Zn, and Co).

5.2 Conclusions - catalyst characterization.

A 15% wt. Co/Al₂O₃ catalyst was prepared by impregnation technique under vacuum and characterized by Temperature-Programmed Reduction (TPR) and N₂ adsorption isotherm techniques. The results show that:

- The TPR is a most important technique used for characterizing the catalyst, that provides information about the degree of temperature and amount of H₂ consumed for the complete reduction of Co₃O₄ to CoO and then to Co on the support surface.
- The measured BET surface area of the Co/Al₂O₃ catalyst is lower than the calculated value (see Appendix C, C.2), due to the pore blockage produced by cobalt oxide clusters.

5.3 Conclusions - FT reaction.

The effect of a range of two parameters, namely: reaction temperature and gas hourly space velocity (GHSV), on the FT reaction in the presence of Cobalt-Alumina based catalyst was measured. The results show that:

- In all tests, at the beginning a higher conversion of CO and a lower conversion of H₂ were observed. Subsequently X_{CO} decreases and X_{H₂} increases gradually until reaching the steady-state conditions approximately after 600-800 min.

- The formation of light hydrocarbons (C₁-C₄) products and CO₂ decreases gradually and the formation of liquid products corresponds to an increase of the chain length.
- A decrease in the production of light hydrocarbons leads to an increase in the selectivity towards gasoline and diesel hydrocarbons.
- The reaction temperature and the gas hourly space velocity do not have significant effects on the conversion of diluted CO while having few effects on the conversion of diluted H₂.
- An increase in the reaction temperature and GHSV leads to a shift of the product towards low molecular weight hydrocarbons.
- The selectivity towards the desired products (e.g. gasoline and diesel hydrocarbons) is 40.3% and 47.2% respectively, and can be achieved at a reaction temperature of 220 °C and a GHSV value of 370 h⁻¹.
- The value of the CO conversion obtained at steady state adopting the minimum values of temperatures and GHSV is about 27%, which is higher than the values reported in the literature with the same H₂/CO ratio for a not diluted condition.
- The reduced amounts of CO₂ demonstrate that the presence of cobalt catalyst reduces substantially the WGS activity.
- The steady state condition has been kept for 10 days and tests repeated several times with no appreciable changes, demonstrating the high stability of the catalyst.

References

- Adesina A. A., 1997. "Hydrocarbon synthesis via Fischer-Tropsch reaction: travails and triumphs", *Applied Catalysis A: General*, Vol. (138), pp. 345-367.
- Agdag O.N. and Sponza D.T., 2007. "Co-digestion of mixed industrial sludge with municipal solid wastes in anaerobic simulated landfilling bioreactors", *Journal of Hazardous Materials*, Vol. (140), pp.75-85.
- Ail S. S. and Dasappa S., 2016. "Biomass to liquid transportation fuel via Fischer - Tropsch synthesis Technology review and current scenario", *Renewable and Sustainable Energy Reviews*, Vol. (58), pp.267-286.
- Alaswad A., Dassisti M., Prescott T. and Olabi A. G., 2015. "Technologies and developments of third generation biofuel production", *Renewable and Sustainable Energy Reviews*, Vol. (51), pp.1446-1460.
- Alexopoulos S., 2012. "Biogas Systems: Basics, Biogas Multifunction, Principle of Fermentation and Hybrid Application with a Solar Tower for the Treatment of Waste Animal Manure", *Journal of Engineering Science and Technology Review*, Vol. (5), pp. 48 -55.
- Altaş L., 2009. "Inhibitory effect of heavy metals on methane-producing anaerobic granular sludge", *Journal of Hazardous Materials*, Vol. (162), pp.1551-1556.
- Araki S., Hino N., Mori T. and Hikazudani S., 2010. "Autothermal reforming of biogas over a monolithic catalyst", *Journal of Natural Gas Chemistry*, Vol. (19), pp.477-481.

- Alvarez R. and Liden G., 2008. "Semi-continuous co-digestion of solid slaughterhouse waste, manure, and fruit and vegetable waste", *Renewable Energy*, Vol. (33), pp.726-734.
- Alvarez J.A., Otero L., Lema J.M., 2010. "A methodology for optimizing feed composition for anaerobic co-digestion of agro-industrial wastes", *Bioresource Technology*, Vol. (101), pp.1153-1158.
- APHA (American Public Health Association), 2005. "Standard Methods for the Examination of Water and Wastewater", American Technical Publishers.
- Appels L., Baeyens J., Degreve J. and Dewil R., 2008. "Principles and potential of the anaerobic digestion of waste-activated sludge", *Progress in Energy and Combustion Science*, Vol. (34), pp. 755-781.
- Ariunbaatar J., Panico A., Frunzo L., Esposito G., Pirozzi F. and Lens P.N.L.,2014. "Pretreatment methods to enhance anaerobic digestion of organic solid waste", *Applied Energy*, Vol. (123), pp.143-156.
- Avraam K., 2012. "Waste to Energy: Opportunities and Challenges for Developing and Transition Economies", Springer London Dordrecht Heidelberg, New York.
- Baoning Z., Petros G. , Ruihong Z., James L., Bryan J. and Xiujin L,2009. "Characteristics and biogas production potential of municipal solid wastes pretreated with a rotary drum reactor", *Bioresource Technology*, Vol. (100), pp. (1122-1129).

- Batstone D. J., Keller J., Angelidaki I., Kalyuzhnyi S. V., Pavlostathis S. G., Rozzi A., Sanders W. T. M., Siegrist H. and Vavilin V. A. ,2002. “The IWA Anaerobic Digestion Model No.1 (ADM1)”, *Water Science & Technology*, Vol. (45), pp. 65-73.
- Bolzonella D., Pavan P., Mace S. and Cecchi F.,2006. “Dry anaerobic digestion of differently sorted organic municipal solid waste: a full-scale experience”, *Water Science & Technology*”, Vol. 53(8), pp.23-32.
- Borja R., Martí'n A., Sa'nchez E., Rinco'n B., Raposo F., 2005. “Kinetic modelling of the hydrolysis, acidogenic and methanogenic steps in the anaerobic digestion of two-phase olive pomace (TPOP)”, *Process Biochemistry*, Vol. (40), pp. 1841-1847.
- Bouallagui H., Lahdheb H., Romdan E., Rachdi B., Hamdi M., 2009a. “Improvement of fruit and vegetable waste anaerobic digestion performance and stability with co-substrates addition”, *Journal of Environmental Management*, Vol. (90), pp.1844-1849.
- Brown D., Shi J. and Li Y., 2012. “Comparison of solid-state to liquid anaerobic digestion of lignocellulosic feedstocks for biogas production”, *Bioresource Technology*, Vol. (124), pp. 379-386.
- Brulé M., Bolduan R., Seidelt S., Schlagermann P., Bott A., 2013. “Modified batch anaerobic digestion assay for testing efficiencies of trace metal additives to enhance methane production of energy crops”, *Environmental Technology*, Vol. 34(13-14), pp. 2047-2058.

- Bukur D. B., Lang X., Rossin J. A., Zimmerman W. H., Rosynek M. P., Yeh E. B., Li C., 1989. "Activation studies with a promoted precipitated iron Fischer-Tropsch catalyst", *Industrial & Engineering Chemistry Research*, Vol.28 (8), pp.1130-1140.
- Bukur D. B., Patel S. A., Lang X., 1990. "Fixed bed and slurry reactor studies of Fischer-Tropsch synthesis on precipitated iron catalyst", *Applied Catalysis*, Vol. 61(1), pp.329-349.
- Bukur D. B., Lang X. and Nowicki L., 2005. "Comparative Study of an Iron Fischer-Tropsch Catalyst Performance in Stirred Tank Slurry and Fixed-Bed Reactors", *Industrial & Engineering Chemistry Research*, Vol. (44), pp. 6038-6044.
- Cabbai V. , Ballico M., Aneggi E., and Goi D., 2013. "BMP tests of source selected OFMSW to evaluate anaerobic co-digestion with sewage sludge", *Waste Management*, Vol. (33), pp. 1626-1632.
- Cai J., Zheng P., Mahmood Q., 2008. "Effect of sulfide to nitrate ratios on the simultaneous anaerobic sulfide and nitrate removal", *Bioresource Technology*, Vol. (99), pp.5520-5527.
- Campuzano R. and González-Martínez S., 2016. "Characteristics of the organic fraction of municipal solid waste and methane production: A review, *Waste management*, Vol. (54), pp.3-12.
- Carrere H. , Dumas C., Battimelli A., Batstone D.J., Delgenes J.P., Steyer J.P., Ferrer I., 2010. "Pretreatment methods to improve sludge anaerobic degradability: A review", *Journal of Hazardous Materials*, Vol. (183), pp.1-15.

- Charisiou N.D., Siakavelas G., Papageridis K.N., Baklavaridis A., Tzounis L., Avraam D.G. and Goula M.A.,2016. “Syngas production via the biogas dry reforming reaction over nickel supported on modified with CeO₂ and/or La₂O₃ alumina catalysts”, *Journal of Natural Gas Science and Engineering*, Vol. (31), pp. 164-183.
- Chen J. L., Ortiz R., Steele T.W.J. and Stuckey D.C.,2014. “Toxicants inhibiting anaerobic digestion: A review”, *Biotechnology Advances*, Vol. (32), pp.1523-1534.
- Cheng K., Subramanian V., Carvalho A., Ordonsky V. V., Wang Y. and Khodakov A. Y., 2016. “The role of carbon pre-coating for the synthesis of highly efficient cobalt catalysts for Fischer–Tropsch synthesis”, *Journal of Catalysis*, Vol. (337), pp. 260-271.
- Cheng J., Gong X., Hua P., Martin Lok C., Ellis P., French S., 2008. “A quantitative determination of reaction mechanisms from density functional theory calculations: Fischer–Tropsch synthesis on flat and stepped cobalt surfaces”, *Journal of Catalysis*, Vol. (254), pp.285-295.
- Chen Y., Cheng J. J. and Creamer K.S., 2008. “Inhibition of anaerobic digestion process: A review”, *Bioresource Technology*, Vol. (99), pp. 4044-4064.
- Chiu S., Chiu J. and Kuo W., 2013. “Biological stoichiometric analysis of nutrition and ammonia toxicity in thermophilic anaerobic co-digestion of organic substrates under different organic loading rates”, *Renewable Energy*, Vol. (57), pp.323-329.

- Chu C., Li Y., Xu K., Ebie Y., Inamori Y. and Konga H., 2008. “A pH- and temperature-phased two-stage process for hydrogen and methane production from food waste”, *International journal of Hydrogen Energy*, Vol. (33), pp.4739-4746.
- Chu W., Chernavskii P.A., Gengembre L., Pankina G. A., Fongarland P. and Khodakov A. Y., 2007. “Cobalt species in promoted cobalt alumina-supported Fischer–Tropsch catalysts”, *Journal of Catalysis*, Vol. (252), pp. 215-230.
- Choudhury H. A. and Moholkar V.S., 2013a. “An Optimization Study of Fischer–Tropsch Synthesis Using Commercial Cobalt Catalyst”, *International Journal of Scientific Engineering and Technology*, Vol. (2), pp. 31-39.
- Choudhury H. A. and Moholkar V. S., 2013b. “Synthesis of Liquid Hydrocarbons by Fischer –Tropsch Process using Industrial Iron Catalyst”, *International Journal of Innovative Research in Science Engineering and Technology*, Vol. (2), pp. 3493-3499.
- Converti A, Del Borghi A., Zilli M., Arni S. and Del Borghi M., 1999. “Anaerobic digestion of the vegetable fraction of municipal refuses: mesophilic versus thermophilic conditions”, *Bioprocess Engineering*, Vol. (21), pp.371-376.
- Cuetos, M.J., Fernández, C., Gómez, X., Morán, A., 2011. “Anaerobic co-digestion of swine manure with energy crop residues”, *Biotechnology and Bioprocess Engineering*, Vol. (16), pp. 1044-1052.

- Cuetos, M.J., Gomez, X., Otero, M., Moran, A., 2008. “Anaerobic digestion of solid slaughterhouse waste (SHW) at laboratory scale: influence of co-digestion with the organic fraction of municipal solid waste (OFMSW)”, *Biochemical Engineering Journal*, Vol. (40), pp. 99-106.
- Dasgupta D. and Wiltowski T., 2011. “Enhancing gas phase Fischer–Tropsch synthesis catalyst design”, *Fuel*, Vol. (90), pp. 174-181.
- Davis B. H., 2001. “Fischer–Tropsch synthesis: current mechanism and futuristic needs”, *Fuel Processing Technology*, Vol. (71), pp. 157-166.
- Demirbas A., 2008. “Biofuels sources, biofuel policy, biofuel economy and global biofuel projections”, *Energy Conversion and Management*, Vol. (49), pp.2106-2116.
- Demirel B. and Scherer P., 2008. “The roles of acetotrophic and hydrogenotrophic methanogens during anaerobic conversion of biomass to methane: a review”, *Reviews in Environmental Science and Bio/Technology*, Vol. (7), pp.173-190.
- Deublein D. and Steinhauser A., 2008. “Biogas from Waste and Renewable Resources: An Introduction”, WILEY-VCH Verlag GmbH & Co. KGaA, Germany.
- Deublein D. And Steinhauser A., 2011. “Biogas from waste and renewable resources: an introduction”, Second Edition, Wiley -VCH Verlag GmbH & Co. KGaA, Germany.
- Dong L., Zhenhong Y., Yongming S., Xiaoying K., Yu Z., 2009. “Hydrogen production characteristics of organic fraction of municipal solid wastes by anaerobic mixed culture fermentation”, *International Journal of Hydrogen Energy*, Vol. (34), pp.812-820.

- Dry M. E., 1996. "Practical and theoretical aspects of the catalytic Fischer-Tropsch process", *Applied Catalysis A: General*, Vol. (138), pp. 319-344.
- Dry M. E., 1999. "Fischer-Tropsch reactions and the environment", *Applied Catalysis A: General*, Vol. (189), pp.185-190.
- Dry M. E., 2001. "High quality diesel via the Fischer-Tropsch Process: a review", *Journal of Chemical Technology and Biotechnology*, Vol. (77), pp.43-50.
- Dry E. M., 2002. "The Fischer-Tropsch process: 1950-2000", *Catalysis Today*, Vol. (71), pp.227-241.
- Duan N., Dong B. , Wu B. and Dai X.,2012. "High-solid anaerobic digestion of sewage sludge under mesophilic conditions: Feasibility study", *Bioresource Technology*, Vol. (104), pp.150-156.
- El-Mashad H.M., Wilko K.P., Loon V., Zeeman G., 2003. "A model of solar energy utilisation in the anaerobic digestion of cattle manure", *Biosystems Engineering*, Vol. (84), pp. 231-238.
- El-Mashad H.M. and Zhang R., 2010. "Biogas production from co-digestion of dairy manure and food waste", *Bioresource Technology*, Vol. (101), pp. 4021-4028.
- Farias F.E.M., Silva F.R.C., Cartaxo S.J.M., Fernandes F.A.N. and Sales F.G., 2007. "Effect of Operating Conditions on Fischer-Tropsch Liquid Products", *Latin American Applied Research*, Vol. (37), pp.283-287.

- Farias F.E.M. , Fernandes F.A.N. and Sales F.G.,2010. “Effect of Operating Conditions on Fischer-Tropsch Liquid Products Produced by Unpromoted and Potassium-Promoted Iron Catalyst”, *Latin American Applied Research*, Vol. (40), pp.161-166.
- Favre E. , Bounaceur R. and Roizard D., 2009. “Biogas, membranes and carbon dioxide capture”, *Journal of Membrane Science*, Vol. (328), pp. 11-14.
- Fei J.H., Yang M.X., Hou Z.Y., and Zheng X. M., 2004. “Effect of the Addition of Manganese and Zinc on the Properties of Copper-Based Catalyst for the Synthesis of Syngas to Dimethyl Ether”, *Energy & Fuels*, Vol. (18), pp. 1584-1587.
- Fengel D. and Wegner G., 1983. “Wood - Chemistry, Ultrastructure, Reactions” De Gruiter, Berlin.
- Fermoso F. G., Bartacek J., Jansen S., Lens P.N.L., 2009. “Metal supplementation to UASB bioreactors: from cell-metal interactions to full-scale application”, *Science of the Total Environment*, Vol. (407), pp.3652 - 3667.
- Fernandez J., Perez M. and Romero L., 2008. “Effect of substrate concentration on dry mesophilic anaerobic digestion of organic fraction of municipal solid waste (OFMSW)”, *Bioresource Technology*, Vol. (99), pp.6075-6080.
- Fernandez B., Porrier P. and Chamy R., 2001. “Effect of inoculum-substrate ratio on the startup of solid waste anaerobic digesters”, *Water Science and Technology*, Vol. (44:4), pp.103-108.

- Feyzi M., Irandoust M. and Mirzaei A. A., 2011. “Effects of promoters and calcination conditions on the catalytic performance of iron–manganese catalysts for Fischer–Tropsch synthesis”, *Fuel Processing Technology*, Vol. (92), pp. 1136-1143.
- Feyzi M., Nadri S. and Joshaghani M., 2013. “Catalytic Performance of Fe–Mn/SiO₂ Nanocatalysts for CO Hydrogenation”, *Journal of Chemistry*, Vol. (2013), pp.1-10.
- Fezzani B. and Cheikh R.B., 2010. “Two-phase anaerobic co-digestion of olive mill wastes in semi-continuous digesters at mesophilic temperature”, *Bioresource Technology*, Vol. (101), pp. 1628-1634.
- Forster-Carneiro T., Pérez M. and Romero L.I., 2008. “Influence of total solid and inoculum contents on performance of anaerobic reactors treating food waste”, *Bioresource Technology*, Vol. (99), pp.6994-7002.
- Franzle S. and Markert B., 2002. “The Biological System of the Elements (BSE)-a brief introduction into historical and applied aspects with special reference on “ecotoxicological identity cards” for different element species (e.g. As and Sn)”, *Environmental Pollution*, Vol. (120), pp.27-45.
- Fratolocchi L., Visconti C.G., Lietti L., Tronconi E., Cornaro U. and Rossini S., 2015. “A novel preparation method for “small” eggshell Co/γ-Al₂O₃ catalysts: A promising catalytic system for compact Fischer–Tropsch reactors”, *Catalysis Today*, Vol. (246), pp.125-132.
- Galadima A. and Muraza O., 2015. “Waste to liquid fuels: potency, progress and challenges: Review paper”, *International Journal of Energy Research*, Vol. (39), pp.1451-1478.

- Galbe M. and Zacchi G., 2007. "Pretreatment of lignocellulosic materials for efficient bioethanol production", *Advances in Biochemical Engineering/Biotechnology*, Vol. (108), pp. 41-65.
- Gallert C. and Winter J., 1997. "Mesophilic and thermophilic anaerobic digestion of source- sorted organic wastes: effect of ammonia on glucose degradation and methane production", *Applied Microbiology and Biotechnology*, Vol. (48), pp. 405-410.
- Gangadharan P. , Kanchi K.C. and Lou H.H.,2012. "Evaluation of the economic and environmental impact of combining dry reforming with steam reforming of methane", *Chemical Engineering Research and Design*, Vol. (90), pp.1956-1968.
- Carlsson M. , Lagerkvist A. and Sagastume M. F., 2012. "The effects of substrate pre-treatment on anaerobic digestion systems: A review", *Waste Management*, Vol. (32), pp.1634-1650.
- Garrote G., Dominguez H., Parajo J.C., 1999. "Hydrothermal processing of lignocellulosic materials", *Holz als Roh- und Werkstoff*, Vol. (57), pp.191-202.
- Gaube J. and Klein H. F., 2008. "Studies on the reaction mechanism of the Fischer–Tropsch synthesis on iron and cobalt", *Journal of Molecular Catalysis A: Chemical*, Vol. (283), pp.60-68.
- Geo J., Juhina D. and Pranab D.,2014. "Generation of biogas from food waste using an anaerobic reactor under laboratory conditions", *International Journal of Scientific Research and Education*, Vol. (2), pp.1453-1465.

- Ghaniyari-Benis S., Borja R., Ali Monemian S., Goodarzi V., 2009. Anaerobic treatment of synthetic medium-strength wastewater using a multistage biofilm reactor, *Bioresource Technology*, Vol. (100), pp.1740-1745.
- Ghosh S., Henry M.P., Sajjad A., Mensinger M.C., Arora J.L., 2000. "Pilot scale gasification of municipal solid wastes by high-rate and two-phase anaerobic digestion (TPAD)", *Water Science & Technology*, Vol. (41), pp.101-110.
- Girardon J.S., Lermontov A.S., Gengembre L., Chernavskii P.A and Constant A. G., Khodakov A. Y., 2005a. "Effect of cobalt precursor and pretreatment conditions on the structure and catalytic performance of cobalt silica-supported Fischer–Tropsch catalysts", *Journal of Catalysis*, Vol. (230), pp. 339-352.
- Girardon J.S., Constant A. G., Gengembre L., Chernavskii P.A., Khodakov A. Y., 2005b. "Optimization of the pretreatment procedure in the design of cobalt silica supported Fischer–Tropsch catalysts", *Catalysis Today*, Vol. (106), pp.161-165.
- Girardon J.S., Quinet E., Constant A. G., Chernavskii P.A., Gengembre L., Khodakov A. Y., 2007. "Cobalt dispersion, reducibility, and surface sites in promoted silica-supported Fischer–Tropsch catalysts", *Journal of Catalysis*, Vol. (248), pp.143-157.
- Gómez X., Cuetos M. J., Cara J., Morán, A. & García A. I. ,2006. "Anaerobic co-digestion of primary sludge and the fruit and vegetable fraction of the municipal solid wastes: Conditions for mixing and evaluation of the organic loading rate", *Renewable Energy*, Vol. (31), pp.2017-2024.

- Goula M. A., Charisiou N. D., Papageridis K. N., Delimitis A., Pachatouridou E., and Iliopoulou E. F., 2015. "Nickel on alumina catalysts for the production of hydrogen rich mixtures via the biogas dry reforming reaction: Influence of the synthesis method", *International Journal of Hydrogen Energy*, Vol. (40), pp.9183-9200.
- Grady J. C.P.L., Daigger G.T. and Lim H.C., 1999. "Biological Waste Water Treatment", Marcel Dekker, New York.
- Guendouz J., Buffiere P., Cacho J., Carrere M., Delgenes J.P., 2010. "Dry anaerobic digestion in batch mode: design and operation of a laboratory-scale, completely mixed reactor," *Waste Management*, Vol.(30), pp.1768-1771.
- Haber J., Block J. H. and Delmon B., 1995. "Manual of methods and procedures for catalyst characterization", *Pure and Applied Chemistry*, Vol. (67), pp.1257-1306.
- Hammond G.P., Kallu S. and Manus M.C., 2008. "Development of biofuels for the UK automotive market", *Applied Energy*, Vol. (85), pp. 506-515.
- Hansen K.H. , Angelidaki I. and Ahring B. K., 1998. "Anaerobic digestion of swine manure: Inhibition by ammonia", *Water Research*, Vol. (32), pp.5-12.
- Harasimowicz M. , Orluk P., Zakrzewska-Trznadel G. and Chmielewski A.G., 2007. "Application of polyimide membranes for biogas purification and enrichment", *Journal of Hazardous Materials*, Vol. (144), pp. 698-702.
- Hayakawa H., Tanaka H. and Fujimoto K., 2007. "Studies on catalytic performance of precipitated iron/silica catalysts for Fischer–Tropsch Synthesis", *Applied Catalysis A: General*, Vol. (328), pp. 117-123.

- He W.Z., Li G.M., Kong L.Z., Wang H., Huang J.W. and Xu J.C., 2008. "Application of hydrothermal reaction in resource recovery of organic wastes", *Resources Conservation and Recycling*, Vol. (52), pp.691-699.
- Heo N.H., Park S.C., Lee J.S. and Kang H., 2003. "Solubilization of waste activated sludge by alkaline pretreatment and biochemical methane potential (bmp) tests for anaerobic co-digestion of municipal organic waste", *Water Science and Technology*, Vol. (48), pp.211-219.
- Ho N. C., Nag-Jong K., Jongwon K. and Chang M. J., 2010. "Biomass-derived Volatile Fatty Acids platform for fuels and chemicals", *Biotechnology and Bioprocess Engineering*, Vol. (15), pp.1-10.
- Hong J., Chernavskii P. A., Khodakov A. Y. and Chu W., 2009. "Effect of promotion with ruthenium on the structure and catalytic performance of mesoporous silica (smaller and larger pore) supported cobalt Fischer–Tropsch catalysts", *Catalysis Today*, Vol. (140), pp.135-141.
- Hong J., Chu W., Chernavskii P. A. and Khodakov A. Y., 2010. "Effects of zirconia promotion on the structure and performance of smaller and larger pore silica-supported cobalt catalysts for Fischer–Tropsch synthesis", *Applied Catalysis A: General*, Vol. (382), pp.28-35.
- Hong J., Marceau E., Khodakov A. Y. Constant A. G., Fontaine C. L., Villain F., Briois V., Chernavskii P.A., 2011. "Impact of sorbitol addition on the structure and performance of silica-supported cobalt catalysts for Fischer–Tropsch synthesis", *Catalysis Today*, Vol. (175), pp. 528- 533.
- Hong-Wei Y. and David E. B., 2007. "Anaerobic co-digestion of algal sludge and waste paper to produce methane", *Bioresource Technology*, Vol. (98), pp.130-134.

- Iglesia E., 1997. "Design, synthesis, and use of cobalt-based Fischer-Tropsch synthesis catalysts", *Applied Catalysis A: General*, Vol. (161), pp. 59-78.
- Igoni A.H., Abowei M.F.N. , Ayotamuno M.J. and Eze. C.L., 2008. "Effect of Total Solids Concentration of Municipal Solid Waste on the Biogas produced in an Anaerobic Continuous Digester", *Journal of food, Agriculture & Environment*, Manuscript EE 07 010, Vol. (X), pp.1-11.
- Ingrid H. Franke-Whittle, Andreas Walter, Christian Ebner and Heribert Insam, 2014. "Investigation into the effect of high concentrations of volatile fatty acids in anaerobic digestion on methanogenic communities", *Waste Management*, Vol. (34), pp.2080-2089.
- Jacobs G., Patterson P. M., Zhang Y., Das T., Li J. and Davis B. H., 2002. "Fischer-Tropsch synthesis: deactivation of noble metal-promoted Co/Al₂O₃ catalysts", *Applied Catalysis A: General*, Vol. (233), pp. 215-226.
- Jalama, K., Coville, N.J., Xiong, H., Hildebrandt, D., Glasser, D., Taylor, S., Carley, A., Anderson, J.A., and Hutchings, G.J., 2011. "A Comparison of Au/Co/Al₂O₃ and Au/Co/SiO₂ Catalysts in the Fischer-Tropsch Reaction", *Applied Catalysis A: General*, Vol. (395:1-2), pp. 1-9.
- Jha A. K., Li J., Nies L. and Zhang L., 2011. "Research advances in dry anaerobic digestion process of solid organic wastes: Review", *African Journal of Biotechnology*, Vol. (10), pp. 14242-14253.

- Jung H., Yang J.I., Yang J. H., Lee H.T., Chun D. H. and Kim H.J., 2010. “Investigation of Fischer–Tropsch synthesis performance and its intrinsic reaction behavior in a bench scale slurry bubble column reactor”, *Fuel Processing Technology*, Vol. (91), pp. 1839-1844.
- Jung I. Y., Yang J. H., Kim H. J., Jung H., Chun D. H. and Lee H.T., 2010. “Highly effective cobalt catalyst for wax production in Fischer–Tropsch synthesis”, *Fuel*, Vol. (89), pp. 237-243.
- Kalloum S., Salem F., Kouki A. and Mokaddem H., 2014. “Influence of inoculums/substrate ratios (ISRs) on the mesophilic anaerobic digestion of slaughterhouse waste in batch mode: Process stability and biogas production”, *Energy Procedia*, Vol. (50), pp. 57-63.
- Karlsson A. , Einarsson P. , Schnürer A. , Sundberg C. , Ejlertsson J., Svensson B. H.,2012. “Impact of trace element addition on degradation efficiency of volatile fatty acids, oleic acid and phenyl acetate and on microbial populations in a biogas digester”, *Journal of Bioscience and Bioengineering*, Vol. (114), pp.446-452.
- Kashyap D.R., Dadhich K.S., Sharma S.K., 2003. “Biomethanation under psychrophilic conditions: a review”, *Bioresource Technology*, Vol. (87), pp. 147-153.
- Kaparaju P., Buendia I., Ellegaard L. and Angelidakia I., 2008. “Effects of mixing on methane production during thermophilic anaerobic digestion of manure: lab-scale and pilot-scale studies”, *Bioresource Technology*, Vol. (99), pp.4919-4928.

- Kapdi S.S., Vijay V.K., Rajesh S.K. and Prasad R. , 2005. “Biogas scrubbing, compression and storage: perspective and prospectus in Indian context”, *Renewable Energy*, Vol. (30), pp. 1195-1202.
- Karaca H. , Fongarland P., Constant A.G. , Khodakov A. Y. , Hortmann K. and DonkS. V., 2009. “Intergranular and intragranular cobalt repartitions in alumina supported Fischere-Tropsch catalysts promoted with platinum”, *Comptes Rendus Chimie*, Vol. (12), pp. 668-676.
- Karaca H., Safonova O. V. , Chambrey S., Fongarland P., Roussel P., Constant A. G., Lacroix M. and Khodakov A.Y., 2011. “Structure and catalytic performance of Pt-promoted alumina-supported cobalt catalysts under realistic conditions of Fischer–Tropsch synthesis”, *Journal of Catalysis*, Vol. (277), pp.14-26.
- Kayhanian M., 1999. “Ammonia inhibition in high-solids biogasification: an overview and practical solutions”, *Environmental Technology*, Vol. (20), pp.355-365.
- Kaygusuz K., 2012. “Energy for sustainable development: A case of developing countries”, *Renewable and Sustainable Energy Reviews*, Vol. (16), pp. 1116-1126.
- Kayhanian M. and Rich D.,1995. “Pilot-scale high solids thermophilic anaerobic digestion of municipal solid waste with an emphasis on nutrient requirements”, *Biomass and Bioeneray*, Vol. (8), pp. 433- 444.
- Kim J., Park C., Kim T.H., Lee M., Kim S., Kim S.W., Lee, J., 2003. “Effects of various pretreatments for enhanced anaerobic digestion with waste activated sludge”, *Journal of Bioscience and Bioengineering*, Vol. (95), pp. 271-275.

- Kleinert A., Feldhoff A. , Schiestel T. and Caro J., 2006. “Novel hollow fibre membrane reactor for the partial oxidation of methane”, *Catalysis Today*, Vol.(118), pp. 44-51.
- Kong, F., Engler, C., Soltes, E., 1992. “Effects of cell-wall acetate, xylan backbone and lignin on enzymatic hydrolysis of aspen wood”, *Applied Biochemistry and Biotechnology*, Vol.(34),pp. 23-35.
- Kongjan P., O-Thong S. and Angelidaki I., 2013. “Hydrogen and methane production from desugared molasses using a two-stage thermophilic anaerobic process”, *Engineering in Life Sciences*, Vol. (13), pp.118-125.
- Kral T.A., Brink K.M., Miller S. L., Mckay C.P., 1998. “Origins of Life and Evolution of the Biosphere”, *The Journal of the International Astrobiology Society*, Vol. (28), pp.311-319.
- Krishna R. R., Hiroshan H., Janardhanan G., Jean E.B., and Thomas L., 2009. “Geotechnical properties of synthetic municipal solid waste”, *International Journal of Geotechnical Engineering*, Vol. (3), pp.429-438.
- Kumabe K., Sato T., Matsumoto K., Ishida Y. and Hasegawa T., 2010. “Production of hydrocarbons in Fischer–Tropsch synthesis with Fe-based catalyst: Investigations of primary kerosene yield and carbon mass balance”, *Fuel*, Vol. (89), pp.2088–2095.
- Lavoie JM., 2014. “Review on dry reforming of methane, a potentially more environmentally-friendly approach to the increasing natural gas exploitation”, *Frontiers in Chemistry*, Vol. (2), pp.1-17.
- Lee D.H., Behera S.K., Kim J., Park H.S., 2009. “Methane production potential of leachate generated from Korean food waste recycling facilities: a lab scale study”, *Waste Management*, Vol. (29), pp.876–882.

- Lee D., Lee S., Bae J., Kang J., Kim K. , Rhee S., Park J., Cho J., Chung J. and Seo D., 2015. "Effect of Volatile Fatty Acid Concentration on Anaerobic Degradation Rate from Field Anaerobic Digestion Facilities Treating Food Waste Leachate in South Korea", *Journal of Chemistry*, Vol. (2015), pp.1-9.
- Leckel D., 2009. "Diesel Production from Fischer-Tropsch: The Past, the Present, and New Concepts", *Energy & Fuels*, Vol. (23), pp. 2342-2358.
- Leikam K. and Stegmann R., 1999. "Influence of mechanical-biological pretreatment of municipal solid waste on landfill behavior", *Waste Management and Research*, Vol. (17), pp.424-429.
- Lesteur M., Bellon-Maurel V., Gonzalez C., Latrille E., Roger J.M., Junqua G., Steyer J.P., 2010. "Alternative methods for determining anaerobic biodegradability: a review", *Process Biochemistry*, Vol. (45), pp. 431-440.
- Levis J.W., Barlaz M.A., Themelis N.J., Ulloa P., 2010. "Assessment of the state of food waste treatment in the United States and Canada", *Waste Management*, Vol. (30), pp. 1486-1494.
- Li C. and Fang H.H.P., 2007. "Inhibition of heavy metals on fermentative hydrogen production by granular sludge", *Chemosphere*, Vol. (67), pp.668-673.
- Li H., Chen L., Liu W. and Zou S., 2012. "Optimized alkaline pretreatment of sludge before anaerobic digestion", *Bioresource Technology*, Vol. (123), pp.189-194.

- Li Y., Park S. Y. and Zhu J., 2011. “Solid-state anaerobic digestion for methane production from organic waste”, *Renewable and Sustainable Energy Reviews*, Vol. (15), pp.821-826.
- Lianhua L., Dong L., Yongming S., Longlong M., Zhenhong Y. and Xiaoying K., 2010. “Effect of temperature and solid concentration on anaerobic digestion of rice straw in South China”, *International Journal of Hydrogen Energy*, Vol. (35), pp.7261-7266.
- Liew L. N., Shi J. and Li Y., 2012. “Methane production from solid-state anaerobic digestion of lignocellulosic biomass”, *biomass and bioenergy*, Vol. (46), pp.125-132.
- Liu X., Li X. and Fujimoto K., 2007. “Effective control of carbon number distribution during Fischer–Tropsch synthesis over supported cobalt catalyst”, *Catalysis Communications*, Vol. (8), pp. 1329-1335.
- Liu C., Yuan X., Zeng G., Li W., Li J., 2008. “Prediction of methane yield at optimum pH for anaerobic digestion of organic fraction of municipal solid waste”, *Bioresource Technology*, Vol. (99), pp. 882-888.
- Liu T. and Sung S., 2002. “Ammonia inhibition on thermophilic acetoclastic methanogens”, *Water Science and Technology*, Vol. (45), pp. 113-120.
- Liu Y., Teng B., Guoa X. ,b, Li Y., Changa J. ,Tian L. Hao X., Wanga Y., Hong-Wei Xiang H. , Xua Y. and Li Y.W.,2007a. “Effect of reaction conditions on the catalytic performance of Fe-Mn catalyst for Fischer-Tropsch synthesis”, *Journal of Molecular Catalysis A: Chemical*, Vol. (272), pp. 182-190.

- Liu Y., Zheng S., Shi B. and Li J., 2007b. “Deuterium tracer study of Fischer–Tropsch synthesis: A method to eliminate accumulation problems”, *Journal of Molecular Catalysis A: Chemical*, Vol. (276), pp. 110-115.
- Lo H.M., Chiang C.F., Tsao H.C., Pai T.Y., Liu M.H., Kurniawan T.A., Chao K.P., Liou C.T., Lin K.C., Chang C.Y., Wang S.C., Banks C.J., Lin C.Y., Liu W.F., Chen P.H., Chen C.K., Chiu H.Y., Wu H.Y., Chao T.W., Chen Y.R., Liou D.W., and Lo F.C., 2012. “Effects of spiked metals on the MSW anaerobic digestion”, *Waste Management & Research*, Vol. (30 :1), pp.32-48.
- Lo Y.C., Saratale G. D., Chen W.M., Bai M.D. and Chang J.S., 2009. “Isolation of cellulose-hydrolytic bacteria and applications of the cellulolytic enzymes for cellulosic biohydrogen production”, *Enzyme and Microbial Technology*, Vol. (44), pp.417-425.
- Lohitharn N., Goodwin J. G. and Lotero E., 2008a. “Fe-based Fischer–Tropsch synthesis catalysts containing carbide-forming transition metal promoters”, *Journal of Catalysis*, Vol. (255), pp.104-113.
- Lohitharn N. , James G. and Goodwin J., 2008b. “Effect of K promotion of Fe and FeMn Fischer–Tropsch synthesis catalysts: Analysis at the site level using SSITKA”, *Journal of Catalysis*, Vol. (260), pp. 7-16.
- Luo M., Hamdeh H. and Davis B. H., 2009. “Fischer-Tropsch Synthesis: Catalyst activation of low alpha iron catalyst”, *Catalysis Today*, Vol. (140), pp.127-134.

- Ma W., Jacobs G., Gao P., Jermwongratanachai T., Shafer W. D., Pendyala V. R. R. , Yen C. H., Klettlinger J.L.S. and Davis B. H., 2014. “Fischer–Tropsch synthesis: Pore size and Zr promotional effects on the activity and selectivity of 25% Co/Al₂O₃ catalysts”, *Applied Catalysis A: General*, Vol. (475), pp. 314-324.
- Macias-Corral M., Samani Z., Hanson A., Smith G., Funk P., Yu H., Longworth J., 2008. “Anaerobic digestion of municipal solid waste and agricultural waste and the effect of co-digestion with dairy cow manure”, *Bioresource Technology*, Vol. (99), pp. 8288-8293.
- Mansouri M., Atashi H, Tabrizi F. F., Mansouri G. and Setareshenas N., 2014. “Fischer–Tropsch synthesis on cobalt–manganese nanocatalyst: studies on rate equations and operation conditions”, *International Journal of Industrial Chemistry*, Vol. (5:14), pp.1-9.
- Marie A. J., Constant A. G., Khodakov A.Y. and Diehl F., 2009. “Cobalt supported on alumina and silica-doped alumina: Catalyst structure and catalytic performance in Fischer - Tropsch synthesis”, *Comptes Rendus Chimie*, Vol. (12), pp. 660-667.
- Masse L., Masse D.I. and Kennedy K.J., 2003. “Effect of hydrolysis pretreatment on fat degradation during anaerobic digestion of slaughterhouse wastewater”, *Process Biochemistry*, Vol. (38), pp.1365-1372.
- Massoud K., George T. and Robert C. B., 2007. “Biomass Conversion Processes for Energy Recovery”, *Handbook of Energy Conservation and Renewable Energy*, Taylor and Francis Group, LLC.

- Mata-Alvarez J., Dosta J., Mace S., Astals S., 2011. “Codigestion of solid wastes: a review of its uses and perspectives including modelling”, *Critical Reviews in Biotechnology*, Vol. (31), pp. 99 -111.
- Mata-Alvarez J., edn, 2003. “Biomethanization of the Organic Fraction of Municipal Solid Wastes”, TJ International Ltd., Cornwall, U.K.
- Menardo S., Cacciatore V. and Balsari P., 2015. “Batch and continuous biogas production arising from feed varying in rice straw volumes following pre-treatment with extrusion”, *Bioresource Technology*, Vol. (180), pp.154-161.
- Michael H. Gerardi, 2003. “The Microbiology of Anaerobic Digesters”, John Wiley & Sons, Inc., Hoboken, New Jersey, USA.
- Micoli L., Bagnasco G., Turco M., Trifuoggi M., Russo Sorge A., Fanelli E., Pernice P., Aronne A., 2013. “Vapour phase H₂O₂ decomposition on Mn based monolithic catalysts synthesised by innovative procedures”, *Applied Catalysis B: Environmental*, Vol. (140-141), pp.516-522.
- Mnqanqeni N.N.M. and Coville N. J., 2008. “The effect of sulfur addition during the preparation of Co/Zn/TiO₂ Fischer–Tropsch catalysts”, *Applied Catalysis A: General*, Vol. (340), pp. 7-15.
- Mohanty P., Pant K.K., Parikh J. and Sharma D.K., 2011. “Liquid fuel production from syngas using bifunctional CuO – CoO –Cr₂O₃ catalyst mixed with MFI zeolite”, *Fuel Processing Technology*, Vol. (92), pp.600-608.

- Morales F., Groot F. M.F., Gijzeman O. L.J., Mens A., Stephan O. and Weckhuysen B. M. , 2005. “Mn promotion effects in Co/TiO₂ Fischer–Tropsch catalysts as investigated by XPS and STEM-EELS”, *Journal of Catalysis*, Vol. (230), pp. 301-308.
- Morales F., Smit E. D., Groot F. M.F., Visser T. and Weckhuysen B. M., 2007. “Effects of manganese oxide promoter on the CO and H₂ adsorption properties of titania-supported cobalt Fischer–Tropsch catalysts”, *Journal of Catalysis*, Vol. (246), pp.91-99.
- Mrafkova L., Goi D., Gallo V. and Colussi I., 2003. “Preliminary Evaluation of Inhibitory Effects of Some Substances on Aerobic and Anaerobic Treatment Plant Biomasses”, *Chemical and Biochemical Engineering Quarterly*, Vol. (17), pp. 243-247.
- Mudhoo A. and Kumar S., 2013. “Effects of heavy metals as stress factors on anaerobic digestion processes and biogas production from biomass”, *International Journal of Environmental Science and Technology*, Vol. (10), pp.1383-1398.
- Muleja A. A., Yao Y., Glasser D. and Hildebrandt D., 2016. “A study of Fischer-Tropsch synthesis: Product distribution of the light hydrocarbons”, *Applied Catalysis A: General*, Vol. (517), pp. 217-226.
- Nabaho D., Niemantsverdriet (Hans) J.W., Claeys M. and Steen E., 2016. “Hydrogen spillover in the Fischer–Tropsch synthesis: An analysis of platinum as a promoter for cobalt–alumina catalysts”, *Catalysis Today*, Vol. (261), pp.17–27

- Nah I.W., Kang Y. W., Hwang K.Y. and Song W.K.,2000. “Mechanical pretreatment of waste activated sludge for anaerobic digestion process”, *Water Research*, Vol. (34), pp. 2362-2368.
- Naik S.N., Goud V. V., Rout P. K. and Dalai A. K.,2010. “Production of first and second generation biofuels: A comprehensive review”, *Renewable and Sustainable Energy Reviews*, Vol. (14), pp. 578-597.
- Najafabadi A. T., Khodadadi A. A., Parnian M. J. and Mortazavi Y., 2016. “Atomic layer deposited Co/ γ -Al₂O₃ catalyst with enhanced cobalt dispersion and Fischer–Tropsch synthesis activity and selectivity”, *Applied Catalysis A: General*, Vol. (511), and pp.31- 46.
- Nalo T., Tasing K., Kumar S. and Bharti A., 2014. “Anaerobic Digestion of Municipal Solid Waste: A Critical Analysis”, *International Journal of Innovative Research in Science, Engineering and Technology*, Vol. (3), pp.224-234.
- Nayono S. E., Gallert C., Winter J., 2010. “Co-digestion of press water and food waste in a biowaste digester for improvement of biogas production”, *Bioresource technology*, Vol. (101), pp.6987- 6993.
- Nielfa A., Cano R., Fdz-Polanco M., 2015. “Theoretical methane production generated by the co-digestion of organic fraction municipal solid waste and biological sludge”, *Biotechnology Reports*, Vol. (5), pp. 14-21.
- Nigam P., Singh A., 2011. “Production of liquid biofuels from renewable resources: Review”, *Progress in Energy and Combustion Science*, Vol. (37), pp. 52- 68.

- Osa A.R., Lucas A. D., Valverde J.L., Romero A., Monteagudo I., Coca P. and Sánchez P., 2011a. "Influence of alkali promoters on synthetic diesel production over Co catalyst", *Catalysis Today*, Vol. (167), pp. 96-106.
- Osa A.R., Lucas A. D., Romero A., Valverde J. L. and Sánchez P., 2011b. "Influence of the catalytic support on the industrial Fischer–Tropsch synthetic diesel production", *Catalysis Today*, Vol. (176), pp. 298-302.
- Osa A.R., Lucas A. D., Romero A., Valverde J. L. and Sánchez P., 2011c. "Fischer–Tropsch diesel production over calcium-promoted Co/alumina catalyst: Effect of reaction conditions", *Fuel*, Vol. (90), pp.1935-1945.
- Osa A.R. , Lucas A. D., Maroto J. D., Romero A., Valverde J.L. and Sánchez P., 2012. "FTS fuels production over different Co/SiC catalysts", *Catalysis Today*, Vol. (187), pp.173- 182.
- Overett M. J., Hill R. O. and Moss J. R., 2000. "Organometallic chemistry and surface science: mechanistic models for the Fischer–Tropsch synthesis", *Coordination Chemistry Reviews*, Vol. (206), pp. 581-605.
- Parawira W., Murto M., Read J.S., Mattiasson B., 2005. "Profile of hydrolases and biogas production during two-stage mesophilic anaerobic digestion of solid potato waste", *Process Biochemistry*, Vol. (40), pp.2945-2952.
- Park M.H. Choi B. K., Park Y.H., Moon D.J., Park N.C. and Kim Y.C., 2015. "Kinetics for steam and CO₂ reforming of methane over Ni/La/Al₂O₃ catalyst", *Journal of Nanoscience and Nanotechnology*, Vol. (15), pp. 5255-5258.
- Park Y., Tsuno H., Hidaka T., Cheon J., 2008. "Evaluation of operational parameters in thermophilic acid fermentation of kitchen waste" *Journal of Material Cycles and Waste Management*, Vol. (10), pp. 46-52.

- Patzlaff J., Liu Y. , Graffmann C. and Gaube J.,1999. “Studies on product distributions of iron and cobalt catalyzed Fischer–Tropsch synthesis”, *Applied Catalysis A: General*, Vol. (186), pp. 109-119.
- Pendyala V. R. R., Jacobs G., Bertaux C., Khalid S. and Davis B. H., 2016. “Fischer–Tropsch synthesis: Effect of ammonia on supported cobalt catalysts”, *Journal of Catalysis*, Vol. (337), pp.80-90.
- Peng K., Li X., Luo C. and Shen Z., 2006. “Vegetation composition and heavy metal uptake by wild plants at three contaminated sites in Xiangxi area China”, *Journal of Environmental Science and Health Part A*, Vol. (40), pp.65-76.
- Perego C. and Villa P, 1997. “Catalyst preparation methods”, *Catalysis Today*, Vol. (34), pp. 281-305.
- Pirozzi D., Ausiello A., Strazza R., Trofa M., Zuccaro G., Toscano G., 2013. “Exploitation of agricultural biomasses for the synthesis of II-generation biodiesel”, *Chemical Engineering Transactions*, Vol. (32), pp. 175-180.
- Poggi-Varaldo HM, Trejo-Espino J, Fernandez-Villagomez G, Esparza-Garcia F, Caffarel-Mendez S and Rinderknecht-Seijas N., 1999. “Quality of anaerobic compost from paper mill and municipal solid wastes for soil amendment”, *Water Science and Technology*, Vol. (40), pp.179-186.
- Post M. F. M., van’t Hoog A. C., Minderhoud J. K., Sie S. T., 1989. “Diffusion Limitations in Fischer-Tropsch Catalysts”, *American Institute of Chemical Engineers*, Vol.35 (7), pp. 1107-114.
- Pour A. N., Zamani Y. , Tavasoli A., Shahri S. M. K. and Taheri S. A., 2008a. “Study on products distribution of iron and iron–zeolite catalysts in Fischer–Tropsch synthesis”, *Fuel*, Vol. (87), pp. 2004-2012.

- Pour A. N., Shahri S.M, Zamani Y., Irani M. and Tehrani S., 2008b. “Deactivation studies of bifunctional Fe-HZSM5 catalyst in Fischer-Tropsch process”, *Journal of Natural Gas Chemistry*, Vol. (17), pp.242-248.
- Pour A. N., Shahri S.M., Bozorgzadeh H. R., Zamani Y., Tavasoli A. and Marvast M. A., 2008c. “Effect of Mg, La and Ca promoters on the structure and catalytic behavior of iron-based catalysts in Fischer-Tropsch synthesis”, *Applied Catalysis A: General*, Vol. (348), pp. 201-208.
- Qiang H., Lang D.L., Li Y.Y., 2012. “High-solid mesophilic methane fermentation of food waste with an emphasis on Iron, Cobalt, and Nickel requirements”, *Bioresource Technology*, Vol. (103), pp. 21–27.
- Qing-Hao H., Xiu-Fen L., He L., Guo-Cheng D., Jian C., 2008. “Enhancement of methane fermentation in the presence of Ni²⁺ chelators”, *Biochemical Engineering Journal*, Vol. (38), pp. 98-104.
- Rafiq M. H., Jakobsen H.A., Schmid R. and Hustad J.E., 2011. “Experimental studies and modeling of a fixed bed reactor for Fischer-Tropsch synthesis using biosyngas”, *Fuel Processing Technology*, Vol. (92), pp.893-907.
- Rahimpour M.R. and Elekaei H. 2009a. “Optimization of a novel combination of fixed and fluidized-bed hydrogen-permselective membrane reactors for Fischer-Tropsch synthesis in GTL technology”, *Chemical Engineering Journal*, Vol.(152), pp. 543-555.

- Rahimpour M.R. and Elekaei H. 2009b. "A comparative study of combination of Fischer–Tropsch synthesis reactors with hydrogen-permselective membrane in GTL technology", *Fuel Processing Technology*, Vol. (90), pp. 747-761.
- Ragsdale S. W., 2008. "Enzymology of the Wood–Ljungdahl pathway of acetogenesis", *Annals of the New York Academy of Sciences*, Vol. (1125), pp.129-136.
- Raposo F., Banks C.J., Siegert I., Heaven S. and Borja R., 2006. "Influence of inoculum to substrate ratio on the biochemical methane potential of maize in batch tests", *Process Biochemistry*, Vol. (41), pp. 1444-1450.
- Regalbuto J. 2007. "Catalyst Preparation Science and Engineering", CRC Press, Taylor and Francis Group, LLC.
- Rincon B., Bujalance L., Fermoso F.G., Martín A. and Borja R., 2013. "Biochemical methane potential of two-phase olive mill solid waste: influence of thermal pretreatment on the process kinetics", *Bioresource Technology*, Vol. (140), pp.249-255.
- Rostrup-Nielsen J.R., 2000. "New aspects of syngas production and use", *Catalysis Today*, Vol. (63), pp.159-164.
- Rofer-Depoorter C.K. 1981. "A Comprehensive Mechanism for the Fischer–Tropsch Synthesis", *Chemical Reviews*, Vol. (81), pp.47-474.
- Roubaud A. and Favrat D., 2005. "Improving performances of a lean burn cogeneration biogas engine equipped with combustion prechambers", *Fuel*, Vol. (84), pp.2001-2007.

- Ryckebosch E., Drouillon M. and Vervaeren H., 2011. “Techniques for transformation of biogas to biomethane: Review”, *Biomass and Bioenergy*, Vol. (35), pp.1633-1645.
- Rytter E., Tsakoumis N. E. and Holmen A., 2016, “On the selectivity to higher hydrocarbons in Co-based Fischer–Tropsch synthesis”, *Catalysis Today*, Vol. (261), pp. 3-16.
- Sadeqzadeh M., Karaca H., Safonova O.V., Fongarland P., Chambrey S., Rouse I. P., Constant A. G., Lacroix M., Ferré D. C., Luck F. and Khodakov A.Y., 2011. “Identification of the active species in the working alumina-supported cobalt catalyst under various conditions of Fischer–Tropsch synthesis”, *Catalysis Today*, Vol. (164), pp.62-67.
- Sethuraman R., Bakhshi N. N., Katikaneni S. P. and Idem R. O., 2001. “Production of C4 hydrocarbons from Fischer–Tropsch synthesis in a follow bed reactor consisting of Co–Ni–ZrO₂ and sulfated-ZrO₂catalyst beds”, *Fuel Processing Technology*, Vol. (73), pp. 197-222.
- Schell D. and Harwood C., 1994. “Milling of lignocellulosic biomass”, *Applied Biochemistry and Biotechnology*, Vol. (45), pp.159-168.
- Schulz H. and Claeys M. 1999. “Kinetic modelling of Fischer–Tropsch product distributions”, *Applied Catalysis A: General*, Vol. (186), pp. 91-107.
- Schwarz J.A., Contescu C. and Contescu A., 1995. “Methods for Preparation of Catalytic Materials”, Vol. (95), pp.477-510
- Shahriari H., Warith M., Hamoda M. and Kennedy K. J., 2012. “Anaerobic digestion of organic fraction of municipal solid waste combining two pretreatment modalities, high temperature microwave and hydrogen peroxide”, *Waste Management*, Vol. (32), pp. 41-52.

- Schulz H., 1999. "Short history and present trends of Fischer–Tropsch synthesis", *Applied Catalysis A: General*, Vol. (186), pp.3-12.
- Shankaranand V.S., Ramesh M.V. and Lonsane B.K., 1992. "Idiosyncrasies of solid-state fermentation systems in the biosynthesis of metabolites by some bacterial and fungal cultures", *Process Biochemistry*, Vol. (27), pp. 33-36.
- Sie S.T. and Krishna R. 1999. "Fundamentals and selection of advanced Fischer–Tropsch reactors", *Applied Catalysis A: General*, Vol. (186), pp. 55-70.
- Siegert I, Banks C., 2005. "The effect of volatile fatty acid additions on the anaerobic digestion of cellulose and glucose in batch reactors", *Process Biochemistry*, Vol. (40), pp.3412-3418.
- Sosnowaki P., Wieczorek A. and Ledakowicz S., 2003. "Anaerobic co-digestion of sewage sludge and organic fraction of municipal solid wastes", *Advances in Environmental Research*, Vol. (7), pp. 609-616.
- Soto M., Mendez R. and Lema J.M., 1993. "Methanogenic and non methanogenic activity tests: theoretical basis and experimental setup", *Water Research*, Vol. (27), pp.1361-1376.
- Starr K., Gabarrell X. , Villalba G. , Talens L. and Lombardi L., 2012. "Life cycle assessment of biogas upgrading technologies", *Waste Management*, Vol. (32), pp. 991-999.
- Steynberg A. and Dry M. ,2004. "Fischer-Tropsch Technology", Elsevier Science & Technology Books.
- Sun Y. and Cheng J., 2002. "Hydrolysis of lignocellulosic materials for ethanol production: a review", *Bioresource Technology*, Vol. (83), pp.1-11.

- Taherzadeh M.J. and Karimi K., 2008. "Pretreatment of lignocellulosic wastes to improve ethanol and biogas production: a review", *International Journal of Molecular Sciences*, Vol. (9), pp.1621-1651.
- Tanahashi M., 1990. "Characterization and degradation mechanisms of wood components by steam explosion and utilization of exploded wood", *Wood Research: bulletin of the Wood Research Institute Kyoto University*, Vol. (77), pp. 49-117.
- Tampio E., Ervasti S., Paavola T., Heaven S., Banks C., and Rintala J., 2014. "Anaerobic digestion of autoclaved and untreated food waste", *Waste Management*, Vol. (34), pp.370-377.
- Teng B., Zhang C., Yang J., Cao D., Chang J., Xiang H. and Li Y., 2005. "Oxygenate Kinetics in Fischer-Tropsch synthesis over an industrial Fe-Mn catalyst", *Fuel*, Vol. (84), pp.791-800.
- Toscano G., Ausiello A., Micoli L., Zuccaro G., Pirozzi D., 2013. "Anaerobic digestion of residual lignocellulosic material to biogas and biohydrogen", *Chemical Engineering Transactions*, Vol. (32), pp.487-492.
- Tristantini D., Lögdberg S., Gevert B., Borg Ø. and Holmen A., 2007. "The effect of synthesis gas composition on the Fischer-Tropsch synthesis over $\text{Co}/\gamma\text{-Al}_2\text{O}_3$ and $\text{Co-Re}/\gamma\text{-Al}_2\text{O}_3$ catalysts", *Fuel Processing Technology*, Vol. (88), pp.643-649.
- Trzcinski A.P., Stuckey D.C., 2010. "Treatment of municipal solid waste leachate using a submerged anaerobic membrane bioreactor at mesophilic and psychrophilic temperatures: analysis of recalcitrants in the permeate using GC-MS", *Water Research*, Vol. (44), pp. 671-680.

- Turco M., Bagnasco G., Cammarano C., Micoli L., Lenarda M., Moretti E Storaro L., Talon A., 2011. "The role of H₂O and oxidized copper species in methanol steam reforming on a Cu/CeO₂/Al₂O₃ catalyst prepared by one-pot sol–gel method, *Applied Catalysis B: Environmental*, Vol.(102), pp.387-394.
- Vavilin V.A., Fernandez B., Palatsi J. and Flotats X., 2008. "Hydrolysis kinetics in anaerobic degradation of particulate organic material: An overview", *Waste Management*, Vol. (28), pp. 939-951.
- Vindis P., Mursec B., Janzekovic M. and Cus F., 2009. "The impact of Mesophilic and thermophilic anaerobic digestion on biogas production", *Journal of Achievements in Materials and Manufacturing Engineering*, Vol. (36:2), pp.192-198.
- Vliet O.P.R., Faaij A. P.C., and Turkenburg W.C., 2009. "Fischer–Tropsch diesel production in a well-to-wheel perspective: A carbon, energy flow and cost analysis", *Energy Conversion and Management*, Vol. (50), pp. 855-876.
- Wang Q. , Kuninobu M., Ogawa H. I. and Kato Y., 1999. "Degradation of volatile fatty acids in highly efficient anaerobic digestion", *Biomass and Bioenergy*, Vol. (16), pp.407-416.
- Wang Y., Zhang Y., Wang J., Meng L., 2009. "Effects of volatile fatty acid concentrations on methane yield and methanogenic bacteria", *Biomass and Bioenergy*, Vol. (33), pp.848-853.

- Wang Y.N., Ma W.P., LuY.J. , Yang J., XuY.Y. , Xiang H.W. , Li Y.W., ZhaoY.L. and ZhangB.J.,2003. “Kinetics modelling of Fischer–Tropsch synthesis over an industrialFe–Cu–K catalyst”, *Fuel*, Vol. (82), pp.195-213.
- Ward A.J., Hobbs, P.J., Holliman, P.J., Jones, D.L., 2008. “Optimization of the anaerobic digestion of agricultural resources”, *Bioresource Technology*, Vol. (99), pp. 7928-7940.
- Weiland P., 2003. “Production and Energetic Use of Biogas from Energy Crops and Wastes in Germany”, *Applied Biochemistry and Biotechnology*, Vol. (109), pp. 263- 274.
- Wijekoon K. C., Visvanathan C., and Abeynayaka A., 2011. “Effect of organic loading rate on VFA production, organic matter removal and microbial activity of a two-stage thermophilic anaerobic membrane bioreactor”, *Bioresource Technology*, Vol.(102),pp. 5353-5360.
- Wilhelm D.J., Simbeck D.R., Karp A.D. and Dickenson R.L.,2001. “Syngas production for gas-to-liquids applications: technologies, issues and outlook”, *Fuel Processing Technology*, Vol. (71), pp.139-148.
- Wonga M. H. and Coville N. J., 2010. “Indium as a chemical promoter in Fe-based Fischer-Tropsch synthesis”, *Applied Catalysis A: General*, Vol. (377), pp.150-157.
- Xiong H., Zhang Y., Liew K. and Li J., 2009. “Ruthenium promotion of Co/SBA-15 catalysts with high cobalt loading for Fischer–Tropsch synthesis”, *Fuel Processing Technology*, Vol. (90), pp.237-246.

- Xu D., Duan H., Li W. and Xu H., 2006. "Investigation on the Fischer-Tropsch Synthesis with Nitrogen-Containing Syngas over $\text{CoPtZrO}_2/\text{Al}_2\text{O}_3$ Catalyst", *Energy & Fuels*, Vol. (20), pp. 955-958.
- Yadvika S., Sreekrishnan T.R., Kohli S. and Rana V., 2004. "Enhancement of biogas production from solid substrates using different techniques: A review", *Bioresource Technology*, Vol. (95), pp.1-10.
- Yang J. H., Kim H. J., Chun D.H., Lee H.T., Hong J. C., Jung H. and Jung I. Y., 2010. "Mass transfer limitations on fixed-bed reactor for Fischer-Tropsch synthesis", *Fuel Processing Technology*, Vol. (91), pp. 285-289.
- Yang S.T. and Okos M.R., 1987. "Kinetic study and mathematical modeling of methanogenesis of acetate using pure cultures of methanogens", *Biotechnology and Bioengineering*, Vol. (30), pp. 661- 667.
- Yates I. C. and Satterfield C. N., 1992. "Hydrocarbon Selectivity from Cobalt Fischer-Tropsch Catalysts", *Energy & Fuels*, Vol. (6), pp.308-314.
- Yenigün O. and Demirel B., 2013. "Ammonia inhibition in anaerobic digestion: A review", *Process Biochemistry*, Vol. (48), pp. 901-911.
- Yi J. , Dong B., Jin J. and Dai X., 2014. "Effect of Increasing Total Solids Contents on Anaerobic Digestion of Food Waste under Mesophilic Conditions: Performance and Microbial Characteristics Analysis", *PLOS ONE*, Vol. (9:7), pp.1-10.
- Zaher U., Cheong D.Y., Wu B., and Chen S., 2007. "Producing energy and fertilizer from organic municipal solid waste", *Ecology Publication 07-07-024*, Department of Biological Systems Engineering/Washington State University.

- Zandvoort M. H., Hullebusch E. D.V., Gieteling J. , Lens P. N.L., 2006. “Granular sludge in full-scale anaerobic bioreactors: Trace element content and deficiencies”, *Enzyme and Microbial Technology*, Vol. (39), pp. 337-346.
- Zennaro R., Tagliabue M., Bartholomew C. H., 2000. “Kinetics of Fischer–Tropsch synthesis on titania-supported cobalt”, *Catalysis Today*, Vol. (58), pp.309-319.
- Zhang C.H., Yang Y., Teng B.T., Li T.Z., Zheng H.Y., Xiang H.W. and Li Y.W.,2006. “Study of an iron-manganese Fischer–Tropsch synthesis catalyst promoted with copper”, *Journal of Catalysis*, Vol. (237), pp.405-415.
- Zhang C., Su H, Baeyens J. and Tan T., 2014. “Reviewing the anaerobic digestion of food waste for biogas production”, *Renewable and Sustainable Energy Reviews*, Vol. (38), pp.383-392.
- Zhang J., Chen J., Li Y., Sun Y., 2002. “Recent Technological Developments in Cobalt Catalysts for Fischer-Tropsch Synthesis, *Journal of Natural Gas Chemistry*, Vol. (11),pp.99-108.
- Zhang L., Lee Y. W. and Jahng D., 2011. “Anaerobic co-digestion of food waste and piggery wastewater: focusing on the role of trace elements”, *Bioresource Technology*, Vol. (102), pp.5048-5059.
- Zhang P., Zeng G., Zhang G., Li Y., Zhang B. and Fan M.,2008. “Anaerobic co-digestion of biosolids and organic fraction of municipal solid waste by sequencing batch process”, *Fuel Processing Technology*, Vol. (89), pp. 485-489.

- Zhang Y., Bao J., Nagamori S. and Tsubaki N., 2009. "A new and direct preparation method of iron-based bimodal catalyst and its application in Fischer–Tropsch synthesis", *Applied Catalysis A: General*, Vol. (352), pp.277-281.
- Zhao G. , Zhang C., Qin S., Xiang H. and Li Y., 2008. "Effect of interaction between potassium and structural promoters on Fischer–Tropsch performance in iron-based catalysts", *Journal of Molecular Catalysis A: Chemical*, Vol. (286), pp. 137-142.
- Zheng S., Liu Y., Li J. and Shi B., 2007. "Deuterium tracer study of pressure effect on product distribution in the cobalt-catalyzed Fischer–Tropsch synthesis", *Applied Catalysis A: General*, Vol. (330), pp. 63-68.
- Zheng Y., Zhao J., Xu F. and Li Y., 2014. "Pretreatment of lignocellulosic biomass for enhanced biogas Production: Review", *Progress in Energy and Combustion Science*, Vol. (42), pp. 35-53.
- Zimmerman W. H., Bukur D. B., 1990. "Reaction kinetics over iron catalyst used for Fischer-Tropsch synthesis", *The Canadian Journal of Chemical Engineering*, Vol. (68:2), pp. 292-301.
- Zupancic G. D., and Jemea A., 2010. "Anaerobic digestion of tannery waste: semi continuous and anaerobic sequencing batch reactor process", *Bioresource technology*, Vol. (101), pp. 26-33.

Appendices

Appendix A

Composition of alkaline copper tartrate solution

Copper Reagent A. Dissolve 2.5 g of Na_2CO_3 (anhydrous), 2.5 g of Sodium potassium tartrate (Rochelle salt), 2g of Sodium bicarbonates NaHCO_3 , and 20 g Sodium sulfate (Na_2SO_4) (anhydrous) in 80 mL of distilled water in a beaker and then diluted to 100 mL.

Copper Reagent B. Dissolve 15 g of Copper sulfate ($\text{CuSO}_4 \cdot 5\text{H}_2\text{O}$) in 80 mL of distilled water in beaker. Then, two drops of concentrated sulfuric acid (H_2SO_4) and diluted to 100 mL.

Finally, the alkaline copper tartrate solution was prepared by mixed 25 mL of Copper Reagent A with 1mL of Copper Reagent B.

Composition of arsenomolybdate reagent

- 1- Dissolve 2.5 gm of ammonium molybdate in 45 mL of distilled water in a beaker, then 2.1 mL of concentrated sulfuric acid H_2SO_4 was added and mix.
- 2- Dissolve 0.3 g of Arsenate ($\text{Na}_2\text{HASO}_4 \cdot 7\text{H}_2\text{O}$) in 25 mL distilled water in a beaker.
- 3- Then mix two beakers and placed in an incubator at 37°C for 24 to 48 hours.

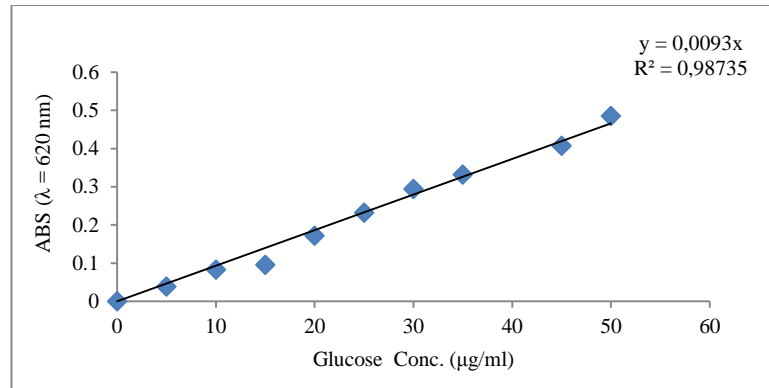


Figure A.1 Calibration line Assay by Nelson-Somogyi for measuring reducing sugars.

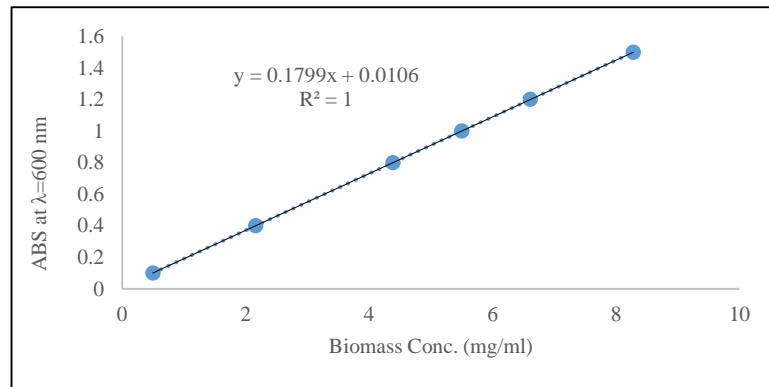


Figure A.2 Calibration curve for biomass growth.

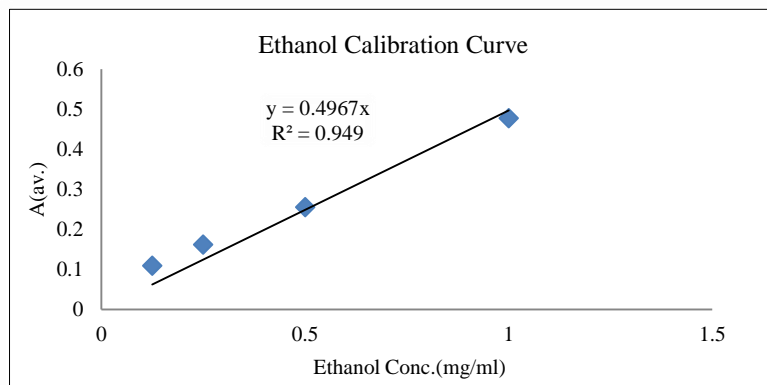
Appendix B

Figure B.1 Calibration curve for ethanol.

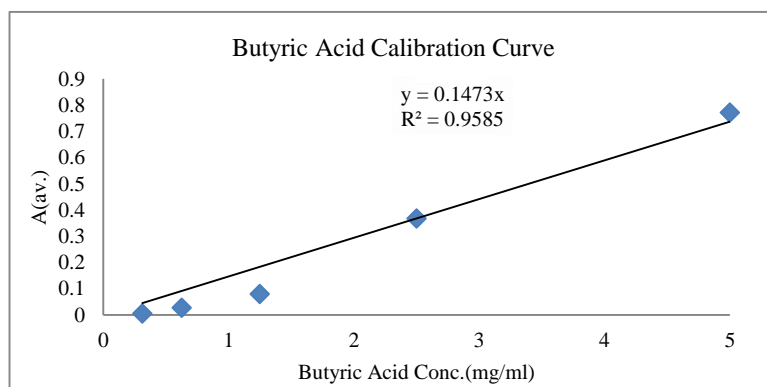


Figure B.2 Calibration curve for butyric acid.

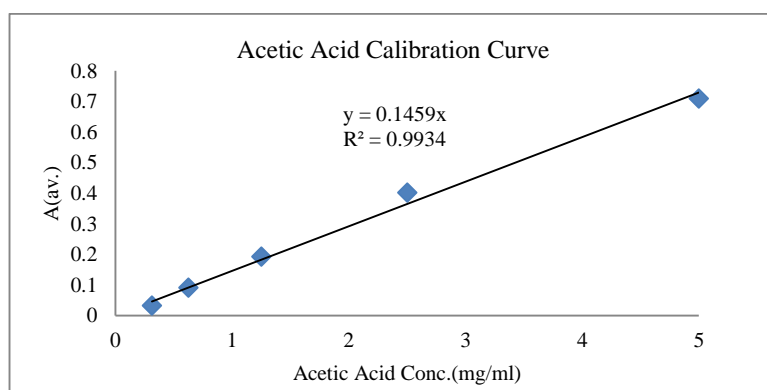


Figure B.3 Calibration curve for acetic acid.

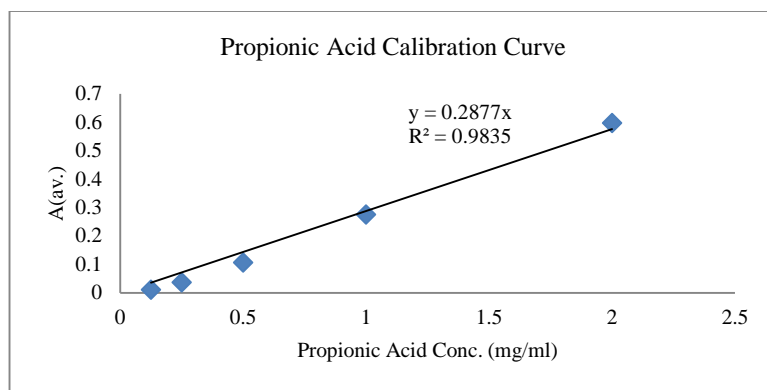


Figure B.4 Calibration curve for propionic acid.

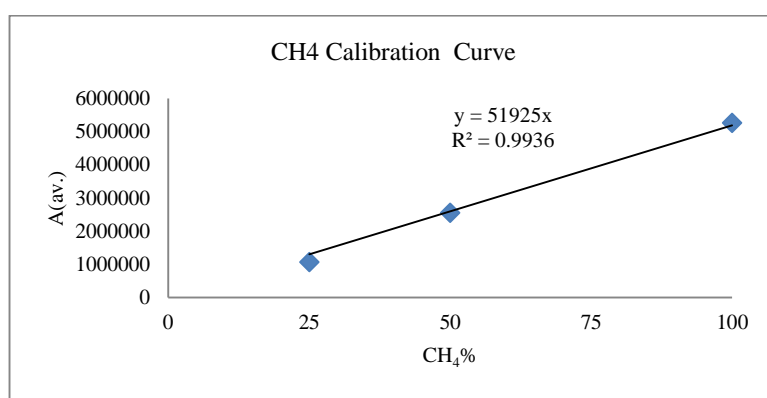


Figure B.5 Calibration curve for methane.

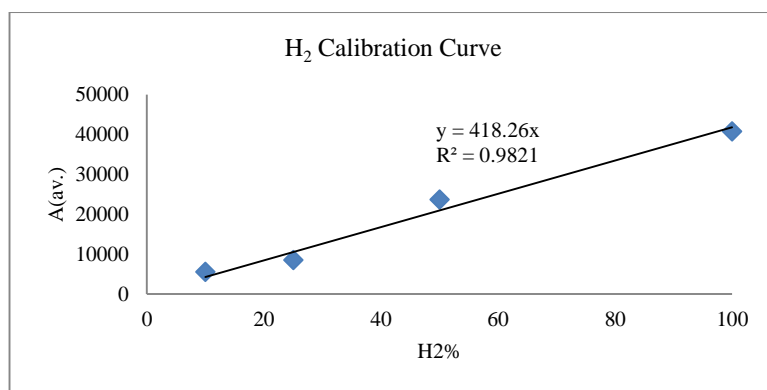


Figure B.6 Calibration curve for hydrogen.

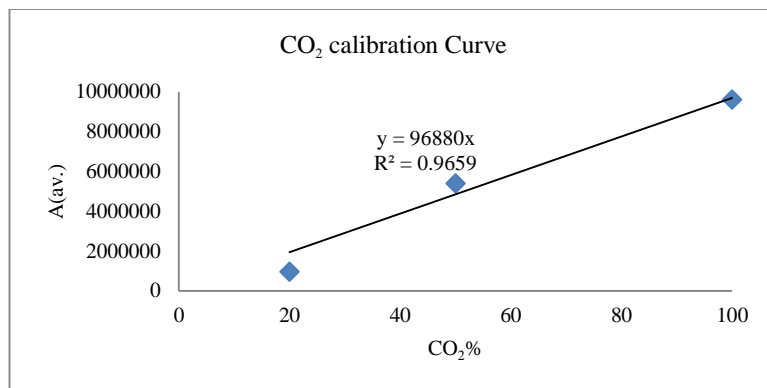


Figure B.7 Calibration curve for carbone dioxide.

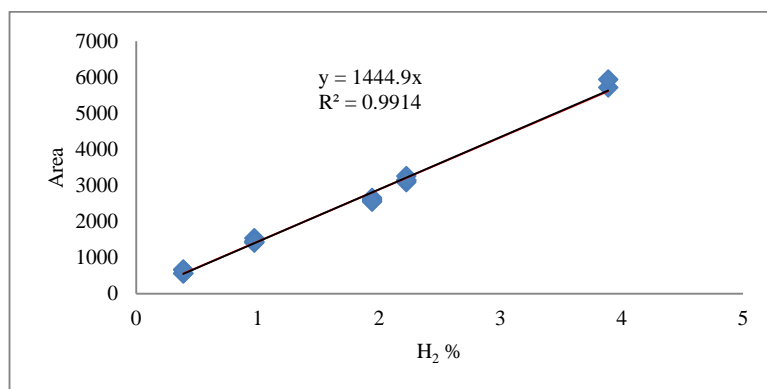


Figure B.8 Calibration curve for hydrogen feed to FT reaction.

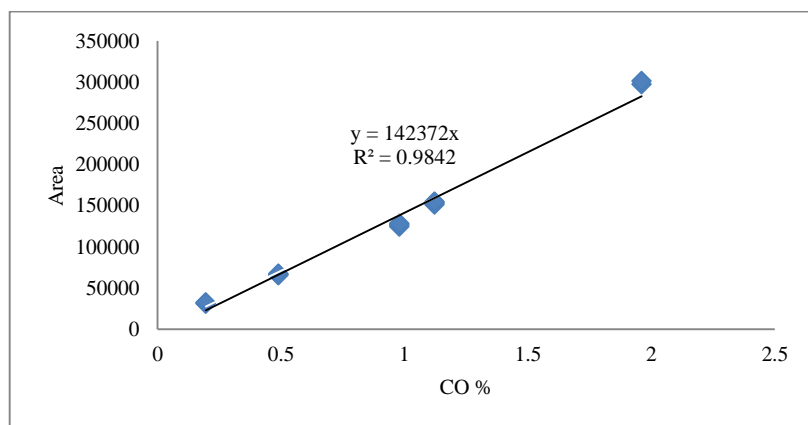
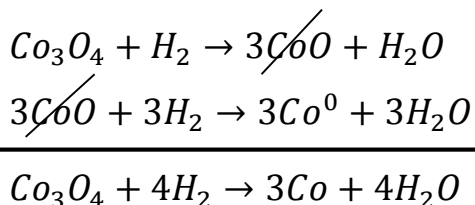


Figure B.9 Calibration curve for carbone monoxide feed to FT reaction.

Appendix C

C.1 Reducibility Calculation

The area of peaks during temperature-programmed reduction (TPR) calculate based on weight of the calcined cobalt catalysts. By assuming the major species of calcined Co catalysts is Co_3O_4 . Based on 15wt% of Co in the $\text{Co}/\text{Al}_2\text{O}_3$. The amount of H_2 that can be consumed by Co_3O_4 is calculated as follow:



Molecular Weight of Co = 58.93 g/mole and $\text{Co}_3\text{O}_4 = 240.79$ g/mole

Catalyst loaded in reactor = 5 g with 15% Co (i.e 0.75 g Co)

Mole of Co = $0.75/58.93 = 0.01273$ mole

$\text{Co}_3\text{O}_4/\text{Co} = 1/3$, mole of $\text{Co}_3\text{O}_4 = 1/3 \times$ mole Co = $1/3 \times 0.01273 = 0.00424$ mole.

$\text{Co}_3\text{O}_4/\text{H}_2 = 1/4$, mole of $\text{H}_2 = 4 \times$ mole of $\text{Co}_3\text{O}_4 = 4 \times 0.00424$ mole = 0.01697 mole of H_2 consumed for 100% reducibility.

For in suit reduction 2 % H_2/Ar mixture at flow rate = 6NL/h. (i.e 0.12 NL/h H_2)

Mole of $\text{H}_2 = 0.12$ (NL/h) $\times 1$ (atm.)/0.08206 (L. atm. /mole. K) $\times 673.15$ K) = 0.002172 mole/h.

For 10 hours = 0.02172 mole.

C.2 Calculation surface area for Co/Al₂O₃

Weight Co/Al₂O₃ catalyst = 5 g.

BET surface area of Al₂O₃=220 m²g⁻¹

Moles of Co₃O₄ after calcination =0.00424 mole (Appendix C, C.1)

Weight of Co₃O₄ =0.00424 mole ×240.79 g/mole =1.021 g.

Weight percentage of Co₃O₄= 1.021/5 = 0.204.

Theoretical surface area = (1-0.204) ×220 m²g⁻¹= 175.12 m²g⁻¹